Energy and carbon metabolism during the awakening from metabolic dormancy in cyanobacteria

Dissertation

der Mathematisch-Naturwissenschaftlichen Fakultät
der Eberhard Karls Universität Tübingen
zur Erlangung des Grades eines
Doktors der Naturwissenschaften
(Dr. rer. nat.)

vorgelegt von

Sofía Doello Román

aus El Puerto de Santa María/Spanien

Tübingen

2021

Gedruckt mit Genehmigung der Mathematisch-Naturwissenschaftlichen Fakultät der Eberhard Karls Universität Tübingen.

Tag der mündlichen Qualifikation:	21.09.2021
Dekan	Prof. Dr. Thilo Stehle
1. Berichterstatter:	Prof. Dr. Karl Forchhammer
2. Berichterstatter:	Prof. Dr. Christiane Wolz
3. Berichterstatter:	Prof. Dr. Gary Sawers

A Carmen Muñoz Delgado,
la más increíble de las mujeres

Contents

ABBREVIATIONS

2-OG	2-oxoglutarate
ABC	ATP-binding cassette
ADP	adenosine diphosphate
ARTO	alternative respiratory terminal oxidase
ATP	adenosine triphosphate
AtpH	c subunit of ATP synthase
CBB	Calvin-Benson-Bassham cycle
CCCP	chlorophenylhydrazone
CCM	carbon concentrating mechanism
Cox	cytochrome c oxidase
Cyt	cytochrome
DBMIB	dibromthymochinon
DCCD	dicyclohexylcarbodiimide
DCMU	dichlorophenyl dimethylurea
DNP	dinitrophenol
ED	Enter Doudoroff
EIPA	ethylisopropilamiloride
EMP	Embden-Meyerhof-Parnas pathway
Fd	ferredoxin
FNR	ferredoxin $NADP^+$ reductase
G6PDH	glucose-6-phosphate dehydrogenase
GDH	glutamate dehydrogenase
GlgA	glycogen synthase
GlgB	glycogen branching enzyme
GlgC	glucose-1-phosphate adenylyltransferase
GlgP	glycogen phosphorylase
GlgX	glycogen debranching enzyme
Gln	glutamine
Glu	glutamate
GOGAT	glutamate synthetase
GS	glutamine synthetase
KCN	potassium cyanide
K_m	Michaelis-Menten constant
NAD^+/ NADH	nicotinamide adenine dinucleotide
$NADP^+$/ NADPH	nicotinamide adenine dinucleotide phosphate
NDH	NAD(P)H dehydrogenase
Pc	plastocyanin
PEPc	phosphoenolpyruvate carboxylase
Pfk	phosphofruktokinase
Pgam	phosphoglycerate mutase
Pgi	phosphoglucoisomerase
Pgm	phosphoglucomutase
PHB	polyhydroxybutyrate
Pi	inorganic phosphate
PQ	plastoquinone
PS	photosystem
RTO	respiratory terminal oxidase
SDH	succinate dehydrogenase
TCA	tricarboxylic acid
V_{max}	maximum velocity
WT	wild type

I. ZUSAMMENFASSUNG

Bakterielle Dormanz spielt eine entscheidende Rolle für das Überleben und die Ausbreitung von Bakterienpopulationen. Cyanobakterien sind eine vielfältige Gruppe von Prokaryoten mit einer außergewöhnlichen Fähigkeit zur Anpassung an unterschiedliche Umweltbedingungen. Eine der häufigsten Herausforderungen, mit denen Cyanobakterien in der Natur konfrontiert sind, ist Stickstofflimitierung. Wenn das einzellige Cyanobakterium *Synechocystis* sp. PCC 6803 einem Mangel an gebundenem Stickstoff unterliegt, durchlaufen die Zellen eine metabolische Anpassung, die zu einem Ruhezustand führt, der es ihnen erlaubt, diese Bedingungen über einen längeren Zeitraum zu überleben. Diese Anpassung folgt einem genetisch festgelegten Programm und beinhaltet den Abbau des größten Teils der Thylakoidmembranen und die Synthese von Glykogen. Im Ruhezustand ist die richtige Kontrolle der Energiehomöostase und des Glykogenstoffwechsels für das Überleben essenziell. In der vorliegenden Arbeit wurde die Regulation des Energie- und Kohlenstoff-Stoffwechsels untersucht.

Es wurde gezeigt, dass dormante Zellen auf einen anderen Mechanismus der ATP-Synthese angewiesen sind als vegetative Zellen. Während des vegetativen Wachstums wird der größte Teil des zellulären ATP von den ATP-Synthasen in einer Reaktion produziert, die einen elektrochemischen Protonengradienten über die Thylakoidmembran erfordert, der durch photosynthetischen oder respiratorischen Elektronentransport erzeugt wird. In stickstoffarmen Zellen ist die Anzahl der Thylakoidmembranen stark reduziert, was eine reduzierte Kapazität der thylakoidalen ATP-Synthese impliziert. Unter diesen Umständen sind die Zellen auf die ATP-Synthasen in der zytoplasmatischen Membran und auf einen extrazellulären elektrochemischen Natriumgradienten für die ATP-Synthese angewiesen. Diese Arbeit entschlüsselte die vorübergehende Nutzung eines elektrochemischen Natriumgradienten zur Energiegewinnung als Überlebensstrategie während widrigen Umweltbedingungen.

Die Zugabe einer Stickstoffquelle zu dormanten Zellen initiiert das Erwachungsprogramm. Die Stickstoffassimilation löst den Glykogenabbau aus, der die notwendige Energie und Stoffwechselzwischenprodukte zur Regeneration der abgebauten Zellbestandteile liefert. Diese Arbeit zeigte, dass der Glykogenabbau durch Dephosphorylierung und Aktivierung der Phosphoglucomutase 1 (Pgm1) ausgelöst wird, die als metabolisches Ventil fungiert, um eine vorzeitige Nutzung der Glykogenspeicher zu vermeiden. Bemerkenswert ist, dass dieser Regulationsmechanismus evolutionär konserviert zu sein scheint. Es konnte gezeigt werden, dass nur eine spezifische Glykogenmobilisierungsstrategie ein erfolgreiches Erwachen ermöglicht, die die Glykogenphosphorylase GlgP2, den oxidativen Pentosephosphat-Weg (OPP) und den Enter-Doudoroff-Weg (ED) einbezieht. Darüber hinaus wurde gezeigt, dass das OPP-Protein (OpcA) und die Glukose-6-Phosphat-Dehydrogenase (G6PDH), die Proteine, die an der ersten Reaktion des OPP- und ED-Weges beteiligt sind, während des Erwachens mit Pgm1 interagieren. Diese Interaktion könnte zur Bildung eines Metabolons führen, dass den Kohlenstoffffluss in Richtung OPP- und ED-Weg kanalisiert, um ein effektives Erwachen aus der Dormanz zu gewährleisten.

II. SUMMARY

Bacterial dormancy plays a crucial role in the survival and spread of bacterial populations. The capability of resuming growth after a dormant period allows bacterial cells to survive in an ever-changing environment. Cyanobacteria represent a diverse group of prokaryotes with an exceptional ability to adapt to different environmental conditions. One of the most common challenges cyanobacteria face in nature is nitrogen limitation. When the unicellular cyanobacterium *Synechocystis* sp. PCC 6803 lacks a source of combined nitrogen, cells undergo a metabolic adaptation that leads to a dormant state that allows them to survive these conditions for a prolonged period of time. This adaptation follows a genetically determined program and involves the degradation of most of the thylakoid membranes and the synthesis of glycogen stores. In the quiescent state, proper control of energy homeostasis and glycogen metabolism are essential for survival. In the present study, the regulation of the energy and carbon metabolism during nitrogen starvation was investigated.

Dormant cells were shown to rely on a different mechanism of ATP synthesis than vegetative cells. During vegetative growth most of the cellular ATP is produced by the ATP synthases in a reaction that requires an electrochemical proton gradient across the thylakoid membrane, which is generated by photosynthetic or respiratory electron transport. In nitrogen-starved cells, the number of thylakoid membranes is very reduced, which implies a reduced capacity of thylakoidal ATP synthesis. Under these circumstances, cells rely on the ATP synthases located in the cytoplasmic membrane and on an extracellular electrochemical sodium gradient for ATP synthesis. This study unraveled the transient utilization of a sodium-motive force for energy generation as a survival strategy in response to adverse environmental conditions.

Addition of a nitrogen source to dormant cells initiates the resuscitation program. Nitrogen assimilation triggers glycogen degradation, which provides the necessary energy and metabolic intermediates to regenerate the degraded cellular components. This work revealed that glycogen catabolism is induced by dephosphorylation and activation of phosphoglucomutase 1 (Pgm1), which acts as a metabolic valve to avoid premature usage of the glycogen stores before a nitrogen source is available. Remarkably, this regulatory mechanism seems to be evolutionary conserved. Only a specific glycogen mobilization strategy was shown to enable successful resuscitation, which involves the glycogen phosphorylase GlgP2, the oxidative pentose phosphate (OPP) pathway and the Enter-Doudoroff (ED) pathway. Furthermore, OPP cycle protein (OpcA) and glucose-6-phosphate dehydrogenase (G6PDH), the proteins involved in the first reaction of the OPP and ED pathways, were shown to interact with Pgm1 during recovery. These interactions might result in the formation of a metabolon that directs the carbon flux into the OPP and ED pathways to ensure effective awakening from dormancy.

III. PUBLICATIONS

1. Accepted publications

Publication 1: Research article

Doello, S., Klotz, A., Makowka, A., Gutekunst, K., and Forchhammer, K. (2018). A specific glycogen mobilization strategy enables rapid awakening of dormant cyanobacteria from chlorosis. *Plant Physiol*. 177, 594–603.

Publication 2: Research article

Koch, M., **Doello, S.**, Gutekunst, K., and Forchhammer, K. (2019). PHB is produced from glycogen turn-over during nitrogen starvation in *Synechocystis* sp. PCC 6803. *Int. J. Mol. Sci*. 20, 1942: 1-14.

Publication 3: Research article

Doello, S., Burkhardt, M., and Forchhammer, K. (2021). The essential role of sodium bioenergetics and ATP homeostasis in the developmental transitions of a cyanobacterium. *Curr. Biol*. 31, 1–10.

Publication 4: Review article

Neumann, N., **Doello, S.** and Forchhammer, K. (2021). Recovery of unicellular cyanobacteria from nitrogen chlorosis: A model for resuscitation of dormant bacteria. *Microb. Physiol*. doi: 10.1159/000515742

Publication 5: Book chapter

Selim, K.A., Zimmer, E., Yehia, H., and **Doello, S.** (2021). Molecular and Cellular Mechanisms Underlying the Microbial Survival Strategies: Insights into Temperature and Nitrogen Adaptations. In: Choudhary D.K., Mishra A., Varma A. (eds) Climate Change and the Microbiome. Soil Biology, vol 63. Springer, Cham. doi: 10.1007/978-3-030-76863-8_36

2. Submitted manuscripts

Publication 6: Research article

Doello, S., Neumann, N., Spät, P., Macek, B., Forchhammer, K. (2021). Regulatory phosphorylation site tunes Phosphoglucomutase 1 as a metabolic valve to control mobilization of glycogen stores. *BioRxiv*. doi: 10.1101/2021.04.15.439997

3. Declaration of author contribution

Publication 1: "*A specific glycogen mobilization strategy enables rapid awakening of dormant cyanobacteria from chlorosis.*"

Under the supervision of Prof. Karl Forchhammer, I planned and performed the ATP, glycogen, PAM, and oxygen evolution measurements, recovery assays, prepared the figures and wrote the manuscript with input from Prof. Kirstin Gutekunst and Prof. Karl Forchhammer.

Publication 2: *"PHB is produced from glycogen turn-over during nitrogen starvation in Synechocystis sp. PCC 6803."*

I conducted all the glycogen measurements, the characterization of the Δ*glgA1* and Δ*glgA2* mutant strains, and edited the manuscript under the supervision of Prof. Karl Forchhammer.

Publication 3: *"The essential role of sodium bioenergetics and ATP homeostasis in the developmental transitions of a cyanobacterium"*

I designed and conducted all the experiments in this publication except for the monitoring of the optical density, glycogen determination and oxygen evolution measurements. I prepared all the figures and wrote the manuscript under the supervision of Prof. Karl Forchhammer.

Publication 4: *"Recovery of unicellular cyanobacteria from nitrogen chlorosis: a model for resuscitation of dormant bacteria"*

I edited the manuscript text and prepared Figure 3 under the supervision of Prof. Karl Forchhammer.

Publication 5: *"Molecular and Cellular Mechanisms Underlying the Microbial Survival Strategies: Insights into Temperature and Nitrogen Adaptations"*

I wrote the section "*Adaptation to nitrogen starvation in non-diazotrophic bacteria".*

Publication 6: "*Regulatory phosphorylation site tunes Phosphoglucomutase 1 as a metabolic valve to control mobilization of glycogen stores.*"

I designed and conducted all the experiments in this publication except for the proteomics analysis, prepared all the figures and wrote the manuscript under the supervision of Prof. Karl Forchhammer.

IV. INTRODUCTION

1. Cyanobacteria

Cyanobacteria or *Cyanophyta* constitute a phylum of gram-negative prokaryotes within the domain Bacteria. They are one of the most ancient organisms on Earth and have triggered key evolutionary events throughout history.[1,2] Cyanobacteria are the only prokaryotes capable of carrying out oxygenic photosynthesis. 2.45 billion years ago, their ability to produce oxygen from the oxidation of water triggered one of the most important environmental changes in our planet, the Great Oxidation Event, causing the atmosphere to change from a reducing to an oxidizing environment and allowing for the origin of life based on aerobic respiration.[1,3] Since then, cyanobacteria have evolved and occupied all kinds of habitats due to their remarkable ability to adapt to changing environmental conditions.[4] Today, they represent a diverse group of prokaryotes that are essential primary biomass producers, contributing to almost a quarter of the CO_2 fixation. Additionally, cyanobacteria are important contributors as nitrogen fixers, since some strains are capable of assimilating atmospheric N_2 into ammonium through the action of the enzyme complex nitrogenase in specialized cells named heterocysts.[5] The *Cyanophyta* can be classified in five different sections. Sections I and II comprise unicellular strains that reproduce by binary or multiple fission, respectively. Sections III and IV consist of filamentous strains that can divide in one plane, with Section III including filamentous strains with no specialized cells, and section IV being formed by filamentous cyanobacteria capable of differentiating specialized cells. Strains belonging to section V include filamentous cyanobacteria that can divide in more than one plane.[6]

1.1 *Synechocystis* sp. PCC 6803 as a model organism

Synechocystis sp. PCC 6803 (from now referred to as *Synechocystis*) is a Section I cyanobacterial strain that was first isolated from a freshwater lake in Berkeley in 1968.[7] Although *Synechocystis* is classified as a fresh water microorganism, it is able to grow in near-coastal areas, and to acclimate to high salt conditions.[8] *Synechocystis* was the first fully sequenced photosynthetic organism and it is accessible for genetic modification due to the availability of mutagenesis tools and its capability to uptake exogenous DNA.[9] While many cyanobacteria are obligated photoautotrophs, *Synechocystis* is metabolically versatile and it is also capable of mixotrophic and light-activated heterotrophic growth at the expense of external carbon sources.[10] *Synechocystis* is a non-diazotrophic organism: It is unable to fix atmospheric N_2 and therefore relies on a source of combined nitrogen for nitrogen assimilation. Given the frequent limitation of such nitrogen sources in the environment, *Synechocystis* has developed a metabolic adaptation to survive periods of nitrogen limitation, which involves the entry into a dormant state.[11] These characteristics make this unicellular cyanobacterium an excellent model organism to investigate questions related to photosynthesis, carbon catabolic pathways, nitrogen assimilation, stress

responses, and metabolic dormancy. *Synechocystis* also has the ability to produce different types of carbon biopolymers utilizing atmospheric CO_2, including glycogen,[12] polyhydroxybutyrate,[13] and cyanophycin,[14] which makes it interesting from a biotechnological and environmental perspective. The different aspects of the metabolism of *Synechocystis* are discussed in the following sections.

2. Energy metabolism in *Synechocystis*

Synechocystis mainly grows photoautotrophically: As long as sufficient light and nutrients are available, energy is provided by oxygenic photosynthesis. Nevertheless, this cyanobacterial strain is a facultative mixotroph, and it is also able to utilize glucose from the environment as a source of energy in combination with the photosynthetic processes. During periods of darkness, energy is solely obtained via respiration.[10] The photosynthetic and the respiratory reactions mainly take place in the thylakoid membranes, although a simplified electron transport chain also exists in the plasma membrane (**Figure 1**).[15] Remarkably, cyanobacteria are the only organisms in which the photosynthetic and the respiratory electron transport chains share common components.[16] The electron transport chain in the thylakoid membranes generates a proton gradient between the cytoplasm and the thylakoid lumen, which is utilized by the F_0F_1-ATP synthases to produce adenosine triphosphate (ATP), the universal energy-carrying molecule.[17] The specific mechanisms of ATP synthesis via photosynthesis and respiration are described below.

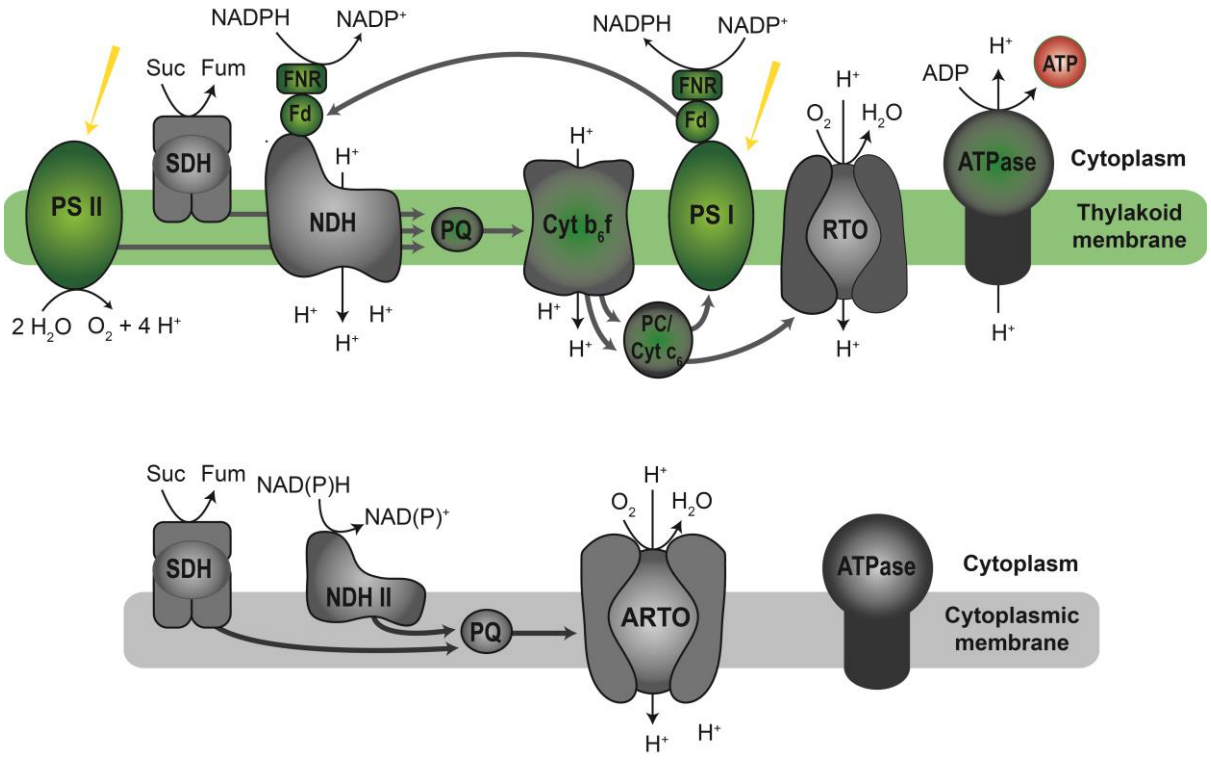

Figure 1. Cyanobacterial photosynthetic and respiratory electron transport chains at the thylakoid (top) and cytoplasmic membrane (bottom). Photosynthetic components are shown in green, respiratory components in grey, and shared components in grey/green.

2.1 Oxygenic photosynthesis

Oxygenic photosynthesis uses the energy obtained from light to produce chemical energy, carbohydrates, and oxygen. This process can be divided into: (i) the light-dependent reactions, in which the energy absorbed from light is converted to ATP and reduction equivalents, and (ii) the carbon reactions, in which the energy from these compounds is used to fix atmospheric CO_2.[18]

The light-dependent reactions start at photosystem II (PSII), a pigment–protein multimeric complex composed of the light-harvesting complex, the reaction center, and the oxygen evolving complex. The energy of light is captured by the light-harvesting complexes, the phycobilisomes. These large structures are composed of proteins associated with a chromophore, the phycobiliproteins, which include phycoerythrin, phycocyanin, phycoerythrocyanin and allophycocyanin. In *Synechocystis*, the phycobilisomes form a hemi-discoidal structure with a core of stacked allophycocyanin trimers and peripheral rods of phycocyanin.[19,20] The phycobilisomes deliver the energy of absorbed light to P_{680}, the reaction center in PSII. When the chlorophyll *a* molecule in P_{680} is excited by the absorption of one photon, it transfers an electron to an oxidized plastoquinone acceptor, reducing it to plastoquinol and leaving a positive charge on P_{680}.[21] The oxidized P_{680} receives then electrons from the oxygen evolving complex, which in turn oxidizes water molecules. Once four electrons have been abstracted from the oxygen evolving complex, two molecules of water are split into four protons, four electrons and a molecule of oxygen. Since the thylakoid membrane presents high impermeability to protons, this process contributes to the formation of a proton gradient between the thylakoid lumen and the cytoplasm. The plastoquinol reduced by PSII diffuses though the membrane and is oxidized by the cytochrome b_6f complex (cyt b_6f) through a series of redox reactions known as the Q cycle. During this process, four protons are released into the thylakoid lumen and two electrons are further transferred from cyt b_6f to the water soluble electron carriers plastocyanin and cytochrome c_6 (cyt c_6).[22] In many cyanobacteria, including *Synechocystis*, plastocyanin is the main electron carrier, and cyt c_6 is only synthesized if copper availability is low. Plastocyanin and cyt c_6 act as electron donors to photosystem I (PSI). When light is absorbed by the antenna complex of PSI, the chlorophyll *a* molecule in the P_{700} reaction center is excited and an electron is transferred to ferredoxin, the final electron acceptor. The missing electron in P_{700} is then rapidly replenished by plastocyanin or cyt c_6. Reduced ferredoxin can mediate electron transfer in a variety of biosynthetic reactions or can produce reducing equivalents in the form of NADPH by transferring electrons to the ferredoxin-$NADP^+$ reductase (FNR).[23]

The above-described process represents the thylakoid membrane linear-photosynthetic electron transport. Alternatively, cyclic electron transport around PSI can occur: The NADPH generated by FNR can be oxidized to $NADP^+$ by the NAD(P)H dehydrogenase (NDH) in the thylakoid membrane, which transfer the electrons to cyt b_6f, thus establishing a cyclic electron flow without requiring PSII. This cyclic electron transfer contributes to the formation of a proton gradient without leading to accumulation of NADPH.[23,24]

In the photosynthetic light-independent or carbon reactions, atmospheric CO_2 is fixed into carbohydrates using the NADH produced in the light-dependent reactions. The process of CO_2 fixation is described in *Section 3.1*.

2.2 Respiration

Respiration comprises the metabolic reactions that use energy-rich molecules and oxygen to produce energy and CO_2. Essentially, respiration can be viewed as the reversed process of oxygenic photosynthesis. In cyanobacteria, most of the respiratory activity takes place in the thylakoid membranes, where the generation of a proton gradient as a consequence of electron transport leads to the synthesis of ATP. This process is also known as oxidative phosphorylation. Respiratory electron transport starts with type I NADPH dehydrogenases (NDH-I) and succinate dehydrogenases (SDH), which oxidize NADPH and succinate and transfer electrons to plastoquinone acceptors. The plastoquinone pool, cyt b_6f, plastocyanin and cyt c_6 are shared components of the photosynthetic and the respiratory electron transport chain. Plastocyanin and cyt c_6 donate electrons to the respiratory terminal oxidases (RTO), which reduce molecular oxygen to water and couple electron transfer with proton translocation.[16,23] Several RTOs have been identified in *Synechocystis*: an *aa3* cytochrome c oxidase (COX), a *bd* quinol oxidase (Cyd), and an alternative terminal oxidase (ARTO). COX is the main type of RTO and accepts electrons from cyt b_6f, while Cyd and ARTO accept electrons directly from plastoquinol.[25] Unlike photosynthesis, which exclusively takes place in the thylakoid membranes, respiration is also carried out at the plasma membrane. Although the main bioenergetic processes occur at the thylakoids, the cyanobacterial plasma membrane also has an important role in energy transduction, and many cellular processes, such as cell motility, nutrient uptake, and efflux pumps are associated with an energized plasma membrane.[26] In *Synechocystis,* the cytoplasmic membrane possesses a rudimentary respiratory chain that includes SDH and type II NAD(P)H dehydrogenases (NDH-II), plastoquinone and ARTO.[23,27,28] Three NDH-II are present in *Synechocystis*: NdbA, NdbB, and NdbC. So far, the role of NDH-II is not well understood.

2.3 ATP synthesis

ATP is the main energy-carrying molecule in the cell. Most of the cellular ATP is synthesized by the F_0F_1-ATP synthase, a membrane-bound molecular machine that produces ATP from adenosine diphosphate (ADP) and inorganic phosphate (P_i) utilizing the energy of an electrochemical proton or sodium gradient as a driving force. The enzyme is formed by two parts: the F_0 and the F_1 complex. F_0 is embedded in the membrane and is responsible for ion translocation, whereas F_1 is the soluble component where ATP synthesis takes place.[29] In *Synechocystis,* ATP synthases are mostly located in the thylakoid membranes, where they use the proton motive force generated by photosynthetic and respiratory electron transport to synthesize ATP. Nonetheless, ATP synthases have also been found in the plasma membrane.[26]

Ion specificity of the ATP synthase is determined in the c-ring within complex F_0. Whether the c-ring binds protons or sodium ions is not dictated by major structural differences, but by slight variations in the amino acid sequence around the ion-binding site. Both protons and sodium ions bind a glutamate residue, and it is the nature of the amino acids surrounding this residue that determine the specificity of the c-ring. Sodium-ATP synthases have several polar groups in their ion-binding site which form a complex network of hydrogen bonds, whereas proton-ATP synthases have more hydrophobic residues.[30,31] The balance between hydrophobic and polar groups makes the c-rings more or less selective towards one ion or the other. Proton-ATP synthases must have a high proton selectivity, since usually the concentration of sodium is much higher than the concentration of protons in physiological conditions. Some ATP synthases possess proton-specific c-rings but bind sodium physiologically, since their proton specificity is not strong enough to overcome the excess of sodium.[30,32]

Proton-ATP synthases are the most ubiquitous, being present in most prokaryotes and all eukaryotes, while sodium-ATP synthases are only found in some extremophiles. Due to their prevalence, proton-ATP synthases have traditionally been considered the primary form of the enzyme, whereas the sodium-ATP synthases have been viewed as an exotic adaptation to survival in extreme environments. However, recent studies have shown that the use of a sodium gradient for ATP synthesis is the ancestral form of membrane bioenergetics, since primitive membranes were impermeable to sodium ions, but permeable to protons. Proton-driven ATP synthesis emerged later in evolution, as membranes developed proton impermeability, and became dominant in modern cells.[33]

2.4 Inhibitors of electron transport and ATP synthesis

The use of different electron transport inhibitors and artificial electron donors and acceptors has largely contributed to understand different aspects of the cellular metabolism. Photosynthetic inhibitors have helped unravelling the role and sequence of electron carriers and energy conserving sites in the electron transport chain.[34] 3-(3,4-dichlorophenyl)-1,1-dimethylurea (DCMU) is a PSII inhibitor that can block electron transfer from PSII to plastoquinone and it is extensively used in photosynthesis research and as herbicide.[35] Dibromthymochinon (DBMIB) represents another major group of inhibitors that block the electron transport chain at cyt b_6f, thereby inhibiting cyclic electron transport around PSI and oxidative phosphorylation at the thylakoid membranes. Cyclic photosynthetic electron flow is also blocked by Antimycin A, an inhibitor of the Q cycle.[36] Additionally, potassium cyanide (KCN) inhibits respiratory electron transport by blocking electron transfer to oxygen via terminal oxidases.[37]

Inhibitors of ATP synthesis are also a helpful tool to elucidate the regulatory mechanisms of the energy metabolism. *N*,*N*'-dicyclohexylcarbodiimide (DCCD) is an inhibitor of the F_0F_1 complex of ATP synthases from mitochondria and most bacteria.[38] Synthesis of ATP can additionally be suppressed by treatment with ionophores that dissipate the ion motive force, which include the protonophores carbonyl cyanide m-

chlorophenylhydrazone (CCCP) and 2,4-dinitrophenol (DNP), and the sodium ionophore monensin. Sodium-driven ATP synthesis can also be inhibited by ethylisopropylamiloride (EIPA), an inhibitor of the sodium channels and sodium/proton antiporters.[31,39]

3. Carbon metabolism in *Synechocystis*

As photoautotrophic organisms, cyanobacteria acquire most of the carbon via carbon dioxide (CO_2) and bicarbonate (HCO_3^-) fixation through the photosynthetic dark reactions using the energy and reduction equivalents generated in the light-dependent reactions. The excess of carbohydrates produced during the day is stored as carbon polymers that are used to maintain metabolism during dark periods (**Figure 2**).[40]

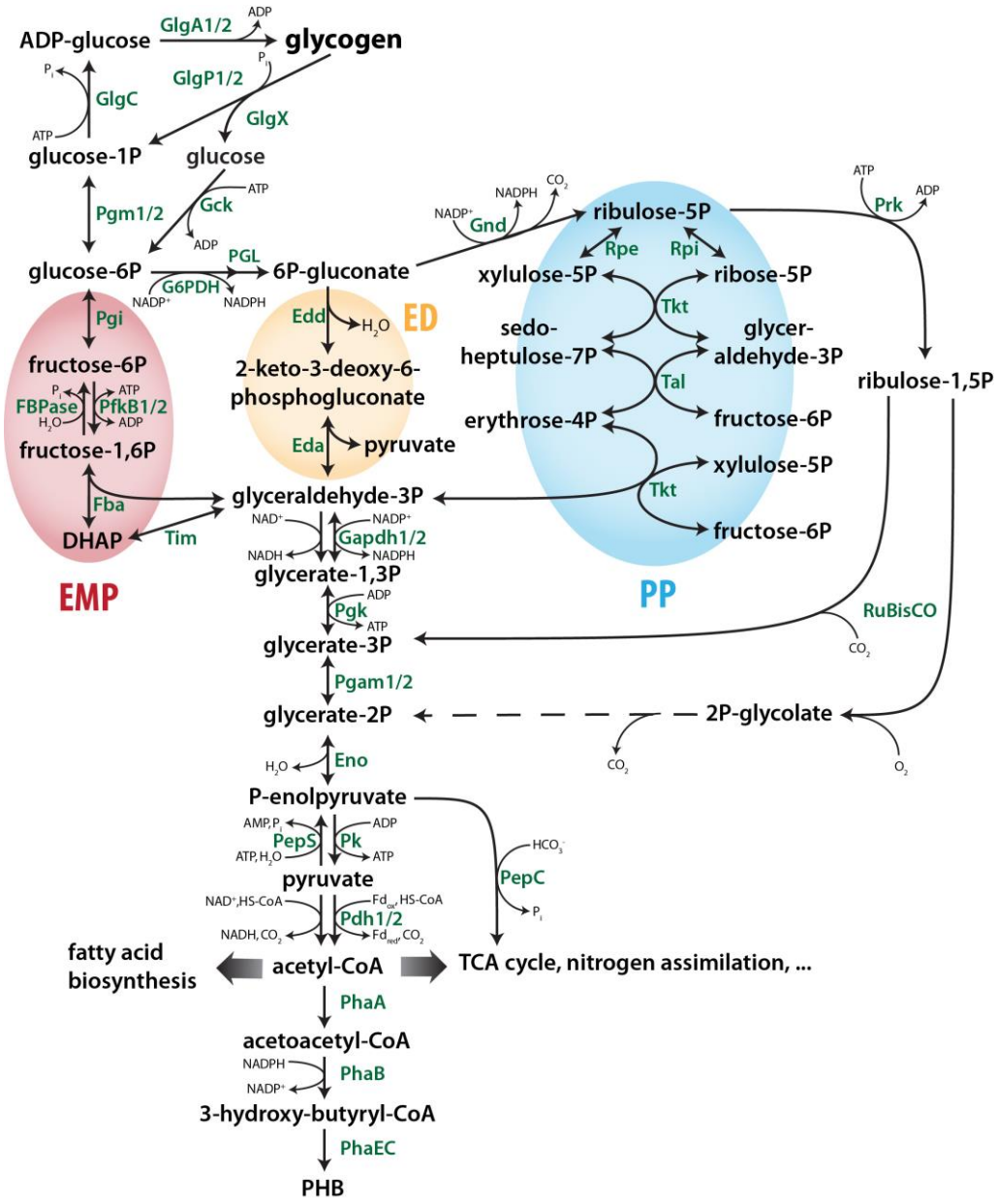

Figure 2. Overview of the carbon metabolism in *Synechocystis*. Adapted from [41].

3.1 Carbon fixation

The main mechanism for carbon fixation used by cyanobacteria is the Calvin-Benson-Bassham (CBB) cycle. In this pathway, CO_2 is condensed with ribulose-1,5-bisphosphate to generate two molecules of 3-phosphoglycerate in the carboxylation reaction catalyzed by ribulose 1,5-bisphosphate carboxylase/oxygenase (RuBisCO). The produced 3-phosphoglycerate can continue the CBB cycle to regenerate ribulose-1,5-bisphosphate or serve as a precursor for different biosynthetic reactions.[5] Besides the carboxylation reaction, RuBisCO can also catalyze an oxygenation reaction, in which ribulose-1,5-bisphosphate is condensed with O_2 instead of CO_2, producing 3-phosphoglycerate and 2-phosphoglycolate. This process is known as photorespiration and it is generally considered to reduce the efficiency of photosynthesis, since the generated 2-phosphoglycolate is toxic and its detoxification requires energy and implies the loss of fixed carbon and nitrogen.[42] Given the low affinity of RuBisCO for CO_2, to avoid high rates of photorespiration cyanobacteria have developed an efficient carbon concentrating mechanism (CCM), which increases the availability of CO_2 around RuBisCO and minimizes its oxygenation activity.[5]

The cyanobacterial CCM includes five different carbon uptake systems that contribute to accumulating inorganic carbon in the cytoplasm: Two for the import of CO_2, and three for the import of HCO_3^-. BCT1, SbtA and BicA, the three HCO_3^- transporters, are located in the plasma membrane, whereas NDH-I_3 and NDH-I_4, the CO_2 transporters, are present in the thylakoid membranes. SbtA and BicA are sodium-dependent HCO_3^- importers. Once in the cytoplasm, inorganic carbon is further transported into the carboxysomes, where RuBisCO and carbonic anhydrase, an enzyme that converts HCO_3^- to CO_2, are located. Carboxysomes are polyhedral microcompartments formed by a protein shell that prevents CO_2 loss, thus providing a CO_2-saturated environment for RuBisCO.[43]

In addition to the CBB cycle, cyanobacteria can also fix CO_2 via the phosphoenolpyruvate carboxylase (PEPC), which catalyzes the β-carboxylation of phosphoenolpyruvate to produce oxaloacetate. PEPC is an essential enzyme that may account for up to 20 % of the total carbon fixation and plays an important anaplerotic role producing carbon skeletons for nitrogen assimilation and amino acid biosynthesis.[44]

3.2 Carbon storage

When the photosynthetically fixed carbon surpasses the need for anabolic reactions, the excess carbon is used to synthesize storage compounds. Accumulation of carbon storage polymers is an important strategy that allows survival during periods of transient starvation.[45] Although most bacterial species store only one type of carbon reserve polymer, *Synechocystis* is able to produce two chemically different carbon storage compounds: glycogen and polyhydroxybutyrate (PHB). However, while glycogen has been recognized as an essential carbon and energy storage during dark periods and nutrient deprivation, the biological role of PHB in cyanobacteria has yet to be established.[46]

3.2.1 Glycogen

Glycogen synthesis is induced in inverse correlation with the growth rate, at dusk and during nutrient imbalance, conditions in which cells accumulate excess sugars.[47] This glucose polymer is produced from the glycerate-3-P obtained from CO_2 fixation, which is metabolized to glucose-1-phosphate (glucose-1P) during the gluconeogenesis. The first committed step of glycogen synthesis is the formation of ADP-glucose by the ADP-glucose pyrophosphorylase or glucose-1P adenylyltransferase (GlgC) from glucose-1P and ATP.[46] ADP-glucose can only be used as a glucosyl donor for the synthesis of glycogen or the osmolyte glucosylglycerol, which is produced under high salt stress.[48] The glycogen synthase (GlgA) transfers the glycosyl group from ADP-glucose to the non-reducing end of a linear glucan chain through a α-(1-4)-glycosylic linkage. In bacteria, the glycogen synthase has been proposed to have the ability to initiate the formation of linear glucan chains by catalyzing its own glycosylation. The branching of these linear chains into a granule is performed by the glycogen branching enzyme (GlgB), a glycosylhydrolase which catalyzes the addition of α-(1-6) ramifications in a transglycosylation reaction: It hydrolyzes an α-(1-4) linkage from a linear glucan chain and transfers a segment composed by 6 to 8 glucose molecules to an α-(1-6) position of a receptor glucan chain.[49]

Glycogen is degraded to provide cells with energy in the form of phosphorylated glucose. Glycogen depolymerization is attained by the combined activity of the glycogen phosphorylase (GlgP) and the glycogen debranching enzyme (GlgX). GlgP is a glycosyltransferase that transfers orthophosphate to the non-reducing end of a linear glucan chain and releases α-D-glucose-1P until a short glucose segment is left in each branch. In cyanobacteria, these segments contain 3-6 molecules of glucose.[50] These shortened segments are further degraded by GlgX, an isoamylase that cleaves the α-(1-6) linkages. Subsequently, phosphoglucomutase (Pgm) converts the glucose-1P produced by GlgP, which is not a usable metabolic intermediate, into glucose-6-phosphate (glucose-6P), a central metabolite that can enter different pathways.[10] Pgm is an evolutionary conserved enzyme, ubiquitous in microorganisms, plants and mammals, that catalyzes the interconversion between glucose-1P and glucose-6P, thus being involved in glycogen synthesis and degradation. This interconversion of phosphohexosugars is one of the most important reactions in carbohydrate metabolism, since the position of the phosphate group determines if the sugar is metabolized in the anabolic or the catabolic direction. A distinctive feature of *Synechocystis* in comparison to other heterotrophic bacteria is the existence of two isoforms of most of the enzymes involved in glycogen metabolism, including the glyceraldehyde-3-P dehydrogenase (Gap), GlgA, GlgP, GlgX and Pgm. In some cases, the different isoenzymes have been shown to have distinctive roles, and often only one of the isoenzymes has proven essential for glycogen synthesis or degradation under specific conditions.[51–54]

3.2.2 Polyhydroxybutyrate

Whereas all cyanobacterial genomes possess the genes for glycogen synthesis, some species, including *Synechocystis*, also contain genes for the production of PHB.[55] This carbon storage compound is a linear and flexible polymer constituted of 3-hydroxybutyrate units. It is made from acetyl-CoA in a three-step biosynthetic process that includes a condensation, a reduction, and a biosynthetic reaction. In the first step, acetoacetyl-CoA is formed from 2 molecules of acetyl-CoA; the enzyme responsible for this reaction is an α-ketothiolase (PhaA). In the second step, PhaB, a reductase, uses NADPH to reduce acetoacetyl-CoA to hydroxybutyryl-CoA. In the final step, a class III PHB synthase (PhaEC) polymerizes hydroxybutyryl-CoA into PHB.[56] Due to its physico-chemical properties, PHB is considered an alternative to thermoplastic polymers, since it can be produced by cyanobacteria in a carbon-neutral manner and has good biodegradation properties. The highest PHB content in *Synechocystis* is observed under nitrogen or phosphate starvation, when cells accumulate up to 20 % of the cell dry weight. In the past decade, *Synechocystis* has been genetically engineered to overproduce PHB. Recently, a PHB super producer strain has been constructed. This strain, named PPT1, lacks the regulator of carbon metabolism PirC, whose role is to direct the photosynthetically fixed carbon towards the synthesis of glycogen (see *Section 4.2*), and contains two genes involved in PHB metabolism, *phaA* and *phaB,* from the known producer strain *Cupriavidus necator*, allowing PHB accumulation up to 80 % of the cell dry weight.[57]

3.3 Carbon catabolism

Sugar catabolism is considered to start with glucose-6P: Besides being the product from glycogen degradation, most of the glucose that enters the cells is converted to glucose-6P via the glucokinase reaction. In *Synechocystis*, glucose-6P can be metabolized through three different glycolytic pathways: The Embden-Meyerhof-Parnas (EMP), the Entner-Doudoroff (ED), and the oxidative pentose phosphate (OPP) pathway.[10] Although they all provide energy and reduction equivalents, these metabolic routes produce different intermediates and ratios of ATP and NADH or NADPH. The EMP pathway has the highest ATP yield and produces NADH but has a greater protein requirement and does not provide pentose sugars, which are important for DNA synthesis. These compounds can be obtained via the OPP pathway, which mainly produces NADPH. The OPP pathway is also the only route that allows complete oxidation of glucose-6P to CO_2 without involving the reactions of the tricarboxylic acid (TCA) cycle: In every run one molecule of CO_2 is released; after six runs, one molecule of glucose-6P is completely converted to CO_2 and NADPH. Thus, the OPP pathway enables efficient production of reduction equivalents that can be used for respiration. The ED pathway was long overlooked and only recently recognized as a glycolytic route in *Synechocystis*. The enzymes involved in the EMP and OPP pathways are also required for the CBB cycle. Therefore, under conditions in which carbohydrate degradation and photosynthesis must operate in parallel, sugar catabolism through the ED pathway is beneficial. Utilization of these different pathways must be tightly regulated to ensure optimal use of the cellular resources.[58]

4. Nitrogen metabolism in *Synechocystis*[1]

Nitrogen is a necessary macronutrient for all living organisms and constitutes a growth-limiting factor in many ecosystems.[59] Cyanobacteria have developed the ability to use a wide range of nitrogen sources: Diazotrophic strains are capable of assimilating atmospheric N_2 via the nitrogenase reaction, while non-diazotrophic strains as *Synechocystis* rely on a source of combined nitrogen, such as ammonium, nitrate, or urea. Nitrate is the most abundant nitrogen source in most habitats. It is taken up via the ATP-binding cassette- (ABC-) transporter NrtABCD. Once in the cytoplasm, nitrate is reduced to nitrite and subsequently to ammonium by the nitrate and nitrite reductases, respectively. These reactions consume electrons from PSI-reduced ferredoxin. Similarly, urea is taken up via the ABC-transporter UrtABCD and converted to ammonium, which is incorporated into the primary metabolism. Ammonium represents the preferred nitrogen source: When nitrogen is available in the form of ammonium, uptake of nitrate and urea is inhibited.[60] This regulation is under the control of the signal transduction protein PII.[61] While the import of nitrate and urea requires ATP consumption, ammonium enters the cells via ammonium permeases of the Amt family. Incorporation of ammonium into organic molecules is achieved via two pathways: The glutamine synthetase – glutamate synthetase (GS-GOGAT) cycle and the glutamate dehydrogenase (GDH) reaction. GDH can directly incorporate ammonium to 2-oxoglutarate (2-OG) to produce glutamate (Glu) consuming NADPH. However, GDH has low affinity for ammonium and this reaction only plays a minor role in ammonium assimilation. The main pathway for nitrogen incorporation is the GS-GOGAT cycle, in which ammonium and Glu are condensed to glutamine (Gln) in the ATP-consuming reaction catalyzed by GS. GOGAT transfers the amino group from Gln to 2-OG to generate two molecules of Glu, thus regaining the Glu molecule initially consumed by GS and providing an additional Glu molecule that serves for the generation of all other nitrogen-containing compounds. The reduction equivalents for the GOGAT reaction are supplied by either NADPH or PSI-reduced ferredoxin.[62] **Figure 3** gives an overview of the process of nitrogen assimilation.

[1] Parts of this section are quotes from Selim, K.A., Zimmer, E., Yehia, H., and Doello, S. (2021). Molecular and Cellular Mechanisms Underlying the Microbial Survival Strategies: Insights into Temperature and Nitrogen Adaptations. In: Climate Change and the Microbiome. Soil Biology, vol 63. Springer, Cham. doi: 10.1007/978-3-030-76863-8_36

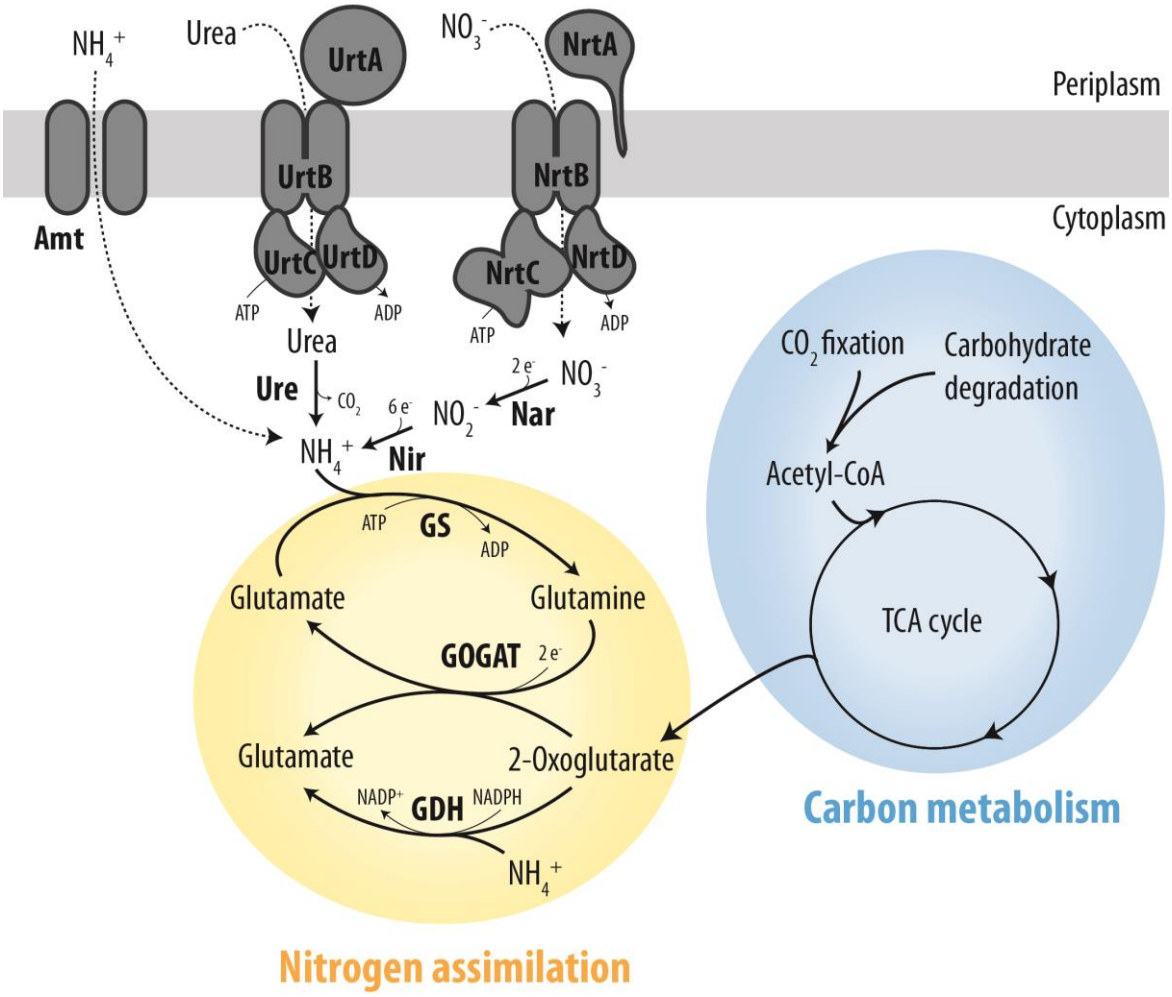

Figure 3. Nitrogen assimilation and interconnection with carbon metabolism in *Synechocystis*.

4.1 Regulation of nitrogen metabolism

Nitrogen assimilation depends on the availability of a carbon skeleton (2-OG) for biosynthesis. Carbon and nitrogen metabolism are thereby closely interconnected. To ensure optimal growth, carbon and nitrogen metabolism must be properly balanced. 2-OG serves as a reporter of the nitrogen status: It promptly accumulates when the nitrogen supply is limited and is rapidly consumed when ammonium is in excess. Receptors of 2-OG include the global nitrogen regulator NtcA and the signal transduction protein PII. NtcA is a global transcription factor that regulates the expression of the genes involved in nitrogen uptake and assimilation. PII is a highly conserved regulatory protein that senses and regulates the carbon/nitrogen balance in bacteria and plants. Under nitrogen limitation, elevated 2-OG levels favor the interaction between NtcA and PipX, a coactivator of NtcA that increases its affinity for its target promoters. Upon increasing nitrogen availability, low 2-OG levels favor the interaction between PII and PipX, which prevents PipX from binding NtcA. Under these conditions, NtcA has low affinity for its target promoters.[63]

4.2 Adaptation to nitrogen limitation in *Synechocystis*

Limitation of a combined nitrogen source is one of the most common hurdles bacteria face in natural environments. In the absence of a combined nitrogen source, *Synechocystis* follows a developmental program that leads to metabolic dormancy and allows survival in these starvation conditions for a prolonged period of time.[11] As described above, the most immediate metabolic change caused by nitrogen depletion is a rise of the 2-OG levels, which results in an NtcA-dependent activation of transcription. One of the targets of NtcA is *nblA*, a gene encoding for a small protein involved in the degradation of the phycobilisomes.[64,65] When nitrogen assimilation stops, the anabolic pathways involved in amino acid and nucleic acid synthesis are halted, which causes ATP and reducing equivalents to accumulate intracellularly. Cells respond by adjusting the photosynthetic apparatus to prevent damage due to overreduction of the photosynthetic electron carriers. This adjustment is achieved via degradation of the light harvesting complexes, the phycobilisomes, which occurs in response to the limitation of various nutrients, but it is particularly rapid under nitrogen deprivation.[11]

NblA is the main protein involved in phycobilisome degradation. Transcription of the *nblA* gene is induced under nitrogen starvation and is controlled by a very complex regulatory network.[66] This intricate system allows a tight regulation of the phycobilisome degradation process, which is essential for survival to environmental changes. In addition to preventing photodamage, phycobilisome disassembly provides amino acids for the proteins involved in glycogen metabolism during acclimation to nitrogen starvation. As a result of the degradation of the light harvesting complexes, cells suffer a color change from blue-green to yellow-orange, gaining a bleached appearance. Therefore, the process of phycobilisome degradation is termed chlorosis.[67]

Another immediate metabolic response to nitrogen starvation is the accumulation of glycogen: When imbalance in the C/N ratio is sensed through elevated levels of 2-OG, the newly photosynthetically fixed carbon is directed towards glycogen synthesis.[12] 3-Phosphoglycerate is the first stable product from the CO_2 fixation reaction catalyzed by RuBisCo. 3-Phosphoglycerate can enter the glycolytic route in the catabolic direction, when it is converted to 2-phosphoglycerate by the phosphoglycerate mutase (Pgam), or in the gluconeogenetic direction, when it is converted to 2,3-bisphosphoglycerate and directed towards glycogen synthesis. The Pgam reaction is a key point in the control of the fate of the photosynthetically fixed carbon. Under nitrogen sufficiency, when 2-OG levels are low, PII binds PirC, a competitive inhibitor of Pgam, and carbon is directed into the catabolic route. When 2-OG levels increase during nitrogen limitation, the PII-PirC complex dissociates and PirC inhibits Pgam, directing carbon into glycogen synthesis.[68] Glycogen accumulation is essential for proper acclimation to nitrogen starvation. Mutants impaired in glycogen synthesis fail to carry out the chlorosis process and do not survive nitrogen depletion.[12] Glycogen accumulation starts almost immediately after the onset of nitrogen starvation and reaches a maximum of 60% of the cell dry weight after 14 hours.[69] After several days of nitrogen starvation, cells begin to accumulate PHB. In contrast to the lethal phenotype that results from abolishing glycogen synthesis, a mutant unable to

accumulate PHB does not show difficulties entering and recovering from nitrogen-induced dormancy. The physiological role of PHB in cell survival during periods of nitrogen starvation has so far not been elucidated.[69–71]

After the first events of adaptation to nitrogen starvation (i.e., chlorosis and glycogen accumulation) have taken place, cells direct their metabolism into a dormant state that allows prolonged survival under these conditions. The chlorotic state is characterized by growth arrest and reduced metabolic activity. Growth arrest occurs after DNA replication, rendering cells ready for division when they can resume metabolic activity and providing a higher polyploidy to protect them in case of DNA damage.[69]

When dormant nitrogen-starved cells encounter a source of combined nitrogen, they are capable of reverting the metabolic and structural changes described above and restore vegetative cell cycle. The process of exiting dormancy is termed resuscitation and it involves a genetically determined program.[69,72] At the metabolic level, the awakening process can be divided into two phases. During the first phase, immediately after nitrogen availability, the genes encoding for the ATP synthesis, nitrogen assimilation and translation machinery are up-regulated. Cells cease the residual photosynthetic activity and induce respiration of glycogen, thus switching to a heterotrophic metabolism. In the second phase, approximately 24 hours after nitrogen availability, cells start to re-green and re-gain photosynthetic activity, entering a mixotrophic phase. Photoautotrophic growth and cell division resume after 48 hours, thereby completing the program.[69] **Figure 4** depicts the morphological and metabolic changes during nitrogen starvation and resuscitation.

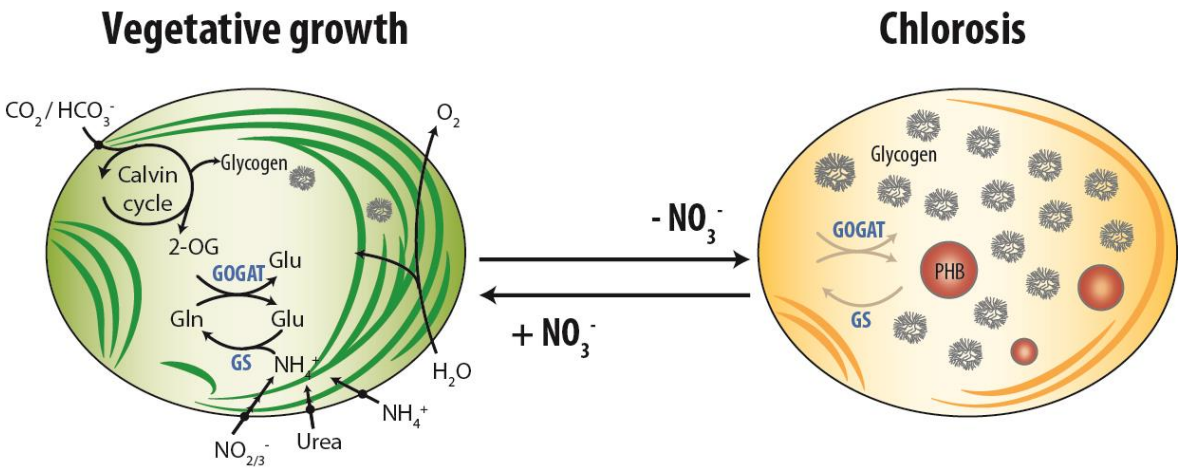

Figure 4. Overview of the metabolic and morphologic adaptation during nitrogen starvation in *Synechocystis*. Adapted from [69].

5. Aim of the investigation

Being able to resume growth after a period of dormancy is a survival strategy of extreme importance for bacterial persistence. Resuscitation of *Synechocystis* from nitrogen-starved conditions has been shown to follow a genetically determined program that allows rapid resumption of vegetative growth upon nitrogen availability. Although the major cellular processes and the transcriptional dynamics that take place have been described,[69] the regulatory mechanisms that control this program have not yet been elucidated. In this work, the switch from a dormant to a recovering metabolism was investigated in detail.

Control of energy homeostasis is critical in the transition into and out of a dormant state. In order to maintain viability in the chlorotic state, cells must be able to produce the minimal amount of ATP to ensure survival. So far, how chlorotic cells obtain ATP had not been studied. In contrast to the low energy requirements during nitrogen starvation, initiation of the resuscitation process implies a high energy demand. Successful resuscitation relies on the ability of dormant cells to provide sufficient energy to sustain the anabolic processes at the onset of resuscitation. Here, the mechanisms of ATP synthesis during nitrogen starvation and resuscitation and the regulation of the energy metabolism were investigated.

Accumulation of carbon reserve polymers plays a crucial role in the survival during transient nutrient starvation. Utilization of carbon stores provides the necessary energy to awake from quiescence. In resuscitating *Synechocystis* cells, glycogen is the major source of carbon: Its degradation starts soon after the addition of nitrogen to chlorotic cells, while PHB, the other carbon storage compound in chlorotic cells, is not degraded during the first 24 h of resuscitation. Nevertheless, the consequences of an impaired glycogen metabolism in survival to nitrogen-starved conditions and the regulation of the synthesis and degradation of this polysaccharide during these developmental transitions had not been studied. The importance of glycogen catabolism, how glycogen degradation is induced, and which metabolic pathways are involved in the resuscitation process were addressed in this work.

V. RESULTS[2]

1. Chlorotic cells rely on sodium bioenergetics for ATP synthesis.

Metabolic quiescence is generally associated with a low energy demand.[73] Addition of a nitrogen source to dormant nitrogen-starved cells induces the awakening process, which implies an increase in the energy requirements due to the initiation of assimilating and anabolic reactions.[69] To better understand the energy metabolism in chlorotic and recovering cells, the ATP content of *Synechocystis* cells at different time points during nitrogen starvation and resuscitation was determined (Figure 2A, Publication 1). When cells were transferred to nitrogen-free medium, the ATP content dropped to approximately ¼ of the level in vegetative cells, and it was subsequently kept at this concentration while cells were nitrogen-deprived. Addition of sodium nitrate triggered a two-fold increase in the ATP content, which was kept at a similar level during the first 24 hours of resuscitation, concurring with the heterotrophic phase. After 48 hours of recovery, the ATP content increased to reach double the levels detected in vegetative cells. At this point, cells have almost completely restored the photosynthetic machinery, while they continue to obtain energy from glycogen degradation, which results in a high ATP content.

The increase in ATP levels upon nitrogen addition to chlorotic cells was detected as soon as 20 min after supplementation with sodium nitrate (Figure 1, Publication 3), thereby representing an astonishing rapid response for cells in a dormant state. Further investigation of this rise in the ATP content revealed a different ATP synthesis mechanism in chlorotic than in vegetative cells. Analysis of this response started with an attempt to identify which major bioenergetic process (i.e., respiration or photosynthesis) was responsible for ATP synthesis after sodium nitrate addition. To answer this question, respiration and photosynthesis were inhibited and ATP levels were measured after supplementation with sodium nitrate. As described below, in *Section 3* of this chapter, chlorotic cells were not able to induce respiration when glycogen degradation was blocked by deletion of the glycogen phosphorylases (Figure 4, Publication 1). Thus, the ATP content in a GlgP deficient mutant (Δ*glgP1/2*) was determined. Chlorotic Δ*glgP1/2* cells showed a similar increase in the ATP levels upon addition of sodium nitrate than WT cells (Figure 1A, Publication 3), indicating that the newly produced ATP does not come from respiration. Photosynthesis was blocked by placing cells in the dark and by treatment with DCMU, DBMIB and Antimycin A (Figure 1B, C and D, Publication 3). None of these treatments suppressed the ATP increase that followed supplementation of chlorotic cells with sodium nitrate. Additionally, dissipation of the proton gradient that powers ATP synthesis by the ATP synthases in the thylakoid membranes by treatment with CCCP and DNP did not affect the ATP increase (Figure 2A and B, Publication 3). This indicated that chlorotic cells rely on a different ATP synthesis mechanism than vegetative cells.

[2] This section summarizes the main results of the research articles listed in *Chapter III* (Publications 1, 2, 3, and 5).

The fact that the lack a proton gradient did not impair ATP synthesis indicated that chlorotic cells may depend on a different motive force to power this process. In some extremophiles, ATP synthesis is coupled to a sodium gradient. The fact that *Synechocystis* uses an electrochemical sodium gradient for other bioenergetic processes (e.g., bicarbonate uptake)[74] suggested sodium could be involved in ATP synthesis in chlorotic cells. In fact, in the previously described experiments, 17 mM sodium nitrate was used to induce resuscitation, which not only resulted in the awakening of the cells, but also in the increase of the sodium motive force. Indeed, when sodium alone (17 mM sodium chloride) was added to chlorotic cells, a rise in the ATP content was measured, and when these cells were further supplemented with potassium nitrate, the ATP levels further increased (Figure 2E, Publication 3). A rise in the ATP content after addition of sodium chloride to chlorotic cells can be explained by the activity of an ATP synthase that can couple a sodium motive force to ATP production. This was proved using drugs to dissipate the sodium gradient (monensin), block sodium transport (EIPA), or inhibit the F-ATPases (DCCD) (Figure 2F, 2G and 3C, Publication 3). All these treatments abolished the ATP increase triggered by addition of sodium chloride to chlorotic cells. Furthermore, addition of more sodium led to more ATP synthesis (Figure 3B, Publication 3), confirming that sodium is used by the ATP synthases to produce ATP in chlorotic cells. Since sodium is more abundant outside than inside the cell, this electrochemical gradient can be used by the ATP synthases in the cytoplasmic membrane to power ATP synthesis. Chlorotic cells seem to maintain a similar membrane potential than vegetative cells, as deduced from their lack of permeability to the fluorescent voltage reporter bis-(1,3-dibutylbarbituric acid)- trimethine oxonol (DiBAC4(3)), which penetrates depolarized cells but does not enter cells with an intact membrane potential (Figure 3A, Publication 3). The extra voltage obtained from the addition of 17 mM sodium chloride constitutes sufficient sodium motive force to drive ATP synthesis. These experiments revealed a sodium-based ATP synthesis mechanism in chlorotic cells that was so far unknown in *Synechocystis*.

In contrast to nitrogen-starved cells, vegetative cells could grow and produce ATP in the absence of sodium as long as they were provided with enough carbon (since sodium is required for bicarbonate import) (Figures 5A, B and C, Publication 3). On the contrary, chlorotic cells showed decreasing optical density when cultivated in sodium-free medium, even in the presence of high carbon (Figure 5D, Publication 3), indicating that cells switch to sodium bioenergetics as a survival strategy to nutrient deprivation. Furthermore, chlorotic cells cultivated in the absence of sodium showed a decreased glycogen content after two weeks of starvation as compared to cells cultivated with sodium (Figure 5E, Publication 3), suggesting that the absence of sodium triggers glycogen catabolism.

Addition of nitrate to chlorotic cells also caused the ATP levels to rise. This effect was absent in the Δ*glgP1/2* mutant and when the GS-GOGAT cycle was blocked, indicating a connection between nitrogen assimilation and glycogen degradation. Inhibition of the terminal respiratory oxidases by KCN also suppressed the nitrate-induced ATP increase, implying that ATP is synthesized by the respiratory activity supported by the reduction equivalents obtained from glycogen catabolism. However, treatment with DBMIB, which exclusively inhibits the respiratory chain at the thylakoid membranes (through inhibition

of cyt b_6f), did not suppress the nitrate-dependent ATP increase, suggesting that the respiratory activity in resuscitating cells takes place at the cytoplasmic membrane (Figure 4, Publication 3), where the ATP synthases use sodium to produce ATP.

2. ATP levels are tuned in each developmental state.

As shown above, after one day of nitrogen starvation cells had a reduced ATP content as compared to vegetative cells. Whether this drop is a consequence of a low metabolic activity or if ATP levels are adjusted after cells are transferred to a nitrogen-free medium remained an open question. To test this, ATP levels were measured shortly after cells were nitrogen deprived. Regardless of the concentration of sodium in the medium, the ATP content dropped as soon as 30 min after nitrogen depletion. A similar drop was observed when the ATP/ADP ratio was measured, indicating the cellular energy charge decreased immediately after nitrogen starvation (Figure 6, Publication 3). At this point, cells still have a full photosynthetic machinery and are metabolically active, implying that cells actively adjust their ATP levels in response to nitrogen depletion.

3. Glycogen catabolism by GlgP2 is essential for survival to nitrogen starvation.

The glycogen content has been shown to decrease after addition of nitrate to chlorotic cells.[69] To test the relevance of glycogen catabolism during resuscitation from nitrogen starvation, mutants lacking the glycogen phosphorylases (Δ*glgP1*, Δ*glgP2*, and Δ*glgP1/2*) were created. These strains were transferred to nitrogen-free medium and their ability to recover on a nitrate-containing agar plate was tested. While Δ*glgP1* showed a similar recovery than the WT, Δ*glgP2* and Δ*glgP1/2* were severely impaired in their capability to resuscitate (Figure 3A, Publication 1). This impairment was due to inability to degrade glycogen, since their glycogen content did not decrease after addition of a nitrogen source, as it did in the WT and the Δ*glgP1* mutant (Figure 3B, Publication 1). Furthermore, no oxygen consumption was detected in the Δ*glgP1/2* strain after supplementation with nitrate, indicating that glycogen catabolism is necessary to switch on respiration (Figure 4, Publication 1). These data highlighted the essential role of glycogen for the survival in nitrogen starved conditions and revealed that GlgP2 is the main glycogen phosphorylase during resuscitation.

4. The OPP and ED pathways ensure successful resuscitation.

To learn what carbon catabolic routes are relevant during resuscitation from nitrogen starvation, mutants deficient in key enzymes of each pathway were created. The EMP pathway was blocked by knocking out the two homologous phosphofructokinases, PfkB1 and PfkB2 (Δ*pfkB1/2*). *Zwf,* the gene encoding for glucose-6-phosphate dehydrogenase (G6PDH), was deleted to block the entry to both, the ED and the OPP pathways (Δ*zwf*).

Inhibition of the ED and OPP pathways individually was achieved by knocking out 2-keto-3-deoxy-6-phosphogluconate (KDPG) aldolase (Eda) and 6-Phosphogluconate dehydrogenase (Gnd), respectively (Δ*eda* and Δ*gnd*). Additionally, an Eda and Gnd double deletion mutant (Δ*gnd/eda*) and a triple mutant lacking PfkB1, PfkB2 and G6PDH (Δ*zwf/pfkB1/2*) were created (Figure 1, Publication 1). These strains were nitrogen-starved for one month and their ability to recover on an agar plate containing nitrate, as well as their glycogen content were analyzed (Figure 5, Publication 1). The Δ*pfkB1/2* mutant recovered as efficiently as the WT and showed similar glycogen levels, implying that the EMP pathway does not play an important role in the resuscitation process. Conversely, the Δ*zwf* and Δ*gnd*/eda strains showed very poor resuscitation and were impaired in glycogen degradation. Although with a less severe phenotype, the single Δ*eda* and Δ*gnd* mutants were also unable to degrade glycogen and affected in their ability to resuscitate. Interestingly, Δ*eda* seemed to recover better than Δ*gnd*. These results indicate that the parallel operation of the OPP and ED pathways plays an essential role in the resuscitation from chlorosis, with the OPP pathway being of especial importance. Moreover, the total inability to recover and degrade glycogen observed in the Δ*zwf/pfkB1/2*, which is blocked in all carbon catabolic pathways, highlighted once again the cruciality of glycogen catabolism for recovery from nitrogen-starved conditions.

5. The EMP pathway connects the glycogen and PHB pools during chlorosis.

Measurement of the glycogen content at various time points after nitrogen starvation revealed a slight decrease in the glycogen levels after the first week of chlorosis, concurring with the accumulation of PHB (Figure 3, Publication 2). Since photosynthetic activity in the chlorotic state is very reduced, this suggests a correlation between glycogen catabolism and PHB synthesis. In line with this hypothesis, previous studies showed that disruption of PHB synthesis results in an increased production of glycogen.[75] To test if the products of glycogen degradation serve as the substrate for PHB synthesis, several mutant strains were analyzed. Single *glgA* deletion mutants (Δ*glgA1* and Δ*glgA2*) were able to produce a similar amount of glycogen but showed a different response to nitrogen-starved conditions: Δ*glgA2* performed a similar chlorotic response than the WT, whereas Δ*glgA1* failed to properly acclimate and kept a greenish color for the first days of nitrogen depletion (non-bleaching phenotype) (Figure 2A, Publication 2). Moreover, the Δ*glgA1* strain showed very poor recovery on nitrate-containing agar plates, in contrast to the Δ*glgA2* mutant, which recovered as efficiently as the WT (Figure 2B, Publication 2). Determination of the PHB levels in both strains revealed a very low PHB content in the Δ*glgA1* mutant, while Δ*glgA2* was not impaired in PHB synthesis (Figure 3A, Publication 2). These results unraveled a different function of the two GlgA isoforms in the acclimation to nitrogen starvation, with GlgA1 playing an essential role. Additionally, these data supported the idea that the glycogen and PHB pools are connected.

If the products from glycogen degradation are used for PHB synthesis, mutants impaired in glycogen catabolism should show an altered PHB content. To test this, the PHB content of the mutants described in *Section 4* of this chapter was measured. The strains Δ*glgP2* and Δ*glgP1/2*, which were unable to degrade glycogen, were impaired in PHB synthesis, while Δ*glgP1* degraded glycogen and accumulated PHB as the WT (Figures 4 and 5, Publication 2). Intriguingly, the Δ*pfkB1/2* strain, which had not shown a phenotype during resuscitation (see above), was strongly impaired in PHB synthesis, whereas Δ*eda*, which had shown poor recovery, contained similar PHB levels than the WT. The Δ*gnd* mutant, which had the strongest resuscitation phenotype, could only accumulate approximately 50% of the PHB measured in the WT (Figure 6, Publication 2). Altogether, these data showed that PHB is produced from glycogen turn-over during nitrogen starvation, and that functionality of the EMP pathway, which does not seem to play an important role in the resuscitation process, is essential for the synthesis of PHB. The OPP pathway also seems to contribute, although to a smaller extent, to PHB synthesis, while the ED pathway does not seem to be involved.

6. The glycogen degrading enzymes are produced during nitrogen starvation.

The above-described experiments revealed that the main glycogen degrading enzymes during the resuscitation process are GlgP2 and the enzymes that lead to the OPP pathway, G6PDH and Gnd (see *Sections 3* and *4* of this chapter). Interestingly, a transcriptomic study carried out on chlorotic and recovering cells[69] showed that the transcription of these enzymes was highly upregulated in chlorotic cells and suppressed during resuscitation, when they are required (Figure 7, Publication 1). The only enzyme involved in glycogen catabolism that showed a different expression pattern was Pgm1, whose expression was downregulated in chlorotic cells and turned up during resuscitation. These results were consistent with those of a quantitative proteomic study, which revealed that GlgP2, G6PDH and Gnd were up-regulated during chlorosis and kept at high abundance during resuscitation.[76] This indicates the proteins are synthesized during nitrogen starvation and not degraded during recovery, although no new protein is produced, as deduced from the transcriptomics data. The abundance of Pgm1 was very low in chlorotic cells and increased during recovery (Figure 2A, Publication 6). Producing the glycogen catabolic enzymes in advance allows cells to rapidly respond to the presence of nitrogen and immediately induce the resuscitation program. However, such anticipatory behavior implies that the activity of these enzymes must be regulated, and they must remain inactive during chlorosis, since degradation of the bulk of the glycogen stores only starts once nitrogen is available.

7. Mobilization of the glycogen stores is controlled via post-translation modification of Pgm1.

In addition to its different expression pattern at the transcriptomic and proteomic level, a quantitative phosphoproteomic study revealed that Pgm1 is a phosphoprotein with two serine phosphorylation sites: Ser 63 and Ser 168.[76] Interestingly, Ser 63 is one of the most phosphorylated residues during nitrogen starvation (Figure 2B, Publication 6). These observations suggested a possible regulatory role of Pgm1 in the control of the initiation of glycogen catabolism. As deduced from homology modelling of the Pgm1 structure, Ser 168 is located in the catalytic center (Figure 2E, Publication 6). This residue is involved in catalysis and must be phosphorylated for the enzyme to be able to carry out the reaction. The phosphorylation dynamics of this residue agrees with Pgm1 being inactive in chlorosis and activated during resuscitation: Phosphorylation of Ser 168 is very low during nitrogen starvation and it increases during recovery. On the contrary, Ser 63, predicted to be on the surface of the enzyme, presents very high phosphorylation under nitrogen-starved conditions, which decreases after addition of a nitrogen source. According to these dynamics, phosphorylation of Ser 63 could have a regulatory role on Pgm1 activity.

The effect of phosphorylation of Ser 63 on Pgm1 activity was investigated by creating different Pgm1 variants in which the serine at position 63 was exchanged for other amino acids, including aspartate (resulting in a phosphomimetic variant, S63D), alanine (S63A), glycine (S63G), and threonine (S63T). *In vitro* characterization of these variants showed that all substitutions strongly affected enzyme activity: The phosphomimetic variant presented almost no activity, the glycine and the threonine variants conserved less than 10 % of the activity, and the alanine variant retained 15 % (Figure 3A, Publication 6). This strongly suggested that phosphorylation of Ser 63 inhibits Pgm1 activity. Analysis of the enzyme kinetics of the Pgm1-S63A variant revealed that the mutation severely affected the reaction velocity, while it did not increase the Michaelis-Menten constant (K_m), indicating that the substrate affinity was not affected (Figure 3B, Publication 6). These parameters suggest that Ser 63 is involved in catalysis and that the lower enzyme activity was not due the substrate being unable to reach the catalytic center.

To elucidate the physiological consequences of an altered phosphorylation of Pgm1 at Ser 63 during chlorosis and resuscitation, several *Synechocystis* mutant strains were created. To mimic a Pgm1 that is permanently phosphorylated at Ser 63, a Pgm1 knockout mutant (Δ*pgm1*) was constructed, since phosphorylation of this residue seemed to inactivate the enzyme. The Δ*pgm1* strain was unable to carry out a proper acclimation response to nitrogen depletion, presenting a non-bleaching phenotype (Figure 4A, Publication 6). This behavior was a consequence of the inability of this strain to accumulate glycogen at the beginning of the chlorosis process (Figure 4C, Publication 6), since Pgm1 is required for the conversion of glucose-6P to glucose-1P, which is the initial substrate for glycogen synthesis. To find out how a permanent lack of phosphorylation at Ser 63 would affect glycogen metabolism, the Pgm1-S63A variant was introduced in the Δ*pgm1* strain. However, the low activity of the Pgm1-S63A variant could not satisfy the cellular demand

for glycogen synthesis and this strain also showed a non-bleaching phenotype (Figure S2, Publication 6). To ensure cells can synthesize enough glycogen at the onset of chlorosis, the Pgm1-S63A variant was introduced in the WT strain, thus resulting in a mutant containing a WT and a mutant copy of the enzyme. This strain could synthesize glycogen upon nitrogen starvation and successfully carried out the chlorosis process. However, after prolonged nitrogen deprivation, the optical density of the cultures began to decrease. After 1 month of nitrogen depletion, cells showed a reduced glycogen content and very poor ability to recover (Figures 4A, D and E, Publication 6). These data indicated that phosphorylation of Pgm1 at Ser 63 is essential to avoid the premature degradation of the glycogen stores during chlorosis.

Curiously, a homologous residue of the phosphorylation site Ser 63 of *Synechocystis* Pgm1 is also found in higher mammals, including human, mouse, and rabbit (Figure 8A, Publication 6). Regulation of glycogen metabolism is of crucial importance in organisms of all kingdoms of life. In humans, glycogen stores are mainly accumulated in the liver and skeletal muscle and supplied to tissues on demand, and Pgm1 deficiency leads to the abnormal use and storage of glycogen.[77] Proper regulation of Pgm1 activity is thereby of critical importance in humans. To test the influence of phosphorylation of human Pgm1 at Ser 20 (the homologous site for Ser 63 of *Synechocystis* Pgm1) on enzyme activity, we created a phosphomimetic human Pgm1 mutant in which the serine residue at position 20 was substituted by aspartate. This phosphomimetic variant of the human Pgm1 showed no activity *in vitro* (Figure 8B, Publication 6), suggesting that control of Pgm1 activity via phosphorylation of this peripheral residue is a regulatory mechanism evolutionary conserved from bacteria to humans.

8. Carbon flux into the glycogen catabolic routes is under redox control.

Analysis of the steady state levels of the products of glycogen degradation showed that glucose-1P and glucose-6P are accumulated in chlorotic cells (Figure 5, Publication 6). High levels glucose-1P can be explained by Pgm1 inhibition. Accumulation of glucose-6P during nitrogen starvation indicates that the enzymes responsible for its catabolism must also be inactivated in the chlorotic state. Although glucose-6P serves as a substrate for two enzymes, G6PDH and Pgi, G6PDH was shown to be the glucose-6P catabolic enzyme involved in the degradation of the bulk of the glycogen stores (see *Section 4*). In the nitrogen-fixing cyanobacterial strains *Anabaena* sp. PCC 7120 and *Nostoc punctiforme*, G6PDH activity is regulated by the redox state of its activator, the OPP cycle protein (OpcA). To clarify if in *Synechocystis* G6PDH responds to the same regulatory mechanism, the enzyme was characterized *in vitro*. Although G6PDH was active on its own, its substrate affinity increased 6-fold in the presence of OpcA (Figure 6A, Publication 6). However, this activating effect was only observed when OpcA was in an oxidized state, while a reduced OpcA was unable to activate G6PDH (Figure 6B, Publication 6). The activity of G6PDH alone was not affected by redox treatment. Thus, it was confirmed that in *Synechocystis*

G6PDH activity is regulated by the redox state of OpcA, which explains the accumulation of glucose-6P in chlorotic cells: Under these conditions the cytoplasm is in a reduced state and G6PDH is not activated by OpcA; during resuscitation, the cytoplasm becomes a more oxidized environment, G6PDH is activated, and glucose-6P can be metabolized via the OPP and ED pathways.

G6PDH and OpcA were identified as Pgm1 interaction partners in an immunoprecipitation experiment carried out using anti-Pgm1 antibodies (Figure S3, Publication 6). *In vitro* analysis of the interaction between these three proteins via biolayer interferometry revealed that OpcA mediates the formation of a complex: OpcA binds Pgm1 and G6PDH, but G6PDH and Pgm1 do not bind in the absence of OpcA (Figures 7A and B, Publication 6). Given the influence of the redox state of OpcA on its ability to activate G6PDH, the interaction of OpcA with Pgm1 and G6PDH was tested under different redox conditions. The interaction with both Pgm1 and G6PDH was strongly favored when OpcA was in an oxidized state, while the redox state of Pgm1 and G6PDH did not have a strong influence on the binding (Figures 7C, 7D, S4A and S4B, Publication 6). Interestingly, the Pgm1-S63D variant was unable to bind OpcA-G6PDH (Figure S4C, Publication 6). These data suggested that Pgm1, OpcA and G6PDH interact forming a dynamic complex when they are in an active state. Further analysis of the Pgm1-OpcA-G6PDH complex using size exclusion chromatography coupled to multiangle light scattering (SEC-MALS) suggested that the three proteins interact forming a hetero-dodecamer composed by a G6PDH tetramer bound to four subunits of OpcA, each of which binds a Pgm1 subunit. Formation of a complex of sequential metabolic enzymes such this might serve as a metabolon to ensure channeling of the glycogen degradation products into the OPP and ED pathways to ensure successful resuscitation from nitrogen starvation.

VI. DISCUSSION

1. Energy metabolism during nitrogen starvation and resuscitation

In natural environments, dormant microorganisms constitute the majority of the microbial population.[78] Dormancy is an extremely important survival strategy for the persistence of bacteria in adverse environments, the development of antibiotic resistances, and the spread of pathogens.[79] Although a variety of mechanisms are employed by different organisms to reach the dormant state, they all must ensure proper homeostatic control of energy balance during this process. In this work, nitrogen-starved *Synechocystis* cells served as a model to unravel how the energy metabolism is regulated in the transitions into and out of metabolic quiescence.

1.1 ATP homeostasis during nitrogen starvation and resuscitation

Metabolic dormancy is generally characterized by low ATP levels. In *Mycobacterium tuberculosis,* the ATP content in dormant nutrient-starved cells is kept at a level five times lower than in growing cells.[73] In *Synechocystis*, nitrogen-depleted cells contain four times less ATP than vegetative cells.[80] However, whether the low ATP levels in dormant cells is a consequence of their reduced metabolic activity, or whether ATP levels are actively tuned down as part of the metabolic adaptation to nutrient starvation remained an open question. *Synechocystis* showed a decreased ATP content 30 min after the transfer to nitrogen-free medium. When cells are nitrogen-starved, they initially have a full photosynthetic apparatus and are metabolically active, implying they have the ability to synthesize ATP and yet the ATP content rapidly sinks and stays at a constant low level throughout nitrogen depletion. Reduction of ATP levels might be a necessary factor for the transition into a dormant state. Besides its role in providing energy for metabolic reactions, ATP has been shown to influence protein solubility and the fluidity of the cytoplasm,[81] factors that are important for the transition into dormancy. The bacterial cytoplasm has glass-forming properties and changes from a liquid-like state when cells are metabolically active to a glass-like state when cells are dormant.[82] A reduced ATP content might thereby be essential for the transition of the cytoplasm into a glass-like state after prolonged nitrogen-deprivation. Moreover, the formation of protein aggregates, which is favored at low ATP levels, plays an important role in the transition into metabolic quiescence.[83] In line with these ideas, those *Synechocystis* mutant strains that showed high ATP levels after being transferred to nitrogen-free medium failed to carry out the chlorosis process and died in the attempt to acclimate to nitrogen depletion. These strains include mutants unable to synthesize glycogen, such as a double GlgA and a GlgC mutant,[12,48,84] suggesting a role of glycogen synthesis in the control of energy balance. In the present study, glycogen degradation was shown to be induced in chlorotic cells when ATP synthesis was compromised (i.e., in the absence of sodium), possibly in an attempt to maintain ATP at a constant level.[85] Although the mechanism of energy dissipation upon nitrogen depletion is not known, glycogen metabolism seems to have an influence on energy homeostasis.

When dormant chlorotic cells are supplemented with a nitrogen source, their energy demand dramatically increases due to the initiation of the nitrogen assimilating reactions and all the other anabolic processes that are induced at the onset of resuscitation. Cells respond accordingly and immediately increase their ATP levels to fulfill this need. **Figure 5** illustrates the change in the ATP levels during the different developmental transitions in correlation with the oxygen production or consumption as an indicator of photosynthetic and respiratory activity, respectively. The conclusions derived from this work revealed a fine regulation of the ATP content to satisfy the requirements of each state in the lifecycle of *Synechocystis*.

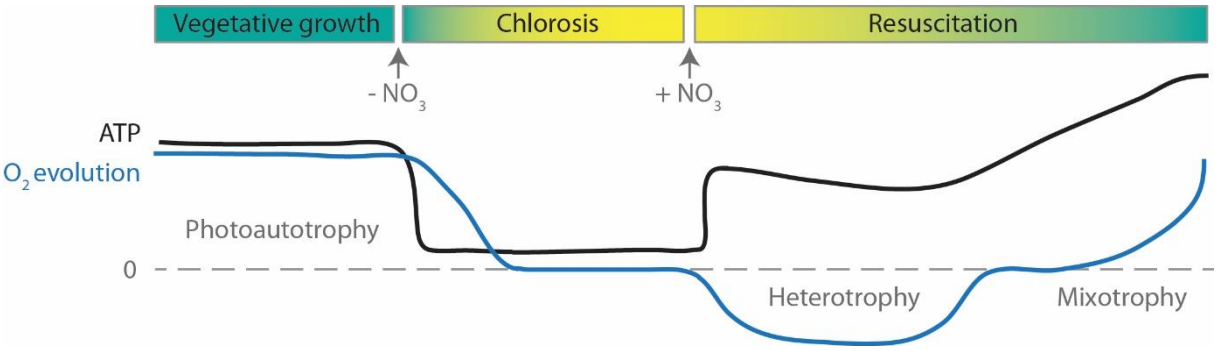

Figure 5. Scheme of the ATP and oxygen levels during nitrogen starvation-induced dormancy and awakening. Units are arbitrary.

1.2 ATP synthesis during chlorosis

As shown in **Figure 5**, the ATP content is kept at a constant low level during nitrogen starvation. Despite having a reduced metabolism, dormant cells still require energy for maintenance and chlorotic cells must ensure sufficient ATP synthesis to sustain viability. In *Synechocystis,* the majority of ATP is produced by the ATP synthases from ADP and inorganic phosphate in a reaction that typically requires an electrochemical proton gradient across the thylakoid membrane, which is generated by photosynthetic or respiratory electron transport.[17] However, nitrogen-starved cells degrade most of their thylakoid membranes during chlorosis, implying that the space for thylakoidal ATP synthases and proton storage is very limited.[69] Nevertheless, ATP synthases have also been found in the cytoplasmic membrane of *Synechocystis*,[86] suggesting that cells may utilize an extracellular electrochemical gradient to fuel the production of ATP. Since cyanobacteria preferably live in alkaline environments, importing protons from the extracellular medium into the cytoplasm to power ATP synthesis seems unlikely. Conversely, cells are exposed to an electrochemical sodium gradient, since the concentration of sodium in the cytoplasm is maintained at a lower level than the extracellular one. The experiments conducted in this work showed that chlorotic cells rely on a sodium motive force and not on a proton motive force to synthesize ATP. Increasing the sodium motive force by adding sodium chloride to chlorotic cells triggered ATP synthesis; the more sodium was added, the more ATP was

produced. Moreover, dissipating the sodium gradient or blocking sodium import inhibited ATP production, while dissolving the proton gradient did not affect it.[85]

The use of an electrochemical sodium gradient to drive ATP synthesis would only be possible if *Synechocystis* possessed an ATP synthase that is capable of binding sodium. As described above (*Section 2.3* of *Chapter IV*), ion specificity is determined in the c-ring in complex F_0. In *Synechocystis*, the c-ring is composed by 14 copies of the c subunit (AtpH).[87] Only one gene in *Synechocystis* encodes for AtpH, implying that the same c-ring should be able to bind protons and sodium. Comparison of the sequence of *Synechocystis*' AtpH with those from other organisms suggested that *Synechocystis* has indeed a promiscuous ATP synthase, since it contains some but not all the amino acids that confer sodium specificity.[85] The ATP synthase from *Methanosarcina acetivorans*, a methanogenic archaeon with an amino acid composition around the ion-binding site in the c-ring similar to *Synechocystis*, presents medium proton specificity but binds sodium physiologically because it is in excess.[32,85] Thus, according to this comparative analysis, the ATP synthases in the thylakoid membranes of *Synechocystis* are able to bind protons due to the high concentration of these ions in the thylakoid lumen, but the ATP synthases in the cytoplasmic membranes should be able to bind sodium ions because the proton concentration in the extracellular medium is too low. The ability to bind both ions allows dormant cells to adapt and survive to an environment where the classical ways to obtain energy are limited. Remarkably, this capacity seems to be exclusive of cyanobacterial strains adapted to high salt concentrations, whereas freshwater species, such as *Arthrospira platensis* and *Synechococcus elongatus,* have ATP synthases with high proton selectivity.[85] The capacity to use sodium for ATP production seems to be conserved by some organisms as an adaptation mechanism to environmental challenges.

1.3 ATP synthesis during resuscitation

The first measured response to the presence of nitrogen in dormant chlorotic cells is an increase in the ATP levels. During the awakening process, the demand of ATP dramatically increases due to the onset of anabolic reactions. Cells seem to respond to this increased energy requirement by immediately producing ATP. The presence of nitrogen is detected through the initiation of its assimilation via the GS-GOGAT cycle, since blocking these reactions abolishes the ATP increase. Inhibition of glycogen degradation and the respiratory terminal oxidases also suppressed the rise in ATP levels at the onset of resuscitation. Functionality of the GS-GOGAT cycle likely sends metabolic signals that trigger glycogen catabolism, which generates reduction equivalents that can be used by the respiratory chain to produce ATP. Given the low abundancy of thylakoid membranes in chlorotic cells and the fact that inhibition of cyt b_6f (which is exclusively found in the thylakoid membranes) did not affect ATP synthesis upon nitrate addition, this respiratory activity probably takes place at the cytoplasmic membrane. Nevertheless, given the alkaline pH of the extracellular medium, the protons exported from the cytoplasm by ARTO, the respiratory oxidase in the cytoplasmic membrane (see *Section 2.2* of *Chapter IV*), would dissipate into the bulk solution. Instead, the proton gradient could directly be

converted into a sodium gradient by neighboring sodium/protons antiporters. After translocation of a proton across the membrane, its diffusion to the aqueous solution is slightly retarded, because the membrane surface is separated from the bulk aqueous phase by an electrostatic barrier. Proton diffusion between closely located enzymes occurs in milliseconds,[88] meaning that the protons translocated by ARTO could be used by sodium/proton antiporters to convert the proton motive force into sodium motive force (**Figure 6**). The existence of such a mechanism is supported by the fact that NADH-II and sodium/proton antiporters are up-regulated in chlorotic cells.[72] This mechanism would allow extrusion of the sodium ions that are imported by the ATP synthases, which is necessary to avoid high concentrations of sodium in the cytoplasm.

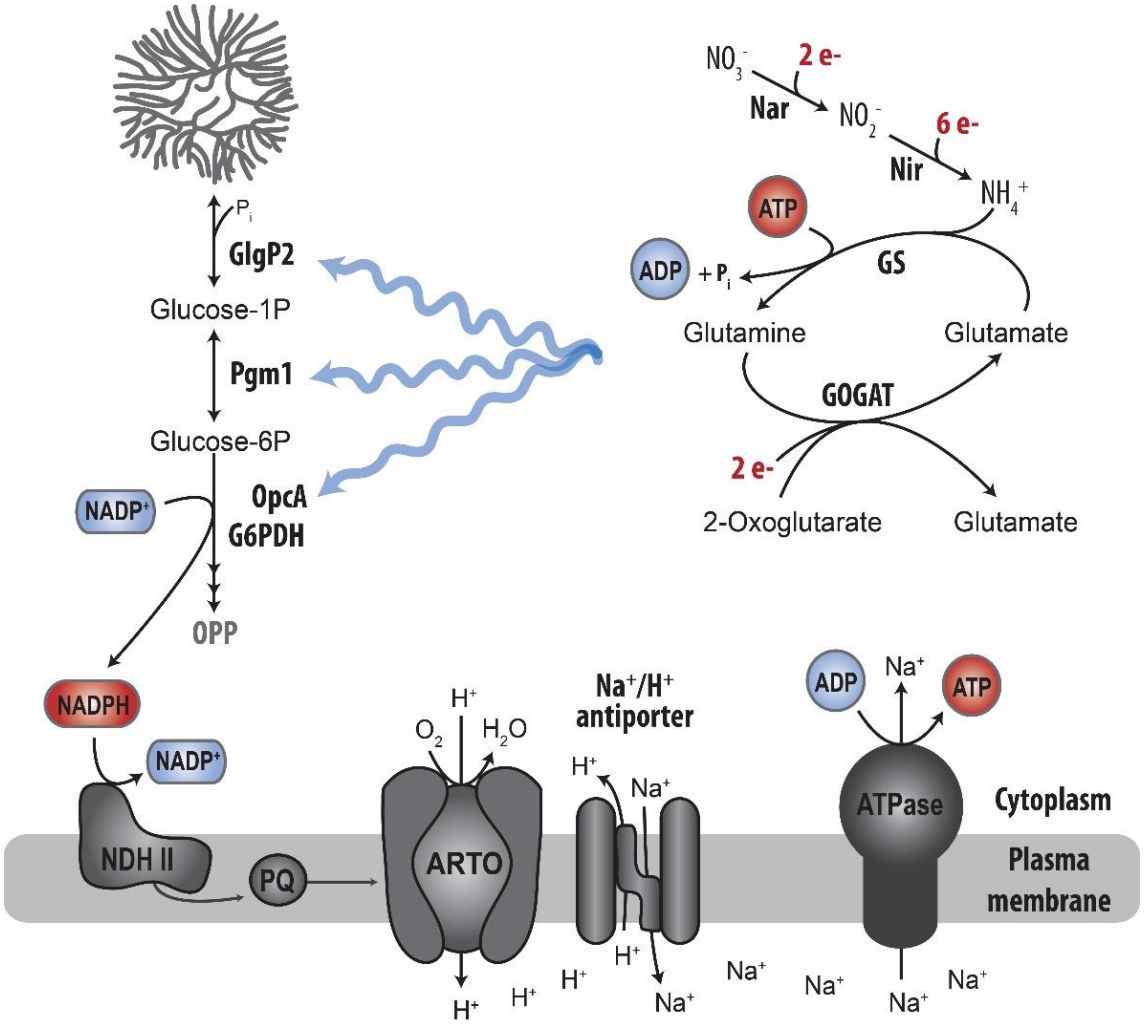

Figure 6. Model of the activation of glycogen catabolism and ATP generation during resuscitation.

1.4 Sodium bioenergetics in vegetative cells

Bioenergetics of *Synechocystis* dormant cells is largely based on sodium. Due to the reduced number of thylakoid membranes, chlorotic and resuscitating cells rely on the cytoplasmic ATP synthases to produce ATP using a sodium motive force. In vegetative cells with a full photosynthetic apparatus, ATP synthesis mainly takes place in the thylakoids. Hence, the lack of an electrochemical sodium gradient across the cytoplasmic membrane does not affect ATP synthesis during vegetative growth. However, sodium gradients are also involved in other processes, such as bicarbonate uptake. When vegetative cells are grown in the absence of sodium, their capability of importing carbon is partially impaired because the bicarbonate transporters SbtA and BicA depend on a sodium gradient. Sodium bioenergetics is thereby also important during vegetative growth, although vegetative cells do not require a sodium motive force to drive ATP synthesis. *Synechocystis* transiently employs a sodium motive force for energy generation as a survival strategy in response to adverse environmental conditions (**Figure 7**).

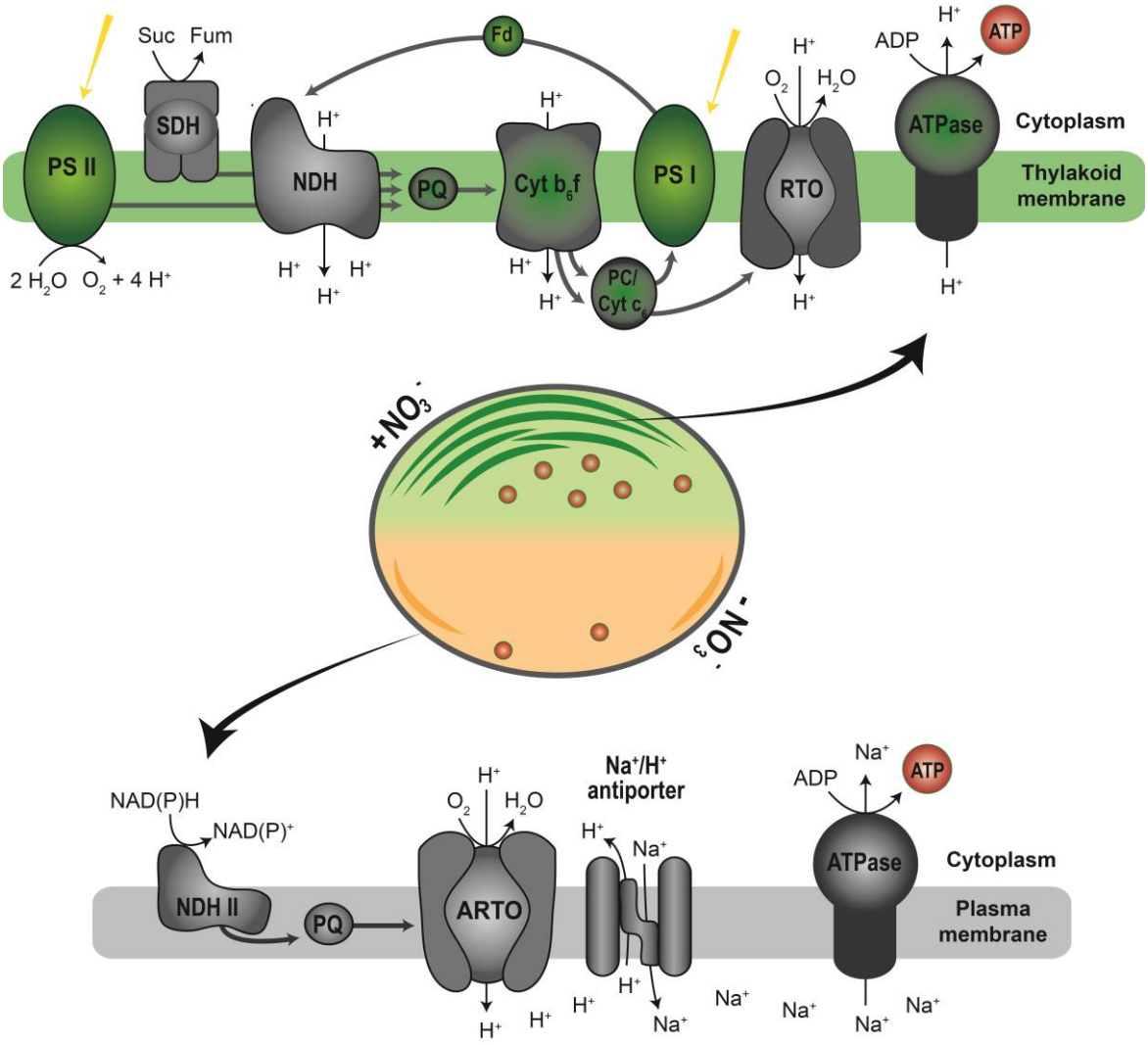

Figure 7. Mechanisms of ATP synthesis in vegetative (top) and chlorotic (bottom) cells. Photosynthetic components are shown in green, respiratory components in grey, and shared components in grey/green.

2. Carbon metabolism during nitrogen starvation and resuscitation

Glycogen accumulation and degradation are essential to overcome periods of nitrogen starvation. Glycogen synthesis is necessary for proper acclimation to nitrogen depletion; inhibition of glycogen synthesis creates a metabolic imbalance that leads to cell death. Glycogen catabolism provides cells with the required energy and metabolic intermediates to rebuild the previously degraded cellular components; inhibition of glycogen degradation renders cells incapable of resuming growth. Although the importance of glycogen in the survival to nitrogen depletion had been recognized before, the specific mechanisms involved in the metabolism of this polysaccharide had not been elucidated. The work presented here showed that only a specific strategy of glycogen synthesis and catabolism, which is subjected to a tight regulation, ensures survival during nitrogen deprivation.

2.1 Glycogen synthesis and degradation strategy

Inability to produce glycogen causes a characteristic non-bleaching phenotype: Cells do not degrade their photosynthetic pigments upon nitrogen depletion, but keep a green color for the first days, progressively looking paler until they lose viability. The molecular mechanism underlying this response is not known, but glycogen synthesis seems to contribute to energy balance, which appears to be essential for a proper acclimation response.[84] This non-bleaching phenotype was previously observed in mutants lacking GlgC and both GlgAs[12] and was confirmed in this study in a mutant lacking Pgm1[89]: All these strains were unable to accumulate glycogen and failed to carry out the chlorosis process. Intriguingly, although the single GlgA knockout mutants produced approximately the same amount of glycogen than the WT, the Δ*glgA1* strain showed a non-bleaching phenotype. The glycogen produced by GlgA2 does not seem to lead to a successful recovery, indicating that glycogen accumulation *per se* does not ensure survival of nitrogen-starved conditions.[41] Analysis of the structural differences between the glycogen contained in the WT, the Δ*glgA1*, and the Δ*glgA2* mutants revealed a different branching pattern in the different strains. Curiously, the glycogen from Δ*glgA1* was more similar to the WT glycogen than the one from Δ*glgA2*.[53] These results could be reproduced during the present work (data not shown) and denote that the different survival phenotypes observed for Δ*glgA1* and the Δ*glgA2* mutants do not originate from the different branching pattern of the granules produced by GlgA1 and GlgA2.

Glycogen catabolism during resuscitation from nitrogen starvation requires the action of GlgP2, whereas GlgP1 does not seem to play a role in this process.[80] The lack of glycogen degradation in the Δ*glgP2* mutant confirms that no other pathway can degrade glycogen. GlgP2 is also responsible for glycogen degradation during periods of darkness, while GlgP1 has only been shown to play a crucial role during heat stress conditions.[51] Although *Synechocystis* possesses two isoforms of most of the enzymes involved in glycogen metabolism, their functional divergence makes them play very distinct roles under different conditions. Additionally, successful resuscitation from nitrogen starvation involves functionality of the OPP and ED pathways.[80] Although the EMP pathway is energetically

more productive (i.e., more ATP is obtained), it does not produce all the metabolic intermediates that are necessary to rebuild all the previously degraded cellular components. Deletion of the EMP pathway seems thereby not to influence resuscitation. When cells begin the recovery process, they initially enter a heterotrophic phase in which they entirely rely on glycogen degradation. During this period, transcription and translation start taking place.[69] These processes require precursors for nucleic and amino acid synthesis. While the CBB cycle is not operating, riboses for RNA synthesis and erythrose-4-phosphate for the synthesis of aromatic compounds can only be obtained from the OPP pathway. In support to this, deletion of the OPP pathway results in the most severe phenotype.[80] Approximately 24 h after the start of resuscitation, cells start to regain photosynthetic activity and enter a mixotrophic phase, in which photosynthesis starts while glycogen degradation continues.[69] The CBB cycle is activated and the ED pathway is probably the most important glycolytic route, since it is the only one that does not share any reactions or intermediates with the CBB cycle.[10,80] In line with this, deletion of the ED pathway has a less severe impact on the efficiency of resuscitation than deletion of the OPP pathway.

2.2 Pgm1 as a metabolic valve that controls mobilization of glycogen stores

Synechocystis acts anticipatory and produces most of the enzymes required for glycogen catabolism already during nitrogen starvation, which allows an immediate response when nitrogen becomes available.[72,80] This implies that the activity of these enzymes must be carefully regulated to avoid premature glycogen degradation. This control is exerted via post-translational modification of Pgm1, the only glycogen related enzyme that follows a different expression pattern. During early chlorosis, Pgm1 activity is required for glycogen synthesis, as shown by the inability to accumulate glycogen of a *pgm1* deletion mutant. After the glycogen stores have been produced, Pgm1 activity is inhibited via phosphorylation at Ser 63. This residue is highly phosphorylated during nitrogen starvation, when Pgm1 must remain inactive to avoid glycogen degradation before a nitrogen source is available. When a non-phosphorylatable variant of Pgm1 (Pgm1-S63A) is present in chlorotic cells, glycogen degradation starts after prolonged nitrogen starvation, causing cells to lose viability, indicating that inactivation of Pgm1 via phosphorylation at Ser 63 is an essential control mechanism for survival of nitrogen-starved conditions. An *in vitro* analysis of a phosphomimetic variant of Pgm1 (Pgm1-S63D) supported the conclusion that the phosphorylated enzyme is inactive. Characterization of the variants Pgm1-S63A, -S63G, and -S63T showed that exchange of Ser 63 for any other amino acid has a negative impact on the reaction velocity but does not affect substrate affinity, since it did not cause the K_m to increase.[89] According to structural studies on related proteins, Ser 63 seems to be involved in a conformational change that converts the catalytic site from an open cleft to a closed pocket.[90] This change of conformation must happen during catalysis in order for the phosphate exchange to properly take place, which explains why any substitutions of Ser 63 negatively affects enzyme activity.[89,90] When this residue is phosphorylated, the negative charge of the phosphate group probably prevents this conformational change, inhibiting the reaction.

Remarkably, this regulatory mechanism seems to be conserved in humans. Regulation of glycogen metabolism is of great importance in organisms of all kingdoms of life. Pgm1 is an evolutionary conserved enzyme and a homologous phosphorylation site of Ser 63 in *Synechocystis* is also found in higher mammals. In humans, Pgm1 deficiency can cause severe disease, yet the functional regulation of this enzyme is poorly understood. Phosphorylation of human Pgm1 on Thr 466 is known to enhance its activity.[91] Ser 20, the homologous of *Synechocystis* Ser 63, had been identified as a phosphorylation site,[92] but the effect of phosphorylation of this residue on enzyme activity had so far not been elucidated. A study involving Pgm1 deficiency patients with mutations on the region of Pgm1 where Ser 20 is located showed that these mutations inhibited enzyme activity up to 96.7 % and caused moderate disease in heterozygote patients.[93] The present study showed that a phosphomimetic variant of human Pgm1 (S20D) is inactive *in vitro*, suggesting that regulation of Pgm1 activity via phosphorylation at this peripheral site is evolutionary conserved.[89]

2.3 Control of carbon flux into the different glycolytic routes in the developmental transitions of *Synechocystis*

Control of Pgm1 activity via phosphorylation at Ser 63 avoids premature degradation of the bulk of the glycogen stores. Nonetheless, residual glycogen catabolism takes place during chlorosis, as shown by the slight decrease in the glycogen content after prolonged nitrogen starvation.[41] This residual catabolic activity may be due to the presence of some dephosphorylated Pgm1 and is necessary to maintain the minimum ATP levels to keep viability in dormant cells. When an non-phosphorylatable Pgm1 is present, as in the strain WT+Pgm1S63A, larger amounts of glycogen are degraded during chlorosis, which leads to cell death.[89] The glucose-6P released by the catabolic reaction of Pgm1 encounters a branching point: It can be metabolized by Pgi and directed into the EMP pathway, or by G6PDH and led to the OPP and ED pathways. As discussed above, the OPP and ED pathways are utilized during resuscitation.[80] However, during nitrogen starvation, the products of glycogen degradation serve as precursors for PHB synthesis, and the main route involved in this conversion is the EMP pathway, the route with the highest ATP yield.[41] Hence, during chlorosis, G6PDH remains inactive and glucose-6P is metabolized by Pgi. Inactivation of G6PDH is achieved through redox control: Its activator protein, OpcA, is a Trx target and can only bind and activate G6PDH when it is in an oxidized state.[89] During chlorosis, the cytoplasm is in reduced conditions, since after cells are nitrogen-starved anabolic processes stop consuming reducing equivalents.[94] Under these circumstances, G6PDH is not activated by OpcA and glucose-6P is metabolized through the EMP pathway and leads to PHB production.

The physiological function of PHB remains enigmatic. In many bacteria, PHB serves as a carbon storage compound that accumulates during nutrient limitation.[95] In some organisms, such as *Arzospirillum brasiliense*, PHB confers tolerance against various environmental stresses, including heat, UV irradiation, desiccation, osmotic shock, and osmotic pressure.[96] A *Synechocystis* Δ*phaEC* mutant did not show any growth disadvantage

as compared to the WT when exposed to these conditions.[71] The fact that PHB is not metabolized when starved cells are transferred to nutrient-rich medium suggests that this polymer does not serve as a reserve compound.[97] A role of PHB as an electron sink to protect against redox stress has been proposed, since its synthesis requires NADPH.[71] The fact that the EMP pathway is the main route involved in PHB synthesis supports this idea: In contrast to the ED and OPP pathways, no NADPH is produced via the EMP pathway, which generates ATP and NADH. During chlorosis, when NADPH production is not desirable, a residual carbon flux from the glycogen pool through the EMP pathway to produce PHB might be beneficial to produce ATP and consume NADPH.

At the onset of resuscitation, functionality of the OPP and ED pathways is required, and G6PDH must be activated.[80] Upon availability of a nitrogen source, the nitrogen assimilatory reactions begin to consume electrons: The reactions catalyzed by the nitrate reductase, nitrate reductase and GOGAT consume a total of 10 electrons. As a consequence, the cytoplasm is oxidized, which enables the activation of G6PDH by OpcA.[89] However, Pgi is upregulated in the early stages of resuscitation, implying that glucose-6P could still be metabolized via the EMP pathway.[72,80] The data derived from the characterization of the different glycolytic mutants strongly suggest that there is a switch in the carbon flux from the EMP to the ED and OPP pathways upon addition of a nitrogen source to chlorotic cells, implying the existence of a mechanism to regulate which enzyme metabolizes glucose-6P.

OpcA-G6PDH were found to form a complex with Pgm1.[89] Interaction between sequential metabolic enzymes at a branch point in a metabolic network has been observed in other pathways, including the TCA cycle, glycolysis and fatty acid biosynthesis. Formation of these complexes, known as metabolons, is thought to allow substrate channeling between two enzymes to avoid the use of a metabolite by a competing enzyme. However, the functional significance of metabolon formation has not yet been fully clarified.[98] Substrate channeling requires that the product of one enzyme is passed as substrate to the next one, thereby preventing its diffusion into the bulk solvent. In the case of the TCA cycle, which might constitute the best-studied example of interaction between sequential metabolic enzymes, there is convincing evidence that metabolites are channeled, but the exact mechanism of substrate transfer and its role in metabolic flux control have not been completely elucidated.[99] The Pgm1-OpcA-G6PDH complex may act as a metabolon to ensure channeling of glucose-6P into the OPP and ED pathways and prevent its metabolization through the EMP pathway, thereby controlling the carbon flux into the glycolytic routes. *In vitro* complex formation was only observed under oxidizing conditions and when Pgm1 was dephosphorylated, suggesting that the metabolon is only formed during resuscitation, when Pgm1 and G6PDH are activated and operation of the OPP and ED pathways is needed.[89] The Pgm1-OpcA-G6PDH complex is thereby probably also relevant in the transition from light to darkness, when these pathways are also utilized. Formation of such a metabolon would allow tight regulation of the carbon flux into the different metabolic routes, which is of exceptional importance to ensure survival in a fluctuating environment. Even though structural and functional evidence of the Pgm1-OpcA-G6PDH complex behaving as a metabolon is still lacking, the data presented here

strongly support its role in substrate channeling, although elucidation of the structure of the complex combined with enzyme kinetic and isotope labeling experiments would be necessary to confirm it. The model of the regulation of the activation of glycogen degradation during resuscitation is depicted in **Figure 8**.

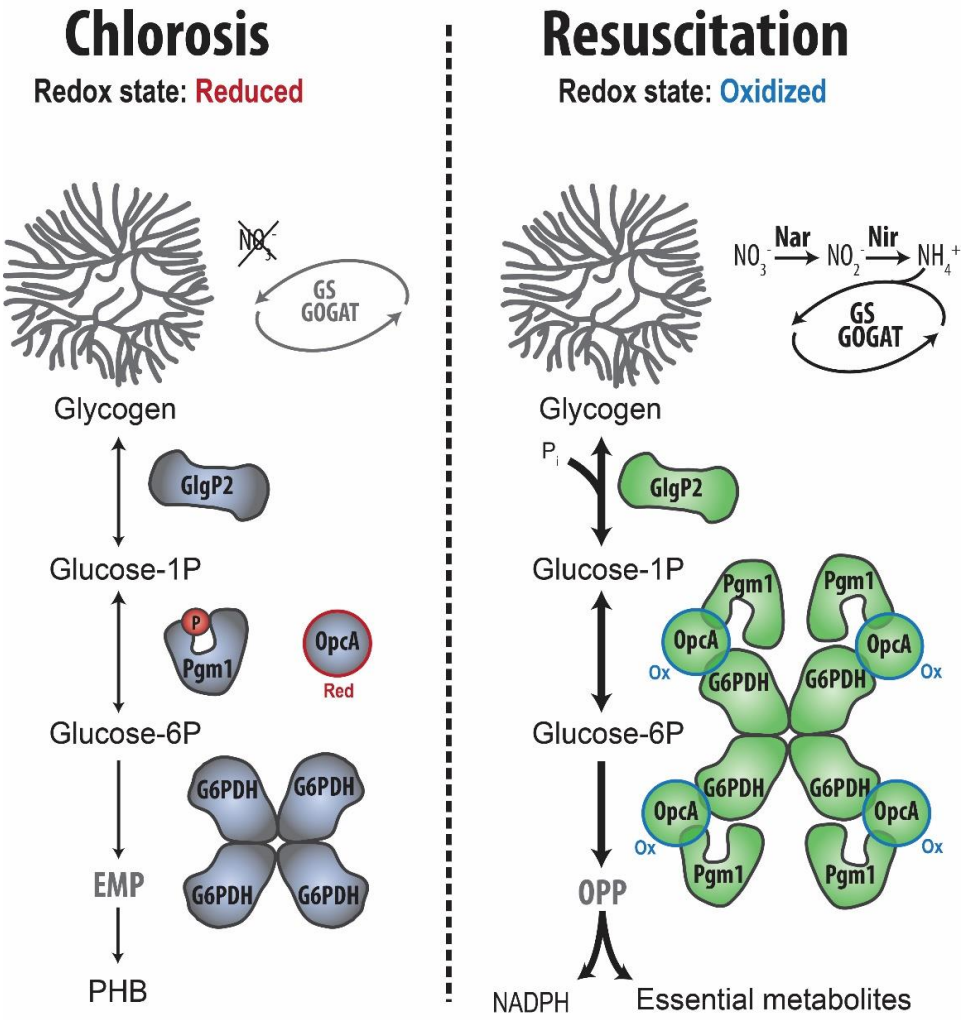

Figure 8. Model of the activation of glycogen catabolism during resuscitation and the control of the carbon flux into the glycolytic routes.

3. Conclusions

This work shed light on the molecular mechanisms underlying the metabolic switch that takes place during awakening from the metabolic dormancy induced by nitrogen starvation in *Synechocystis*. The mechanisms of energy generation during chlorosis and resuscitation were elucidated. This knowledge increases our understanding of the regulation of energy homeostasis during bacterial dormancy, an issue of high relevance in the maintenance of bacterial biodiversity, the spread of pathogens and the development of antibiotic resistances. How widespread the ability to employ sodium-dependent ATP synthesis to survive periods of unfavorable environmental conditions is among bacteria remains an open question. Furthermore, this study unraveled how the control of the utilization of the glycogen reserves is exerted, a matter of great importance in organisms of all kingdoms of life. The pathways that are used in each phase of the transition into and out of the dormant state were clarified, additionally offering a hint of how carbon flux into the different glycolytic routes might be controlled. Nonetheless, to prove the existence of a mechanism of substrate channeling between the glycogen degrading enzymes and its effect in metabolic control, further efforts will be necessary.

VII. REFERENCES

1. Schirrmeister, B. E., Sanchez-Baracaldo, P. & Wacey, D. Cyanobacterial evolution during the Precambrian. *Int. J. Astrobiol.* **15**, 187–204 (2016).
2. Komarek, J., Kastovsky, J., Mares, J. & Johansen, J. R. Taxonomic classification of cyanoprokaryotes (cyanobacterial genera) 2014, using a polyphasic approach. *Preslia* 295–335 (2014). doi:10.1353/ctt.0.0006
3. Blankenship, R. E. How Cyanobacteria went green. *Science (80-.).* **355**, 1372–1374 (2017).
4. Houmard, J. How Do Cyanobacteria Perceive and Adjust to Their Environment? in *Molecular Ecology of Aquatic Microbes* (ed. Joint, I.) 153–170 (Springer Berlin Heidelberg, 1995).
5. Durall, C. & Lindblad, P. Mechanisms of carbon fixation and engineering for increased carbon fixation in cyanobacteria. *Algal Res.* **11**, 263–270 (2015).
6. Rippka, R., Deruelles, J., Waterbury, J. B., Herdman, M. & Stanier, R. Y. Generic Assignments, Strain Histories and Properties of Pure Cultures of Cyanobacteria. *Microbiology* **111**, 1–61 (1979).
7. Zavřel, T., Očenášová, P. & Červený, J. Phenotypic characterization of Synechocystis sp. PCC 6803 substrains reveals differences in sensitivity to abiotic stress. *PLoS One* **12**, 1–21 (2017).
8. Iijima, H., Nakaya, Y., Kuwahara, A., Hirai, M. Y. & Osanai, T. Seawater cultivation of freshwater cyanobacterium Synechocystis sp. PCC 6803 drastically alters amino acid composition and glycogen metabolism. *Front. Microbiol.* **6**, 1–10 (2015).
9. Ikeuchi, M. & Tabata, S. Synechocystis sp. PCC 6803 – a useful tool in the study of the genetics of cyanobacteria. *Photosynth. Res.* 73–83 (2001).
10. Chen, X. *et al.* The Entner–Doudoroff pathway is an overlooked glycolytic route in cyanobacteria and plants. *Proc. Natl. Acad. Sci.* **113**, 5441–5446 (2016).
11. Forchhammer, K. & Schwarz, R. Nitrogen chlorosis in unicellular cyanobacteria – a developmental program for surviving nitrogen deprivation. *Environ. Microbiol.* **21**, 1173–1184 (2019).
12. Gründel, M., Scheunemann, R., Lockau, W. & Zilliges, Y. Impaired glycogen synthesis causes metabolic overflow reactions and affects stress responses in the cyanobacterium Synechocystis sp. PCC 6803. *Microbiol. (United Kingdom)* **158**, 3032–3043 (2012).
13. Schlebusch, M. & Forchhammer, K. Requirement of the nitrogen starvation-induced protein s110783 for polyhydroxybutyrate accumulation in synechocystis sp. strain PCC 6803. *Appl. Environ. Microbiol.* **76**, 6101–6107 (2010).
14. Watzer, B. *et al.* Metabolic pathway engineering using the central signal processor PII. *Microb. Cell Fact.* **14**, 1–12 (2015).

15. Baers, L. L. *et al.* Proteome mapping of a cyanobacterium reveals distinct compartment organization and cell-dispersed metabolism. *Plant Physiol.* **181**, 1721–1738 (2019).

16. Westermark, S. & Steuer, R. Toward multiscale models of cyanobacterial growth: A modular approach. *Front. Bioeng. Biotechnol.* **4**, 1–24 (2016).

17. Imashimizu, M. *et al.* Regulation of F0F1-ATPase from Synechocystis sp. PCC 6803 by γ and ε subunits is significant for light/dark adaptation. *J. Biol. Chem.* **286**, 26595–26602 (2011).

18. Bryant, D. A. & Frigaard, N. U. Prokaryotic photosynthesis and phototrophy illuminated. *Trends Microbiol.* **14**, 488–496 (2006).

19. Singh, N. K., Sonani, R. R., Prasad Rastogi, R. & Madamwar, D. The phycobilisomes: An early requisite for efficient photosynthesis in cyanobacteria. *EXCLI J.* **14**, 268–289 (2015).

20. Pagels, F., Guedes, A. C., Amaro, H. M., Kijjoa, A. & Vasconcelos, V. Phycobiliproteins from cyanobacteria: Chemistry and biotechnological applications. *Biotechnology Advances* **37**, 422–443 (2019).

21. Shevela, D., Björn, L. O. & Govindjee. *Photosynthesis: Solar Energy for Life*. (World Scientific Publishing, 2018). doi:https://doi.org/10.1142/10522

22. Hervás, M., Navarro, J. A. & De La Rosa, M. A. Electron Transfer between Membrane Complexes and Soluble Proteins in Photosynthesis. *Acc. Chem. Res.* **36**, 798–805 (2003).

23. Lea-Smith, D. J., Bombelli, P., Vasudevan, R. & Howe, C. J. Photosynthetic, respiratory and extracellular electron transport pathways in cyanobacteria. *Biochim. Biophys. Acta - Bioenerg.* **1857**, 247–255 (2016).

24. Yamori, W., Makino, A. & Shikanai, T. A physiological role of cyclic electron transport around photosystem I in sustaining photosynthesis under fluctuating light in rice OPEN. *Nat. Publ. Gr.* (2016). doi:10.1038/srep20147

25. Hart, S. E., Schlarb-Ridley, B. G., Bendall, D. S. & Howe, C. J. Terminal oxidases of cyanobacteria. *Biochem. Soc. Trans.* **33**, 832–835 (2005).

26. Huang, F. *et al.* Proteomics of Synechocystis sp. strain PCC 6803: identification of plasma membrane proteins. *Mol. Cell. Proteomics* **1**, 956–966 (2002).

27. Schultze, M. *et al.* Localization of cytochrome b6f complexes implies an incomplete respiratory chain in cytoplasmic membranes of the cyanobacterium Synechocystis sp. PCC 6803. *Biochim. Biophys. Acta - Bioenerg.* **1787**, 1479–1485 (2009).

28. Pils, D. & Schmetterer, G. Characterization of three bioenergetically active respiratory terminal oxidases in the cyanobacterium Synechocystis sp. strain PCC 6803. *FEMS Microbiol. Lett.* **203**, 217–222 (2001).

29. Deckers-hebestreit, G. & Altendorf, K. THE F 0 F 1 -TYPE ATP SYNTHASES OF BACTERIA : Structure and Function of the F 0 Complex. 791–824 (1996).

30. Leone, V., Pogoryelov, D., Meier, T. & Faraldo-Gómez, J. D. On the principle of ion selectivity in Na+/H+-coupled membrane proteins: Experimental and

theoretical studies of an ATP synthase rotor. *Proc. Natl. Acad. Sci. U. S. A.* **112**, E1057–E1066 (2015).

31. Schulz, S. *et al.* A New Type of Na+-Driven ATP Synthase Membrane Rotor with a Two-Carboxylate Ion-Coupling Motif. *PLoS Biol.* **11**, (2013).

32. Schlegel, K., Leone, V., Faraldo-Gómez, J. D. & Müller, V. Promiscuous archaeal ATP synthase concurrently coupled to Na + and H + translocation. *Proc. Natl. Acad. Sci. U. S. A.* **109**, 947–952 (2012).

33. Mulkidjanian, A. Y., Galperin, M. Y., Makarova, K. S., Wolf, Y. I. & Koonin, E. V. Evolutionary primacy of sodium bioenergetics. *Biol. Direct* **3**, 1–19 (2008).

34. Trebst, A. Inhibitors in the functional dissection of the photosynthetic electron transport system. *Photosynth. Res.* **92**, 217–224 (2007).

35. Pansook, S., Incharoensakdi, A. & Phunpruch, S. Effects of the Photosystem II Inhibitors CCCP and DCMU on Hydrogen Production by the Unicellular Halotolerant Cyanobacterium Aphanothece halophytica. *Sci. World J.* **2019**, (2019).

36. Teuber, M., Rögner, M. & Berry, S. Fluorescent probes for non-invasive bioenergetic studies of whole cyanobacterial cells. *Biochim. Biophys. Acta - Bioenerg.* **1506**, 31–46 (2001).

37. Ikeuchi, M. & Tabata, S. Synechocystis sp. PCC 6803 – a useful tool in the study of the genetics of cyanobacteria. *Photosynth. Res.* **70**, 73–83 (2001).

38. Hong, S. & Pedersen, P. L. ATP Synthase and the Actions of Inhibitors Utilized To Study Its Roles in Human Health, Disease, and Other Scientific Areas. *Microbiol. Mol. Biol. Rev.* **72**, 590–641 (2008).

39. Müller, V., Aufurth, S. & Rahlfs, S. The Na+ cycle in Acetobacterium woodii: Identification and characterization of a Na+ translocating F1F0-ATPase with a mixed oligomer of 8 and 16 kDa proteolipids. *Biochim. Biophys. Acta - Bioenerg.* **1505**, 108–120 (2001).

40. Saha, R. *et al.* Diurnal Regulation of Cellular Processes in the Cyanobacterium Synechocystis sp. Strain PCC 6803: Insights from Transcriptomic, Fluxomic, and Physiological Analyses. *MBio* **7**, 1–14 (2016).

41. Koch, M., Doello, S., Gutekunst, K. & Forchhammer, K. PHB is produced from Glycogen turn-over during nitrogen starvation in Synechocystis sp. PCC 6803. *Int. J. Mol. Sci.* **20**, 1–14 (2019).

42. Hagemann, M., Eisenhut, M., Hackenberg, C. & Bauwe, H. Pathway and importance of photorespiratory 2-phosphoglycolate metabolism in cyanobacteria. *Adv. Exp. Med. Biol.* **675**, 91–108 (2010).

43. Badger, M. R. & Price, G. D. CO2 concentrating mechanisms in cyanobacteria: Molecular components, their diversity and evolution. *J. Exp. Bot.* **54**, 609–622 (2003).

44. Scholl, J., Dengler, L., Bader, L. & Forchhammer, K. Phosphoenolpyruvate carboxylase from the cyanobacterium Synechocystis sp. PCC 6803 is under global metabolic control by PII signaling. *Mol. Microbiol.* **114**, 292–307 (2020).

45. Preiss, J. Bacterial glycogen synthesis and its regulation. *Annu. Rev. Microbiol.* 419–458 (1984).

46. Zilliges, Y. Glycogen, a dynamic cellular sink and reservoir for carbon. in *Cell Biology of Cyanobacteria* (ed. Flores, E.) (Caister Academic Press, 2014).

47. Klotz, A. & Forchhammer, K. Glycogen, a major player for bacterial survival and awakening from dormancy. *Future Microbiol.* **12**, 101–104 (2017).

48. Díaz-Troya, S., Roldán, M., Mallén-Ponce, M. J., Ortega-Martínez, P. & Florencio, F. J. Lethality caused by ADP-glucose accumulation is suppressed by salt-induced carbon flux redirection in cyanobacteria. *J. Exp. Bot.* **71**, 2005–2017 (2020).

49. Preiss, J. & Romeo, T. Molecular biology and regulatory aspects of glycogen biosynthesis in bacteria. *Prog. Nucleic Acid Res. Mol. Biol.* **47**, 299–329 (1994).

50. Kobayashi, T. *et al.* Comparison of chain-length preferences and glucan specificities of isoamylase-type α-glucan debranching enzymes from rice, cyanobacteria, and bacteria. *PLoS One* **11**, 1–21 (2016).

51. Fu, J. & Xu, X. The functional divergence of two glgP homologues in Synechocystis sp. PCC 6803. *FEMS Microbiol. Lett.* **260**, 201–209 (2006).

52. Liu, L., Hu, H. H., Gao, H. & Xu, X. D. Role of two phosphohexomutase genes in glycogen synthesis in Synechocystis sp. PCC6803. *Chinese Sci. Bull.* **58**, 4616–4621 (2013).

53. Yoo, S. H., Lee, B. H., Moon, Y., Spalding, M. H. & Jane, J. L. Glycogen synthase isoforms in synechocystis sp. PCC6803: Identification of different roles to produce glycogen by targeted mutagenesis. *PLoS One* **9**, (2014).

54. Mills, L. A., McCormick, A. J. & Lea-Smith, D. J. Current knowledge and recent advances in understanding metabolism of the model cyanobacterium Synechocystis sp. PCC 6803. *Biosci. Rep.* **40**, 1–33 (2020).

55. Beck, C., Knoop, H., Axmann, I. M. & Steuer, R. The diversity of cyanobacterial metabolism: Genome analysis of multiple phototrophic microorganisms. *BMC Genomics* **13**, 1–17 (2012).

56. Hauf, W., Watzer, B., Roos, N., Klotz, A. & Forchhammer, K. Photoautotrophic polyhydroxybutyrate granule formation is regulated by cyanobacterial phasin PhaP in Synechocystis sp. strain PCC 6803. *Appl. Environ. Microbiol.* **81**, 4411–4422 (2015).

57. Koch, M. *et al.* Maximizing PHB content in Synechocystis sp. PCC 6803: a new metabolic engineering strategy based on the regulator PirC. *Microb. Cell Fact.* **19**, 1–12 (2020).

58. Makowka, A. *et al.* Glycolytic shunts replenish the Calvin-Benson-Bassham cycle as anaplerotic reactions in Cyanobacteria. *Mol. Plant* **13**, 471–482 (2020).

59. Vitousek, P. M. & Howarth, R. W. Nitrogen limitation on land and sea: How can it occur? *Biogeochemistry* **13**, 87–115 (1990).

60. Flores, E. & Herrero, A. Nitrogen assimilation and nitrogen control in cyanobacteria. *Biochem. Soc. Trans.* **33**, 164–167 (2005).

61. Watzer, B. *et al.* The signal transduction protein PII controls ammonium, nitrate and urea uptake in cyanobacteria. *Front. Microbiol.* **10**, 1–20 (2019).

62. Bolay, P., Muro-Pastor, M. I., Florencio, F. J. & Klähn, S. The distinctive regulation of cyanobacterial glutamine synthetase. *Life* **8**, 1–21 (2018).

63. Zhang, C. C., Zhou, C. Z., Burnap, R. L. & Peng, L. Carbon/Nitrogen Metabolic Balance: Lessons from Cyanobacteria. *Trends Plant Sci.* **23**, 1116–1130 (2018).

64. Espinosa, J., Forchhammer, K. & Contreras, A. Role of the Synechococcus PCC 7942 nitrogen regulator protein PipX in NtcA-controlled processes. *Microbiology* **153**, 711–718 (2007).

65. Llácer, J. L. *et al.* Structural basis for the regulation of NtcA-dependent transcription by proteins PipX and PII. *Proc. Natl. Acad. Sci. U. S. A.* **107**, 15397–15402 (2010).

66. Klotz, A., Reinhold, E., Doello, S. & Forchhammer, K. Nitrogen Starvation Acclimation in Synechococcus elongatus: Redox-Control and the Role of Nitrate Reduction as an Electron Sink. *Life* **5**, 888–904 (2015).

67. Allen, M. M. & Smith, A. J. Nitrogen chlorosis in blue-green algae. *Arch. Mikrobiol.* **69**, 114–120 (1969).

68. Orthwein, T. *et al.* The Novel PII-Interacting Regulator PirC (Sll0944) Identifies 3-Phosphoglycerate Mutase (PGAM) as Central Control Point of Carbon Storage Metabolism in Cyanobacteria. *bioRxiv* **292599**, (2020).

69. Klotz, A. *et al.* Awakening of a Dormant Cyanobacterium from Nitrogen Chlorosis Reveals a Genetically Determined Program. *Curr. Biol.* **26**, 2862–2872 (2016).

70. Damrow, R., Maldener, I. & Zilliges, Y. The multiple functions of common microbial carbon polymers, glycogen and PHB, during stress responses in the non-diazotrophic cyanobacterium synechocystis sp. PCC 6803. *Front. Microbiol.* **7**, 1–10 (2016).

71. Koch, M., Berendzen, K. W. & Forchhammer, K. On the role and production of polyhydroxybutyrate (Phb) in the cyanobacterium synechocystis sp. pcc 6803. *Life* **10**, (2020).

72. Spät, P., Klotz, A., Rexroth, S., Maček, B. & Forchhammer, K. Chlorosis as a Developmental Program in Cyanobacteria: The Proteomic Fundament for Survival and Awakening. *Mol. Cell. Proteomics* **17**, 1650–1669 (2018).

73. Rittershaus, E., Baek, S. & Sassetti, C. The normalcy of dormancy. *Cell Host Microbe* **13**, 643–651 (2013).

74. Burnap, R. L., Hagemann, M. & Kaplan, A. Regulation of CO2 concentrating mechanism in cyanobacteria. *Life* **5**, 348–371 (2015).

75. Velmurugan, R. & Incharoensakdi, A. Disruption of polyhydroxybutyrate synthesis redirects carbon flow towards glycogen synthesis in synechocystis sp. PCC 6803 Overexpressing glgC/glgA. *Plant Cell Physiol.* **59**, 2020–2029 (2018).

76. Spät, P., Klotz, A., Rexroth, S., Maček, B. & Forchhammer, K. Chlorosis as a developmental program in cyanobacteria: The proteomic fundament for survival and awakening. *Mol. Cell. Proteomics* **17**, 1650–1669 (2018).

77. Lee, Y., Stiers, K. M., Kain, B. N. & Beamer, L. J. Compromised catalysis and potential folding defects in in vitro studies of missense mutants associated with hereditary phosphoglucomutase 1 deficiency. *J. Biol. Chem.* **289**, 32010–32019 (2014).

78. Greening, C., Grinter, R. & Chiri, E. Uncovering the Metabolic Strategies of the Dormant Microbial Majority: towards Integrative Approaches. *mSystems* **4**, 1–5 (2019).

79. Lewis, K. Persister Cells. *Annu. Rev. Microbiol.* **64**, 357–372 (2010).

80. Doello, S., Klotz, A., Makowka, A., Gutekunst, K. & Forchhammer, K. A specific glycogen mobilization strategy enables rapid awakening of dormant cyanobacteria from chlorosis. *Plant Physiol.* **177**, 594–603 (2018).

81. Patel, A. *et al.* ATP as a biological hydrotrope. *Science (80-.).* **356**, 753–756 (2017).

82. Parry, B. R. *et al.* The bacterial cytoplasm has glass-like properties and is fluidized by metabolic activity. *Cell* **156**, 183–194 (2014).

83. Pu, Y. *et al.* ATP-Dependent Dynamic Protein Aggregation Regulates Bacterial Dormancy Depth Critical for Antibiotic Tolerance. *Mol. Cell* **73**, 143-156.e4 (2019).

84. Cano, M. *et al.* Glycogen Synthesis and Metabolite Overflow Contribute to Energy Balancing in Cyanobacteria. *Cell Rep.* **23**, 667–672 (2018).

85. Doello, S., Burkhardt, M. & Forchhammer, K. The essential role of sodium bioenergetics and ATP homeostasis in the developmental transitions of a cyanobacterium. *Curr. Biol.* **31**, 1–10 (2021).

86. Huang, F. *et al.* Proteomics of Synechocystis sp. strain PCC 6803: identification of plasma membrane proteins. *Mol. Cell. Proteomics* **1**, 956–966 (2002).

87. Pogoryelov, D. *et al.* The oligomeric state of c rings from cyanobacterial F-ATP synthases varies from 13 to 15. *J. Bacteriol.* **189**, 5895–5902 (2007).

88. Mulkidjanian, A. Y., Heberle, J. & Cherepanov, D. A. Protons @ interfaces: Implications for biological energy conversion. *Biochim. Biophys. Acta - Bioenerg.* **1757**, 913–930 (2006).

89. Doello, S., Neumann, N., Spät, P., Maček, B. & Forchhammer, K. Regulatory phosphorylation site tunes Phosphoglucomutase 1 as a metabolic valve to control mobilization of glycogen stores . (2021). doi:https://doi.org/10.1101/2021.04.15.439997

90. Müller, S. *et al.* Crystal structure analysis of the exocytosis-sensitive phosphoprotein, pp63/parafusin (phosphoglucomutase), from paramecium reveals significant conformational variability. *J. Mol. Biol.* **315**, 141–153 (2002).

91. Gururaj, A., Barnes, C. J., Vadlamudi, R. K. & Kumar, R. Regulation of phosphoglucomutase 1 phosphorylation and activity by a signaling kinase. *Oncogene* **23**, 8118–8127 (2004).

92. Bian, Y. *et al.* An enzyme assisted RP-RPLC approach for in-depth analysis of human liver phosphoproteome. *J. Proteomics* **96**, 253–262 (2014).

93. Beamer, L. J. Mutations in hereditary phosphoglucomutase 1 deficiency map to key regions of enzyme structure and function. *J. Inherit. Metab. Dis.* **38**, 243–256 (2015).

94. Hauf, W. *et al.* Metabolic changes in Synechocystis PCC6803 upon nitrogen-starvation: Excess NADPH sustains polyhydroxybutyrate accumulation. *Metabolites* **3**, 101–118 (2013).

95. Anderson, A. J. & Dawes, E. A. Occurrence, metabolism, metabolic role, and industrial uses of bacterial polyhydroxyalkanoates. *Microbiol. Rev.* **54**, 450 LP – 472 (1990).

96. Kadouri, D., Jurkevitch, E. & Okon, Y. Involvement of the Reserve Material Poly-β-Hydroxybutyrate in Azospirillum brasilense Stress Endurance and Root Colonization. *Appl. Environ. Microbiol.* **69**, 3244 LP – 3250 (2003).

97. Koch, M., Orthwein, T., Alford, J. T. & Forchhammer, K. The Slr0058 Protein From Synechocystis sp. PCC 6803 Is a Novel Regulatory Protein Involved in PHB Granule Formation. *Front. Microbiol.* **11**, 1–13 (2020).

98. Sweetlove, L. J. & Fernie, A. R. The role of dynamic enzyme assemblies and substrate channelling in metabolic regulation. *Nat. Commun.* **9**, 2136 (2018).

99. Zhang, Y. *et al.* Protein-protein interactions and metabolite channelling in the plant tricarboxylic acid cycle. *Nat. Commun.* **8**, 15212 (2017).

VIII. APPENDIX

1. Publication 1 (Accepted)

Research article

Sofía Doello, Alexander Klotz, Alexander Makowka, Kirstin Gutekunst, and Karl Forchhammer

A specific glycogen mobilization strategy enables rapid awakening of dormant cyanobacteria from chlorosis.

2018. *Plant Physiology*. 177, 594–603

A Specific Glycogen Mobilization Strategy Enables Rapid Awakening of Dormant Cyanobacteria from Chlorosis[1]

Sofia Doello,[a,2] Alexander Klotz,[a,2] Alexander Makowka,[b] Kirstin Gutekunst,[b] and Karl Forchhammer[a,3]

[a]University of Tübingen, Interfaculty Institute of Microbiology and Infection Medicine Tübingen, 72076 Tübingen, Germany

[b]Christian-Albrechts-University, Department of Biology, Botanical Institute, 24118 Kiel, Germany

ORCID IDs: 0000-0002-4025-3016 (S.D.); 0000-0003-4666-8607 (A.K.); 0000-0003-3199-8101 (K.F.)

Many organisms survive stressful conditions via entry into a dormant state that can be rapidly exited when the stressor disappears; this ability provides a strong selective advantage. In the cyanobacterium *Synechocystis* sp. PCC 6803, the exit from nitrogen chlorosis takes less than 48 h and is enabled by the impressive metabolic flexibility of these cyanobacteria, which pass through heterotrophic and mixotrophic phases before reentering photoautotrophic growth. Switching between these states requires delicate coordination of carbohydrate oxidation, CO_2 fixation, and photosynthesis. Here, we investigated the contribution of the different carbon catabolic routes by assessing mutants of these pathways during nitrogen chlorosis and resuscitation. The addition of nitrate to nitrogen-starved cells rapidly starts the awakening program. Metabolism switches from maintenance metabolism, characterized by residual photosynthesis and low cellular ATP levels, to an initial heterotrophic phase, characterized by respiration and an immediate increase in ATP levels. This respiration relies on glycogen breakdown catalyzed by the glycogen phosphorylase GlgP2. In the following transient mixotrophic phase, photosynthesis and CO_2 fixation restart and glycogen is consumed. During the mixotrophic phase, parallel operation of the oxidative pentose phosphate cycle and the Entner-Doudoroff pathway is required for resuscitation to proceed; the glycolytic route via the Embden-Meyerhof-Parnas pathway has minor importance. Our data suggest that, during resuscitation, only the Entner-Doudoroff and oxidative pentose phosphate pathways supply the metabolic intermediates necessary for the anabolic reactions required to reconstitute a vegetative cell. Intriguingly, the key enzymes for glycogen catabolism are already expressed during the preceding chlorotic phase, in apparent preparation for rapid resuscitation.

Cyanobacteria are oxygenic photoautotrophic organisms adapted to a wide range of environments (Stanier and Cohen-Bazire, 1977). Nitrogen shortage represents one of the most common growth limitations in terrestrial and marine ecosystems (Vitousek and Howarth, 1991). Nondiazotrophic cyanobacteria, including *Synechocystis* sp. PCC 6803 (hereafter *Synechocystis*), respond to the lack of a usable nitrogen source by undergoing a process called chlorosis (Allen and Smith, 1969; Luque and Forchhammer, 2008). This adaptation mechanism is characterized by the degradation of photosynthetic pigments, which causes cells to turn from a blue-green to a yellow color. During chlorosis, the cells divide one more time and then enter cell cycle arrest, where they degrade the bulk of cellular proteins and the photosynthetic apparatus, leaving only residual photosynthetic activity. Additionally, they tune down their metabolism by minimizing energy-consuming reactions, such as protein synthesis and anabolic processes. These molecular adaptations lead the cells into a dormant state that allows them to survive for a long period of time (Görl et al., 1998; Sauer et al., 2001). The energy produced by the residual photosynthetic activity seems to be sufficient to keep cells alive, since they consume almost no ATP. Furthermore, chlorotic cells rapidly accumulate reserve polymers, including glycogen and polyhydroxybutyrate (PHB; Sauer et al., 2001; Schlebusch and Forchhammer, 2010).

Synechocystis is capable of rapidly recovering from chlorosis when a usable nitrogen source becomes available (Klotz et al., 2016). The resuscitation process occurs in two major phases. First, the energy necessary to reinstall central cellular processes is rapidly provided by carbohydrate oxidation and respiration. Second, phase 2 starts approximately 16 h after the addition of nitrate and is characterized by reconstitution of the photosynthetic apparatus; after 48 h, cells have turned green again and photosynthesis resumes. We have demonstrated previously that glycogen is the major reserve polymer required for resuscitation. Although cells also accumulate PHB during nitrogen

[1]This work was supported by the German Research Council (Deutsche Forschungsgemeinschaft, DFG) GRK 1708 "Molecular Principles of Bacterial Survival Strategies", the DFG SFB 766 (A11), grant GU 1522/1-1, and by BMBF (FP3 09).

[2]These authors contributed equally to the article.

[3]Address correspondence to karl.forchhammer@uni-tuebingen.de.

The author responsible for distribution of materials integral to the findings presented in this article in accordance with the policy described in the Instructions for Authors (www.plantphysiol.org) is: Karl Forchhammer (karl.forchhammer@uni-tuebingen.de).

K.F. conceived the research plans; A.K. performed and supervised experiments; K.G. supervised experiments; S.D. and A.M. performed experiments; S.D., K.F., K.G., A.K., and A.M. analyzed the data; S.D., K.F., and K.G. wrote the article.

www.plantphysiol.org/cgi/doi/10.1104/pp.18.00297

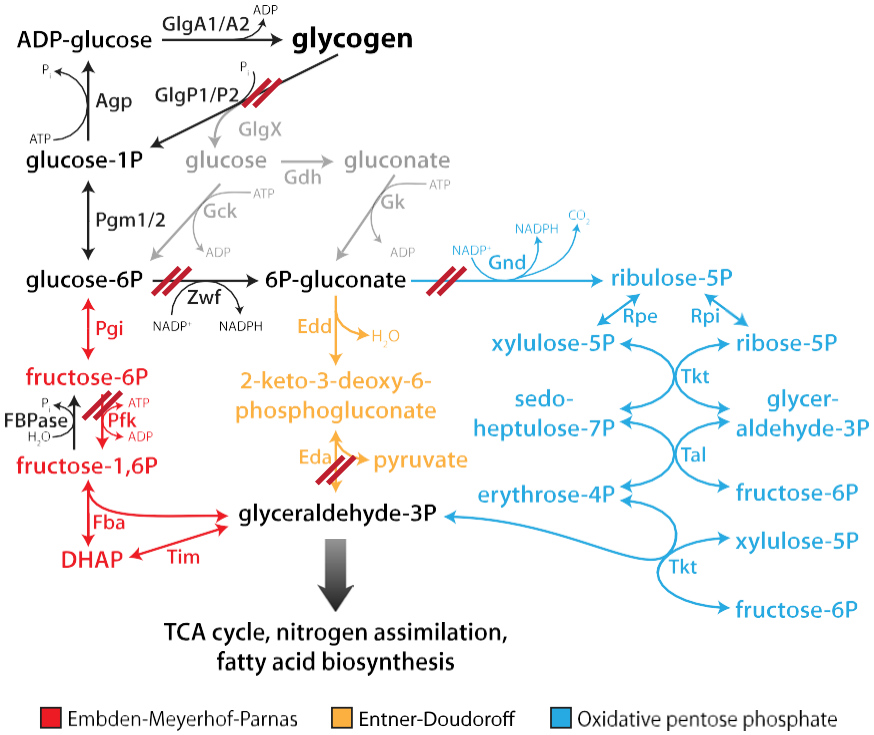

Figure 1. Depiction of glycogen catabolism in *Synechocystis*. Deletion of specific genes is indicated as a double red line. These deletions resulted in a total of nine mutants that were analyzed in this study: Δ*glgP1*, Δ*glgP2*, Δ*glgP1/2*, Δ*pfkB1/2*, Δ*zwf*, Δ*zwf/pfkB1/2*, Δ*gnd*, Δ*eda*, and Δ*gnd/eda*. TCA, Tricarboxylic acid.

starvation, no significant decrease in PHB content is observed during the first phase of resuscitation, and a PHB-free mutant is able to recover from chlorosis as efficiently as the wild type (Klotz et al., 2016). By contrast, mutants deficient in glycogen synthesis present a nonbleaching phenotype and die during prolonged nitrogen starvation, which implies that glycogen synthesis is necessary for chlorosis (Gründel et al., 2012). Upon nitrogen depletion, cells accumulate glycogen up to 60% of the cell's dry weight, and this glycogen is used as a substrate for respiration during resuscitation (Klotz and Forchhammer, 2017).

Glycogen is a biopolymer composed of α-d-glucosyl units connected by α-1,4 linkages and branched through α-1,6 linkages, which account for approximately 7% to 10% of the total linkages, and are organized in a specific way (Shearer and Graham, 2002). The synthesis and degradation of glycogen granules involve several enzymes with specific activities (Preiss, 1984). Among them, glycogen phosphorylase catalyzes the phosphate-dependent splitting of the α-1,4 linkage, thereby releasing Glc-1-P. *Synechocystis* harbors two homologous glycogen phosphorylase genes, *glgP1* and *glgP2* (corresponding to sll1356 and slr1367). Fu and Xu (2006) showed the different physiological roles of these two enzymes: GlgP1 seems to be important during heat stress, whereas GlgP2 provides the main glycolytic activity during day/night cycles. This functional divergence suggests that these two enzymes also may play different roles during resuscitation from nitrogen starvation-induced chlorosis.

The Glc-1-P molecule released by glycogen phosphorylase is converted to Glc-6-P by phosphoglucomutase (Pgm) and then can be channeled into different glycolytic routes. *Synechocystis* also has two homologs of Pgm, Pgm1 (sll0726) and Pgm2 (slr1334), although Pgm1 is responsible for 97% of the activity (Liu et al., 2013). Conventionally, cyanobacteria were known to oxidize Glc-6-P via the Embden-Meyerhof-Parnas (EMP) pathway (glycolysis) and the oxidative pentose phosphate (OPP) pathway. However, *Synechocystis* was recently discovered to also possess the Entner-Doudoroff (ED) glycolytic pathway (Chen et al., 2016). Therefore, there are three possible degradation routes for Glc-6-P in *Synechocystis* (Fig. 1). The role of these different pathways in the process of resuscitation was hitherto unclear.

Here, we investigated the importance of different routes of glycogen degradation for energy metabolism and their regulation during nitrogen starvation and resuscitation. We employed various deletion mutants to identify the crucial pathways in glycogen catabolism during resuscitation. Our results demonstrate that the two glycogen phosphorylase paralogs have different functions and that the ED and OPP pathways play a major role in resuscitation. The fact that the key enzymes for glycogen degradation are already expressed during nitrogen starvation demonstrates that *Synechocystis*

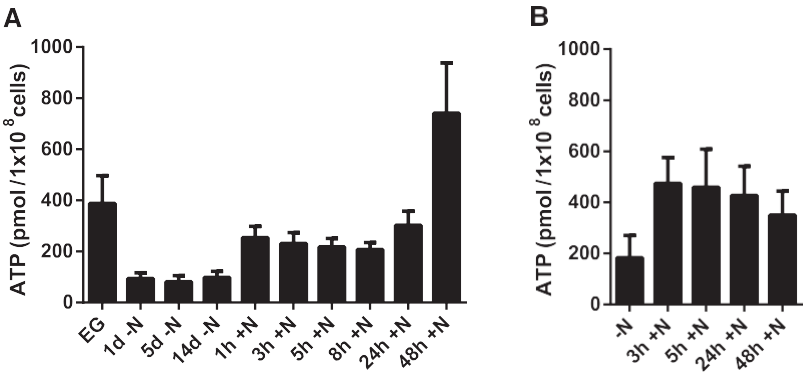

Figure 2. Determination of ATP content during exponential growth (EG), nitrogen starvation (−N), and resuscitation (+N) of the wild type (A) and Δ*glgP1/2* (B). The ATP content was normalized to 1 × 10^8 cells. At least three biological replicates were measured; error bars represent the SD.

anticipates the awakening process and is prepared for rapid glycogen degradation, once nitrogen is available. To maintain this machinery in a quiescent state unless it is needed requires a sophisticated, yet unknown, mechanism of regulation.

RESULTS

Energy Metabolism during Nitrogen Starvation and Resuscitation in *Synechocystis*

In order to better understand energy metabolism during nitrogen starvation and resuscitation, we measured the ATP content of *Synechocystis* during these phases. As shown in Figure 2A, after nitrogen depletion, the ATP level dropped from ~400 to ~100 nm 10^8 $cells^{-1}$ mL^{-1} and stayed constant at this level while the cells were in dormancy. After providing the cells with nitrate, the ATP level almost immediately increased to ~250 nm 10^8 $cells^{-1}$ mL^{-1}, a level that was intermediate between that in exponentially growing cells and that during nitrogen starvation. The ATP content then stayed constant during the first phase of resuscitation until about 24 h. Thereupon, concomitant with the onset of photosynthetic electron transport, the ATP levels increased strongly and, at 48 h, reached a value 2 times higher than in exponentially growing cells (greater than 700 nm 10^8 $cells^{-1}$ mL^{-1}). At this time point, photosynthetic activity is completely restored, although cells have not yet resumed cell division (Klotz et al., 2016). These results are consistent with the metabolic adaptations of *Synechocystis* during nitrogen starvation and resuscitation (Klotz et al., 2016).

GlgP2 Is the Crucial Enzyme for Glycogen Degradation during Resuscitation

To understand the importance of glycogen degradation during resuscitation, mutants deficient in the two homologous glycogen phosphorylases (*glgP1* and *glgP2*) were generated. The two genes were replaced by antibiotic resistance cassettes, resulting in a total of three strains: Δ*glgP1*, Δ*glgP2*, and the double mutant Δ*glgP1/2*. We starved these three phosphorylase-deficient mutants for 1 month and analyzed their ability to recover from nitrogen starvation on BG_{11} solid agar plates in comparison with the *Synechocystis* wild type (Fig. 3A). Δ*glgP1* presented no phenotype, since it was able to recover with the same efficiency as the wild type. However, neither Δ*glgP2* nor Δ*glgP1/2* could efficiently recover from nitrogen starvation. Wemeasured the ability of Δ*glgP2* and Δ*glgP1/2* to degrade glycogen by measuring the glycogen content of these mutants during resuscitation (Fig. 3B). Our results showed that neither of the two mutants degraded a significant amount of glycogen after nitrate addition. These findings indicate that glycogen degradation is essential for recovery from nitrogen chlorosis and that GlgP2 is the major glycogen-degrading enzyme during resuscitation.

Glycogen Degradation Is Necessary for Turning on Respiration during Resuscitation

Degradation of glycogen is necessary for successful resuscitation, but it is not known how glycogen degradation affects the onset of respiration and the switch to heterotrophic metabolism upon the addition of nitrate. To address this, we further characterized the Δ*glgP1/2* mutant by measuring its oxygen evolution during resuscitation. Figure 4 shows a comparison of how oxygen is consumed/produced in the wild type and Δ*glgP1/2*. While the wild type turned on respiration soon after nitrate addition, no significant oxygen consumption was observed for Δ*glgP1/2* in the first 24 h of recovery. Rather, this mutant exhibited a tiny amount of oxygen evolution after 6 h of resuscitation, while the wild type was still respiring. In the wild type, residual photosynthesis is completely suppressed after the addition of nitrate (Klotz et al., 2016), suggesting that ATP is obtained from respiration. Suppression of photosynthesis during illumination might be due to the induction of respiration, resembling an inverse Kok effect. The Kok effect describes the phenomenon that, during exponential growth, photosynthesis inhibits respiration (Healey and Myers, 1971), the opposite of which seems to occur during *Synechocystis* resuscitation. In the Δ*glgP1/2* mutant, since respiration is not turned on, residual photosynthesis may continue

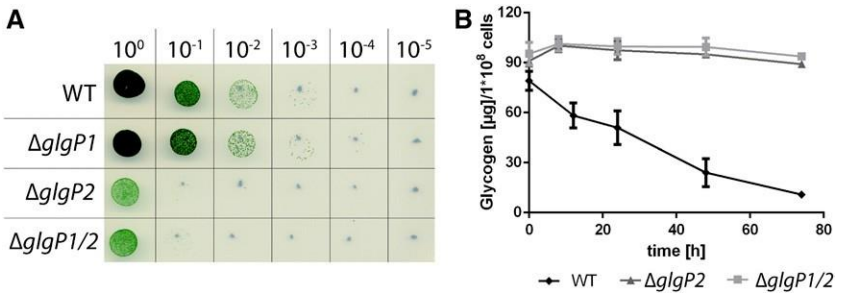

Figure 3. Characterization of glycogen phosphorylase-deficient mutants (Δ*glgP1*, Δ*glgP2*, and Δ*glgP1/2*). A, Spot assay on solid BG_{11} agar of the phosphorylase-deficient mutants to test resuscitation from long-term chlorosis. Dilutions are indicated on the top row. B, Determination of the glycogen content during resuscitation from 1-month chlorosis of Δ*glgP2* and Δ*glgP1/2*. The glycogen content was normalized to 1×10^8 cells. At least three biological replicates were measured. Error bars represent the SD. WT, Wild type.

after nitrate addition. To test this hypothesis, we used pulse-amplitude modulation (PAM) fluorometry to determine the PSII activity of the Δ*glgP1/2* mutant during resuscitation (Supplemental Fig. S1). In fact, instead of being suppressed, the PAM-measured PSII activity increased slightly during the first hours of resuscitation, confirming that Δ*glgP1/2*, unable to degrade glycogen, does not turn on respiration but, instead, continues its residual photosynthesis.

To investigate how this residual photosynthesis in the Δ*glgP1/2* strain affects its energy metabolism, we measured the ATP levels during resuscitation (Fig. 2B). Strikingly, as in the wild type, the ATP concentration increased after the addition of nitrate and stayed constant during the first few hours of resuscitation. However, in contrast to the wild type, wherein a further increase in ATP levels was observed after 24 h, the ATP levels in the mutant decreased at the later time points, consistent with its inability to recover from chlorosis. Conversely, in the dark, only a small increase in ATP levels was observed in the Δ*glgP1/2* mutant (Supplemental Fig. S2).

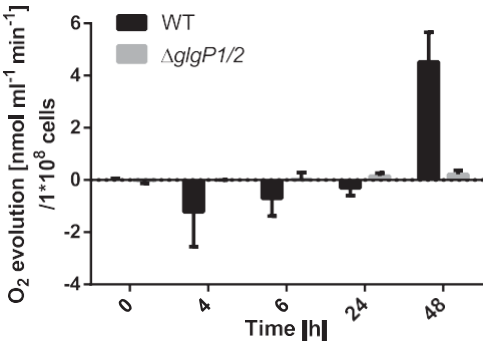

Figure 4. Oxygen evolution of Δ*glgP1/2* and the wild type (WT) during recovery. At least three biological replicates were measured; error bars represent the SD.

Functionality of the ED and OPP Pathways Plays a Key Role during Resuscitation

To determine the importance of the different glycolytic routes during resuscitation, mutants of the key enzymes of these pathways were analyzed. Phosphofructokinase (Pfk), unique to the EMP pathway, catalyzes the phosphorylation of Fru-6-P to Fru-1,6-bisphosphate. *Synechocystis* harbors two *pfk* paralogs, *pfkB1* and *pfkB2*. Glc-6-P dehydrogenase (Zwf) converts Glc-6-P to 6-phosphogluconate, which can be further metabolized via the ED or OPP pathway. 6-Phosphogluconate dehydrogenase (Gnd) is unique to the OPP pathway, catalyzing the conversion of 6-phosphogluconate to ribulose-5-phosphate. The key enzyme unique to the ED pathway is 2-keto-3-deoxy-6-phosphogluconate (KDPG) aldolase (Eda), which converts KDPG into glyceraldehyde-3-phosphate and pyruvate. The following mutants were analyzed: single mutants Δ*eda*, Δ*gnd*, and Δ*zwf*, the double mutants Δ*pfkB1/2* and Δ*gnd/eda*, and the triple mutant Δ*zwf/pfkB1/2*. A depiction of the blocked pathways is shown in Figure 1. The mutants were starved for 1 month and then resuscitated on solid BG_{11} agar plates in parallel with the wild type (Fig. 5A). If the possible bypass via Glc dehydrogenase (Gdh) and gluconate kinase (Gk; indicated in gray in Fig. 1) can be neglected, the deletion of *zwf* and *pfkB1/2* should block all glycogen catabolic pathways. In fact, the respective mutant Δ*zwf/pfkB1/2* could not recover from nitrogen starvation. This result confirmed that Glc, which arises as a minor by-product from the hydrolytic activity of the debranching enzyme (GlgX), is not efficiently metabolized via Gdh and Gk. In contrast to the *zwf* mutant, no substantial difference between the recovery of Δ*pfkB1/2* and the wild type could be observed, indicating that the EMP pathway does not play a role in resuscitation. Deletion of the ED pathway alone in Δ*eda* resulted in poorer recovery compared with the wild type, whereas when the OPP pathway alone was interrupted in Δ*gnd*, the effect was even more pronounced. Interruption of both the ED and OPP pathways in Δ*zwf* resulted in a mutant

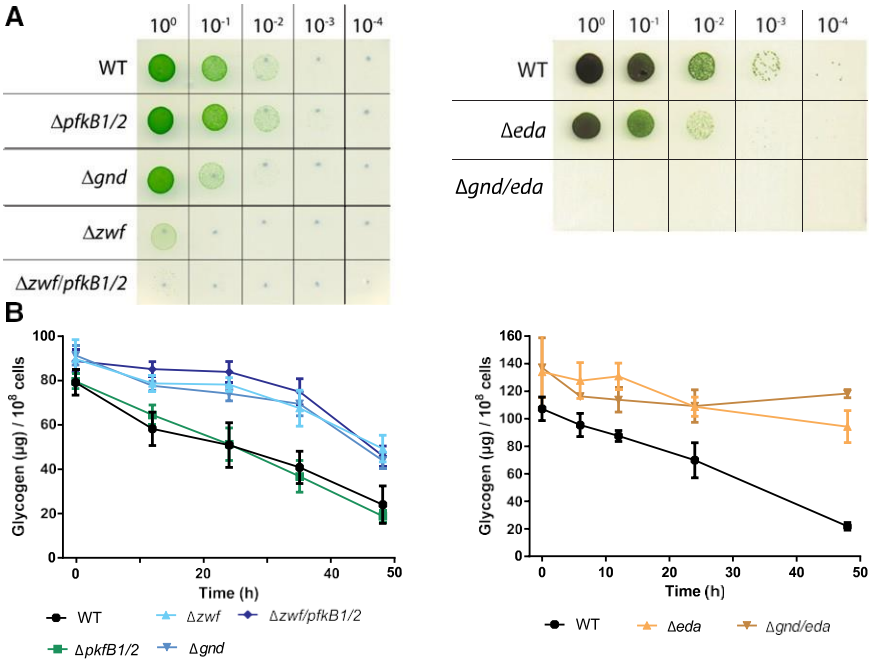

Figure 5. Characterization of glycolytic mutants Δ*pfkB1/2*, Δ*zwf*, Δ*zwf/pfkB1/2*, Δ*gnd*, Δ*eda*, and Δ*gnd/eda*. A, Spot assay on solid BG_{11} agar of glycolytic mutants to test resuscitation from long-term chlorosis. Dilutions are indicated in the top row. B, Determination of the glycogen content of glycolytic mutants during resuscitation from 1-month chlorosis of the same mutants. The glycogen content was normalized to 1×10^8 cells. At least three biological replicates were measured; error bars represent the SD. WT, Wild type.

that recovered poorly, demonstrating that the EMP pathway could only very inefficiently compensate for the loss of the ED and OPP pathways (compare Δ*zwf/pfkB1/2* and Δ*zwf*). Strikingly, the double mutant Δ*gnd/eda* could not recover at all. Since, in both mutants, neither the OPP nor the ED pathway is functioning, we expected no difference in recovery between Δ*zwf* and Δ*gnd/eda*. Thus, there must be another reason why Δ*zwf* recovered, albeit inefficiently, whereas Δ*gnd/eda* did not recover at all. We hypothesized that 6P-gluconate might accumulate in Δ*gnd/eda* but not in Δ*zwf*, thereby possibly inhibiting CO_2 fixation as soon as photosynthesis starts. 6P-gluconate is known to bind to Rubisco with the potential to inhibit CO_2 fixation. Measurement of 6P-gluconate levels under chlorotic conditions confirmed that this metabolite heavily accumulated in Δ*gnd/eda*, whereas it was barely detectable in either Δ*zwf* or wild-type cells (Fig. 6A). In agreement with this, CO_2 fixation was severely impaired in Δ*gnd/eda*, whereas the wild type first evolved CO_2 as a consequence of respiration and only then turned on CO_2 fixation with the onset of photosynthesis (Fig. 6B). Taken together, these results indicate that the EMP pathway does not play an important role in resuscitation, whereas the OPP and ED pathways are the main glycogen-degrading routes during this process. As the Δ*eda* mutant showed a slightly better recovery than the Δ*gnd* mutants, it appears that the OPP pathway plays a more crucial role than the ED pathway during resuscitation. Furthermore, initiation of CO_2 fixation via the Calvin-Benson cycle following the respiratory phase is essential for a successful recovery.

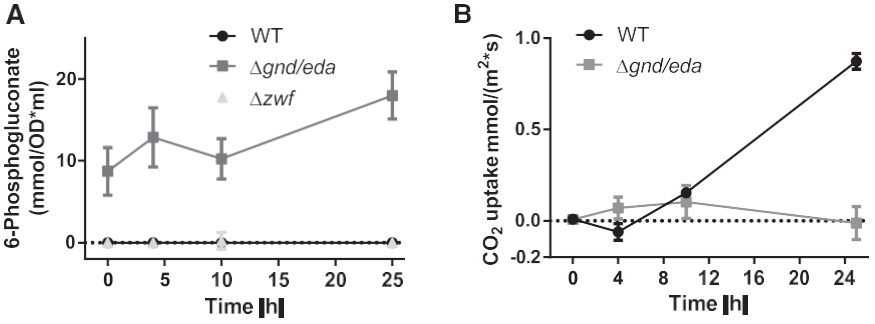

Figure 6. Intracellular 6-phosphogluconate content and CO_2 uptake of mutants blocked in the ED and OPP pathways (Δ*gnd/eda* and Δ*zwf*). A, Intracellular 6-phosphogluconate content during resuscitation from chlorosis of the wild type (WT), Δ*gnd/eda*, and Δ*zwf*. Slightly negative values were set to 0. B, CO_2 uptake of the wild type and Δ*gnd/eda* during resuscitation. At least three biological replicates were measured; error bars represent the SD.

To reveal how the various mutations affect glycogen consumption, we measured the glycogen content of all six glycolytic mutants during resuscitation. As shown in Figure 5B, the initiation of resuscitation caused a linear degradation of glycogen in the wild type as well as in Δ*pfkB1/2*. However, Δ*zwf*, Δ*zwf/pfkB1/2*, Δ*gnd*, Δ*eda*, and Δ*gnd/eda* seemed to accumulate more glycogen than the wild type and showed a much slower degradation of this polymer. Degradation of a portion of the glycogen (20%–40%) in these mutants is possible because they have a functional GlgP2, but degradation of hexose phosphates is totally or partially blocked, and this inhibits further glycogen degradation. To prove this, we measured the levels of Glc-6-P and Fru-6-P in the wild type and Δ*zwf/pfkB1/2*, which is blocked in all hexose phosphate degradation routes. Already during nitrogen starvation, both hexose phosphates accumulated in Δ*zwf/pfkB1/2* when compared with the wild type. After the onset of resuscitation, the levels of both sugars dropped below the detection limit in the wild type, indicating their fast consumption. By contrast, in the Δ*zwf/pfkB1/2* triple mutant, the level of Glc-6-P continued to increase and that of Fru-6-P is maintained at high levels, confirming the inability of the mutant to metabolize these molecules (Supplemental Fig. S3). These results show that glycogen breakdown is activated by nitrate addition independent of the start of the glycolytic reactions, explaining the degradation of glycogen in the various glycolytic mutants.

Synechocystis Is Prepared for Glycogen Degradation during Nitrogen Starvation

Previously, we performed a transcriptomic analysis of cells undergoing chlorosis and resuscitation (Klotz et al., 2016). The transcriptional regulation of the genes involved in glycogen catabolism is shown in Figure 7. The experiments described above led us to conclude that GlgP2 is the major glycogen-degrading enzyme during resuscitation, while GlgP1 does not play a relevant role here. In accord, our transcriptomic data set revealed that *glgP1* is not subjected to strong regulation, whereas *glgP2* is strongly up-regulated during nitrogen starvation but repressed when resuscitation is induced. Intriguingly, the genes for the key enzymes for the OPP and ED pathways, *zwf* and *gnd*, which play a major role in recovery from chlorosis, showed a similar regulation to *glgP2*: they were up-regulated during nitrogen starvation and down-regulated during resuscitation. A quantitative proteomic analysis of chlorotic and recovering cells (Spaet et al., 2018) revealed that protein levels of GlgP2, Zwf, and Gnd were indeed higher during nitrogen starvation than in exponentially growing cells (Supplemental Fig. S4), confirming that the *glgP2*, *zwf*, and *gnd* genes are not only transcribed but also translated into proteins during chlorosis. This shows that the cells produce the glycogen-degrading enzymes together with the glycogen granules, so that degradation can start as soon as nitrogen is available again. During resuscitation, *glgP2*, *zwf*, and *gnd* transcripts decrease while the protein levels are maintained, indicating that these enzymes are not turned over as long as they are active. Of the glycogen-degrading enzymes, the major phosphoglucomutase Pgm1 is the only one that is regulated in a different way. The *pgm1* gene is repressed during chlorosis and turned on during resuscitation, and the same trend is observed at the protein level. Moreover, Pgm1 is strongly subjected to posttranslational modification via Ser phosphorylation at two sites (Spaet et al., 2018), indicating that it might play a key role in the control of glycogen degradation upon nitrate addition.

To further reveal the activation of the glycogen-degrading enzymes in chlorotic cells, we measured the oxygen-exchange rate after dark incubation in the wild type and the Δ*glgp1/2* mutant (Supplemental Fig. S5). In the light, chlorotic wild-type cells neither consume nor produce oxygen; however, upon transfer to darkness, a low but clearly measurable consumption of oxygen could be observed. By contrast, Δ*glgp1/2* was unable to start respiration in the dark, like due to its inability to initiate respiration upon nitrate addition (see above). These results suggest that the equipment of chlorotic cells with the glycogen-degrading enzymes serves a double role: it allows rapid resuscitation when nitrate becomes available again and it enables cells to use glycogen for survival in the dark.

DISCUSSION

Synechocystis is able to survive long-term periods of nitrogen starvation and to rapidly resuscitate after the readdition of a usable nitrogen source. Glycogen, which quickly accumulates during nitrogen starvation and plays a major role in the transition to chlorosis, is rapidly mobilized upon the onset of resuscitation (Klotz et al., 2016). In this study, we investigated the importance of glycogen degradation for revival and the implication of the different glycogen catabolic pathways during resuscitation.

When *Synechocystis* is exposed to nitrogen starvation, cells tune down their metabolism and remain alive with minimal photosynthetic activity (Klotz et al., 2016). The metabolic adaptations during chlorosis reduce both energy consumption and generation, reaching a metabolic equilibrium that allows them to survive for a long time under starvation conditions. In agreement with the assumption that, even in the dormant state, a minimal amount of energy is necessary to keep cells alive (Sauer et al., 2001), ATP levels were shown to be maintained at a level that corresponds to one-fourth of the value at exponential growth (Fig. 2A). We propose that this residual level is adjusted to keep dormant cells alive. Chlorotic cells consume only very low amounts of ATP, since they perform almost no anabolic reactions or protein synthesis. As such, ATP regeneration should be tuned down correspondingly. In agreement, our previous transcriptomic data showed that genes encoding the F-ATPase machinery

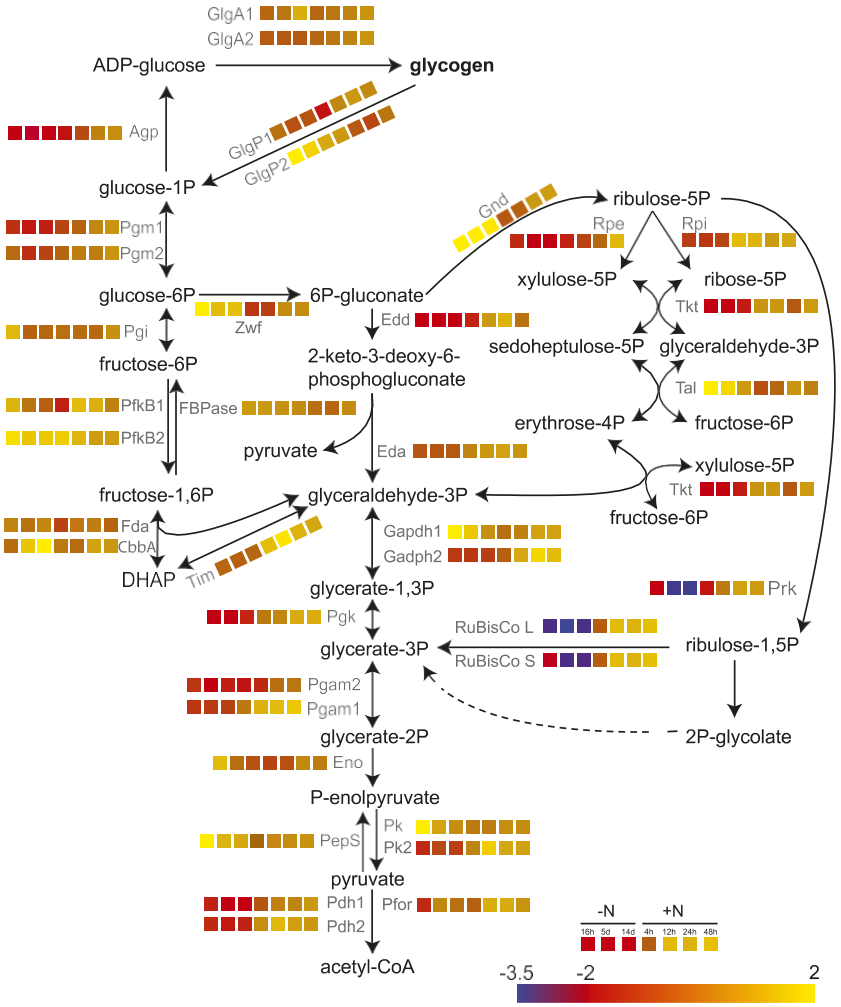

Figure 7. Transcriptional regulation of genes needed for glycogen catabolism during nitrogen starvation (16 h, 5 d, and 14 d) and resuscitation (4, 12, 24, and 48 h). Analysis was performed using a high-resolution microarray (Agilent; format, 8 × 60 K; slide layout = IS-62976-8-V2) as described by Klotz et al. (2016). Relative transcript abundance normalized to exponential growth is shown as $\log_2$ and encoded in a color code from blue ($2^{-3.5}$) to yellow (2^2).

were strongly repressed in long-term chlorotic cells (Klotz et al., 2016). When resuscitation was initiated by the addition of nitrate, the first genes that were induced comprised all components for the translational apparatus, for nitrogen assimilation, and the F0-ATPase subunits. This implies an increased need for ATP due to the onset of anabolism and protein synthesis, which must be matched with an increased capacity for ATP regeneration by reinstallation of the F-ATPase machinery (Klotz et al., 2016). In line with this scenario, the measurement of ATP levels revealed a sudden increase of ATP upon the addition of nitrate. This first increase reaches a plateau, lying between the levels in dormant and vegetative growing cells. This plateau indicates that the increased need for ATP is perfectly balanced by the increased capacity to regenerate ATP. Only after 24 h of the resuscitation process does the concentration of ATP start to increase further, reaching almost double the value of normal growing cells after 48 h. At this point, cells have restored the powerful energy-generating photosynthetic machinery, but they have not yet consumed all reserve polymers and have not yet entered exponential growth, which gives rise to a transient surplus of energy.

This study confirmed our previous assumption that glycogen degradation is pivotal for resuscitation. Characterization of the individual glycogen phosphorylase mutants (Δ*glgP1* and Δ*glgP2*) revealed that only GlgP2 plays a crucial role for glycogen breakdown during recovery from chlorosis. GlgP2 also is known to be responsible for glycogen degradation during periods of darkness (Fu and Xu, 2006). By contrast, GlgP1 has only been shown to play a crucial role during heat stress conditions (Fu and Xu, 2006), and any further physiological function remains elusive. Both Δ*glgP2* and the Δ*glgP1/2* double mutant were unable to

degrade glycogen during resuscitation (Fig. 3B), confirming that no other pathway can degrade glycogen. Furthermore, we showed that glycogen degradation is essential for the initiation of respiration upon nitrate addition, since no significant oxygen consumption is observed in the Δ*glgP1/2* double mutant (Fig. 4). In the wild type, respiration during the first hours of resuscitation leads to a complete inhibition of photosynthesis (Klotz et al., 2016). The Δ*glgP1/2* double mutant, however, does not respire and, therefore, photosynthesis is not shut down. Rather, it seems that these mutant cells attempt to awake their metabolism when nitrate is added and use the remaining photosynthetic machinery to produce ATP (Fig. 2B). However, due to the lack of metabolic intermediates provided by glycogen catabolism, resuscitation is abortive. Nevertheless, the initial increase in ATP in these mutants suggests that the ATP levels are actively regulated by an unknown metabolic trigger, which responds to the addition of nitrate.

Glycogen phosphorylase catalyzes the excision of a Glc-1-P molecule by breaking the α-1,4 linkage. This Glc-1-P can be further catabolized via three different glycolytic routes, namely, the EMP, ED, and OPP pathways. Our findings indicate that the ED and OPP pathways are the major glycogen-degrading routes during resuscitation, since the mutants blocked in either or both pathways (Δ*zwf*, Δ*gnd*, Δ*eda*, and Δ*gnd/eda*) are either retarded or inhibited in their ability to recover from chlorosis and degrade glycogen. The lack of phenotype of the Δ*pfkB1/2* mutant indicates that the EMP pathway does not play a crucial role in this process (Fig. 5). However, a minor contribution of the EMP pathway in glycogen breakdown might not be specific to the resuscitation process. During resuscitation, a first heterotrophic phase (0–24 h +N), in which glycogen is degraded and fuels respiration, is followed by a gradual increase in photosynthetic activity, while glycogen degradation continues (16–48 h; Klotz et al., 2016). It appears that CO_2 fixation is activated as soon as photosynthesis is initiated. The concomitant use of glycogen as a carbon source with photosynthetic energy generation and CO_2 fixation resembles mixotrophic conditions. Finally, cells reenter fully autotrophic conditions under which they again rely only on photosynthesis. The restoration of transcription and translation takes place early in resuscitation (Klotz et al., 2016) and requires precursors for nucleic and amino acids. As long as the Calvin-Benson cycle is not running, ribose components for the synthesis of RNA and erythrose-4-phosphate for the synthesis of aromatic compounds can be provided exclusively via the OPP pathway. In line with this, deleting genes that participate in the OPP pathway has the severest impact on the cell's ability to recover from chlorosis (Δ*gnd*, Δ*zwf*, Δ*zwfpfkB1/B2*, and Δ*gnd/eda*). Following the first respiratory phase, mixotrophic conditions are created when glycogen degradation continues while photosynthesis starts. During this phase, the Calvin-Benson cycle, which in many steps is a reversal of the OPP pathway, is activated. The transcriptomic data (Klotz et al., 2016) show that genes encoding enzymes of the Calvin-Benson cycle (e.g. Prk, RubiscoL, RubiscoS, Pgk, Gapdh2, Tkt, Rpi, and Rpe) are already up-regulated in the early phase of resuscitation (4 h +N). Under mixotrophic conditions, the ED pathway is probably the most physiologically important (Chen et al., 2016). The ED pathway does not share reactions and intermediates with the Calvin-Benson cycle; this allows concomitant glycogen breakdown via the ED pathway and operation of the reductive pentose phosphate cycle. The ED pathway might thus be especially important in the mixotrophic phase of resuscitation. Furthermore, this pathway provides a shortcut for the delivery of pyruvate to the tricarboxylic acid cycle. In line with this, the impact of deletion of the ED pathway on resuscitation is less severe than deletion of the OPP pathway. Remarkably, deletion of both *gnd* and *eda* completely abrogated resuscitation, whereas deletion of *zwf* resulted in a mutant that was still able to recover poorly (Fig. 5A). In line with this, we detected an overaccumulation of 6P-gluconate in Δ*gnd/eda* but not in Δ*zwf* (Fig. 6A). 6P-gluconate is known to compete with ribulose-1,5-bisphosphate for binding to Rubisco (Badger and Lorimer, 1981). It follows that CO_2 fixation is impaired in Δ*gnd/eda* in addition to the lack of the OPP and ED pathways (Fig. 6B). The limited recovery of Δ*zwf* is thus probably enabled by a minor consumption of Glc-6-P via the EMP pathway in the early phase followed by CO_2 fixation as soon as photosynthesis starts (compare Δ*zwf* and Δ*zwf/pfkB1/2* in Fig. 5A). However, in Δ*gnd/eda*, the consumption of Glc-6-P via the EMP pathway is not followed by CO_2 fixation and, accordingly, resuscitation is not successful. These results convincingly show that the awakening of dormant cyanobacteria from chlorosis requires glycogen breakdown in the early phase followed by CO_2 fixation.

A transcriptomic analysis of the chlorosis and resuscitation processes revealed that *Synechocystis* anticipates and prepares for glycogen degradation during nitrogen starvation (Klotz et al., 2016). Transcription of *glgP2*, *zwf*, and *gnd*, which we found to be the main enzymes in glycogen catabolism during resuscitation, was up-regulated during nitrogen starvation and turned down during resuscitation (Fig. 7). Moreover, quantitative proteomic analyses (Spaet et al., 2018) showed that the GlgP2, Zwf, and Gnd protein levels also increased during chlorosis and are maintained after the addition of nitrate. This indicates that the cells anticipate the resuscitation process and produce the proteins necessary to degrade glycogen while they undergo chlorosis, which allows an immediate response when a nitrogen source is available. Furthermore, chlorotic cells are able to rapidly turn on respiration in the dark (Supplemental Fig. S5), which substantiates that GlgP2 is present and active during chlorosis. These findings raised the question of how glycogen mobilization is initiated, since most of the enzymes involved in the first steps of glycogen catabolism (GlgP2,

Zwf, and Gnd) are present throughout the course of chlorosis and resuscitation, yet glycogen degradation only starts after the addition of nitrate. This requires a mechanism that prevents unintended degradation of glycogen during chlorosis by GlgP2. Direct regulation of GlgP2 activity is conceivable; however, posttranslational control of glycogen phosphorylase activity in cyanobacteria has not been demonstrated so far. Another key enzyme that might control glycogen degradation is Pgm1. This enzyme has been described as a target of thioredoxin regulation in *Synechocystis* (Lindahl and Florencio, 2003) and showed conspicuous protein Ser phosphorylation dynamics during chlorosis and resuscitation (Spaet et al., 2018). Whatever the mechanism involved, glycogen mobilization must be activated upon the onset of nitrogen assimilation as well as after transfer to darkness. How these signals are perceived by the cells and transmitted to activate the necessary enzymes requires further investigation. These studies will lead to insights into how cyanobacteria coordinate metabolic transitions, which is poorly understood. The awakening of dormant *Synechocystis* cells from chlorosis offers a unique model system in which to study the delicate interplay of carbohydrate oxidation, CO_2 fixation, and photosynthesis.

MATERIALS AND METHODS

Cultivation of *Escherichia coli*

Escherichia coli was grown in Luria-Bertani medium at 37°C (Bertani, 1951). For growth on solid medium, 1.5% (w/v) agar-agar was added to the regular Luria-Bertani medium. Strains containing plasmids have been propagated with the appropriate concentration of antibiotics.

Cyanobacterial Cultivation Conditions

All *Synechocystis* sp. PCC 6803 strains used in this study were grown in BG_{11} supplemented with 5 mm $NaHCO_3$, as described previously (Rippka et al., 1979). A list of the strains used is provided in Supplemental Table S1. Two kinds of wild-type strains, Glc sensitive and Glc tolerant, were used; both strains responded equally during nitrogen starvation and resuscitation. Cultivation was performed with continuous illumination (40–50 µmol photons m^{-2} s^{-1}) and shaking (130–140 rpm) at 27°C. Induction of nitrogen starvation and resuscitation was induced as described previously (Schlebusch and Forchhammer, 2010; Klotz et al., 2016). If mutants or strains containing antibiotic markers were used, the precultures were propagated with the appropriate concentration of antibiotics. Biological replicates were inoculated with the same precultures but propagated, nitrogen starved, and resuscitated independently in different flasks under identical conditions.

Isothermal, Single-Reaction DNA Assembly (Gibson Cloning)

Cloning was performed as described by Gibson et al. (2009) using primers containing sequences of the specific vector backbones (Supplemental Table S2). pUC19 (New England Biolabs) was used for the generation of cyanobacterial mutants.

ATP Determination

One-milliliter aliquots of bacterial cultures were taken and immediately frozen in liquid nitrogen. ATP was extracted by boiling and freezing samples three times consecutively (boiling at 100°C and freezing in liquid nitrogen) and spinning them down at 25,000*g* for 1 min at 4°C. ATP in the supernatant was quantified with the ATP Determination Kit (Molecular Probes; A22066) following the manufacturer's protocol. A total of 450 µL of a reaction mix containing 25 mm Tricine buffer, pH 7.8, 5 mm $MgSO_4$, 0.1 mm EDTA, 0.1 mm sodium azide, 1 mm DTT, 0.5 mm d-luciferin, and 1.25 µg mL^{-1} firefly luciferase was mixed with 50 µL of the samples, and the luminescence was read in a luminometer (Sirius Luminometer; Berthold Detection Systems). An ATP standard curve was generated and used to calculate ATP content in the collected samples.

Spot Assay

Serial dilutions of chlorotic cultures were prepared (10^0, 10^{-1}, 10^{-2}, 10^{-3}, 10^{-4}, and 10^{-5}), starting with an OD_{750} of 1.5 µL of these dilutions, dropped on solid BG_{11} agar plates, and cultivated at 50 µmol photons m^{-2} s^{-1} and 27°C for 5 to 7 d.

Glycogen Determination

Glycogen determination was performed as described previously (Gründel et al., 2012) with modifications described by Klotz et al. (2015).

Oxygen Evolution Measurement

Oxygen evolution was measured in vivo using a Clark-type oxygen electrode (Hansatech DW1). Light was provided from a high-intensity white light source (Hansatech L2). Oxygen evolution of 2 mL of recovering cultures at an OD_{750} of 0.5 was measured at room temperature and 50 µmol photons m^{-2} s^{-1}.

PAM

PSII activity was analyzed in vivo with a WATER-PAM chlorophyll fluorometer (Walz). All samples were dark adapted for 5 min before measurement. The maximal PSII quantum yield was determined with the saturation pulse method (Schreiber et al., 1995). Cultures were diluted 1:20 in BG_{11} medium before the measurements in a final volume of 2 mL.

Quantification Assay for 6P-Gluconate

A total of 100 µL of cells with an OD_{750} of 50 was pelleted, resuspended in 1 mL of 0.2 m HCl, and incubated at 95°C for 15 min. The solution was centrifuged (10 min at 18,000*g* at room temperature), and the supernatant was transferred to a new cup and neutralized with 1 mL of 1 m Tris-HCl (pH 8). The solution was divided into two parts (2 × 900 µL) for a positive and a blank sample. A total of 90 µL of 11 mm $NADP^+$ solution was added to all samples as well as 10 µL of 5 units mL^{-1} Gnd (Megazyme) solution to all positive samples and 10 µL of water to all blank samples. Absorption at 340 nm was measured, and blank sample absorption values were subtracted from positive sample absorption values. The 6-phosphogluconate concentration was then calculated by using a standard curve.

Quantification Assay for Glc-6-P

A total of 100 µL of cells with an OD_{750} of 50 was pelleted, resuspended in 1 mL of 0.2 m HCl, and incubated at 95°C for 15 min. The solution was centrifuged (10 min at 18,000*g* at room temperature), and the supernatant was transferred to a new cup and neutralized with 1 mL of 1 m Tris-HCl (pH 8). The solution was divided into two parts (2 × 900 µL) for a positive and a blank sample. A total of 90 µL of 11 mm $NADP^+$ solution was added to all samples as well as 10 µL of 5 units mL^{-1} Glc-6-P dehydrogenase (Sigma-Aldrich) solution to all positive samples and 10 µL of water to all blank samples. Absorption at 340 nm was measured, and blank sample absorption values were subtracted from positive absorption values. Glc-6-P concentration was then calculated by using a standard curve.

Quantification Assay for Fru-6-P

A total of 100 µL of cells with an OD_{750} of 50 was pelleted, resuspended in 1 mL of 0.2 m HCl, and incubated at 95°C for 15 min. The solution was centrifuged (10 min at 18,000*g* at room temperature), and the supernatant was

transferred to a new cup and neutralized with 1 mL of 1 m Tris-HCl (pH 8). The solution was divided into two parts (2 × 900 µL) for a positive and a blank sample. A total of 90 µL of 11 mm $NADP^+$ solution containing 5 units mL^{-1} Glc-6-P dehydrogenase (Sigma-Aldrich) was added to all samples as well as 10 µL of 5 units mL^{-1} phosphoglucose isomerase (Boehringer Mannheim) solution to all positive samples and 10 µL of water to all blank samples. Absorption at 340 nm was measured, and blank sample absorption values were subtracted from positive absorption values. Fru-6-P concentration was then calculated by using a standard curve.

CO_2 Gas-Exchange Measurement

BG_{11} medium devoid of bicarbonate was mixed with agar, heated, and poured onto cutoff lids of 5-mL centrifugation cups. After solidification of the agar, 100 µL of cells with an OD_{750} of 50 was added and dried in front of a ventilator while being exposed to 50 µE of light emitted by a fluorescent tube. Two such lids were loaded simultaneously into the cuvette of a GFS-3000 gas-exchange measuring system from Walz containing an atmosphere of 400 µL L^{-1} CO_2 and 60% humidity at 28°C. The cuvette was exposed to 50 µE of light emitted by a fluorescent tube. After a short adaptation period, CO_2-exchange rates were monitored for 90 s, while measurements were taken every 15 s. The six measurements were averaged. In order to correct for diffusion of CO_2 into or out of the agar, the CO_2 exchange of cell-free agar lids was measured and subtracted from sample values.

Accession Numbers

Sequence data from this article can be found in the UniProt database under accession numbers P73511 (GlgP1), P73546 (GlgP2), P74643 (Pgm1), P73411 (Zwf), P72830 (PfkB1) Q55988 (PfkB2), P52208 (Gnd), and Q55872 (Eda). The accession number of the microarray data cited in this article is GEO:GSE83363.

Supplemental Data

The following supplemental materials are available.

Supplemental Figure S1. PSII quantum yield determined by PAM fluorometry of *Synechocystis* wild type and Δ*glgP1/2* during recovery from chlorosis.

Supplemental Figure S2. ATP content during nitrogen starvation and resuscitation of Δ*glgP1/2* in the absence of light.

Supplemental Figure S3. Glc-6-P and Fru-6-P levels in *Synechocystis* wild type and Δ*zwf/pfkB1/2* during nitrogen starvation and resuscitation.

Supplemental Figure S4. Expression ratios of transcripts and proteins of the main enzymes involved in glycogen degradation during resuscitation.

Supplemental Figure S5. Oxygen-exchange rate of chlorotic Δ*glgP1/2* and wild-type cells in the light and after 3 min of incubation in the dark.

Supplemental Table S1. List of strains used.

Supplemental Table S2. List of primers used in this study.

ACKNOWLEDGMENTS

We thank Lars Nichelmann for assistance with the CO_2 fixation measurements and Selina Schwarzbach for involvement in ATP measurements.

Received March 8, 2018; accepted April 9, 2018; published April 27, 2018.

LITERATURE CITED

Allen MM, Smith AJ (1969) Nitrogen chlorosis in blue-green algae. Arch Mikrobiol **69**: 114–120

Badger MR, Lorimer GH (1981) Interaction of sugar phosphates with the catalytic site of ribulose-1,5-bisphosphate carboxylase. Biochemistry **20**: 2219–2225

Bertani G (1951) Studies on lysogenesis. I. The mode of phage liberation by lysogenic Escherichia coli. J Bacteriol **62**: 293–300

Chen X, Schreiber K, Appel J, Makowka A, Fähnrich B, Roettger M, Hajirezaei MR, Sönnichsen FD, Schönheit P, Martin WF, (2016) The Entner-Doudoroff pathway is an overlooked glycolytic route in cyanobacteria and plants. Proc Natl Acad Sci USA **113**: 5441–5446

Fu J, Xu X (2006) The functional divergence of two glgP homologues in Synechocystis sp. PCC 6803. FEMS Microbiol Lett **260**: 201–209

Gibson DG, Young L, Chuang RY, Venter JC, Hutchison CA III, Smith HO (2009) Enzymatic assembly of DNA molecules up to several hundred kilobases. Nat Methods **6**: 343–345

Görl M, Sauer J, Baier T, Forchhammer K (1998) Nitrogen-starvation-induced chlorosis in Synechococcus PCC **7942**: adaptation to long-term survival. Microbiology **144**: 2449–2458

Gründel M, Scheunemann R, Lockau W, Zilliges Y (2012) Impaired glycogen synthesis causes metabolic overflow reactions and affects stress responses in the cyanobacterium Synechocystis sp. PCC 6803. Microbiology **158**: 3032–3043

Healey FP, Myers J (1971) The Kok effect in *Chlamydomonas reinhardi*. Plant Physiol **47**: 373–379

Klotz A, Forchhammer K (2017) Glycogen, a major player for bacterial survival and awakening from dormancy. Future Microbiol **12**: 101–104

Klotz A, Reinhold E, Doello S, Forchhammer K (2015) Nitrogen starvation acclimation in Synechococcus elongatus: redox-control and the role of nitrate reduction as an electron sink. Life (Basel) **5**: 888–904

Klotz A, Georg J, Bučinská L, Watanabe S, Reimann V, Januszewski W, Sobotka R, Jendrossek D, Hess WR, Forchhammer K (2016) Awakening of a dormant cyanobacterium from nitrogen chlorosis reveals a genetically determined program. Curr Biol **26**: 2862–2872

Lindahl M, Florencio FJ (2003) Thioredoxin-linked processes in cyanobacteria are as numerous as in chloroplasts, but targets are different. Proc Natl Acad Sci USA **100**: 16107–16112

Liu L, Hu HH, Gao H, Xu XD (2013) Role of two phosphohexomutase genes in glycogen synthesis in Synechocystis sp. PCC6803. Chin Sci Bull **58**: 4616–4621

Luque I, Forchhammer K (2008) Nitrogen assimilation and C/N balance sensing. *In* **A Herrero, E Flores**, eds, The Cyanobacteria: Molecular Biology, Genomics and Evolution. Caister Academic Press, Norfolk, UK, pp 335–382

Preiss J (1984) Bacterial glycogen synthesis and its regulation. Annu Rev Microbiol **38**: 419–458

Rippka R, Deruelles J, Waterbury JB, Herdman M, Stanier RY (1979) Generic assignments, strain histories and properties of pure cultures of cyanobacteria. Microbiology **111**: 1–61

Sauer J, Schreiber U, Schmid R, Völker U, Forchhammer K (2001) Nitrogen starvation-induced chlorosis in Synechococcus PCC **7942**: low-level photosynthesis as a mechanism of long-term survival. Plant Physiol **126**: 233–243

Schlebusch M, Forchhammer K (2010) Requirement of the nitrogen starvation-induced protein Sll0783 for polyhydroxybutyrate accumulation in Synechocystis sp. strain PCC 6803. Appl Environ Microbiol **76**: 6101–6107

Schreiber U, Endo T, Mi H, Asada K (1995) Quenching analysis of chlorophyll fluorescence by the saturation pulse method: particular aspects relating to the study of eukaryotic algae and cyanobacteria. Plant Cell Physiol **36**: 873–882

Shearer J, Graham TE (2002) New perspectives on the storage and organization of muscle glycogen. Can J Appl Physiol **27**: 179–203

Spaet P, Klotz A, Sascha R, Boris M, Karl F (2018) Chlorosis as a developmental program in cyanobacteria: the proteomic fundament for survival and awakening. BioRxivhttps://doi.org/10.1101/325761

Stanier RY, Cohen-Bazire G (1977) Phototrophic prokaryotes: the cyanobacteria. Annu Rev Microbiol **31**: 225–274

Vitousek PM, Howarth RW (1991) Nitrogen limitation on land and in the sea: how can it occur. Biogeochemistry **13**: 87–115

2. Publication 2 (Accepted)

Research article

Moritz Koch, Sofía Doello, Kirstin Gutekunst, and Karl Forchhammer

PHB is produced from Glycogen turn-over during nitrogen starvation in Synechocystis sp. PCC 6803.

2019. *International Journal of Molecular Sciences*. 20, 1942: 1-14.

International Journal of
Molecular Sciences

MDPI

Article

PHB is Produced from Glycogen Turn-over during Nitrogen Starvation in *Synechocystis* sp. PCC 6803

Moritz Koch [1], Sofía Doello [1], Kirstin Gutekunst [2] and Karl Forchhammer [1,*]

[1] Interfaculty Institute of Microbiology and Infection Medicine Tübingen, Eberhard-Karls-Universität Tübingen, 72076 Tübingen, Germany; moritz.koch@uni-tuebingen.de (M.K.); sofia.doello@gmail.com (S.D.)
[2] Department of Biology, Botanical Institute, Christian-Albrechts-University, 24118 Kiel, Germany; kgutekunst@bot.uni-kiel.de
* Correspondence: karl.forchhammer@uni-tuebingen.de; Tel.: +49-7071-29-72096

Received: 4 April 2019; Accepted: 18 April 2019; Published: 20 April 2019

Abstract: Polyhydroxybutyrate (PHB) is a polymer of great interest as a substitute for conventional plastics, which are becoming an enormous environmental problem. PHB can be produced directly from CO_2 in photoautotrophic cyanobacteria. The model cyanobacterium *Synechocystis* sp. PCC 6803 produces PHB under conditions of nitrogen starvation. However, it is so far unclear which metabolic pathways provide the precursor molecules for PHB synthesis during nitrogen starvation. In this study, we investigated if PHB could be derived from the main intracellular carbon pool, glycogen. A mutant of the major glycogen phosphorylase, GlgP2 (*slr1367* product), was almost completely impaired in PHB synthesis. Conversely, in the absence of glycogen synthase GlgA1 (*sll0945* product), cells not only produced less PHB, but were also impaired in acclimation to nitrogen depletion. To analyze the role of the various carbon catabolic pathways (EMP, ED and OPP pathways) for PHB production, mutants of key enzymes of these pathways were analyzed, showing different impact on PHB synthesis. Together, this study clearly indicates that PHB in glycogen-producing *Synechocystis* sp. PCC 6803 cells is produced from this carbon-pool during nitrogen starvation periods. This knowledge can be used for metabolic engineering to get closer to the overall goal of a sustainable, carbon-neutral bioplastic production.

Keywords: cyanobacteria; bioplastic; PHB; sustainable; glycogen; metabolic engineering; Synechocystis

1. Introduction

Cyanobacteria are among the most widespread organisms on our planet. Their ability to perform oxygenic photosynthesis allows them to grow autotrophically with CO_2 as the sole carbon source [1]. Additionally, many cyanobacteria acquired the ability to fix nitrogen, one of the most limiting nutrients [2]. However, many others are not able to fix nitrogen, one of them being the well-studied model organism *Synechocystis* sp. PCC 6803 (hereafter: *Synechocystis*) [3]. Nitrogen starvation starts a well-orchestrated survival process in *Synechocystis*, called chlorosis [4]. During chlorosis, *Synechocystis* degrades not only its photosynthetic machinery, but also accumulates large quantities of biopolymers, namely glycogen and poly-hydroxy-butyrate (PHB) [5]. Glycogen synthesis following the onset of nitrogen starvation serves transiently as a major sink for newly fixed CO_2 [6] before CO_2 fixation is tuned down during prolonged nitrogen starvation. During resuscitation from chlorosis, a specific glycogen catabolic metabolism supports the re-greening of chlorotic cells [7]. By contrast to the pivotal role of glycogen, the function of the polymer PHB remains puzzling, since mutants impaired in PHB synthesis survived and recovered from chlorosis as awild-type [8,9]. Nevertheless, many different cyanobacterial species produce PHB, implying a hitherto unrecognized functional importance [10].

In other microorganisms PHB fulfills various functions during conditions of unbalanced nutrient availability and can also protect cells against low temperatures or redox stress [11–13]. Understanding the intracellular mechanisms that lead to PHB production could help to elucidate the physiological role of this polymer. Regardless of the physiological significance of PHB, this polymer has been recognized as a promising alternative for current plastics, which contaminate terrestrial and aquatic ecosystems [14]. PHB can serve as a basis for completely biodegradable plastics, with properties comparable to petroleum-derived plastics [15,16]. Since *Synechocystis* produces PHB only under nutrient limiting conditions, this phenomenon can be exploited to temporally separate the initial biomass production from PHB production induced by shifting cells to nitrogen limiting conditions [10].

One of the biggest obstacles preventing economic PHB production in cyanobacteria remains the low level of intracellular PHB accumulation [17]. While chemotrophic bacteria are capable of producing more than 80% PHB of their cell dry mass, (e.g., *Cupriavidus necator*), most cyanobacteria naturally produce less than 20% of their cell dry mass [15]. Additionally, their growth rate is too slow to compete with the PHB production in chemotrophic bacteria. There have been many attempts in the past to further improve the intracellular PHB production, often with limited [1] success [18–20]. One of the most successful approaches has been achieved by random mutagenesis, leading to up to 37% PHB of the cell dry mass [21]. However, more directed approaches involving genetic engineering are often limited by a lack of knowledge about how the cells' metabolism works in detail. For example, until today, it was still unknown from which carbon metabolites PHB was derived. There have been several different studies analyzing the intracellular fluxes in cyanobacteria [22]. However, most of them did not analyze the carbon flow during prolonged nitrogen starvation. One of these studies showed that in nitrogen-starved photosynthetically grown cyanobacteria up to 87% of the carbon in PHB is derived from intracellular carbon sources rather than from newly fixed CO_2 [23]. However, until now, it was not clearly resolved which metabolic routes provide the precursors for PHB synthesis. This knowledge would lay the foundation for future metabolic engineering approaches to create overproduction strains. Hence, the goal of this study was to find out where the carbon for the PHB production is coming from and which pathways it is taking until it reaches PHB.

It has been shown that disruption of PHB synthesis results in an increased production of glycogen; however, an overproduction of glycogen did not lead to higher amounts of PHB [24]. Another study that also investigated the accumulation of glycogen in a PHB-free mutant Δ*phaC*, could not detect any differences in growth or glycogen accumulation [8].

An important aspect in the issue concerning the relation between glycogen and PHB metabolism deals with the contribution of various carbon metabolic pathways for the production of precursors for PHB under conditions of nitrogen limitation. *Synechocystis* is able to catabolize glucose via three parallel operating glycolytic pathways [25] (Figure 1): the Embden-Meyerhof-Parnas (EMP) pathway, the oxidative pentose phosphate (OPP) pathway [26], and the Entner Doudoroff (ED) pathway [25]. When nitrogen-starved cells recover from chlorosis, they require the parallel operating OPP and ED pathways, whereas the EMP pathway seems dispensable [7]. Metabolic analysis of mutants overexpressing the transcriptional regulator *rre37* showed a correlated upregulation of PHB synthesis and EMP pathway genes (*phaAB* and *pfkA*, respectively) [27]. However, so far is has not been investigated, how important these pathways for the production of PHB during nitrogen starvation.

This work started with the initial aim to define whether PHB synthesis depends on the metabolism of glycogen. Since the initial results implied that PHB is strongly affected by glycogen catabolism, we further investigated the importance of the different carbon pathways EMP, ED and OPP for the production of PHB. These findings shall help to further understand the intracellular PHB metabolism in cyanobacteria, which can be used to create more efficient PHB overproduction strains, making the production of PHB as a bioplastic more cost efficient.

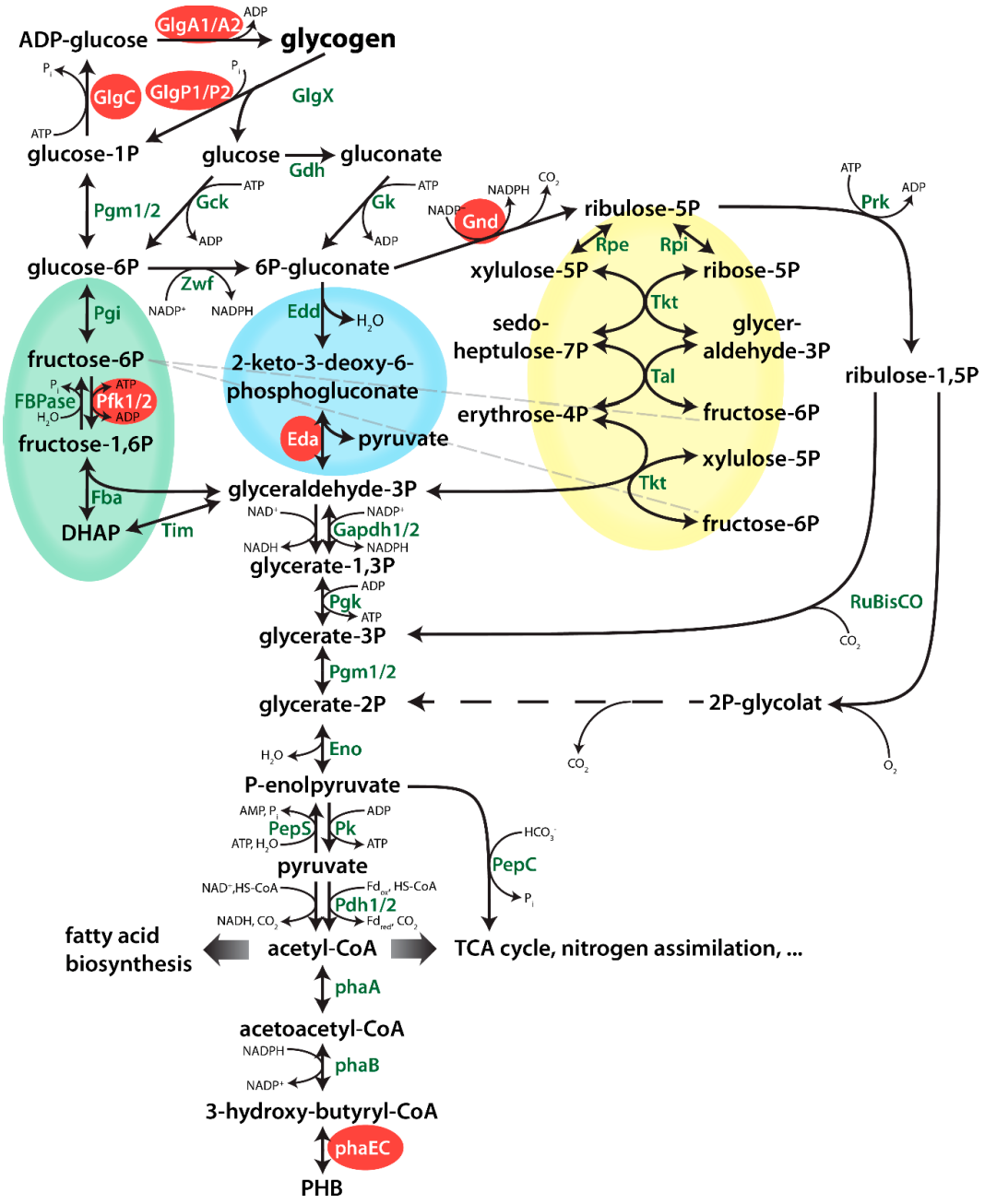

Figure 1. Overview of central metabolism of Synechocystis. Genes which were deleted in this study are highlighted in with a red background. Dotted lines represent several enzymatic reactions. The EMP, ED and OPP (Embden-Meyerhof-Parnas, Entner-DoudoroffOxidative Pentose Phosphate) pathways are highlighted in green, blue and yellow, respectively.

2. Results

Following the onset of nitrogen-starvation, large quantities of fixed carbon are stored in *Synechocystis* cells as glycogen granules. Long-term starvation experiments of *Synechocystis* cultures have shown that, while cells are chlorotic, glycogen is slowly degraded, following its initial rapid accumulation but PHB is slowly and steadily accumulating [9]. Considering that chlorotic cells are photosynthetically inactive, these data could indicate a potential correlation between the turn-over of glycogen and the synthesis of PHB. An overview of the metabolic pathways connecting the glycogen pool with PHB is shown in Figure 1. To substantiate the hypothesis that PHB might be derived from

glycogen turn-over, we investigated PHB accumulation in various mutant strains, in which key steps in different pathways are interrupted. The respective mutations are shown in Figure 1. All strains used in this work were characterized previously, with their phenotypes, including growth behaviours, described in the respective publications (see Table A1). Furthermore, all mutants used in these studies were fully segregated to ensure clear phenotypes.

2.1. Impact of Glycogen Synthesis on PHB Production

To analyze the role of glycogen synthesis on the production of PHB, we first analyzed the accumulation of these biopolymers during nitrogen starvation in mutants with defects in glycogen synthesis. The double mutant of the two glycogen synthase genes *glgA1* (*sll0945*) and *glgA2* (*sll1393*) is unable to acclimate to nitrogen deprivation and rapidly dies upon shifting cells to nitrogen free $BG11^0$ medium [8] and, therefore, could not be analyzed. Instead, we used a knockout mutant of the glucose-1-phosphate adenylyltransferase (*glgC*, *slr1176*) and two knockout strains of each of the isoforms of the glycogen synthase, *glgA1* (*sll0945*) and *glgA2* (*sll1393*). Yoo et al. [28] reported that the single *glgA1* and *glgA2* mutants were still able to produce similar amounts of glycogen as the wild-type (WT), since one glycogen synthase is still present, and this seems to be sufficient to reach the wild-type levels of glycogen. However, the structure of the glycogen produced by the two isoforms seemed to slightly differ in chain-length distribution [28]. In that study, no distinguishing phenotype of the two mutant strains had been reported. In the present study, the cultures were shifted to nitrogen free medium $BG11^0$ and further incubated under constant illumination of 40 µmol photons m^{-2} s^{-1}. Under these experimental conditions, the Δ*glgA1* mutant showed an impaired chlorosis reaction, whereas the Δ*glgA2* mutant performed chlorosis as the wild-type strain (Figure 2A). To further determine the viability of two weeks nitrogen-starved cells, serial dilutions were dropped on nitrate-supplemented BG11 plates. As shown in Figure 2B, the Δ*glgA1* mutant was severely impaired in recovering from nitrogen starvation, whereas Δ*glgA2* could recover from chlorosis with the same efficiency as the wild-type (Figure 2B).

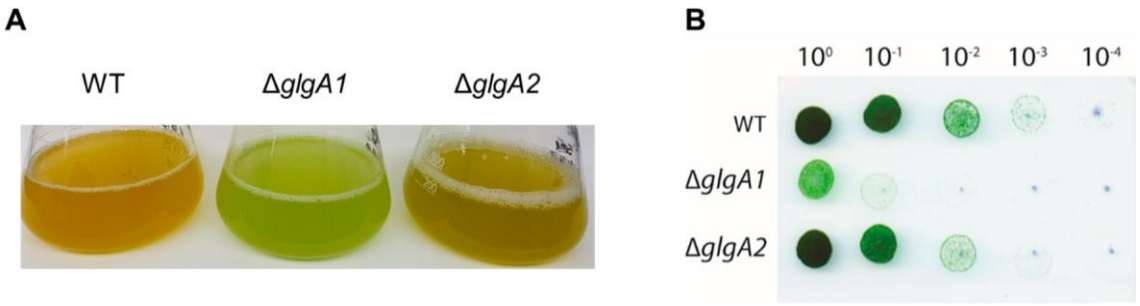

Figure 2. Characterization of the glycogen synthase mutants, Δ*glgA1* and Δ*glgA2*. (**A**) Cultures after five days of nitrogen starvation. (**B**) Recovery assay of chlorotic wild-type (WT) and mutants Δ*glgA1* and Δ*glgA2*, using the drop agar method. Cultures that were nitrogen-starved for 14 days were serially diluted from 1 to 1:10,000 and from each dilution, a drop of 5 µL was plated on BG11 agar and grown for seven days.

During the course of three weeks of nitrogen starvation, the quantities of PHB and glycogen that accumulate in the cells were determined (Figure 3A,B).

In the wild-type, the amount of glycogen already peaked after the first week and slowly decreased in the following two weeks (Figure 3B). As previously reported by Yoo et al. [28], the single Δ*glgA1* and Δ*glgA2* mutants initially accumulated similar amounts of glycogen to the wild-type, but in contrast to the wild-type, the level of glycogen remained high. The PHB content in the *glgA2* mutant was similar to the wild-type for the first seven days of nitrogen starvation, but PHB accumulation slowed down afterwards (Figure 3B). By contrast, the *glgA1* mutant was strongly impaired in PHB production. Together, the phenotype of the *glgA1* and *glgA2* mutants indicates that glycogen synthase GlgA1 plays

a much more important role in nitrogen starvation acclimation than GlgA2, although the amount of glycogen produced by these two strains is almost the same. One explanation could be that the subtle differences in the glycogen produced form the two isoenzymes might result in different functions, with GlgA1-produced glycogen being much more relevant for the maintenance metabolism in chlorotic cells and for the resuscitation from chlorosis than glycogen produced by GlgA2. In clear correlation with the redundant role of GlgA2, the *glgA2* mutant was not impaired in PHB synthesis, whereas mutation of the functionally important *glgA1* gene resulted in strongly impaired PHB synthesis.

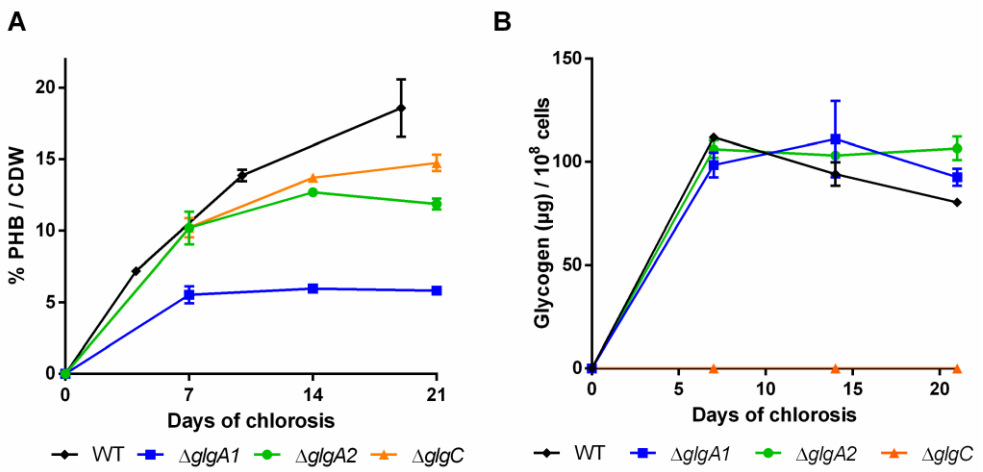

Figure 3. Polyhydroxybutyrate (PHB) content in percentage of cell dry weight (CDW) (**A**) and cellular glycogen content (**B**) of mutants impaired in the glycogen synthesis. Cultures were shifted to nitrogen free medium at day 0 and were subsequently grown for 21 days. Each point represents a mean of three independent biological replicates.

The *glgC* mutant was previously characterized by Grundel et al. [6]. They showed that Δ*glgC* is not able to perform a proper nitrogen-starvation acclimation response: it maintains its pigments while it loses viability, which was also observed in our experiments. Namakoshi et al. [29] showed that this mutant is unable to synthesize glycogen, which is also in line with our results. Under our conditions, unlike previously described by Damrow et al. [8], the *glgC* mutant did not show an increased amount of PHB compared to the WT, but seemed to accumulate less PHB instead (Figure 3A). It has to be noted though that Damrow et al. [8] investigated only one single timepoint, after seven days of nitrogen starvation. In addition, these results should be treated with care, since PHB content is normalized to cell dry weight, which shrinks in the *glgC* mutant due to progressive cell lysis. Consequently, the cell density was severely diminished at the end of the experiment (OD_{750} of 0.51, compared to ~1.15 of other mutants and the wild-type). The differences between our study and that of Damrow et al. [8] thus may result from differences in cell lysis rather than from differences in PHB synthesis. When the relatively low cell density of the *glgC* mutant is considered, it produces much less PHB per volume compared to the wild-type.

2.2. Impact of Glycogen Degradation on PHB Production

If glycogen turn-over would result in PHB accumulation during chlorosis, synthesis of PHB should be abrogated when glycogen degradation is impaired. To test this assumption, mutants in catabolic glycogen phosphorylase genes (*glgP*) were investigated with the same methods as described above. Glycogen can be degraded by the two glycogen phosphorylase isoenzymes, encoded by *glgP1* (slr1356) and *glgP2* (slr1367) [7]. A detailed study by Doello et al. [7] showed that GlgP2 is the main enzyme responsible for glycogen degradation during resuscitation from nitrogen chlorosis. Knocking out GlgP1 (Δ*glgP1*) does not affect the efficiency of recovery, whereas knocking out GlgP2 (Δ*glgP2*) or both phosphorylases (Δ*glgP1l2*) completely impairs the ability to degrade glycogen [7]. Here, we

investigated glycogen and PHB accumulation during three weeks of nitrogen starvation in these glycogen phosphorylases mutants.

Although the initial amount of glycogen was higher in the *glgP1* mutant compared to the WT (Figure 4B), the amount decreased during the course of the experiment. By contrast, no glycogen degradation occurred in the Δ*glgP2* and Δ*glgP1l2* double mutant. This correlates with the specific requirement of chlorotic cells for GlgP2 for resuscitation from nitrogen starvation, as it has been previously described [7].

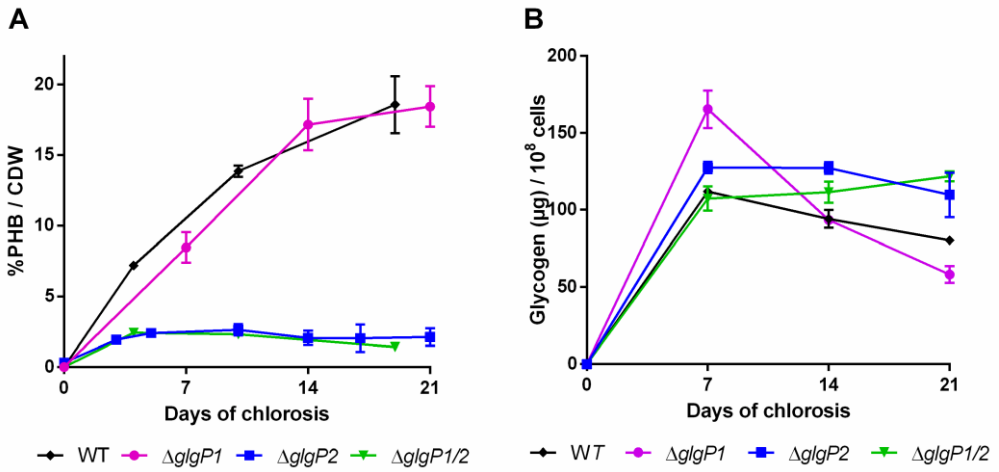

Figure 4. PHB content in percentage of cell dry weight (CDW) (**A**) and glycogen content (**B**) of mutants impaired in the glycogen degradation. Cultures were shifted to nitrogen free medium at day 0 and were subsequently grown for 21 days. Each point represents a mean of three independent biological replicates.

Intriguingly, the different mutants showed a drastic difference in the amounts of PHB being produced (Figure 4A): While the Δ*glgP1* strain produced similar amounts of PHB as the wild-type, a strong decrease was observed for the Δ*glgP2* strain. The same phenotype was observed for the double knockout mutant, indicating that origin of the effect is based on the absence of *glgP2*. The PHB synthesis phenotypes were further confirmed by fluorescence microscopy after staining PHB with Nile red (Figure 5). PHB granules appear as bright red fluorescing intracellular granular structures. In agreement with the results from PHB quantification by HPLC analysis, the Δ*glgP1* strain showed similar amounts and distribution of PHB granules than the wild-type. By contrast, only very small granules, if at all visible, could be detected in the strains Δ*glgP2* and Δ*glgP1l2*.

Altogether, the inability of the mutants Δ*glgP2* and Δ*glgP1l2* to accumulate PHB demonstrates unequivocally that glycogen catabolism through GlgP2 is required for the ongoing PHB synthesis during prolonged nitrogen starvation.

2.3. Impact of Mutations in Carbon Catabolic Pathway on PHB Production

The experiments outlined above revealed that specific glycogen synthesizing or degrading enzymes have a strong effect on the amounts of PHB being produced and that glycogen turn-over via GlgP2 provides the carbon skeletons for PHB synthesis. To investigate how the released glucose phosphate molecules are metabolized downstream of glycogen, knockouts of the three most important glycolytic routes [25] were checked for their PHB and glycogen production during chlorosis. While the strain Δ*eda* (*sll0107*) lacks the ability to metabolize molecules via the ED pathway, Δ*gnd* is not able to use the OPP pathway. Additionally, the strain Δ*pfk1l2* lacks both phosphofructokinases, which causes an interruption of the EMP pathway. Also, the individual knockouts of both isoforms, Δ*pfk1* and Δ*pfk2*, were investigated.

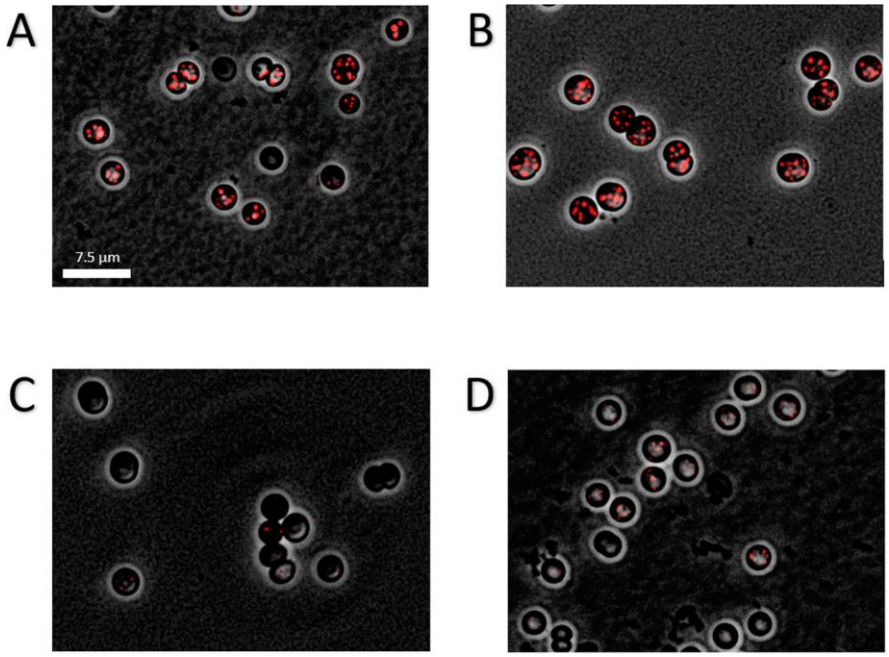

Figure 5. Fluorescence microscopic picture of Nile-red stained PHB granules in chlorotic cells. Cultures where grown for 14 days in nitrogen depleted medium BG11^0. Shown is an overlay of phase contrast with a CY3 channel of the WT (**A**), Δ*glgP1* (**B**), Δ*glgP2* (**C**) and Δ*glgP1l2* (**D**). Scale bar corresponds to 7.5 µm.

Again, the di**ff**erent mutant strains and a WT control were grown for three weeks under nitrogen deprived conditions and PHB and glycogen content was quantified (Figure 6).

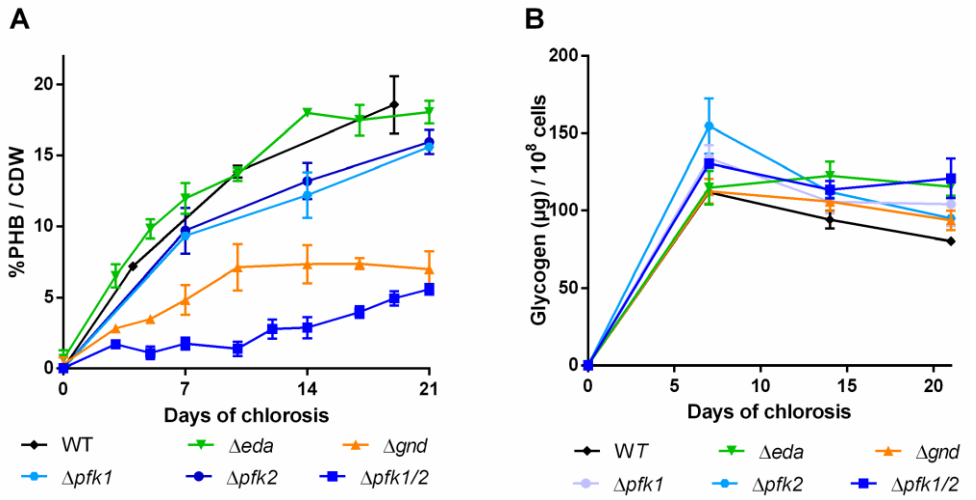

Figure 6. PHB content in percentage of cell dry weight (CDW) (**A**) and glycogen content (**B**) of mutants with disrupted carbon pathway. Cultures were shifted to nitrogen free medium at day 0 and were subsequently grown for 21 days. Each point represents a mean of three independent biological replicates.

Distortion of the ED pathway (Δ*eda*) did not result in any PHB phenotype different from the WT and the glycogen content remained high during the course of the experiment. In the Δ*gnd* mutant, a slower increase of PHB than in the WT was observed within the first ten days (Figure 6A) and PHB accumulation subsequently ceased. When the EMP pathway was blocked (Δ*pfk1l2*), only very little PHB was produced in the first two weeks of the chlorosis. Thereafter though, PHB production slightly

increased and finally reached similar levels as in the Δ*gnd* mutant. The total amount of glycogen over the time of chlorosis did not decrease in this mutant. The single Δ*pfk* mutants showed PHB contents similar to the WT, indicating that the two isoenzymes are able to replace each other's function. Taken together, it appears that EMP and OPP pathways contribute to PHB production, whereas the ED pathway does not play a role.

2.4. Impact of PHB Formation on Glycogen Synthesis

In order to check how the PHB production affects the accumulation of glycogen, a PHB-free mutant, namely Δ*phaEC*, was checked for its production of carbon polymers (Figure 7).

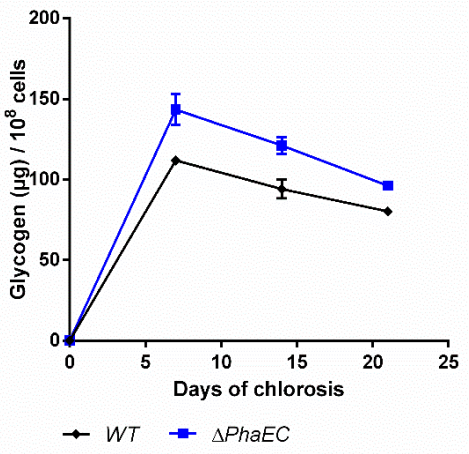

Figure 7. Glycogen content of wild-type and mutant lacking the PHB synthase genes (*PhaEC*). Cultures were shifted to nitrogen free medium at day 0 and were subsequently grown for 21 days. Each point represents a mean of three independent biological replicates.

As expected, the mutant was unable to synthesize PHB (data not shown [8]). Compared to the WT, the mutant produced moderately higher amounts of glycogen and degrades it slightly faster, so that at the end of the experiments, the glycogen levels were quite similar.

3. Discussion

As recently shown by isotope labeling experiments [23], the majority of the carbon from PHB is coming from intracellular metabolites, which contribute around 74% to the carbon within PHB. Additionally, a random mutagenized strain, which is an overproducer of PHB, shows also a strongly accelerated decay of glycogen [30]. Here, we provide clear evidence that the intracellular glycogen pool and its products provide the carbon metabolites for PHB synthesis during nitrogen starvation. In the absence of glycogen degradation, as it is the case in the Δ*glgP2* and the Δ*glgP1/2* double mutant, PHB synthesis is almost completely abrogated. In the Δ*glgP2* mutant, the remaining GlgP1 enzyme is apparently not efficiently catabolizing glycogen, which agrees with its lack of function for the resuscitation from chlorosis. By contrast, GlgP2 is required for glycogen catabolism and resuscitation from chlorosis [7]. From these data, it is reasonable to hypothesize that during chlorosis, GlgP2 slowly degrades glycogen, and the degradation products end up in the PHB pool.

Like the two glycogen phosphorylase isoenzymes, the two glycogen synthase isoenzymes GlgA1 and GlgA2 appear to have specialized functions. Even though both Δ*glgA1* and Δ*glgA2* synthesized similar amounts of glycogen, deletion of *glgA1* resulted in a mutant with reduced bleaching, viability and PHB content whereas Δ*glgA2* was less affected. This indicates that glycogen produced by GlgA1 is important for resuscitation and growth. On the other hand, GlgA2 produced glycogen appeared less important or its function is yet unknown. Previous publications did not see such a difference, which may be explained by a much shorter time of nitrogen starvation used in their study [6]. Taken together, those mutants (*glgP2* and Δ*glgA1*) that were less viable under nitrogen starvation, did also

synthesize less PHB. It remains to be demonstrated, if the different impact that GlgA1 and GlgA2 exert on viability and PHB synthesis originates from the slightly different branching patterns [28] of the glycogen, that they synthesize.

In the Δ*glgC* mutant, PHB is formed, although no glycogen is produced (Figure 3), which seems to contradict the hypothesis of glycogen-derived PHB [8,28]. Taking into account the above results, it appears likely that the carbon metabolites used for PHB can under certain conditions bypass the glycogen pool. When *glgC* is knocked out, glucose-1P (and its precursor, glucose-6P) cannot be further converted into ADP-glucose and may accumulate. The glucose-phosphates could then be downstream metabolized to glyceraldehyde-3P and further converted into PHB. By contrast, when *glgA1* is mutated, the newly fixed carbon can be converted by GlgC to ADP-glucose and subsequently enters the GlgA2-synthesized inactive glycogen pool, where it cannot be further metabolized into PHB. A similar connection between PHB and glycogen has already been described in other organisms (*Sinorhizobium meliloti*), where PHB levels were lower in a mutant lacking *glgA1* [31]. Since the GlgA1/GlgA2 double mutant rapidly dies upon nitrogen starvation [6], the impact of the complete absence of glycogen due to glycogen synthase deficiency on PHB synthesis cannot be experimentally tested.

Furthermore, we observed that a slower degradation of glycogen often correlates with a low-PHB-phenotype, as seen in the case of Δ*glgA1*, Δ*glgP2*, Δ*glgP1/2* and Δ*pfk1/2* (Figures 3, 4 and 6, respectively). This further supports the hypothesis, that only when glycogen gets degraded during the process of chlorosis, PHB is formed. In two cases, Δ*glgP1/2* and Δ*pfk1/2*, the amount of glycogen was even increasing during the later course of nitrogen starvation. This hints towards an ongoing glycogen formation during nitrogen chlorosis, which gets only visible once glycogen degradation is disturbed. Apparently, glycogen metabolism is much more dynamic than presumed from the relative static pool size observed in the wild-type. A steady glycogen synthesis may be counterbalanced by ongoing degradation, together resulting in only a slow net change of its pool size.

The residual metabolism in nitrogen starved chlorotic cells [9,32] is probably required to ensure long-term survival through repair of essential biomolecules such as proteins, DNA and RNA, osmoregulation, regulated shifts in metabolic pathways and the preparation for a quick response as soon as nutrients are available again [33,34]. According to these needs, non-growing starved cells still require a constant supply of ATP, reduction equivalents and the ability to produce cellular building blocks for survival. In line with this, we observed that PHB production was mainly achieved via the EMP pathway, which has the highest ATP yield among the three main carbon catalytic pathways (EMP, OPP, ED). In addition, we found that the OPP pathway is involved in PHB synthesis as well. This pathway provides metabolites for biosynthetic purposes as the repair of biomolecules for maintenance. By contrast, deletion of the ED pathway, which has a lower ATP yield in comparison to the EMP pathway and is physiologically probably most important in connection with photosynthesis and the Calvin–Benson cycle [7,25], did not impair PHB production under nitrogen starvation. Nevertheless, the glycogen levels did not decrease in the Δ*gnd* mutant, implying that mutation of the ED pathway affects the dynamics of glycogen turn-over discussed above.

Finally, we observed that the various carbon catabolic pathways have different functional importance for PHB production, in a time-dependent manner: While the mutant Δ*gnd* (blocking the OPP pathway) produced PHB in the first phase of the experiment but later stopped its synthesis, the Δ*pfk1/2* mutant (impaired in the EMP pathway) was initially blocked in PHB accumulation but later started to produce it (Figure 4). Interestingly, the time point, at which the Δ*gnd* mutant stopped PHB production matched its start in the Δ*pfk1/2* mutant. This could indicate a consecutive role of EMP and OPP pathway during nitrogen chlorosis. Although the exact function of the EMP pathway remains unknown, we show here for the first time a phenotype of a cyanobacterial mutant lacking this pathway. This suggested to also investigate the deletion of the individual knockouts. Deletion of only one of the Pfk isoenzymes (*pfk1*: sll1196 and *pfk2*: sll0745) resulted in mutants that produced about 80% of the PHB of WT cells, whereas the PHB production of the double mutant Δ*pfk1/2* was severely reduced. Pfk1 and Pfk2 can thus obviously compensate for the loss of the respective other, even though PHB

production is highest if both enzymes are present. This observation is well in line with transcriptomic studies, which detected an increase in expression of both Pfk isoenzymes during nitrogen starvation [5]. The observation that both EMP and OPP pathway are of importance during arrested growth under nitrogen starvation is in agreement with earlier investigations that reported the upregulation of the sugar catabolic genes *pfk1*, *pfk2*, *zwf*, *gnd* and *gap1* concomitantly with glycogen accumulation [5,35]. EMP and OPP pathway thus support PHB production in non-growing, nitrogen-starved cells, whereas ED and OPP pathway are most important during resuscitation form nitrogen chlorosis after feeding the cells with nitrate [7].

The mutant Δ*phaEC* did not produce any PHB and degraded glycogen similarly to the WT (Figure 7). This indicates that there is no direct feedback between these two polymer pools. In the absence of PHB synthesis, metabolites form glycogen degradation could be leaked by overflow reactions. Under unbalanced metabolic situations, it has been shown that cyanobacteria can excrete metabolites into the medium to control their intracellular energy status [6,36,37]. In any case, this result demonstrates that PHB and glycogen do not compete for CO_2 fixation products, but glycogen is epistatic over PHB synthesis.

Previous studies showed that, under nitrogen starvation, certain genes are upregulated, which are under the regulation of SigE, a group 2 σ factor [38]. Among these genes are glycogen degrading enzymes like *glgP1* and *glgP2* and *glgX*, but also the key enzymes for the pathways further downstream, namely *pfk* and *gnd*. The fact that all these genes are expressed simultaneously with the genes of the PHB synthesis [9], demonstrate that all relevant transcripts of the key enzymes required for the conversion from glycogen to PHB are present during nitrogen starvation. Our finding that PHB is mainly synthesized from glycogen degradation during nitrogen chlorosis is supported by a recent study, where a *Synechocystis* sp. PCC 6714 strain with enhanced PHB accumulation was created by random mutagenesis. Transcriptome analysis revealed that this strain exhibits an increased expression of glycogen phosphorylase [21]. This indicates that manipulation of glycogen metabolism may be a key for improved PHB synthesis.

Gaining further insights into the intracellular carbon fluxes could provide more information on how PHB production is regulated. Once the regulation is understood, this knowledge could be used to redirect the large quantities of glycogen towards PHB. This knowledge could be used in metabolic engineering approaches to either completely reroute the carbon from glycogen (making up more than 60% of the CDW) to PHB, for example by overexpression of glycogen degrading enzymes, or even from inorganic carbon to PHB directly. Therefore, the new insights from this work can be exploited for biotechnological applications to further increase the amounts of PHB being produced in cyanobacteria.

4. Materials and Methods

4.1. Cyanobacterial Cultivation Conditions

For standard cultivation, *Synechocystis* sp. PCC 6803 cells were grown in 200 mL BG_{11} medium, supplemented with 5 mM $NaHCO_3$ [39]. A list of the used strains of this study is provided in Table A1. Two different wild-type strains, a Glc sensitive and a Glc tolerant one, were used. Both strains showed the same behavior during normal growth as well as during chlorosis. Appropriate antibiotics were added to the different mutants to ensure the continuity of the mutation. The cells were cultivated at 28 °C, shaking at 120 rpm and constant illumination of 40–50 µmol photons m^{-2} s^{-1}. Nitrogen starvation was induced as described previously [40]. In short, exponentially growing cells (OD 0.4–0.8) were centrifuged for 10 min at 4000 *g*. The cells were washed in 100 mL of BG_0 (BG_{11} medium without $NaNO_3$) before they were centrifuged again. The resulting pellet was resuspended in BG_0 until it reached an OD of 0.4.

4.2. Microscopy and Staining Procedures

To observe PHB granules within the cells, 100 µL of cyanobacterial cells were centrifuged (1 min at 10,000× *g*) and 80 µL of the supernatant discarded. Nile Red (10 µL) was added and used to resuspend the pellet in the remaining 20 µL of the supernatant. From these mixtures, 10 µL were taken and applied on an agarose coated microscope slide to immobilize the cells. The Leica DM5500B microscope (Leica, Wetzlar, Germany) was used with a 100× /1.3 oil objective for fluorescence microscopy. To detect Nile red stained PHB granules, an excitation filter BP 535/50 was used, together with a suppression filter BP 610/75. A Leica DFC360FX (Leica, Wetzlar, Germany)) was used for image acquisition.

4.3. PHB Quantification

PHB content within the cells was determined as described previously [41]. Roughly 15 mL of cells were harvested and centrifuged at 4000 *g* for 10 min at 25 °C. The resulting pellet was dried for 3 h at 60 °C in a speed-vac (Christ, Osterode, Germany), before 1 mL of concentrated H_2SO_4 was added and boiled for 1 h at 100 °C to break up the cells and to convert PHB to crotonic acid. From this, 100 µL were taken and diluted in 900 µL 0.014 M H_2SO_4. To remove cell debris, the samples were centrifuged for 10 min at 10,000 *g*, before 500 µL of the supernatant were transferred to 500 µL 0.014 M H_2SO_4. After an additional centrifugation step with the same conditions as above, the supernatant was used for HPLC analysis on a Nucleosil 100 C 18 column (Agilent, Santa Clara, CA, USA) (125 by 3 mm). As a liquid phase, 20 mM phosphate buffer (pH 2.5) was used. Commercially available crotonic acids was used as a standard with a conversion ratio of 0.893. The amount of crotonic acid was detected at 250 nm.

4.4. Glycogen Quantification

Intracellular glycogen content was measured by harvesting 2 mL of cyanobacterial culture. The cells were washed twice with 1 mL of ddH_2O. Afterwards the pellet was resuspended in 400 µL KOH (30% *w/v*) and incubated for 2 h at 95 °C. For the subsequent glycogen precipitation, 1200 µL ice cold ethanol (final concentration of 70%) were added. The mixture was incubated at –20 °C for 2–24 h. Next, the solution was centrifuged at 4 °C for 10 min at 10,000 *g*. The pellet was washed twice with 70% and 98% ethanol and dried in a speed-vac for 20 min at 60 °C. Next, the pellet was resuspended in 1 mL of 100 mM sodium acetate (pH 4.5) and 8 µL of an amyloglucosidase solution (4.4 U/µL) were added. For the enzymatic digest, the cells were incubated at 60 °C for 2 h. For the spectrometical glycogen determination, 200 µL of the digested mixture was used and added to 1 mL of O-toluidine-reagent (6% O-toluidine in 100% acetic acid). The tubes were incubated for 10 min at 100 °C. The samples were cooled down on ice for 3 min, before the OD_{635} was measured. The final result was normalized to the cell density at OD_{750}, where OD_{750} = 1 represents 10^8 cells. A glucose standard curve was used to calculate the glucose contents in the sample from their OD540.

4.5. Drop Agar Method

Serial dilutions of chlorotic cultures were prepared (10^0, 10^{-1}, 10^{-2}, 10^{-3}, 10^{-4} and 10^{-5}) starting with an OD_{750} of 1. Five microliters of these dilutions were dropped on solid BG_{11} agar plates and cultivated at 50 µmol photons m^{-2} s^{-1} and 27 °C for 7 days.

Author Contributions: Conceptualization, M.K. and K.F.; Methodology, M.K., S.D. and K.F.; Investigation, M.K. and S.D.; Writing-Original Draft Preparation, M.K., S.D. and K.F.; Writing-Review & Editing, M.K., S.D., K.G. and K.F.; Supervision, K.F.; Project Administration, M.K. and K.F.

Funding: This research was funded by the Studienstiftung des Deutschen Volkes and the RTG 1708 "Molecular principles of bacterial survival strategies". We acknowledge support by Deutsche Forschungsgemeinschaft and Open Access Publishing Fund of University of Tübingen.

Acknowledgments: We would like to thank Yvonne Zilliges for providing the mutants Δ*glgA1*, Δ*glgA2* and Δ*glgC*. Furthermore, we thank Eva Nussbaum for maintaining the strain collection and Andreas Kulick for assistance with HPLC analysis.

Conflicts of Interest: The authors declare no conflict of interest.

Appendix A

Table A1. List of used strains.

Strain	Background	Relevant Marker of Genotype	Reference
Synechocystis sp. PCC 6803 GS	GS	-	Pasteur culture collection
Synechocystis sp. PCC 6803 GT	GT	-	Chen et al. 2016
Δ*glgA1*	GT	*sll0945::kmR*	Gründel et al. 2012
Δ*glgA2*	GT	*sll1393::cmR*	Gründel et al. 2012
Δ*glgC*	GT	*slr1176::cmR*	Damrow et al. 2012
Δ*glgP1*	GS	*sll1356::kmR*	Doello et al. 2018
Δ*glgP2*	GS	*slr1367::spR*	Doello et al. 2018
Δ*glgP1l2*	GS	*sll1356::kmR*, *slr1367::spR*	Doello et al. 2018
Δ*eda*	GT	*sll0107::gmR*	Chen et al. 2016
Δ*gnd*	GT	*sll0329::gmR*	Chen et al. 2016
Δ*pfkB1l2*	GT	*sll1196::kmR*, *sll0745::spR*	Chen et al. 2016
Δ*phaEC*	GS	*slr1829*, *slr1830::kmR*	Klotz et al. 2016

References

1. Soo, R.M.; Hemp, J.; Parks, D.H.; Fischer, W.W.; Hugenholtz, P. On the origins of oxygenic photosynthesis and aerobic respiration in Cyanobacteria. *Science* **2017**, *355*, 1436–1440. [CrossRef] [PubMed]
2. Vitousek, P.M.; Howarth, R.W. Nitrogen Limitation on Land and in the Sea—How Can. It Occur. *Biogeochemistry* **1991**, *13*, 87–115. [CrossRef]
3. Kaneko, T.; Tanaka, A.; Sato, S.; Kotani, H.; Sazuka, T.; Miyajima, N.; Sugiura, M.; Tabata, S. Sequence analysis of the genome of the unicellular cyanobacterium *Synechocystis* sp. strain PCC6803. I. Sequence features in the 1 Mb region from map positions 64% to 92% of the genome. *DNA Res.* **1995**, *2*, 153–166. [CrossRef]
4. Forchhammer, K.; Schwarz, R. Nitrogen chlorosis in unicellular cyanobacteria—a developmental program for surviving nitrogen deprivation. *Environ. Microbiol.* **2018**. [CrossRef] [PubMed]
5. Osanai, T.; Oikawa, A.; Shirai, T.; Kuwahara, A.; Iijima, H.; Tanaka, K.; Ikeuchi, M.; Kondo, A.; Saito, K.; Hirai, M.Y. Capillary electrophoresis-mass spectrometry reveals the distribution of carbon metabolites during nitrogen starvation in *Synechocystis* sp. PCC 6803. *Environ. Microbiol.* **2014**, *16*, 512–524. [CrossRef] [PubMed]
6. Grundel, M.; Scheunemann, R.; Lockau, W.; Zilliges, Y. Impaired glycogen synthesis causes metabolic overflow reactions and affects stress responses in the cyanobacterium *Synechocystis* sp. PCC 6803. *Microbiology* **2012**, *158*, 3032–3043. [CrossRef] [PubMed]
7. Doello, S.; Klotz, A.; Makowka, A.; Gutekunst, K.; Forchhammer, K. A Specific Glycogen Mobilization Strategy Enables Rapid Awakening of Dormant Cyanobacteria from Chlorosis. *Plant Physiol.* **2018**, *177*, 594–603. [CrossRef]
8. Damrow, R.; Maldener, I.; Zilliges, Y. The Multiple Functions of Common Microbial Carbon Polymers, Glycogen and PHB, during Stress Responses in the Non-Diazotrophic Cyanobacterium *Synechocystis* sp. PCC 6803. *Front. Microbiol.* **2016**, *7*, 966. [CrossRef]
9. Klotz, A.; Georg, J.; Bučinská, L.; Watanabe, S.; Reimann, V.; Januszewski, W.; Sobotka, R.; Jendrossek, D.; Hess, W.R.; Forchhammer, K. Awakening of a Dormant Cyanobacterium from Nitrogen Chlorosis Reveals a Genetically Determined Program. *Curr. Biol.* **2016**, *26*, 2862–2872. [CrossRef]
10. Ansari, S.; Fatma, T. Cyanobacterial Polyhydroxybutyrate (PHB): Screening, Optimization and Characterization. *PLoS ONE* **2016**, *11*, e0158168. [CrossRef]
11. Nowroth, V.; Marquart, L.; Jendrossek, D. Low temperature-induced viable but not culturable state of Ralstonia eutropha and its relationship to accumulated polyhydroxybutyrate. *FEMS Microbiol. Lett.* **2016**, *363*, fnw249. [CrossRef]

12. Batista, M.B.; Teixeira, C.S.; Sfeir, M.Z.T.; Alves, L.P.S.; Valdameri, G.; Pedrosa, F.O.; Sassaki, G.L.; Steffens, M.B.R.; de Souza, E.M.; Dixon, R.; et al. PHB Biosynthesis Counteracts Redox Stress in Herbaspirillum seropedicae. *Front. Microbiol.* **2018**, *9*, 472. [CrossRef] [PubMed]
13. Urtuvia, V.; Villegas, P.; González, M.; Seeger, M. Bacterial production of the biodegradable plastics polyhydroxyalkanoates. *Int. J. Biol. Macromol.* **2014**, *70*, 208–213. [CrossRef] [PubMed]
14. Li, W.C.; Tse, H.F.; Fok, L. Plastic waste in the marine environment: A review of sources, occurrence and effects. *Sci. Total Environ.* **2016**, *566*, 333–349. [CrossRef] [PubMed]
15. Drosg, B.; Gattermayr, F.; Silvestrini, L. Photo-autotrophic Production of Poly(hydroxyalkanoates) in Cyanobacteria. *Chem. Biochem. Eng. Q.* **2015**, *29*, 145–156. [CrossRef]
16. Martin, K.; Lukas, M. Cyanobacterial Polyhydroxyalkanoate Production: Status Quo and Quo Vadis? *Curr. Biotechnol.* **2015**, *4*, 464–480.
17. Singh, A.; Sharma, L.; Mallick, N.; Mala, J. Progress and challenges in producing polyhydroxyalkanoate biopolymers from cyanobacteria. *J. Appl. Phycol.* **2017**, *29*, 1213–1232.
18. Lau, N.S.; Foong, C.P.; Kurihara, Y.; Sudesh, K.; Matsui, M. RNA-Seq Analysis Provides Insights for Understanding Photoautotrophic Polyhydroxyalkanoate Production in Recombinant *Synechocystis* sp. *PLoS ONE* **2014**, *9*, e86368. [CrossRef]
19. Khetkorn, W.; Incharoensakdi, A.; Lindblad, P.; Jantaro, S. Enhancement of poly-3-hydroxybutyrate production in *Synechocystis* sp. PCC 6803 by overexpression of its native biosynthetic genes. *Bioresour. Technol.* **2016**, *214*, 761–768. [CrossRef]
20. Carpine, R. Genetic engineering of *Synechocystis* sp. PCC6803 for poly-β-hydroxybutyrate overproduction. *Algal Res. Biomass Biofuels Bioprod.* **2017**, *25*, 117–127. [CrossRef]
21. Kamravamanesh, D.; Kovacs, T.; Pflügl, S.; Druzhinina, I.; Kroll, P.; Lackner, M.; Herwig, C. Increased poly-beta-hydroxybutyrate production from carbon dioxide in randomly mutated cells of cyanobacterial strain *Synechocystis* sp. PCC 6714: Mutant generation and characterization. *Bioresour. Technol.* **2018**, *266*, 34–44. [CrossRef]
22. Steuer, R.; Knoop, H.; Machné, R. Modelling cyanobacteria: From metabolism to integrative models of phototrophic growth. *J. Exp. Bot.* **2012**, *63*, 2259–2274. [CrossRef]
23. Dutt, V.; Srivastava, S. Novel quantitative insights into carbon sources for synthesis of poly hydroxybutyrate in Synechocystis PCC 6803. *Photosynth. Res.* **2018**, *136*, 303–314. [CrossRef]
24. Rajendran, V.; Incharoensakdi, A. Disruption of polyhydroxybutyrate synthesis redirects carbon flow towards glycogen synthesis in *Synechocystis* sp. PCC 6803 overexpressing glgC/glgA. *Plant Cell Physiol.* **2018**, *59*, 2020–2029.
25. Chen, X.; Schreiber, S.; Appel, J.; Makowka, A.; Fähnrich, B.; Roettger, M.; Hajirezaei, M.R.; Sönnichsen, F.D. The Entner-Doudoroff pathway is an overlooked glycolytic route in cyanobacteria and plants. *Proc. Natl. Acad. Sci. USA* **2016**, *113*, 5441–5446. [CrossRef]
26. Yu, J.; Liberton, M.; Cliften, P.F.; Head, R.D.; Jacobs, J.M.; Smith, R.D.; Koppenaal, D.W.; Brand, J.J.; Pakrasi, H.B. Synechococcus elongatus UTEX 2973, a fast growing cyanobacterial chassis for biosynthesis using light and CO2. *Sci. Rep.* **2015**, *5*, 8132. [CrossRef] [PubMed]
27. Osanai, T.; Oikawa, A.; Numata, K.; Kuwahara, A.; Iijima, H.; Doi, Y.; Saito, K.; Hirai, M.Y. Pathway-level acceleration of glycogen catabolism by a response regulator in the cyanobacterium Synechocystis species PCC 6803. *Plant Physiol.* **2014**, *164*, 1831–1841. [CrossRef] [PubMed]
28. Yoo, S.H.; Lee, B.H.; Moon, Y.; Spalding, M.H.; Jane, J.L. Glycogen Synthase Isoforms in *Synechocystis* sp. PCC6803: Identification of Different Roles to Produce Glycogen by Targeted Mutagenesis. *PLoS ONE* **2014**, *9*, e91524. [CrossRef]
29. Namakoshi, K.; Nakajima, T.; Yoshikawa, K.; Toya, Y.; Shimizu, H. Combinatorial deletions of glgC and phaCE enhance ethanol production in *Synechocystis* sp. PCC 6803. *J. Biotechnol.* **2016**, *239*, 13–19. [CrossRef]
30. Kamravamanesh, D.; Slouka, C.; Limbeck, A.; Lackner, M.; Herwig, C. Increased carbohydrate production from carbon dioxide in randomly mutated cells of cyanobacterial strain *Synechocystis* sp. PCC 6714: Bioprocess. understanding and evaluation of productivities. *Bioresour. Technol.* **2019**, *273*, 277–287. [CrossRef] [PubMed]
31. Wang, C.X.; Saldanha, M.; Sheng, X.; Shelswell, K.J.; Walsh, K.T.; Sobral, B.W.; Charles, T.C. Roles of poly-3-hydroxybutyrate (PHB) and glycogen in symbiosis of Sinorhizobium meliloti with *Medicago* sp. *Microbiology* **2007**, *153*, 388–398. [CrossRef] [PubMed]

32. Sauer, J.; Schreiber, U.; Schmid, R.; Völker, U.; Forchhammer, K. Nitrogen starvation-induced chlorosis in Synechococcus PCC 7942. Low-level photosynthesis as a mechanism of long-term survival. *Plant Physiol.* **2001**, *126*, 233–243. [CrossRef][PubMed]
33. Lever, M.A.; Rogers, K.L.; Lloyd, K.G.; Overmann, J.; Schink, B.; Thauer, R.K.; Hoehler, T.M.; Jørgensen, B.B. Life under extreme energy limitation: A synthesis of laboratory- and field-based investigations. *FEMS Microbiol. Rev.* **2015**, *39*, 688–728. [CrossRef]
34. Kempes, C.P.; van Bodegom, P.M.; Wolpert, D.; Libby, E.; Amend, J.; Hoehler, T. Drivers of Bacterial Maintenance and Minimal Energy Requirements. *Front. Microbiol.* **2017**, *8*, 31. [CrossRef]
35. Osanai, T.; Azuma, M.; Tanaka, K. Sugar catabolism regulated by light- and nitrogen-status in the cyanobacterium *Synechocystis* sp. PCC 6803. *Photochem. Photobiol. Sci.* **2007**, *6*, 508–514. [CrossRef] [PubMed]
36. Cano, M.; Holland, S.C.; Artier, J.; Burnap, R.L.; Ghirardi, M.; Morgan, J.A.; Yu, J. Glycogen Synthesis and Metabolite Overflow Contribute to Energy Balancing in Cyanobacteria. *Cell Rep.* **2018**, *23*, 667–672. [CrossRef]
37. Benson, P.J.; Purcell-Meyerink, D.; Hocart, C.H.; Truong, T.T.; James, G.O.; Rourke, L.; Djordjevic, M.A.; Blackburn, S.I.; Price, G.D. Factors Altering Pyruvate Excretion in a Glycogen Storage Mutant of the Cyanobacterium, Synechococcus PCC7942. *Front. Microbiol.* **2016**, *7*, 475. [CrossRef]
38. Osanai, T.; Kanesaki, Y.; Nakano, T.; Takahashi, H.; Asayama, M.; Shirai, M.; Kanehisa, M.; Suzuki, I.; Murata, N.; Tanaka, K. Positive regulation of sugar catabolic pathways in the cyanobacterium *Synechocystis* sp. PCC 6803 by the group 2 sigma factor sigE. *J. Biol. Chem.* **2005**, *280*, 30653–30659. [CrossRef]
39. Rippka, R.; Deruelles, D.; Waterbury, J.B.; Herdman, M.; Stanier, R.Y. Generic Assignments, Strain Histories and Properties of Pure Cultures of Cyanobacteria. *J. Gen. Microbiol.* **1979**, *111*, 1–61. [CrossRef]
40. Schlebusch, M.; Forchhammer, K. Requirement of the Nitrogen Starvation-Induced Protein Sll0783 for Polyhydroxybutyrate Accumulation in *Synechocystis* sp. Strain PCC 6803. *Appl. Environ. Microbiol.* **2010**, *76*, 6101–6107. [CrossRef]
41. Taroncher-Oldenburg, G.; Nishina, K.; Stephanopoulos, G. Identification and analysis of the polyhydroxyalkanoate-specific beta-ketothiolase and acetoacetyl coenzyme A reductase genes in the cyanobacterium *Synechocystis* sp. strain PCC6803. *Appl. Environ. Microbiol.* **2000**, *66*, 4440–4448. [CrossRef] [PubMed]

3. Publication 3 (Accepted)

Research article

Sofía Doello, Markus Burkhardt, and Karl Forchhammer

The essential role of sodium bioenergetics and ATP homeostasis in the developmental transitions of a cyanobacterium.

2021. *Current Biology.* 20, 31, 1-10

Current Biology

The essential role of sodium bioenergetics and ATP homeostasis in the developmental transitions of a cyanobacterium

Graphical Abstract

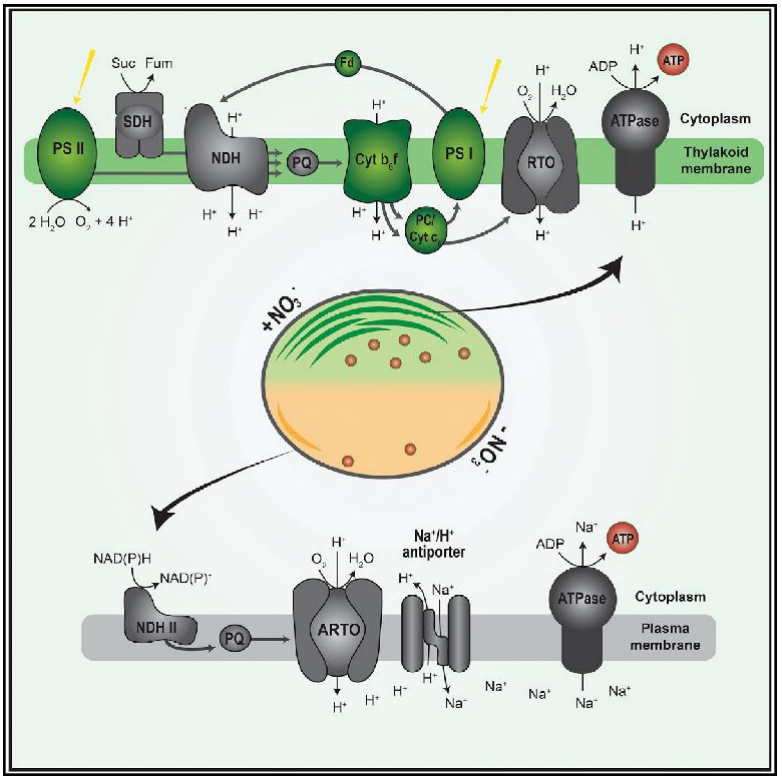

Highlights

- *Synechocystis* engages sodium bioenergetics during nitrogen starvation
- Sodium-dependent ATP synthesis is only essential during metabolic dormancy
- ATP levels are finely tuned according to the metabolic requirements

Authors

Sofia Doello, Markus Burkhardt, Karl Forchhammer

Correspondence

karl.forchhammer@uni-tuebingen.de

In Brief

How do dormant cells obtain energy to survive and resume growth after prolonged nutrient starvation? Doello et al. use nitrogen-starved *Synechocystis* cells to investigate the regulation of ATP homeostasis during dormancy and unravel a critical role for sodium bioenergetics and a precise regulation of the energy metabolism in dormant cells.

Doello et al., 2021, Current Biology *31*, 1606–1615
April 26, 2021
https://doi.org/10.1016/j.cub.2021.01.065

CellPress
OPEN ACCESS

Current Biology

Article

The essential role of sodium bioenergetics and ATP homeostasis in the developmental transitions of a cyanobacterium

Sofia Doello,[1] Markus Burkhardt,[1] and Karl Forchhammer[1,2,*]
[1]Interfaculty Institute of Microbiology and Infection Medicine, University of Tübingen, Auf der Morgenstelle 28, 72076 Tübingen, Germany
[2]Lead contact
*Correspondence: karl.forchhammer@uni-tuebingen.de
https://doi.org/10.1016/j.cub.2021.01.065

SUMMARY

The ability to resume growth after a dormant period is an important strategy for the survival and spreading of bacterial populations. Energy homeostasis is critical in the transition into and out of a quiescent state. *Synechocystis* sp. PCC 6803, a non-diazotrophic cyanobacterium, enters metabolic dormancy as a response to nitrogen starvation. We used *Synechocystis* as a model to investigate the regulation of ATP homeostasis during dormancy, and we unraveled a critical role for sodium bioenergetics in dormant cells. During nitrogen starvation, cells reduce their ATP levels and engage sodium bioenergetics to maintain the minimum ATP content required for viability. When nitrogen becomes available, energy requirements rise, and cells immediately increase ATP levels, employing sodium bioenergetics and glycogen catabolism. These processes allow them to restore the photosynthetic machinery and resume photoautotrophic growth. Our work reveals a precise regulation of the energy metabolism essential for bacterial survival during periods of nutrient deprivation.

INTRODUCTION

Dormant micro-organisms are vastly represented in natural environments.[1] Dormancy highly contributes to the survival of bacterial populations, the spreading of pathogens, and the development of antibiotic resistances.[2] The molecular processes that lead bacterial cells into a dormant state are diverse but generally characterized by growth arrest and residual metabolic activity.[3] Despite having a reduced metabolism, dormant cells still require energy for maintenance.[1] In fact, energy homeostasis is critical for the survival of dormant cells.[3] However, how the energy metabolism is regulated when bacterial cells enter and exit periods of dormancy is to date poorly understood.

Cyanobacteria represent a diverse group of prokaryotes endowed with the ability to adapt to changing environmental conditions, which has allowed them to colonize a wide range of ecosystems.[4] One of the most common hurdles cyanobacteria face in natural environments is limitation of combined nitrogen.[5] *Synechocystis* sp. PCC 6803 (*Synechocystis*) is a non-diazotrophic cyanobacterial strain that survives periods of nitrogen starvation by entering metabolic quiescence, thus representing a good model to study fundamental aspects of bacterial dormancy.[6] *Synechocystis* can survive prolonged periods of nitrogen starvation by undergoing nitrogen-chlorosis, a process characterized by the degradation of most of the thylakoid membranes. Cells enter cell cycle arrest and shut down their metabolism. Most of the photosynthetic apparatus is degraded, leaving cells with residual photosynthetic capacity, and energetically costly processes, like anabolic reactions, are halted.[6] In this resting state, the intracellular ATP concentration is about ¼ of the level during vegetative growth.[7] In addition, as cells degrade most of their cellular components, they synthesize reserve polymers, which are essential for exiting dormancy and resuming growth. Glycogen is the main storage molecule during nitrogen starvation: its synthesis and degradation are crucial for cell survival under these conditions.[6–8]

When nitrogen becomes available to dormant cells, they immediately initiate a highly organized resuscitation program.[6,9] During the first stages of the resuscitation process, cells catabolize the accumulated glycogen to obtain energy and metabolic intermediates to restore the previously degraded cellular components. When the photosynthetic machinery is restored, cells switch back to phototrophic metabolism.[6] Upon nitrogen addition, the energy requirement of chlorotic cells suddenly increases due to the initiation of anabolic reactions, such as the glutamine synthetase/glutamate synthase (GS/GOGAT) reaction cycle. Concomitantly with the increased energy demand, the low ATP content of dormant cells rapidly increases to an intermediate level, which represents approximately 50% of the ATP content of a vegetative growing cell.[7] So far, how dormant cells produce this ATP has remained unknown. Intriguingly, we observed a rapid increase in ATP levels also in mutant cells unable to degrade glycogen.[7] This observation prompted us to investigate the source of the rise in ATP content in resuscitating cells. The aim of this study was to reveal how dormant cells maintain the required ATP levels to keep viability and how they obtain the necessary energy to awaken from dormancy.

Current Biology *31*, 1606–1615, April 26, 2021

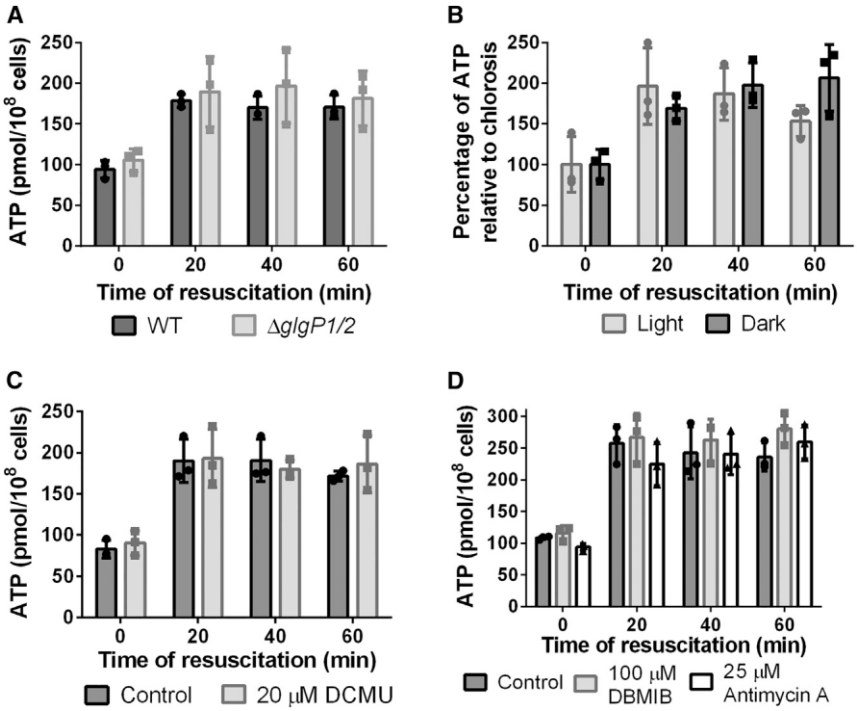

Figure 1. The rapid increase in ATP levels upon $NaNO_3$ addition is independent of glycogen catabolism and photosynthesis

(A) ATP content normalized to 1 3 10^8 cells of WT and D*glgP1/2* chlorotic cells after addition of 17 mM $NaNO_3$.

(B) WT chlorotic cells after incubation for 1 h in darkness and addition of 17 mM $NaNO_3$.

(C and D) WT chlorotic cells treated with (C) 20 mM DCMU and (D) 100 mM DBMIB and 25 mM antimycin A. Cells were treated for 5 min before the first measurement (0 min). Resuscitation was then induced by addition of 17 mM $NaNO_3$. At least three biological replicates were measured; error bars represent the SD; asterisks represent the statistical significance.

See also Figures S1 and S2.

RESULTS

The rapid ATP increase in response to nitrogen availability is independent of glycogen degradation and photosynthesis

Upon nitrogen addition, cells start the resuscitation program and their energy demands increase. Cells must then produce ATP to support nitrogen assimilation and biosynthetic processes. We measured the intracellular ATP levels within the first hour of resuscitation and observed an increase of ~100% in the ATP content 20 min after the addition of $NaNO_3$, and these levels were maintained for the first hour of recovery (Figure 1A). This ATP increase constitutes the fastest measured response of chlorotic cells to the presence of nitrogen,[6] but how it is produced is not yet understood.

A rise in the ATP levels might seem an obvious consequence of activating a dormant metabolism and entering a transient phase of heterotrophy. It is tempting to assume that the increased ATP values at the start of resuscitation come from the onset of glycogen catabolism, which is induced soon after the addition of $NaNO_3$ to dormant cells.[6] Previously, we observed that a mutant lacking the glycogen phosphorylases (D*glgP1/2*) displayed elevated ATP levels 3 h after $NaNO_3$ addition, but these cells did not further recover. Here, we compared the short-term response in ATP levels between D*glgP1/2* and wild type (WT) in more detail and found that $NaNO_3$ triggered a similar rapid ATP increase in the D*glgP1/2* mutant as it did in the WT, implying that the onset of ATP synthesis does not depend on glycogen catabolism (Figure 1A). Respiration of other metabolites can be excluded, because D*glgP1/2* does not show any oxygen consumption upon addition of $NaNO_3$. In fact, the rise in ATP levels happened before cells perform respiration at full capacity. During nitrogen-chlorosis, cells display residual photosynthetic activity, which is completely repressed after a few hours of resuscitation, when degradation of glycogen is fully operating.[7] Pulse-amplitude modulation (PAM) fluorometry measurements revealed that, 1 h after nitrate addition, much after an ATP increase is measurable, glycogen catabolism has not yet suppressed PSII activity (Figure S1). After 2 h of resuscitation, when cells are fully respirating, the PSII activity disappears and only resumes when cells have partially restored their photosynthetic machinery (~12 h after nitrate addition). Thus, the increase in ATP levels during early resuscitation could depend on photosynthesis instead of respiration. To test this possibility, we measured the ATP content of dark-incubated cells (Figure 1B). Although ATP levels were overall lower in the dark than in the light, addition of $NaNO_3$ caused a similar increase under both conditions. To completely exclude the role of photosynthesis on the rise of ATP levels, we treated chlorotic cells with different photosynthetic inhibitors. Exposure to dichlorophenyl dimethylurea (DCMU), which blocks the electron transfer from PSII to the plastoquinone (PQ) (Figure 1C), dibromthymochinon (DBMIB), which inhibits the electron flow from PQ to the cytochrome b_6f (Cyt b_6f), and antimycin A, which disrupts the Q cycle in Cyt b_6f (Figure 1D), did not affect the cell's ability to produce ATP after addition of $NaNO_3$, although treated cells showed impaired resuscitation from nitrogen starvation (Figure S2).

The ATP increase relies on a sodium motive force

Respiration and photosynthesis are the two main bioenergetic processes that generate an electrochemical proton gradient that can be used by the ATP synthase to power ATP production. When both processes were blocked, nitrogen-starved cells could still increase ATP levels upon addition of $NaNO_3$. To elucidate the contribution of proton motive force (*PMF*) to the ATP increase, chlorotic cells were treated with the protonophores carbonyl cyanide m-chlorophenyl hydrazone (CCCP) and 2,3-dinitrophenol (DNP). Protonophores make membranes permeable to protons, destroying proton gradients. Although treatment with CCCP and DNP prevented resuscitation (Figure S2), it did

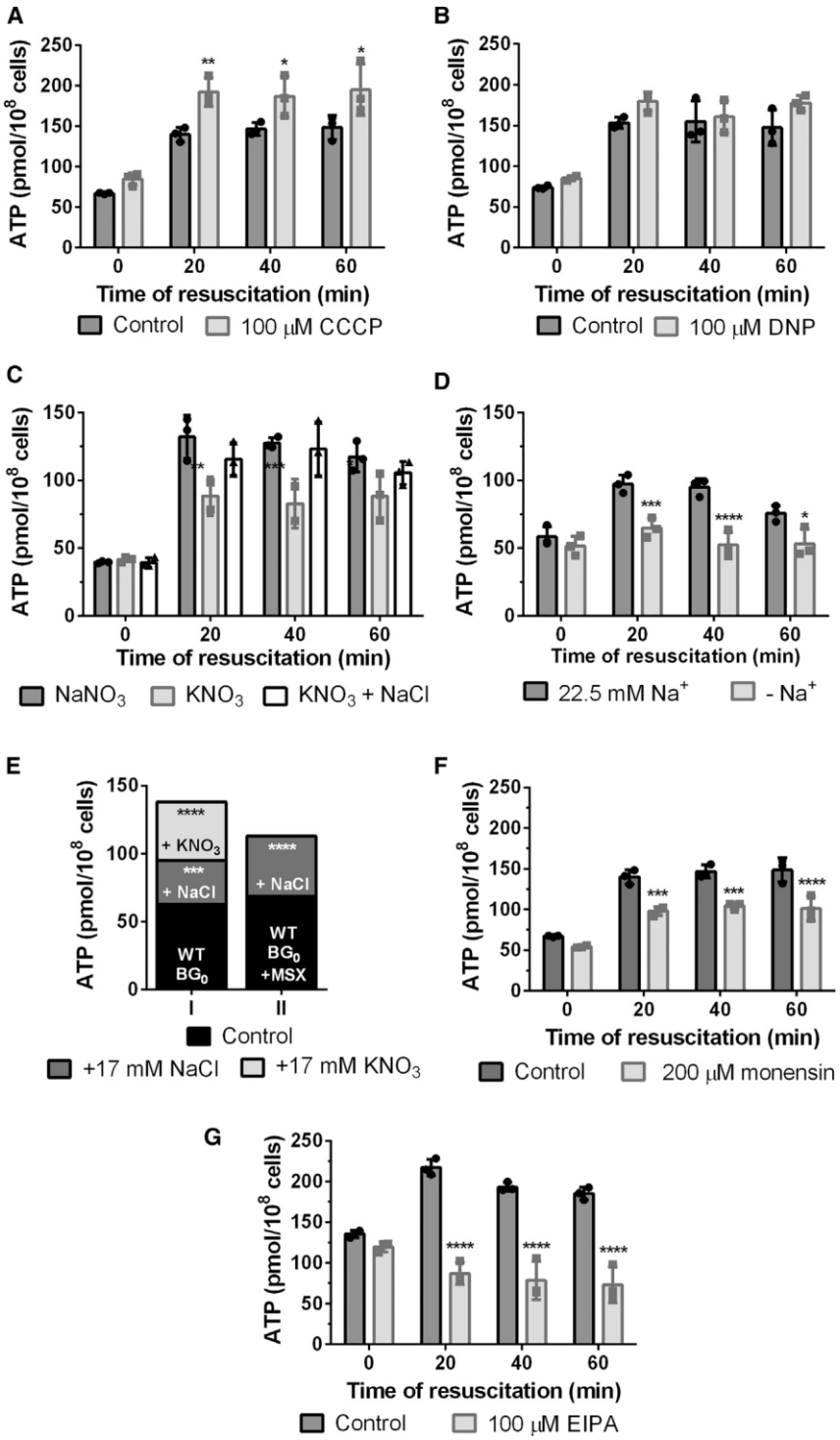

Figure 2. The rise of cellular ATP upon $NaNO_3$ addition does not rely on a proton gradient and is a response to both increased sodium concentrations and nitrogen assimilation

(A and B) ATP content normalized to 1 $3\ 10^8$ cells of WT chlorotic cells treated with (A) 100 mM CCCP and (B) 100 mM DNP. Cells were treated for 5 min before the first measurement (0 min). Resuscitation was then induced by addition of 17 mM $NaNO_3$.

(C) Cells were resuscitated using either 17 mM $NaNO_3$, 17 mM KNO_3, or 17 mM KNO_3 + 17 mM NaCl.

(D) Cells were washed twice with $BG_{11\text{-}0Na}$ sodium-free medium and resuscitated with 17 mM KNO_3.

(E) ATP content normalized to 1 $3\ 10^8$ cells of chlorotic cells in $BG_{11\text{-}0}$ (black), after supplementation with 17 mM NaCl (dark gray), and after additional supplementation with 17 mM KNO_3 (light gray). Column I: untreated WT chlorotic cells supplemented with 17 mM NaCl and 17 mM KNO_3 are shown. Column II: WT chlorotic cells treated with 200 mM MSX and supplemented with 17 mM NaCl and 17 mM KNO_3 are shown.

(F) Chlorotic cells treated with 200 mM monensin.

(G) Chlorotic cells treated with 100 mM EIPA.

In (F) and (G), cells were treated for 5 min before the first measurement (0 min) and then resuscitation was induced by addition of 5 mM NH_4Cl + 17 mM NaCl. At least three biological replicates were measured; error bars represent the SD; asterisks represent the statistical significance. See also Figure S2.

not abolish the rise in ATP levels (Figures 2A and 2B). In fact, treatment with CCCP led to a higher ATP production in chlorotic cells after addition of $NaNO_3$, indicating that ATP synthesis does not depend on an electrochemical proton gradient. However, protons are not the only ions that can be used for ATP synthesis, as some ATP synthases can also use a sodium motive force (*SMF*) to power ATP production.[10] Sodium ions are more abundant in the extracellular medium than in the cytoplasm and form a gradient across the plasma membrane that can be utilized by sodium-binding ATP synthases to produce ATP. Besides the thylakoidal ATP synthases, which translocate proton from the thylakoid lumen to the cytoplasm to produce ATP, *Synechocystis* also possesses ATP synthases in the plasma membrane,[11] which might use an *SMF*.

The above experiments were performed by adding 17 mM $NaNO_3$ to chlorotic cells in nitrogen-free $BG_{11\text{-}0}$ medium, increasing the sodium concentration 4-fold. This raised the question whether the rapid increase of intracellular ATP is connected to the sudden rise in sodium levels. To test this, recovery experiments were performed by the addition of 17 mM KNO_3 to cells in $BG_{11\text{-}0}$ (Figure 2C). In this case, the concentration of sodium remained constant. Remarkably, the ATP increase was significantly lower than in the previous experiments with the addition of 17 mM $NaNO_3$. The rapid rise in ATP levels could be restored when 17 mM NaCl was added together with KNO_3 to dormant cells (Figure 2C). When sodium was completely removed from the medium by washing with $BG_{11\text{-}0Na}$ (in which sodium salts have been

substituted by potassium salts), addition of KNO_3 triggered almost no increase of ATP levels (Figure 2D). These results demonstrated that sodium plays an important role in ATP synthesis in chlorotic cells. However, whether or not the addition of a nitrogen source also contributes to the rise in ATP levels remained unclear. To address this question, sodium and nitrogen were added to dormant cells sequentially (Figure 2E). The sole addition of 17 mM NaCl to chlorotic cells in BG_{11-0} caused a partial increase of the ATP levels within 20 min, compared to the standard resuscitation experiment. When 20 min after supplementation with NaCl a nitrogen source was added to the cells in the form of KNO_3 (Figure 2E, column I), a further rise in ATP levels was observed after 1 h. This indicates that the rise in ATP levels after addition of $NaNO_3$ to chlorotic cells has two components: one due to the increase in the sodium concentration and another one due to the presence of nitrogen. To distinguish whether cells sense the presence of nitrogen or detect it through initiating assimilation via the GS-GOGAT cycle, cells were treated with the GS inhibitor L-methionine sulfoximine (MSX). This treatment completely abolished the nitrogen-dependent component of the ATP increase (Figure 2E, column II), indicating that activation of nitrogen assimilation is required for the nitrogen-dependent ATP increase.

To corroborate the role of sodium in ATP synthesis during chlorosis, nitrogen-starved cells were treated with monensin, a sodium ionophore, and ethyl-isopropyl amiloride (EIPA), an inhibitor of sodium channels and sodium/proton antiport. To exclude any indirect effects caused by possible interference of the inhibitors with nitrate transport, the effect of monensin and EIPA on the ATP content was measured after adding a combination of NH_4Cl and NaCl to chlorotic cells. Treatment with monensin led to lower ATP levels than the untreated control (Figure 2F). Strikingly, exposure to EIPA completely abolished the ATP increase (Figure 2G), proving the key role of sodium bioenergetics in chlorotic cells.

An increase in the sodium motive force provides a source of free energy for dormant cells

The results above showed that ATP synthesis was stimulated in dormant cells by increasing the concentration of sodium, which contributes to a rise in the *SMF*. The ion motive force (*IMF*) is the electrochemical gradient of an ion across the membrane and depends on the membrane potential and the concentration of the ion at both sides of the membrane. For an ion with charge z, its *IMF* is

$$IMF\delta mV\Phi = V_m - \frac{RT}{zF} ln\text{-}\frac{C_{out}}{C_{in}};$$

where V_m is the membrane potential, R the gas constant, F the Faraday constant, C_{in} the concentration of ion inside the cell, and C_{out} the concentration of ion outside the cell.[12] Raising the extracellular sodium concentration from 5.5 mM to 17 mM contributes to the *SMF* with approximately −30 mV, which suggests that, for increasing ATP synthesis, there should already be sufficient V_m in chlorotic cells. To estimate this residual V_m, we used the fluorescent voltage reporter bis-(1,3-dibutylbarbituric acid)-trimethine oxonol (DiBAC4(3)). DiBAC4(3) penetrates depolarized cells, exhibiting enhanced fluorescence in the cytoplasm, but does not enter cells with an intact V_m. As a control, we used cells killed by heat inactivation and vegetative cells. Killed cells showed high permeability to DiBAC4(3), whereas no signs of fluorescence were detected in vegetative cells (Figure 3A). 1-month-chlorotic cells showed a more heterogeneous population: although most cells showed no fluorescence, some were stained by DiBAC4(3). This heterogeneity agrees with the fact that, after a month of nitrogen starvation, not all cells keep viability. However, most chlorotic cells did not show fluorescence, indicating they maintain a similar membrane potential than vegetative cells, which, in addition to the extra voltage obtained after addition of 17 mM NaCl, constitutes sufficient *SMF* to drive ATP synthesis.

To confirm that the ATP increase depends on a rise of the *SMF*, we provided cells with different concentrations of NaCl (Figure 3B). Supplementation with 17 mM NaCl triggered an ~100% increase in ATP levels, whereas addition of 50 mM NaCl led to an ~150% increase, which agrees with the proposed models for ATP yield as a function of the *IMF*.[13,14] To ascertain whether the ATP synthases are responsible for this change in ATP levels, we treated chlorotic cells with N,N'-dicyclohexylcarbodiimide (DCCD), an F-ATPase inhibitor. DCCD-treated cells showed a reduced response to NaCl as compared to untreated cells (Figure 3C), confirming that the non-nitrogen-dependent component of the ATP increase is a purely physico-chemical effect of increasing the concentration of sodium and that it relies on the activity of the ATP synthases.

The nitrogen-dependent component of the ATP increase requires respiration

The metabolically induced ATP increase required activation of the GS-GOGAT cycle, but how initiation of nitrogen assimilation leads to ATP synthesis remained to be addressed. Our previous data showed that addition of a nitrogen source to dormant cells induced glycogen degradation.[6] Glycogen degradation supports ATP synthesis by producing reduction equivalents to support respiration and to a smaller extent by substrate-level phosphorylation. To reveal the contribution of glycogen catabolism on the metabolically induced ATP-level increase, we tested the effect of NaCl and KNO_3 on D*glgP1/2*. As the MSX-treated cells, D*glgP1/2* only reacted to sodium and did not show the nitrogen-dependent component of the ATP increase (Figure 4, column B), confirming that this second component depends on glycogen degradation. To elucidate whether respiration is required to generate ATP upon nitrate addition, we measured the ATP content of chlorotic cells after treatment with potassium cyanide (KCN), which prevents electron transfer from the terminal oxidases to oxygen, inhibiting the respiratory chain. KCN-treated cells increased their ATP levels after addition of NaCl, but not after supplementation with KNO_3 (Figure 4, column C). This indicated that respiration is essential for the metabolically induced increase of ATP levels during early resuscitation. Interestingly, treatment with DBMIB, which blocks the electron transport chain at the Cyt b_6f, did not inhibit the nitrogen-dependent component of the ATP increase (Figure 4, column D), suggesting that respiration takes place on the plasma membrane, because cytochrome b_6f is a specific component of the thylakoid membranes.[15]

Sodium requirement depends on the cellular growth stage

Hitherto, it remained unclear whether cells engage sodium bioenergetics exclusively during nitrogen-chlorosis or whether

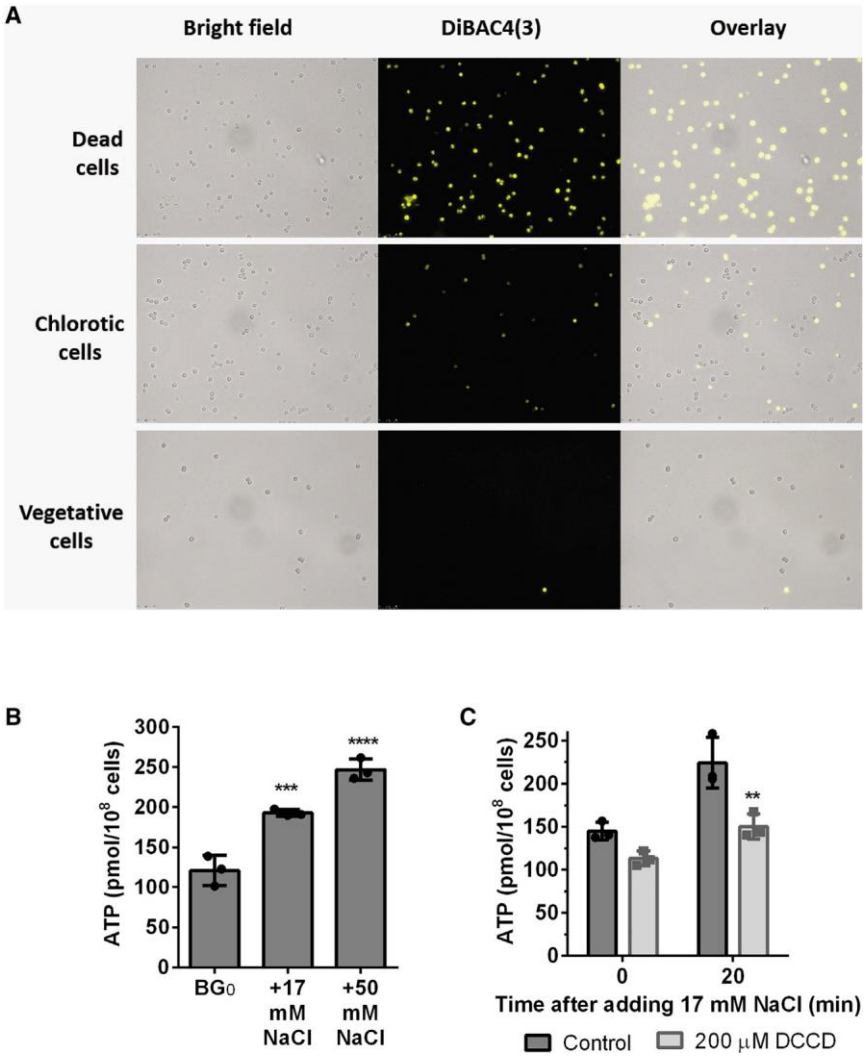

Figure 3. Chlorotic cells maintain a membrane potential, and the amount of ATP produced by the ATP synthases is proportional to the increase in the extracellular concentration of sodium

(A) Microscopic pictures of dead, chlorotic, and vegetative cells stained with DiBAC4(3), which penetrates depolarized cells, showing enhanced fluorescence in the cytoplasm.

(B and C) ATP content normalized to 1×10^8 cells of (B) WT chlorotic cells before and 30 min after addition of 17 mM and 50 mM NaCl and (C) WT chlorotic cells treated with 200 mM DCCD before and 20 min after addition of 17 mM NaCl. Cells were treated for 5 min before the first measurement (0 min). At least three biological replicates were measured; error bars represent the SD; asterisks represent the statistical significance.

sodium-dependent ATP synthesis is a part of *Synechocystis* metabolism in general. To answer this question, vegetative cells were treated with monensin and EIPA. The ATP content of vegetative cells was not affected after treatment with monensin for 30 min (Figure 5A), although EIPA slightly reduced it by 25% (Figure 5B). However, treatment with EIPA also completely inhibited PSII activity (Figure S3), suggesting that the lower ATP levels might be a consequence of inhibition of photosynthesis rather than a direct effect on sodium-dependent ATP synthesis. This indicates that, although sodium bioenergetics plays a key role during nitrogen starvation, vegetative cells do not rely on sodium-dependent ATP synthesis.

To further elucidate the role of sodium on the metabolism of *Synechocystis*, vegetative and nitrogen-starved cells were cultivated in sodium-free medium. Under atmospheric gas conditions in shaking flasks, vegetative cells could not grow in the absence of sodium. However, growth in sodium-free medium could be restored when cells were supplemented with 2% CO_2 (Figure 5C). This is due to the requirement of sodium for bicarbonate uptake through the SbtA and BicA transporters.[16,17] Thus, sodium-dependent bicarbonate transport is essential for growth under atmospheric CO_2 supply, but cells do not require sodium with elevated CO_2 concentrations. Conversely, nitrogen-starved cells showed a decreasing optical density when cultivated in sodium-free medium, even when they were supplemented with 2% CO_2 (Figure 5D), indicating a requirement for sodium beyond the need for inorganic carbon transport.

In the presence of sodium, during the first 24 h of chlorosis, cells synthesize large amounts of glycogen. In sodium-free medium and under atmospheric gas conditions, cells accumulate only ~50% of the amount of glycogen after 2 days of nitrogen starvation as compared to the standard medium, and upon further incubation, glycogen levels decreased (Figure 5E). When cells were nitrogen starved under standard conditions for 24 h, until they reached the maximum glycogen content and were then transferred to sodium-free medium, the glycogen concentration progressively decreased after sodium removal (Figure 5E). This suggests that the absence of sodium triggers glycogen catabolism. When resuscitation of chlorotic cells in sodium-free medium was initiated by the addition of KNO_3 (conditions in which only a low ATP increase was observed), they showed higher respiration rates than cells resuscitating under standard conditions (Figure 5F). However, these cells never re-greened and eventually lost viability, as shown by the complete loss of photosynthetic activity (Figure S1).

ATP levels are rapidly tuned depending on the metabolic requirements

So far, the analysis of sodium requirement in vegetative and chlorotic cells showed that vegetative cells require sodium for bicarbonate transport, whereas chlorotic cells require sodium for ATP synthesis. When cells are nitrogen starved, they are initially photosynthetically competent. To elucidate how ATP levels are affected after transferring vegetative cells to nitrogen-deprived

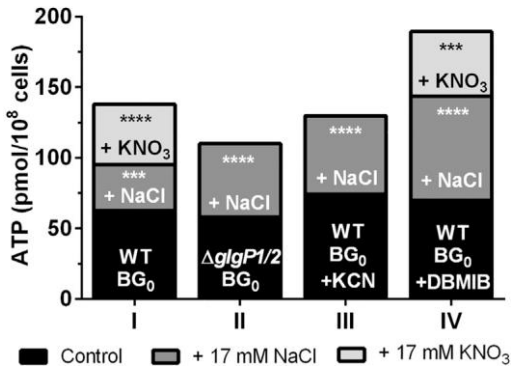

Figure 4. The nitrogen-dependent component of the ATP increase requires respiration of glycogen

ATP content normalized to 1 3 10⁸ cells of chlorotic cells in BG_{11-0} (black), after supplementation with 17 mM NaCl (dark gray), and after additional supplementation with 17 mM KNO_3 (light gray). Column I: WT chlorotic cells are shown. Column II: D*glgP1/2* chlorotic cells are shown. Column III: WT chlorotic cells treated with 1 mM KCN cells are shown. Column IV: WT chlorotic cells treated with 200 mM DBMIB are shown. At least three biological replicates were measured; error bars represent the SD; asterisks represent the statistical significance.

conditions at different sodium concentrations, we analyzed the ATP content of vegetative cells after they were transferred either into regular BG_{11-0} (5.5 mM sodium) or into BG_{11-0} supplemented with 17 mM NaCl (22.5 mM). After 30 min shifting to nitrogen-deficient medium, the ATP levels dropped to approximately 1/3 of the initial value, regardless of the sodium concentration. Subsequently, the ATP content was maintained at this low level during long-term chlorosis (Figure 6A). To ensure that the decrease in ATP levels was caused by lowered energy charge and not by reduced levels of adenine nucleotides, we determined the ATP/ADP ratio, which dropped in a similar manner than ATP levels decreased (Figure 6B). This indicates a reduced energy charge rather than a decrease of nitrogen-containing compounds after nitrogen removal and implies that cells adjust ATP levels as a response to the metabolic imbalance caused by nitrogen depletion.

DISCUSSION

Synechocystis engages sodium bioenergetics during nitrogen starvation

During nitrogen-chlorosis, *Synechocystis* re-arranges its metabolism to reach a dormant state that allows cell survival for a prolonged time. This metabolic adaptation includes reduction of energy consumption and production. Thus, chlorotic cells keep ATP at the minimum level to ensure survival (~50–100 pmol/10⁸ cells).[7] When a nitrogen source is added to chlorotic cells, the ATP demand dramatically increases due to the ammonium-assimilating GS reaction, which consumes one ATP per reaction, and all the following anabolic processes that are induced at the onset of resuscitation.[6,9] Based on measurements of the glutamine levels on vegetative and chlorotic cells,[18,19] the glutamine content can easily increase around 10 mM upon addition of $NaNO_3$ to dormant cells, which implies that approximately 10^7 molecules of glutamine per cell (considering a cell volume of 2 mm³) have to be synthesized by the GS-GOGAT cycle, requiring 10^7 molecules of ATP. Cells respond accordingly and increase ATP levels by about ~100% to power the anabolic reactions.

Most of the cellular ATP is produced by the ATP synthases from ADP and inorganic phosphate. In cyanobacteria, this reaction typically requires an electrochemical proton gradient across the thylakoid membrane, which is generated by photosynthetic or respiratory electron transport.[20] However, chlorotic cells could still increase ATP levels within several minutes, even when the two main bioenergetic processes that generate a proton gradient were inhibited. We could identify the nature of this increase in the ATP content and dissect it into two components: one that is purely sodium dependent and a second one that was triggered by ammonium assimilation and supported by glycogen-dependent respiration.

Because chlorotic cells have largely degraded their thylakoids, the space for thylakoidal ATP synthases and proton storage is very limited.[6] Previous studies have reported the presence of ATP synthases in the plasma membrane of *Synechocystis*,[11] which suggests that cells could use an extracellular electrochemical gradient to power ATP synthesis. Although cyanobacteria preferably grow under alkaline conditions, where protons are not abundant, *PMF* is not the only *IMF* that can be coupled to ATP synthesis. The fact that *Synechocystis* uses an *SMF* for other bioenergetic processes (e.g., bicarbonate uptake)[17] suggested that an electrochemical sodium gradient might be involved in ATP synthesis in chlorotic cells.

The first component of the rise in intracellular ATP that was triggered by addition of $NaNO_3$ to chlorotic cells can be explained by an increase in the *SMF*. This first component was prevented by treatment with DCCD, suggesting that the ATP synthases in the plasma membrane of *Synechocystis* can use an electrochemical sodium gradient to power ATP synthesis. The ATP synthase is formed by a membrane complex (F_0), which transports the ions across the membrane, and a cytoplasmic complex (F_1), where ATP is synthesized. Ion specificity is determined in the c-ring in complex F_0. In *Synechocystis*, there is just one gene that encodes for the c subunit that forms the c-ring (AtpH). Whether the c-ring binds protons or sodium ions depends on slight variations in the amino acid sequence around the ion-binding site. Both protons and sodium ions bind a glutamate residue, but sodium-ATPases have polar groups around this glutamate residue, whereas proton-ATPases have hydrophobic groups.[10,21] The balance between hydrophobic and polar groups makes the c-rings more or less selective toward one ion or the other. Proton-ATPases must have high proton selectivity, because usually the concentration of sodium is much higher than the concentration of protons in physiological conditions. Some organisms, like *Methanosarcina acetivorans*, possess proton-specific c-rings that can bind sodium physiologically because their proton specificity is not strong enough to overcome the excess of sodium.[21,22] Figure 7A shows an alignment of the sequence of *Synechocystis'* AtpH with those from *Ilyobacter tartaricus*, *M. acetivorans*, and *Arthrospira platensis*, with weak, medium, and strong proton selectivity, respectively, as well as the AtpH from *Synechococcus elongatus* PCC 7942, a freshwater cyanobacterial strain, and the 2 AtpH homologs from *Synechococcus* sp. PCC 7002, a marine cyanobacterial strain. There are 5 key amino acids around the main ion-binding residue

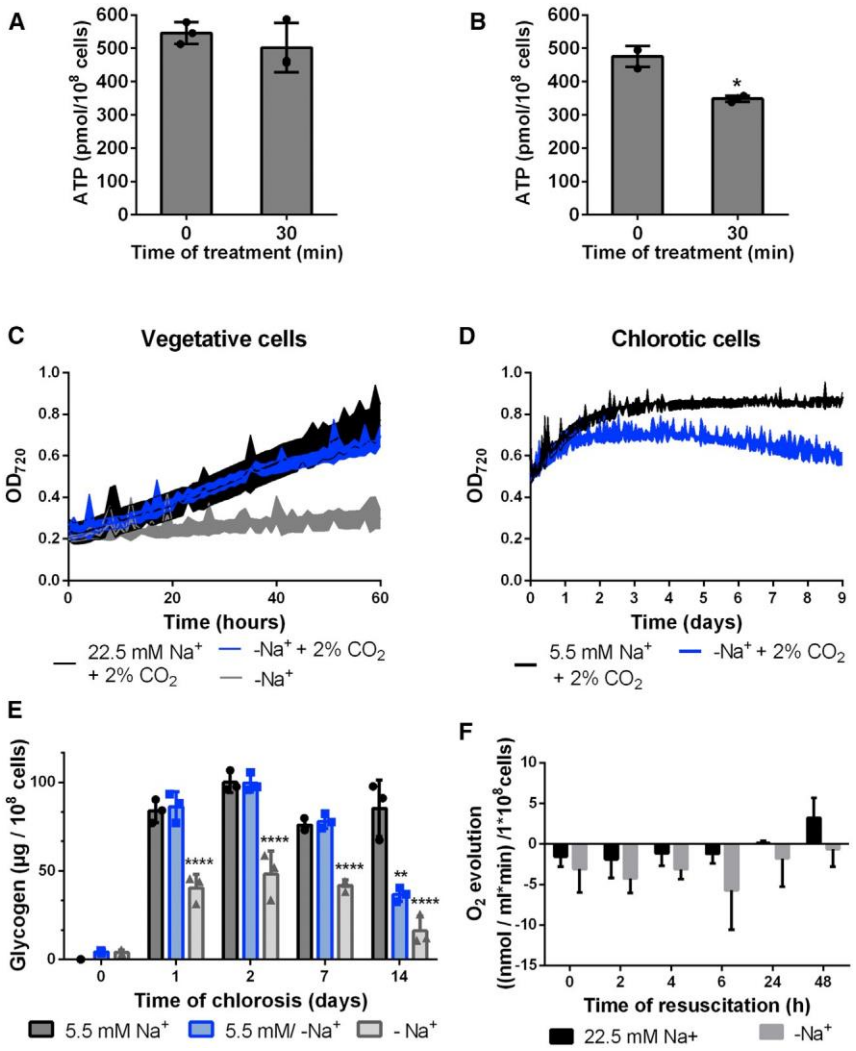

Figure 5. Sodium is required for bicarbonate uptake, but not for ATP synthesis, during vegetative growth

(A) ATP content normalized to 1 3 10⁸ cells of vegetative cells treated with 200 mM monensin for 30 min.

(B) ATP content normalized to 1 3 10⁸ cells of vegetative cells treated with 100 mM EIPA for 30 min (see also Figure S3).

(C) Optical density at 720 nm of vegetative cells in regular BG_{11} supplemented with 2% CO_2 (black line) and in $BG_{11\text{-}Na}$ sodium-free medium with ambient air (gray line) and 2% CO_2 supplementation (blue line).

(D) Optical density at 720 nm of chlorotic cells in regular $BG_{11\text{-}0}$ supplemented with 2% CO_2 (black line) and in $BG_{11\text{-}0\text{-}Na}$ sodium-free medium supplemented with 2% CO_2 (blue line).

(E) Glycogen content normalized to 1 3 10⁸ cells throughout chlorosis of WT cells in medium containing 5.5 mM sodium (black bars, standard conditions), sodium-free medium (gray bars), and cells that were cultivated in standard conditions, i.e., 5.5 mM sodium, for 24 h and then transferred to sodium-free medium (blue bars).

(F) Oxygen evolution of resuscitating WT cells in medium containing 22.5 mM sodium (black bars, standard conditions) and sodium-free medium (gray bars). At least three biological replicates were measured; error bars represent the SD; asterisks represent the statistical significance.

See also Figure S1.

(marked in red) that favor sodium binding: 3 sodium-binding residues (in orange) and 2 residues that bind a stabilizing water molecule (in green). *I. tartaricus* possesses all 5 residues (Figure 7B), although *M. acetivorans* lacks the residues that bind the stabilizing water molecule, which gives the c-ring a higher proton selectivity than the one of *I. tartaricus*. *A. platensis* has hydrophobic amino acids surrounding the glutamate residue, which confers the c-ring high proton selectivity. *Synechocystis*, like *M. acetivorans*, also contains the polar residues that interact with the sodium ion, but not the residues that interact with the stabilizing water molecule, presenting medium proton selectivity. A moderate proton specificity permits the ATP synthases in the thylakoid membranes to bind protons, because the concentration of protons in the thylakoid lumen is high. However, those ATP synthases located in the plasma membrane of dormant cells that live in an alkaline environment are more likely to bind sodium. This enzyme promiscuity allows dormant cells to adapt and survive to an environment where the classical ways to obtain energy are limited. Interestingly, in contrast to *Synechocystis*, which is a brackish water micro-organism and is adapted to high salt concentrations, the fresh-water cyanobacterium *S. elongatus* presents a c-ring with high proton selectivity, although the marine cyanobacterium *Synechococcus* sp. PCC 7002 possesses two AtpH homologs, one with high and one with low proton selectivity. This observation suggests that the switch to sodium bioenergetics under nutrient starvation is likely to be a survival strategy developed only by micro-organisms adapted to high salt concentrations.

The second component of the ATP increase was prevented by treatment with MSX, a specific GS inhibitor, and was absent in a mutant unable to degrade glycogen and when respiration was inhibited by KCN. This suggests that initiation of nitrogen assimilation triggers glycogen catabolism, which contributes to ATP synthesis by supporting respiration. However, inhibition of Cyt b_6f using DBMIB did not prevent the nitrogen-dependent component of the ATP increase. Because Cyt b_6f is only present in the thylakoid membranes, these results suggested that respiration occurs in the plasma membrane during early resuscitation. Previous studies suggested a simpler electron transport chain for the plasma membrane in which electrons are transferred from NAD(P)H dehydrogenases type II (NDH II) to the plastoquinone pool (PQ) and further to an alternative respiratory terminal oxidase (ARTO), without involving Cyt b_6f.[23] Pils and Schmetterer[24] could show that ARTO is energetically active and can energize the plasma membrane in *Synechocystis*. We propose that the

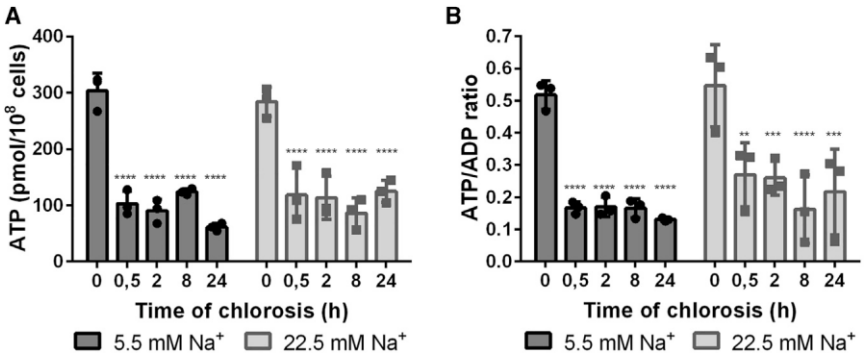

Figure 6. The ATP concentration is rapidly reduced after nitrogen step-down even in the presence of high sodium

(A) ATP content normalized to 1×10^8 cells of WT cells after nitrogen deprivation in standard conditions (5.5 mM sodium, black bars) and high-sodium conditions (22.5 mM sodium, gray bars).

(B) ATP/ADP ratio of WT cells after nitrogen deprivation in standard conditions (5.5 mM sodium, black bars) and high-sodium conditions (22.5 mM sodium, gray bars). At least three biological replicates were measured; error bars represent the SD; asterisks represent the statistical significance.

protons transported from the cytoplasm to the periplasmic space by ARTO could be directly used by closely located sodium/protons antiporters to extrude sodium ions from the cytoplasm, immediately converting *PMF* into *SMF*, which can be used for ATP synthesis (Figure 7C). When a proton is translocated across the membrane, its diffusion to the aqueous solution is retarded, because the membrane surface is separated from the bulk aqueous phase by an electrostatic barrier, and proton diffusion between neighboring enzymes occurs in milliseconds.[25] Close cooperation of ARTO and sodium/proton antiporters could avoid protons dissipating into the aqueous solution and would explain the insensitivity of chlorotic cells toward CCCP. In fact, not only did CCCP not prevent a rise in ATP levels in chlorotic cells, but it led to a higher ATP increase than in untreated cells instead. Treatment with CCCP dissipates the proton gradient and allows higher respiration rates, because the proton pumps do not have to work against a gradient,[26] which can lead to an increased sodium-dependent ATP synthesis. In support to this model, NDH II and sodium/proton antiporters are upregulated in chlorotic cells.[9] Interestingly, NdbA (slr0851), one of the three NDH II isoenzymes in *Synechocystis*, is the third most upregulated protein in chlorotic cells. Moreover, this model is in accordance with the extreme sensitivity of chlorotic cells toward the inhibitor of sodium/proton antiport, EIPA. These results show that bioenergetics of chlorotic cells is largely based on sodium, which allows dormant cells to keep the minimum intracellular ATP concentration to maintain cell viability during metabolic quiescence, even in an alkaline environment.

Energy homeostasis in *Synechocystis*

In contrast to chlorotic cells, vegetative cells do not rely on sodium-dependent ATP synthesis but require sodium primarily for sodium-dependent bicarbonate uptake. During vegetative growth, the major ATP synthesis machinery is located in the thylakoid membranes, where photosynthetic and respiratory complexes generate a *PMF* to power ATP synthesis.[20] Upon nitrogen starvation, nitrogen assimilation and most anabolic processes are halted and ATP levels would be expected to increase, because at this point, the ATP synthesis machinery is still intact and the most energy consuming reactions in the cell stop taking place. However, when cells were transferred to nitrogen-free medium, ATP levels rapidly decreased, independently of the concentration of sodium in the medium, suggesting the existence of a powerful yet unexplored regulatory mechanism of tuning ATP levels.

Reduced ATP levels have previously been reported in bacterial cells during metabolic dormancy. In *Mycobacterium tuberculosis*, the ATP content in nutrient-starved cells is maintained at a constant level that is 5-fold lower than in growing cells.[3] However, whether the decreased ATP content is a consequence of a reduced metabolic activity during bacterial dormancy or whether low ATP levels are required to reach this metabolic state has not been elucidated. In *Synechocystis*, mutants unable to synthesize glycogen (D*glgA1/2* and D*glgC*) present higher ATP levels than the WT and fail to perform a proper acclimation response to nitrogen starvation, which leads to death.[27–29] However, this phenotype is alleviated when synthesis of glucosylglycerol, which is produced from ADP-glucose under conditions of high salt stress, is induced in the D*glgA1/2* mutant, showing the importance of an energy dissipation pathway for acclimation to nitrogen starvation.[29] These findings, together with our observation that ATP levels rapidly drop after nitrogen step-down, even in the presence of high sodium, strongly support the idea that a decreased ATP content is important for adaptation of the metabolism to nitrogen starvation. Reduction of the ATP levels may play a role in re-directing the metabolism into dormancy, because some cellular processes that are important for this transition, such as the formation of protein aggregates, are promoted by decreased cellular ATP concentrations.[30] Also, ATP has been shown to act as a biological hydrotrope that influences the fluidity of the cytoplasm.[31] Adaptation of the cytoplasm from a fluid to a glass-like state has important implications on molecular diffusion inside the cells and plays a relevant role in bacterial adaptation to dormancy.[32] Low ATP levels might be a necessary factor for the transition of the cytoplasm into a glass-like state after prolonged exposure to nitrogen-depleted conditions.

We observed that glycogen degradation is induced in the absence of sodium in chlorotic cells, probably in an attempt to maintain the ATP content to a minimum. Similarly, during resuscitation in sodium-free medium, cells respired more (i.e., degraded more glycogen) than in presence of high sodium, most likely to compensate for the lack of sodium-dependent ATP synthesis. These findings support the previously proposed idea that glycogen metabolism is controlled by the intracellular energy charge and plays an important role in energy homeostasis. Nevertheless, the exact molecular mechanism that allows

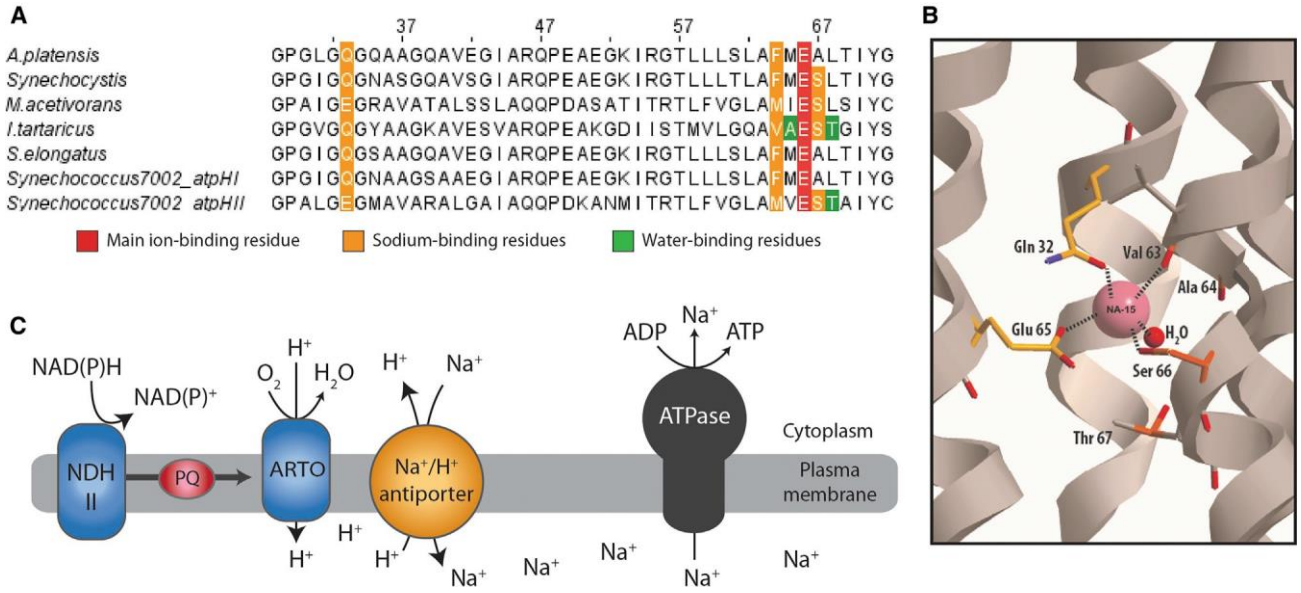

Figure 7. Proposed mechanism of sodium-dependent ATP synthesis in *Synechocystis*

(A) Alignment of the sequence of the ion-binding site of AtpH from *Arthrospira platensis*, *Synechocystis*, *Methanosarcina acetivorans*, *Ilyobacter tartaricus*, *Synechococcus elongatus*, and *Synechococcus* sp. PCC 7002 (AtpH I and AtpH II). Residues involved in Na^+ coordination are indicated in colors.

(B) Na^+ coordination in the c-ring from *I. tartaricus*.

(C) Proposed mechanism for maintaining a Na^+ gradient.

energy dissipation upon nitrogen removal needs yet to be elucidated.[28]

This study sheds light on the regulation of the energy metabolism during bacterial dormancy, which plays a crucial role in the survival and spread of bacterial populations. It remains to be seen how common the phenomenon of engaging sodium bioenergetics to adjust ATP levels to the specific metabolic requirements of each phase of the life cycle is among bacterial species that undergo similar developmental transitions than *Synechocystis*.

STAR+METHODS

Detailed methods are provided in the online version of this paper and include the following:

- d KEY RESOURCES TABLE
- d RESOURCE AVAILABILITY
  - B Lead contact
  - B Materials availability
  - B Data and code availability
- d EXPERIMENTAL MODEL AND SUBJECT DETAILS
- d METHOD DETAILS
  - B Growth curves
  - B ATP determination
  - B ADP determination
  - B Membrane potential determination
  - B Glycogen determination
  - B Oxygen evolution measurement
  - B Pulse amplification measurement (PAM)
- d QUANTIFICATION AND STATISTICAL ANALYSIS

SUPPLEMENTAL INFORMATION

Supplemental Information can be found online at https://doi.org/10.1016/j.cub.2021.01.065.

ACKNOWLEDGMENTS

We thank Dr. Libera Lo Presti for her assistance in writing this manuscript and Armen Mulkidjanian for very helpful discussions. This work was supported by the German Research Council (DFG) FOR 2816 ''The Autotrophy-Heterotrophy Switch in Cyanobacteria: Coherent Decision-Making at Multiple Regulatory Layers,'' GRK 1708 ''Molecular Principles of Bacterial Survival Strategies,'' and EXC 2124 ''Controlling Microbes to Fight Infections.''

AUTHOR CONTRIBUTIONS

S.D. and K.F. designed the experiments. S.D. and M.B. conducted the experiments. S.D. and K.F. analyzed the data and wrote the manuscript.

DECLARATION OF INTERESTS

The authors declare no competing interests.

Received: September 29, 2020
Revised: November 30, 2020
Accepted: January 19, 2021
Published: February 10, 2021

REFERENCES

1. Greening, C., Grinter, R., and Chiri, E. (2019). Uncovering the metabolic strategies of the dormant microbial majority: towards integrative approaches. mSystems *4*, 1–5.
2. Lewis, K. (2010). Persister cells. Annu. Rev. Microbiol. *64*, 357–372.

3. Rittershaus, E.S., Baek, S.H., and Sassetti, C.M. (2013). The normalcy of dormancy: common themes in microbial quiescence. Cell Host Microbe *13*, 643–651.
4. Houmard, J. (1995). How do cyanobacteria perceive and adjust to their environment? In Molecular Ecology of Aquatic Microbes, I. Joint, ed. (Springer Berlin Heidelberg), pp. 153–170.
5. Vitousek, P.M., and Howarth, R.W. (1991). Nitrogen limitation on land and sea: how can it occur? Biogeochemistry *13*, 87–115.
6. Klotz, A., Georg, J., Bucinská, L., Watanabe, S., Reimann, V., Januszewski, W., Sobotka, R., Jendrossek, D., Hess, W.R., and Forchhammer, K. (2016). Awakening of a dormant cyanobacterium from nitrogen chlorosis reveals a genetically determined program. Curr. Biol. *26*, 2862–2872.
7. Doello, S., Klotz, A., Makowka, A., Gutekunst, K., and Forchhammer, K. (2018). A specific glycogen mobilization strategy enables rapid awakening of dormant cyanobacteria from chlorosis. Plant Physiol. *177*, 594–603.
8. Klotz, A., and Forchhammer, K. (2017). Glycogen, a major player for bacterial survival and awakening from dormancy. Future Microbiol. *12*, 101–104.
9. Spät, P., Klotz, A., Rexroth, S., Maček, B., and Forchhammer, K. (2018). Chlorosis as a developmental program in cyanobacteria: the proteomic fundament for survival and awakening. Mol. Cell. Proteomics *17*, 1650–1669.
10. Schulz, S., Iglesias-Cans, M., Krah, A., Yildiz, O., Leone, V., Matthies, D., Cook, G.M., Faraldo-Gómez, J.D., and Meier, T. (2013). A new type of Na(+)-driven ATP synthase membrane rotor with a two-carboxylate ion-coupling motif. PLoS Biol. *11*, e1001596.
11. Huang, F., Parmryd, I., Nilsson, F., Persson, A.L., Pakrasi, H.B., Andersson, B., and Norling, B. (2002). Proteomics of Synechocystis sp. strain PCC 6803: identification of plasma membrane proteins. Mol. Cell. Proteomics *1*, 956–966.
12. Benarroch, J.M., and Asally, M. (2020). The microbiologist's guide to membrane potential dynamics. Trends Microbiol. *28*, 304–314.
13. Cherepanov, D.A., Mulkidjanian, A.Y., and Junge, W. (1999). Transient accumulation of elastic energy in proton translocating ATP synthase. FEBS Lett. *449*, 1–6.
14. Kaim, G., and Dimroth, P. (1999). ATP synthesis by F-type ATP synthase is obligatorily dependent on the transmembrane voltage. EMBO J. *18*, 4118–4127.
15. Schultze, M., Forberich, B., Rexroth, S., Dyczmons, N.G., Roegner, M., and Appel, J. (2009). Localization of cytochrome b6f complexes implies an incomplete respiratory chain in cytoplasmic membranes of the cyanobacterium Synechocystis sp. PCC 6803. Biochim. Biophys. Acta *1787*, 1479–1485.
16. Shibata, M., Katoh, H., Sonoda, M., Ohkawa, H., Shimoyama, M., Fukuzawa, H., Kaplan, A., and Ogawa, T. (2002). Genes essential to sodium-dependent bicarbonate transport in cyanobacteria: function and phylogenetic analysis. J. Biol. Chem. *277*, 18658–18664.
17. Burnap, R.L., Hagemann, M., and Kaplan, A. (2015). Regulation of CO2 concentrating mechanism in cyanobacteria. Life (Basel) *5*, 348–371.
18. Mèrida, A., Candau, P., and Florencio, F.J. (1991). Regulation of glutamine synthetase activity in the unicellular cyanobacterium Synechocystis sp. strain PCC 6803 by the nitrogen source: effect of ammonium. J. Bacteriol. *173*, 4095–4100.
19. Hauf, W., Schlebusch, M., Hüge, J., Kopka, J., Hagemann, M., and Forchhammer, K. (2013). Metabolic changes in Synechocystis PCC6803 upon nitrogen-starvation: Excess NADPH sustains polyhydroxybutyrate accumulation. Metabolites *3*, 101–118.
20. Imashimizu, M., Bernat, G., Sunamura, E., Broekmans, M., Konno, H., Isato, K., Rögner, M., and Hisabori, T. (2011). Regulation of F0F1-ATPase from Synechocystis sp. PCC 6803 by γ and ε subunits is significant for light/dark adaptation. J. Biol. Chem. *286*, 26595–26602.
21. Leone, V., Pogoryelov, D., Meier, T., and Faraldo-Gómez, J.D. (2015). On the principle of ion selectivity in Na+/H+-coupled membrane proteins: experimental and theoretical studies of an ATP synthase rotor. Proc. Natl. Acad. Sci. USA *112*, E1057–E1066.
22. Schlegel, K., Leone, V., Faraldo-Gómez, J.D., and Müller, V. (2012). Promiscuous archaeal ATP synthase concurrently coupled to Na+ and H+ translocation. Proc. Natl. Acad. Sci. USA *109*, 947–952.
23. Baers, L.L., Breckels, L.M., Mills, L.A., Gatto, L., Deery, M.J., Stevens, T.J., Howe, C.J., Lilley, K.S., and Lea-Smith, D.J. (2019). Proteome mapping of a cyanobacterium reveals distinct compartment organization and cell-dispersed metabolism. Plant Physiol. *181*, 1721–1738.
24. Pils, D., and Schmetterer, G. (2001). Characterization of three bioenergetically active respiratory terminal oxidases in the cyanobacterium Synechocystis sp. strain PCC 6803. FEMS Microbiol. Lett. *203*, 217–222.
25. Mulkidjanian, A.Y., Heberle, J., and Cherepanov, D.A. (2006). Protons @ interfaces: implications for biological energy conversion. Biochim. Biophys. Acta *1757*, 913–930.
26. Pansook, S., Incharoensakdi, A., and Phunpruch, S. (2019). Effects of the photosystem II inhibitors CCCP and DCMU on hydrogen production by the unicellular halotolerant cyanobacterium *Aphanothece halophytica*. ScientificWorldJournal *2019*, 1030236.
27. Gründel, M., Scheunemann, R., Lockau, W., and Zilliges, Y. (2012). Impaired glycogen synthesis causes metabolic overflow reactions and affects stress responses in the cyanobacterium Synechocystis sp. PCC 6803. Microbiology (Reading) *158*, 3032–3043.
28. Cano, M., Holland, S.C., Artier, J., Burnap, R.L., Ghirardi, M., Morgan, J.A., and Yu, J. (2018). Glycogen synthesis and metabolite overflow contribute to energy balancing in cyanobacteria. Cell Rep. *23*, 667–672.
29. Díaz-Troya, S., Roldán, M., Mallén-Ponce, M.J., Ortega-Martínez, P., and Florencio, F.J. (2020). Lethality caused by ADP-glucose accumulation is suppressed by salt-induced carbon flux redirection in cyanobacteria. J. Exp. Bot. *71*, 2005–2017.
30. Pu, Y., Li, Y., Jin, X., Tian, T., Ma, Q., Zhao, Z., Lin, S.-Y., Chen, Z., Li, B., Yao, G., et al. (2019). ATP-dependent dynamic protein aggregation regulates bacterial dormancy depth critical for antibiotic tolerance. Mol. Cell *73*, 143–156.e4.
31. Patel, A., Malinovska, L., Saha, S., Wang, J., Alberti, S., Krishnan, Y., and Hyman, A.A. (2017). ATP as a biological hydrotrope. Science *356*, 753–756.
32. Parry, B.R., Surovtsev, I.V., Cabeen, M.T., O'Hern, C.S., Dufresne, E.R., and Jacobs-Wagner, C. (2014). The bacterial cytoplasm has glass-like properties and is fluidized by metabolic activity. Cell *156*, 183–194.
33. Rippka, R., Deruelles, J., Waterbury, J.B., Herdman, M., and Stanier, R.Y. (1979). Generic assignments, strain histories and properties of pure cultures of cyanobacteria. Microbiology *111*, 1–61.
34. Waterhouse, A.M., Procter, J.B., Martin, D.M.A., Clamp, M., and Barton, G.J. (2009). Jalview Version 2–a multiple sequence alignment editor and analysis workbench. Bioinformatics *25*, 1189–1191.
35. Schlebusch, M., and Forchhammer, K. (2010). Requirement of the nitrogen starvation-induced protein Sll0783 for polyhydroxybutyrate accumulation in Synechocystis sp. strain PCC 6803. Appl. Environ. Microbiol. *76*, 6101–6107.
36. Schreiber, U., Endo, T., Mi, H., and Asada, K. (1995). Quenching analysis of chlorophyll fluorescence by the saturation pulse method: Particular aspects relating to the study of eukaryotic algae and cyanobacteria. Plant Cell Physiol. *36*, 873–882.

STAR+METHODS

KEY RESOURCES TABLE

REAGENT or RESOURCE	SOURCE	IDENTIFIER
Experimental models: organisms/strains		
Synechocystis sp. PCC 6803	[33]	PCC 6803
Synechocystis sp. PCC 6803 D*glgP1/2*	[7]	N/A
Software and algorithms		
GraphPad PRISM version 6.01	La Jolla, CA, USA	https://www.graphpad.com/
COBALT: Multiple Alignment Tool - NCBI	Bethesda, MD, USA	http://www.ncbi.nlm.nih.gov/projects/cobalt/
Jalview 2	[34]	https://www.jalview.org/
Other		
BG_{11} Medium	[33]	N/A
$BG_{11\text{-}0}$ Medium	[35]	N/A
BG_{11} Sodium-free Medium	This study	$BG_{11\text{-}Na}$
$BG_{11\text{-}0}$ Sodium-free Medium	This study	$BG_{11\text{-}0\text{-}Na}$
ATP determination kit	Molecular Probes	A22066
ADP Assay Kit	Sigma-Aldrich	MAK133
Bis-(1,3-Dibutylbarbituric Acid)-trimethine oxonol	AAT Bioquest	21411
Amyloglucosidase	Sigma-Aldrich	10115

RESOURCE AVAILABILITY

Lead contact

Further information and questions or inquiries about data and resources should be directed to and will be fulfilled by the lead author, Karl Forchhammer (karl.forchhammer@uni-tuebingen.de).

Materials availability

No unique reagents were created for this study.

Data and code availability

This study did not generate datasets or code.

EXPERIMENTAL MODEL AND SUBJECT DETAILS

The cyanobacterial strains used in this study are listed in the Key resources table. All strains were grown in BG_{11} supplemented with 5 mM $NaHCO_3$ for vegetative growth, as described previously[33]. The concentration of sodium in standard BG_{11} medium is 22.5 mM. Nitrogen starvation was induced as previously described by a 2-step wash with $BG_{11\text{-}0}$ medium supplemented with 5 mM $NaHCO_3$, which contains all BG_{11} components except for $NaNO_3$ [6,35]. The concentration of sodium in standard $BG_{11\text{-}0}$ medium is 5.5 mM. Resuscitation was induced by addition of 17 mM $NaNO_3$ to cells residing in $BG_{11\text{-}0}$ (standard conditions). When indicated, 17 mM $NaNO_3$ was substituted by 17 mM KNO_3 or 5 mM NH_4Cl in recovery experiments, with or without supplementation with 17 mM NaCl, as specified. When stated, cells were transferred to sodium-free ($BG_{11\text{-}Na}$ or $BG_{11\text{-}0\text{-}Na}$) medium, where all sodium salts were replaced by potassium salts. When specified, cells were treated with the inhibitors DCMU (20 mM), DBMIB (100 mM), Antimycin A (25 mM), CCCP (100 mM), DNP (100 mM), MSX (200 mM), monensin (200 mM), EIPA (100 mM) and DCCD (200 mM) for 5 min before the experiment was started unless otherwise indicated. Cultivation was performed with continuous illumination (50 to 60 mmol photons m^{-2} s^{-1}) and shaking (130 to 140 rpm) at 27°C. D*glgP1/2* pre-cultures were cultivated with the appropriate concentration of antibiotics[7] . Biological replicates were inoculated with the same pre-cultures, but propagated, nitrogen-starved and resuscitated independently in different flasks under identical conditions.

METHOD DETAILS

Growth curves

Growth curves were generated using a Multi-cultivator OD-1000 with a Gas Mixing System GMS 150 (Photosystems Instruments, Drasov, Czech Republic). Vegetative cells were grown in BG_{11} or $BG_{11\text{-}Na}$ medium with and without supplementation with 2%

CO_2. Nitrogen starvation was induced as described above, followed by cultivation in $BG_{11\text{-}0}$ or $BG_{11\text{-}0\text{-}Na}$ medium supplemented with 2% CO_2. The OD was monitored at 720 nm. Three biological replicates per condition were measured.

ATP determination

1 mL aliquots of bacterial cultures were taken and immediately frozen in liquid nitrogen. ATP was extracted by boiling and freezing samples 3 times consecutively (boiling at 100°C, freezing in liquid nitrogen) and spinning them down at 25,000 g for 1 min at 4°C. ATP in the supernatant was quantified with the ''ATP determination kit'' (Molecular Probes (A22066), Oregon, USA) following the manufacturer's protocol. 50 ml of a reaction mix containing reaction buffer, luciferin, and firefly luciferase were mixed with 10 ml of the samples and the luminescence was quantified in a luminometer (Sirius Luminometer, Berthold Detection Systems). An ATP standard curve was generated and used to calculate ATP content in the collected samples. For every condition, at least three biological replicates were measured.

ADP determination

1 mL aliquots of bacterial cultures were taken and immediately frozen in liquid nitrogen. ATP was extracted by boiling and freezing samples 3 times consecutively (boiling at 100°C, freezing in liquid nitrogen) and spinning them down at 25,000 g for 1 min at 4°C. ATP in the supernatant was quantified with the ''ADP Assay Kit'' (MAK133, Sigma-Aldrich, Missouri, USA) following the manufacturer's protocol. 90 ml of a reaction mix containing reaction buffer, luciferin, and firefly luciferase were mixed with 10 ml of the samples and the luminescence was quantified in a luminometer to determine the RLU_{ATP}. Subsequently, ''ADP enzyme'' was added to the samples and the luminescence was measured again after a 2-min incubation to determine the RLU_{ADP}. An ADP standard curve was generated. The luminescence corresponding to ADP was calculated (RLU_{ADP}-RLU_{ATP}) and the ADP content in the samples was determined using the standard curve. For every condition, at least three biological replicates were measured.

Membrane potential determination

The dye Bis-(1,3-Dibutylbarbituric Acid)-trimethine oxonol (DiBAC4(3)) was purchased from AAT Bioquest (Hamburg, Germany; cat. no. 21411). Vegetative, chlorotic and dead cells (killed by boiling at 99°C for 20 min) were stained with 10 mM DiBAC4(3) (dissolved in DMSO) for 30 min in the dark. 10 mL of stained cells were dropped on an agarose-coated microscopy slide. A Leica DM5500 B (Wetzlar, Germany) with an 100x /1.3 oil objective was used to image cells. A yellow fluorescent protein (YFP) filter (excitation: 490-510 nm; emission 520-550 nm) was used to detect DiBAC4(3).

Glycogen determination

Glycogen content was determined as described by Gründel et al.[27] with modifications established by Klotz et al.[6]. 2 mL-samples were collected, span down, and washed with distilled water. Cells were lysed by incubation in 30% KOH at 95°C for 2 h. Glycogen was precipitated by addition of cold ethanol to a final concentration of 70% followed by an overnight incubation at −20°C. The precipitated glycogen was pelleted by centrifugation at 15000 g for 10 min and washed with 70% ethanol and 98% absolute ethanol, consecutively. The precipitated glycogen was dried and digested with 35 U of amyloglucosidase (10115, Sigma-Aldrich) in 1 mL of 100 sodium acetate pH 4.5 for 2 h. 200 ml of the samples were mixed with 1 mL of 6% O-toluidine in acetic acid and incubated at 100°C for 10 min. Absorbance was then read at 635 nm. A glucose calibration curve was used to determine the amount of glycogen in the samples. For every condition, at least three biological replicates were measured.

Oxygen evolution measurement

Oxygen evolution was measured *in vivo* using a Clark-type oxygen electrode DW1 (Hansatech, King's Lynn, Norfolk, UK). Light was provided from a high-intensity white light source LS2 (Hansatech). Oxygen evolution of 2 mL recovering cultures at an OD_{750} of 0.5 was measured at room temperature and 50 mmol photons m^{-2} s^{-1}. Three biological replicates per condition were measured.

Pulse amplification measurement (PAM)

PSII activity was analyzed *in vivo* with a WATER-PAM chlorophyll fluorometer (Walz GmbH, Effeltrich, Germany). All samples were dark-adapted for 5 min before measurement. The maximal PSII quantum yield (F_v/F_m) was determined with the saturation pulse method[36]. Cultures were diluted 1:20 before the measurements in a final volume of 2 mL. Three biological and three technical replicates were measured (three measurements of each biological replicate).

QUANTIFICATION AND STATISTICAL ANALYSIS

Statistical details for each experiment can be found in the figure legends. For all experiments, 3 biological replicates were analyzed. Samples taken from cultures that were inoculated with the same pre-cultures, but propagated, nitrogen-starved and resuscitated independently in different flasks under identical conditions were considered different biological replicates. Every measured data point, as well as the mean and SD of the 3 replicates are shown in the graphs. GraphPad PRISM was used to perform paired Student's t tests to determine the statistical significance. Asterisks in the figures were used to symbolize the p value: One asterisk represents p **%** 0.05, two asterisks p **%** 0.01, three asterisks p **%** 0.001, and four asterisks p **%** 0.0001.

4. Publication 4 (Accepted)

Literature review

Niels Neumann, Sofía Doello, and Karl Forchhammer

Recovery of unicellular cyanobacteria from nitrogen chlorosis: A model for resuscitation of dormant bacteria.

2021. M*icrobial Physiology.* doi: 10.1159/000515742

Microbial Physiology

Review Article

Microb Physiol
DOI: 10.1159/000515742

Received: January 8, 2021
Accepted: March 6, 2021
Published online: April 20, 2021

Recovery of Unicellular Cyanobacteria from Nitrogen Chlorosis: A Model for Resuscitation of Dormant Bacteria

Niels Neumann Sofia Doello Karl Forchhammer

Interfaculty Institute of Microbiology and Infection Medicine Tübingen, Eberhard Karls University Tübingen, Tübingen, Germany

Keywords
Metabolic quiescence · Cell cycle arrest · Glycogen metabolism · ATP homeostasis · Starvation

Abstract
Nitrogen starvation induces developmental transitions in cyanobacteria. Whereas complex multicellular cyanobacteria of the order Nostocales can differentiate specialized cells that perform nitrogen fixation in the presence of oxygenic photosynthesis, non-diazotrophic unicellular strains, such as *Synechococcus elongatus* or *Synechocystis* PCC 6803, undergo a transition into a dormant non-growing state. Due to loss of pigments during this acclimation, the process is termed chlorosis. Cells maintain viability in this state for prolonged periods of time, until they encounter a useable nitrogen source, which triggers a highly coordinated awakening process, termed resuscitation. The minimal set of cellular activity that maintains the viability of cells during chlorosis and ensures efficient resuscitation represents the organism's equivalent of the BIOS, the basic input/output system of a computer, that helps "booting" the operation system after switching on. This review summarizes the recent research in the resuscitation of cyanobacteria, representing a powerful model for the awakening of dormant bacteria.

Introduction

Nutrient starvation can be detrimental to organisms when it leads to metabolic disorder that impairs vitalcellular processes. A successful strategy to survive such periods of nutrient deprivation that is particularly widespread in prokaryotes is the transition into a dormant state. In this state, the metabolic processes are reduced to an absolute minimum. The remaining activities just ensure survival and enable the dormant cells to awake and resume growth once the limiting nutrient becomes available again. It is assumed that in natural environments a majority of the bacteria reside in a dormant state, and these cells comprise a "seed bank" – a reservoir – that can be resuscitated when favourable conditions occur. This mechanism is largely responsible for the fitness of bacterial populations and contributes to the sudden appearance of bacteria in the environment and the spreading of antibiotic resistances and bacterial pathogens. An example of dormant bacteria acting as a reservoir of antibiotic resistance is presented in the study by Udikovic-Kolic et al. [2014], where manure supplementation of soil is shown to result in proliferation of diverse soil-resident bacteria, some carrying antibiotic resistance genes.

The ways in which the cells enter dormancy and recover from the dormant stage are rather diverse. Some bacteria form endospores or exospores, others create en-

karger@karger.com
www.karger.com/mip

Correspondence to:
Karl Forchhammer, karl.forchhammer @ uni-tuebingen.de

capsulated cysts or even generate apparently non-differentiated persister cells, which is the case in *Mycobacterium tuberculosis* [Keren et al., 2011]. Despite the differences among these quiescent states, a common requirement in this survival strategy is the ability to reactivate metabolism upon encountering permissive conditions.

Studying the molecular mechanisms supporting these cellular processes is complicated for several reasons. A bacterial population that has undergone the transition into a dormant state is usually highly heterogeneous, since phenotypical variation can be beneficial in the emergence from starvation-induced growth arrest [Moreno-Gámez et al., 2020]. In many cases, includingpopulations of nutrient-starved *Flavobacterium columnare* and *Brucella suis* cells, only a small proportion of the cells remain viable [Arias et al., 2012; AlDahouk et al., 2013]; in others, such as the germination of akinetes of filamentous heterocyst-forming cyanobacteria, re-activation of metabolism is highly asynchronous [Perez et al., 2018]. This heterogeneity precludes the employment of powerful molecular methods that rely on homogenous populations, such as metabolomics, proteomic or transcriptomic studies. Therefore, in many cases, the behaviour of dormant cells can only be studied using single-cell analysis, which still has many limitations. One of the rare cases where transition into and out of the dormant state occurs in a population-wide coherent manner is the case of nitrogen starvation-induced chlorosis in some unicellular cyanobacterial strains, such as *Synechococcus elongatus* and *Synechocystis* PCC 6803. Following a brief description of nitrogen starvation-induced chlorosis, the present article provides a consolidated review of our current knowledge on the resuscitation of these cyanobacteria from prolonged nitrogen chlorosis.

Entry into Chlorosis

That nitrogen starvation leads to bleaching of cyanobacterial cultures was already described in 1910 and this process was termed "chlorosis" [Boresch, 1910]. Only about 70 years later, studies in *S. elongatus* showed that the rapid bleaching caused by nitrogen starvation, a colour change from deep blue-green to yellowish-greenish, was mainly caused by the degradation of the blue phycobiliproteins [Allen and Smith, 1969]. These proteins constitute the light-harvesting antenna system for the photosynthetic reaction centres, the phycobilisomes (PBS) [Grossman et al., 1993]. By screening for mutants with a non-bleaching phenotype on nutrient-deficient plates in the 1990s, *nbl* (non-bleaching) genes were identified in the laboratory of A. Grossman [Collier and Grossman, 1994]. These *nbl*-genes are responsible for phycobiliprotein degradation upon various stress conditions, including nitrogen starvation or high-light stress. Until the mid-1990s, it was assumed that the chlorotic cells lost viability, until a study by Görl et al. [1998] showed that chlorotic *Synechococcus* cells maintain viability for extended periods of time [reviewed in Schwarz and Forchhammer, 2005]. This study revealed a gradual decline in cellular activities following the initial phycobiliprotein degradation, until the cells entered a dormant-like state with almost no detectable metabolic activity. Based on these observations, the chlorosis process could be divided into 3 phases, with phase 1 being the rapid degradation of phycobiliprotein occurring within 1–2 days, followed by phase 2, the gradual decline of metabolic activity (concomitant with a decline in chlorophyll *a*) within the following 8–14 days, and finally, the terminal phase 3, the dormant state with a low basal level of photosynthetic activity [Görl et al., 1998]. Concomitant with the gradual decline of metabolic activity, the cells undergo substantial intracellular re-organization through proteolysis, in particular with respect to the degradation of the intracellular membrane system, the thylakoids, which accommodate the molecular machines of the photosynthetic electron transport chain including photosystem I and II. However, a low level of photosynthetic activity involving PSI and PSII activity is preserved during prolonged chlorosis, which was shown to be required to maintain long-term cell viability [Sauer et al., 2001]. Since no net yield of photosynthesis could be determined, it was suggested that the photosynthetic electrons are recycled through a water-to-water cycle, where oxygen, produced through water splitting at PSII, serves as electron acceptor for PSI-reduced ferredoxin [Sauer et al., 2001]. Considering the severe decomposition of intracellular structures after long-term chlorosis, it is astonishing that cells readily re-green within 2 days and resume growth following the addition of a nitrogen source [Görl et al., 1998; Sauer et al., 1999; Sauer et al., 2001; reviewed in Schwarz and Forchhammer, 2005].

Synechocystis sp. 6803 is a unicellular cyanobacterium only distantly related to *S. elongatus* [Robertson et al., 2001]. It is metabolically more versatile than *S. elongatus* as it is not strictly photoautotrophic and is able to synthesize various reserve polymers not present in *S. elongatus,* such as the nitrogen storage compound cyanophycin (CP) [Stephan et al., 2000] or the polymer polyhydroxybutyrate (PHB) [Hauf et al., 2013; reviewed in Koch et al., 2020]. Despite these differences, the basic nitrogen-star-

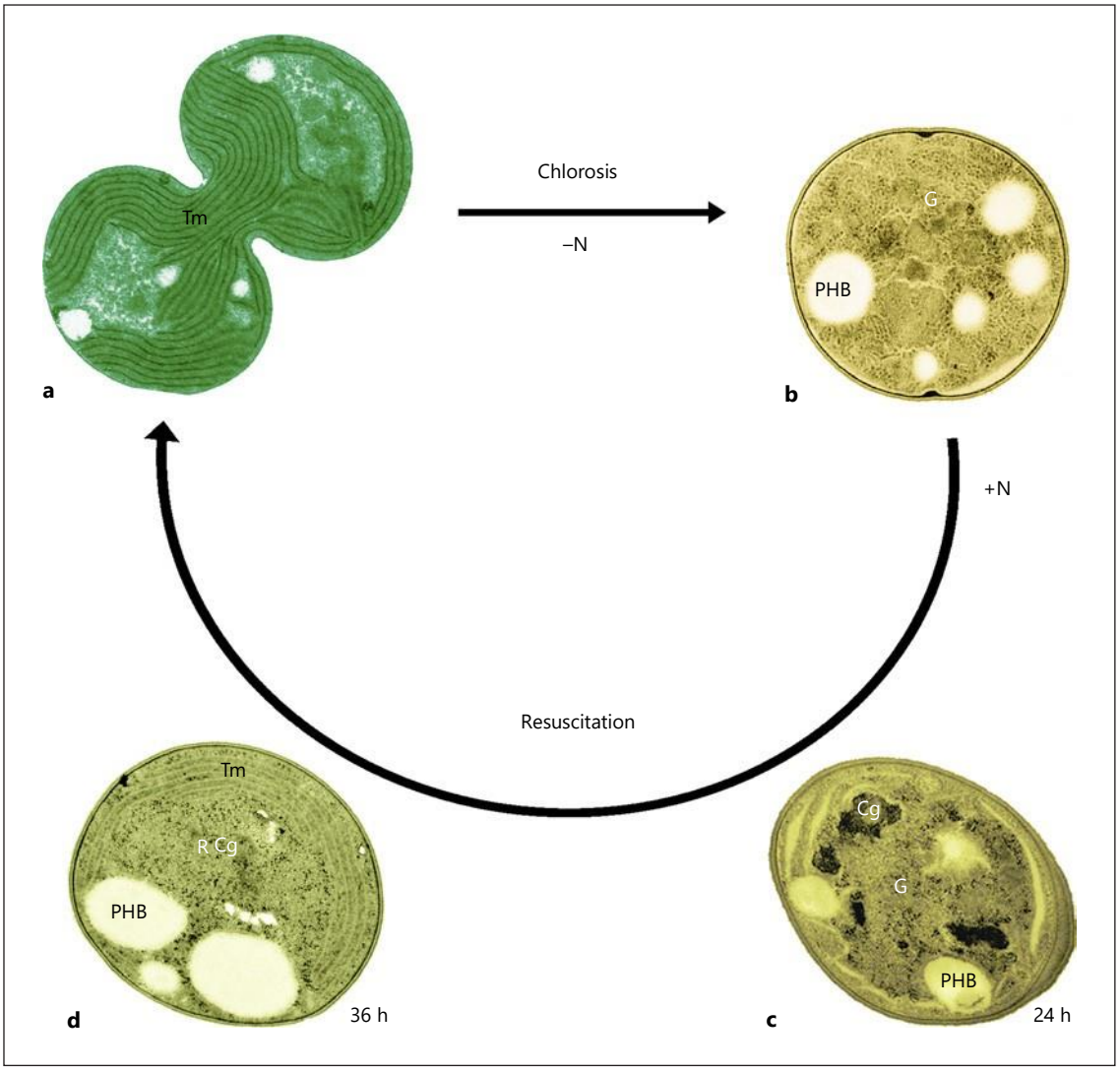

Fig. 1. *Synechocystis* cells during developmental transitions through nitrogen starvation and resuscitation. **a** Cell in exponential growth phase. **b** Chlorotic cell starved for 1 month. **c** Cells during the first 24 h of resuscitation. **d** Cells after 36 h of resuscitation. G, glycogen granules; PHB, polyhydroxybutyrate granules; Cg, cyanophycin granules; Tm, thylakoid membrane; R, ribosomes.

vation acclimation response seems to be highly conserved. Similar to *S. elongatus*, *Synechocystis* employs a set of *nbl* genes under the control of a conserved sensor kinase (Hik33/NblS) to degrade phycobiliproteins, which degrades the photosynthetic apparatus and tunes down metabolic activity until a dormant-like state is attained, from which it rapidly recovers after supplementation with combined nitrogen [reviewed in Schwarz and Forchhammer, 2005]. A distinguishing feature of the strains is the accumulation of large amounts of PHB in *Synechocystis* during prolonged chlorosis [Schlebusch and Forchhammer, 2010; Hauf et al., 2013; Damrow et al., 2016]. However, mutants defective in PHB synthesis are neither impaired in the chlorosis response, nor in the ability to recover from nitrogen starvation [Klotz et al., 2016; Koch et al., 2020], indicating that PHB metabolism is not directly involved in surviving nitrogen deprivation. Unlike PHB, glycogen seems to be a major carbon polymer supporting nitrogen starvation; both *Synechocystis* and *S. elongatus* rapidly accumulate large amounts of this polymer upon nitrogen limitation or upon inhibition of glutamine synthetase (GS) activity [Klotz et al., 2015]. However, mutants that are defective in glycogen synthesis (*glgC* mutants or *glgA1/glgA2* double mutants) display

metabolic deficiencies during nitrogen starvation and are impaired in phycobiliprotein degradation and, therefore, show a non-bleaching phenotype. After a few days under nitrogen-deficient medium, they lose viability [Gründel et al., 2012; Hickman et al., 2013]. The synthesis of glycogen is accompanied by the concomitant induction of expression of glycogen catabolic genes, for which the SigE and Rre37 regulators are responsible [Azuma et al., 2011; Osanai et al., 2014]. Although this appears paradoxical, it illustrates that a genetic program exists that "anticipates" the recovery from nitrogen starvation (see below).

Resuscitation from Chlorosis: A Global Analysis

A first global and comprehensive analysis of the resuscitation of chlorotic *Synechocystis* cells was performed by Klotz et al. [2016]. When fully developed, long-term chlorotic *Synechocystis* cells were supplied with nitrate, and it could be shown that they started to re-green and regain photosynthetic activity after about 24 h. After about 2 days, photosynthetic performance was almost completely restored, and after 3 days, cell division was resumed. Figure 1 provides a graphical representation of these developmental transitions. At a first glance, the retarded appearance of photosynthetic pigments might give the impression that the cells only respond to the addition of a nitrogen source with a delay of approximately a day. However, examination at the molecular level reveals that the apparent 24-h lag phase is in fact a highly dynamic period. As shown by transcriptomic and proteomicanalysis, the basic operating system of the cells, whichduring chlorosis has been turned down to a minimum, must be re-established before the cells are able to re-green and rebuild the complex intracellular machineries of photosynthesis [Klotz et al., 2016; Spat et al., 2018]. It transpired that the entire process follows a highly orchestrated genetically encoded program, evident at all levels of cellular activity.

At the metabolic level, resuscitation can be divided into two principal phases. In the first phase, immediately after nitrate addition, cells turn on a heterotrophic-like metabolism, based on glycogen consumption and oxygen-dependent respiration. In the second phase, after about 24 h, when the photosystems reappear, cells switch to a mixotrophic metabolism, where glycogen utilization co-occurs with CO_2 fixation and oxygenic photosynthesis. Only in the fully recovered state do they finally resume the classical photoautotrophic metabolism and return to vegetative growth. A key to the understanding of the resuscitation program is the underlying glycogen metabolism, which provides the cells with energy and metabolic precursors (see Fig. 2 for an overview of the principal pathways of glycogen metabolism in *Synechocystis*). Therefore, glycogen is pivotal to the viability ofchlorotic cells. The *Synechocystis* genome harbours two paralogous genes for glycogen synthetases, *glgA1* (sll0945) and *glgA2* (sll1393). Knockout of only one of the two *glgA* paralogues results in mutants that synthesize the same amount of glycogen as the wild type following nitrogen step down. Nevertheless, these two mutants display striking phenotypic differences upon nitrogen starvation. Whereas the *glgA2* mutants are able to carry a wild-type response to chlorosis, the *glgA1* mutants as well as the *glgA1/glgA2* double mutants show impaired chlorosis: instead of a step-wise degradation of the photosynthetic pigments, the mutants do not initially respond to nitrogen depletion, but after a while they turn white and lose viability [Koch et al., 2019]. This suggests that only glycogen produced by GlgA1 is relevant for survival. The molecular basis of this difference is unclear and is currently under investigation.

Similar non-redundant pairs of glycogen metabolic genes are found for the paralogues of glycogen phosphorylase, *glgP1* (sll1356) and *glgP2* (slr1367), as well as for the paralogues for glycogen-debranching enzyme *glgX1* (slr0237) and *glgX2* (slr1857). The analysis of the respective mutants showed that only GlgP2 supports the resuscitation program. The *glgP2* mutants (still able to produce GlgP1), as well as the *glgP1/glgP2* double knockout mutants, are unable to be resuscitated from chlorosis, although the initial process of chlorosis proceeds normally, as deduced from the ordered degradation of pigments [Doello et al., 2018]. The poor resuscitation of the various *glgA* and *glgP* mutants is depicted in Figure 2b. The glycogen phosphorylase reaction releases Glc-1P, which is further converted by phosphoglucomutase (PGM, sll0726) to generate Glc-6P (see Fig. 2a). This metabolite can either enter the Embden-Meyerhof-Parnas pathway (EMP), or it can be oxidized by glucose-6P dehydrogenase (encoded by the *zwf*gene) to 6P-gluconate, which is further metabolized by the oxidative pentose phosphate (OPP) cycle or the Entner-Doudoroff (ED) pathway. Whereas mutants with a deficient EMP pathway recover almost like the wild type from the chlorotic state, *zwf* knockout mutants are strongly impaired in resuscitation. A mutant deficient in only the ED pathway is less severely affected than a mutant with an impairment in the OPP pathway, showing that the latter is the most important glycogen catabolic pathway in recovering chlorotic cells [Doello et al., 2018].

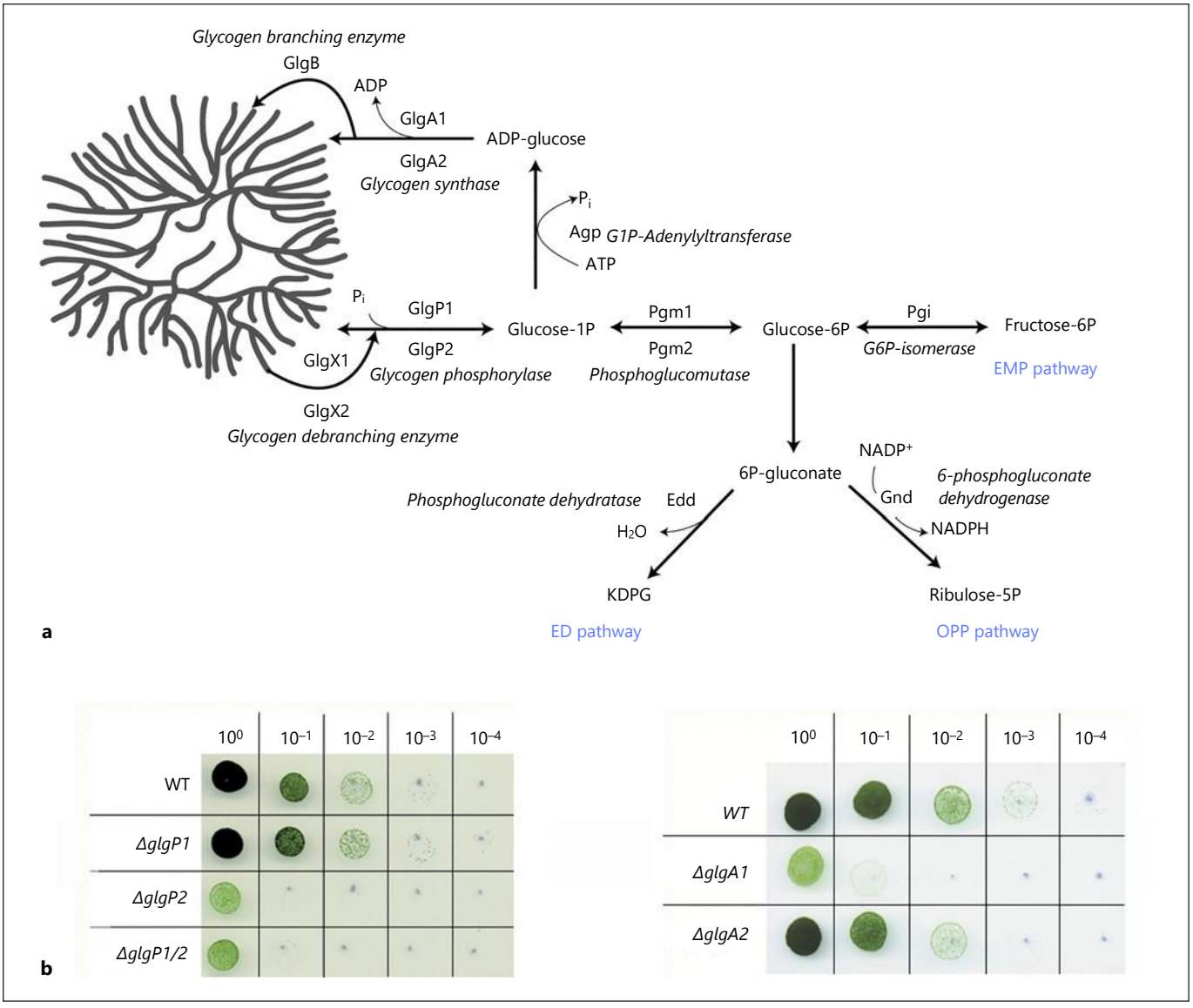

Fig. 2. Schematic representation of glycogen metabolism in *Synechocystis* and its involvement in chlorosis and resuscitation. **a** Depiction of reactions in glycogen metabolism and glycogen catabolic pathways in *Synechocystis*. **b** Resuscitation of chlorotic cells tested by drop plate assay. From a serial dilution of chlorotic cultures (0–10^{-4} dilution as indicated), 5 µL were dropped on nitrate-supplied BG11 plates and incubated until colonies appeared. Resuscitation efficiency of wild type (WT) is compared to various mutants deficient in glycogen phosphorylase (Δ*glgP1*, Δ*glgP2*, Δ*glgP1/2*) or glycogen synthase (Δ*glgA1*, Δ*glgA2*).

When the cells started to respire and to degrade glycogen upon the addition of nitrate to chlorotic cultures, the low level of photosynthetic activity, which is still measurable in the chlorotic state, is completely shut down. Photosynthetic oxygen evolution only reappears at the end of the first phase of resuscitation, indicating a switch to a mixotrophic metabolism. During this period, which takes place about 1 day after addition of the nitrogen source, re-greening becomes visible, indicating the re-installation of the photosynthetic machinery. Electron micrographs reveal that in this second phase of resuscitation, the cells reconstruct the thylakoid system de novo (see Fig. 1d). After about 2 days, most of the cells have recovered their photosynthetic machineries and are able to switch metabolism toward vegetative growth. With the onset of cell division, 2–3 days after the addition of a ni-

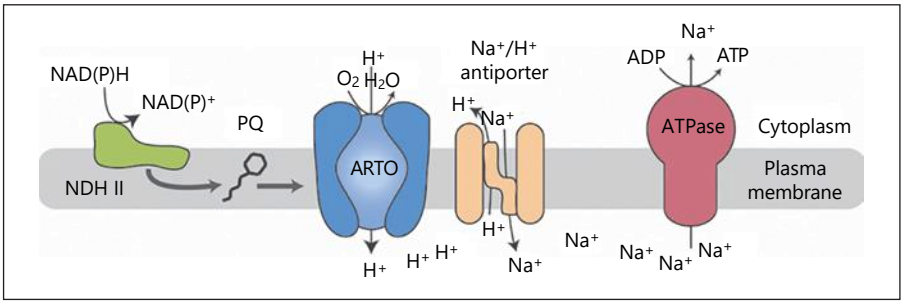

Fig. 3. Sodium-dependent bioenergetic processes in nitrogen-starved cells. Depiction of the components of the respiratory chain and the ATP synthesis machinery in the plasma membrane of *Synechocystis*.

trogen source, the resuscitation program is complete, and the cells exhibit typical vegetative growth. During chlorosis, the cells apparently become arrested in a pre-divisional state; they contain on average double the amount of chromosomal DNA than actively growing cells. At the end of the resuscitation program, the average cell size, as well as the average chromosome copy number, decrease to half the values of chlorotic cells, which is indicative of ongoing cell division [Klotz et al., 2016].

The Start of Resuscitation

Bioenergetics of Awakening

During chlorosis, metabolic reactions are reduced to a minimum and the intracellular energy charge is kept low; the ATP content is maintained at a basal level, which constitutes the minimum to maintain cell survival. Thus,the ATP levels in nitrogen-starved cells are reduced by up to 25% of the value in vegetatively growing cells. Upon addition of a nitrogen source to chlorotic cells, the first detected cellular response is a rapid increase in the ATP content. However, the extent of this increase is dependent on the form in which nitrogen is provided. Addition of sodium nitrate to chlorotic cells triggers a 100% increase in the ATP content within 20 min, whereas supplementation with potassium nitrate leads to a slower increase in the ATP levels (approximately 20–30% less compared to sodium nitrate). Doello et al. [2021] investigated this peculiar phenomenon and have discovered a so far unrecognized and unique bioenergetic strategy in nitrogen-starved cells.

During prolonged chlorosis, the thylakoid membranes, which accommodate the majority of the F-type ATPase complexes, are degraded. Consequently, chlorotic cells rely on the ATP synthases located in the plasma membrane, which are able to use a sodium motive force to power ATP synthesis. When resuscitation is started by the addition of sodium nitrate, the sudden rise of the extracellular sodium concentration leads to an increased sodium motive force, which causes an instantaneous increase in the ATP levels. When potassium nitrate is used to induce resuscitation, the concentration of sodium remains constant, and the increase in the ATP content results from a metabolically regulated response to the availability of a nitrogen source.

When nitrogen assimilation initiates, the cellular ATP demand dramatically increases due to the high turnover rate of the energy-consuming GS reaction. A concomitant increase in ATP synthesis is, therefore, essential to ensure efficient nitrogen assimilation and to avoid drainage of the cellular ATP levels. How cells achieve this tight control of the ATP homeostasis has not yet been entirely deciphered; however, it has been shown that activation of the GS reaction is involved in this regulatory mechanism, because the increase in ATP levels in response to the availability of nitrogen is sensitive to MSX, a specific GS inhibitor. Additionally, upon addition of a nitrogen source, ATP synthesis requires glycogen degradation and respiration. This was demonstrated by the lack of an increase in the ATP content in a GlgP-negative mutant, which is impaired in glycogen catabolism, and in wild-type cells when they are treated with potassium cyanide (KCN), an inhibitor of the respiration. Moreover, specific inhibition of electron transfer from the plastoquinone pool (PQ) to the cytochrome b_6f complex, which is exclusively found in the thylakoid membranes, reveals that respiration takes place at the plasma membrane in chlorotic cells undergoing the early steps of resuscitation [Doello et al., 2021]. It is, therefore, tempting to speculate that nitrogen assimilation through the GS reaction initiates glycogen breakdown, thereby generating reducing equivalents, which then activate respiration at the cytoplasmic membrane. The plasma membrane is equipped with an alternative respiratory chain consisting of a type II NADH:quinone oxidoreductase (NDH II) and an alternative respiratory terminal oxidase (ARTO) [Baers et al., 2019]. In fact, we could show that NDH II is one of the most highly accumulated proteins in the chlorotic state

[Spat et al., 2018]. In vegetative cells, this respiratory system is coupled to the generation of a sodium motive force to energize sodium-dependent bicarbonate uptake [Pils and Schmetterer, 2001]. In nitrogen-starved cells, where inorganic carbon fixation is arrested, this bioenergetic system ensures energy provision in the standby mode and to support the initial phase of resuscitation (Fig. 3).

Resumption of Nitrogen Assimilation

The activity of GS is subject to tight regulation. In cyanobacteria, GS activity is controlled by the inhibitory proteins IF7 and IF17, whose synthesis is under global nitrogen control and is strongly downregulated during nitrogen starvation [Bolay et al., 2018]. Moreover, the cells express a second, nitrogen starvation-specific GS gene, *glnN* [Reyes and Florencio, 1994]. In *S. elongatus*, GlnN helps recovery of the cells from long-term nitrogen starvation [Sauer et al., 1999]. Thus, the cells maintain highly active nitrogen assimilation capacity during chlorosis. As soon as nitrogen becomes available again, GS starts working, thereby initiating the resuscitation program. Nitrogen assimilation then operates at full capacity, with the inhibitory peptides IF7 and IF187 only being induced toward the end of resuscitation [Spat et al., 2018]. In agreement with these findings is the observation that the non-coding regulatory RNA NsiR4, which prevents expression of IF7, remains highly expressed in the initial phase of resuscitation. The assimilation of combined nitrogen initially exceeds the pace of protein synthesis, since the entire translational machinery first has to be re-installed. The excess of assimilated nitrogen is transiently stored as CP [Watzer and Forchhammer, 2018], which is deposited as a granular structure in the cytoplasm (see Fig. 1c; structures indicated by Cg). When the protein synthesis machinery is fully operational, the CP material is recycled for synthesis of cellular building blocks. This strategy enables cells to store any available nitrogen for subsequent utilization in an environment with fluctuating and transient nitrogen supply. Physiological comparison of mutants deficient in CP synthase (cphA) with wild-type cells demonstrated that in the absence of CP synthesis cells are unable to recover completely when nitrogen is only transiently available to the cells. By contrast, wild-type cells can resuscitate successfully and return to vegetative growth [Watzer and Forchhammer, 2018].

Early Events in Transcriptional Regulation

To reveal the molecular events occurring during the process of resuscitation, a detailed transcriptome study has been performed [Klotz et al., 2016]. To achieve this, a high-density microarray covering the entire chromosome and the 7 plasmids was used, probing all 8,916 transcripts of coding and non-coding RNA. RNA was extracted at 5 different time points (after 0, 4, 12, 24 and 48 h after nitrate addition), starting with fully developed chlorotic cells and finishing with completely re-greened cells. A total of 1,570 differentially regulated genes were detected, which corresponds to 17.6% of the entire transcriptome. Of these genes, approximately one-third comprises non-coding RNA. The changes in the transcriptome during the resuscitation process perfectly reflect the chronological order of cellular processes. The majority of the differentially regulated genes belong to the early responding genes, whose expression changes after about 4 h. They comprise 425 and 626 up- or downregulated genes, respectively, compared with the dormant state. The upregulated group of genes includes the entire set of genes encoding the translational apparatus, as well as metabolic genes, particularly those involved in nitrate/nitrite assimilation, genes encoding enzymes for co-factor biosynthesis, ATP synthesis and CO_2 fixation. The latter finding is striking, as it hints at a role for CO_2 fixation prior to the onset of photosynthesis. In agreement with this suggestion, Doello et al. [2018] detected CO_2 fixation activity as soon as 10 h after the initiation of resuscitation, well before the onset of oxygen evolution. Surprisingly, the genes encoding the enzymes required for glycogen catabolism are not strongly upregulated at the transcriptional level. In fact, the glycogen catabolic genes are already upregulated in response to the nitrogen step down, concomitant with the synthesis of glycogen. Proteome analyses confirm that the respective proteins are maintained at elevated levels throughout the chlorotic state. This demonstrates an "anticipatory principle" in the acclimation toward nitrogen starvation. The decisive catabolic enzymes are prepared in standby mode, awaiting the availability of nutrient. This necessarily implies that the enzymes, such as glycogen phosphorylase, have to be kept in an inactive state, in order to prevent premature glycogen consumption. Preliminary data indicate a key role for PGM in the control of glycogen breakdown [unpubl. data].

As deduced from the dynamics of the transcriptome, the early responses reflect the re-installation of the basic operation system of the cells, the core anabolic reactions, energy metabolism and the translational apparatus, enabling the cells to re-configure the complex cellular structures that were degraded during chlorosis. As deduced from this study, the transcriptional machinery itself, in particular the components of the RNA polymerase, does

not change in expression as strongly as the translational machinery. The changes are more subtle and affect specific regulatory components. During nitrogen starvation, the transcriptional machinery switches from use of the house-keeping SigA-dependent RNA polymerase to use of alternative sigma factors, in particular, SigB, SigC and SigE [Imamura and Asayama, 2009; Heilmann et al., 2017]. In particular, SigC has been shown to promote late-stage gene expression and nitrogen promoter recognition [Asayama et al., 2004]. SigE mediates induced expression of various carbon catabolic genes during nitrogen starvation (see above). During resuscitation, however, the transcriptional machinery has to be re-wired toward SigA-dependent transcription, which is responsible for the expression of the core operating system of the cell. The extensive re-organization of the transcriptome agrees with a dominant role for different sigma factors that affect global transcriptional patterns [Srivastava et al., 2020]. The small non-coding 6S RNA may have a key role in sigma factor transition. The 6S RNA is widely distributed in prokaryotes and acts as a global regulatory RNA involved in growth control. *Synechocystis* mutants with mutations in *ssaA* show delayed recovery from the chlorotic state [Heilmann et al., 2017]. The authors of that work also performed in vivo pull-down analysis of the RNA polymerase complex, and the data suggest that the 6S RNA promotes the recruitment of the housekeeping sigma factor SigA to the RNA polymerase core complex, concurrently supporting displacement of group 2 sigma factors, such as SigB, C and E. An early transition back to SigA-dependent transcription explains the extensive transcriptional response observed at the onset of resuscitation in the study by Klotz et al. [2016].

The Second Phase of Resuscitation: Restoration of Photosynthesis

Only after the re-launch of the basic components of the metabolic machinery can the cells afford to re-install the photosynthetic machinery. This is because it imposes a high metabolic burden on the cells through the coordinated synthesis of lipids for thylakoid membranes, the large amounts of tetrapyrroles and all the proteins required for the photosynthetic complexes, from the PBS antenna to the reaction centres. The timing of chlorophyll biosynthesis is especially crucial, because free chlorophyll is toxic to the cells. All these processes must, therefore, occur in a highly coordinated manner. How this is achieved is still poorly understood. The two aforementioned transcriptome and proteome studies [Klotz et al., 2016; Spat et al., 2018], however, provide preliminary insights into this process. Remarkably, the first cellular response upon nitrogen addition is in fact to suppress any residual photosynthetic activity. This early negative impact on photosynthesis is in good agreement with the observation that the function of some of the early regulated gene products is to prevent premature synthesis of photosynthetic components. For example, transient expression of the non-coding RNA PsrR1 supresses chlorophyll biosynthesis and PBS gene expression [Georg et al., 2014] and expression of several PSII-related and chlorophyll biosynthesis-related genes are repressed in the early stage of resuscitation. The logic of this strategy might also be related to the diurnal lifestyle of cyanobacteria. In nature, the cyanobacteria are constantly subjected to the daily availability of light energy for a certain length of time. The awakening of the cells relies exclusively on glycogen-dependent energy metabolism, which allows utilization of nitrogen sources independent of light availability. This ensures a secure progression of resuscitation until the entire basic operation system is completely re-installed. Only then do the cells start to reconstitute the photosynthetic apparatus. The corresponding process works extremely precisely and is finely tuned at all levels. This is clearly illustrated for chlorophyll biosynthesis [Spat et al., 2018], whereby a decisive step in chlorophyll biosynthesis is the conversion of protochlorophyllide to chlorophyllide, for which light-dependent and light-independent isoenzymes exist in *Synechocystis*. At the proteome level, the enzymes are undetectable in the chlorotic state and in the early phase of resuscitation. The light-dependent protochlorophyllide reductase (Por) only becomes detectable in the middle phase of resuscitation [Spat et al., 2018], whereas the light-independent isoenzymes ChlB and ChlL are still absent. In agreement with this, the expression of the corresponding genes is repressed during the early phase of resuscitation (see above). This strategy ensures that chlorophyll biosynthesis can start as soon as the basic operation system is re-installed and light is available. The final biosynthetic enzyme, chlorophyll synthase (ChlG) is already present prior to the induction of Por synthesis, so that using this strategy the cells are prepared to convert the highly toxic chlorophyllide molecule into chlorophyll *a*, which is then incorporated into chlorophyll-binding proteins, which have to be synthesized simultaneously.

Another crucial step in the re-installation of the photosynthetic machinery is the assembly of the photosynthetic protein complexes in newly synthesized thylakoid membranes. Here, quantitative analyses of the phosphoproteome have yielded first intriguing insights into what

is occurring. Among the phosphoproteins whose degree of phosphorylation changed dynamically over the time course of resuscitation, the largest functional group is indeed the proteins related to photosynthesis [Spat et al., 2018]. These proteins can be grouped in 5 classes according to the pattern of phosphorylation change. The few residual proteins of the PBS rods are highly phosphorylated during chlorosis and the phosphorylation level gradually decreases during resuscitation. Phosphorylation of the phycobiliproteins could be related to protein stability and turnover. Other photosynthetic proteins, such as PBS core proteins or some components of PSI and PSII, show a transient increase in phosphorylation. The Vipp1 proteins, for example, which play a decisive role in thylakoid membrane biogenesis [Heidrich et al., 2017], show a particularly complex phosphorylation pattern with 8 detected phosphorylation sites, occurring on 2 clustered regions of the protein. The phosphorylation level remains high during the initial resuscitation phase, with some sites even showing initially increased phosphorylation, until time point 24 h. Subsequently, phosphorylation of all sites decreases, which occurs concomitantly with the accumulation of newly synthesized Vipp1 protein and the emergence of stacked thylakoid membranes. Vipp1 was shown to form large multimeric structures that form rings and rods [Theis et al., 2019] and control the formation of thylakoid membranes [Westphal et al., 2001]. Phosphorylation of Vipp1 might thus keep this protein in an inactive state, until the progression of resuscitation advances to the stage where Vipp1 activity comes into play. Based on this study, protein phosphorylation has thus emerged to add another layer of regulator complexity controlling the timing of resuscitation.

Conclusions

The analysis of the nitrogen starvation-induced transition of *Synechocystis* into a dormant-like chlorotic state and resuscitation form this state has revealed new insights into dormancy and awakening. Organisms from most diverse origins tune down cellular activities to a minimum in order to survive extended periods of adverse environmental conditions, such as nutrient starvation. Under these circumstances, they all need to find the answer to a major issue: What is the minimal activity necessary to maintain viability?

In order to resuscitate cells from the dormant state, a minimal initial energy is necessary, and a minimal set of the most fundamental cellular functions has to be maintained; in order to make new protein, at least some ribosomes and translation factors need to be in place. This minimal set of cellular activities represents the organism's equivalent of the BIOS, the basic input/output system of a computer, that helps re-boot the operation system after being switched on. In analogy, the same tasks have to be performed when resuscitation from the dormant state is executed. We have learned by using chlorosis in *Synechocystis* as a model system that evolution has prepared cells with a sophisticated genetic program to achieve this task. Moreover, it appears that already at the stage when the cells enter the dormant state, they anticipate the future awakening and prepare essential components to allow rapid resuscitation. The revival of nutrient starvation-induced *Bacillus subtilis* spores is another example of the existence of a highly organized developmental program to awaken from dormancy and reconstruct a cell [Sinai et al., 2015]. Another lesson learned from these investigations is the identification of the functions of genes that have been annotated as "hypothetical," since their roles appear only under extreme conditions, and some of these may even belong to the cellular BIOS.

Conflict of Interest Statement

The authors have no conflicts of interest to declare.

Funding Sources

Work in the Forchhammer laboratory was funded by the RTG 1708 "Molecular principles of bacterial survival strategies" and by DFG-funded Research Unit SCyCode (FOR2816). We further acknowledge support by Open Access Publishing Fund of University of Tübingen and Infrastructural Funding from the Cluster of Excellence EXC 2124 "Controlling Microbes to Fight Infections."

Author Contributions

Conceptualization: K.F.; writing, original draft preparation: K.F.; review and editing: N.N., S.D. and K.F.

References

Al Dahouk S, Jubier-Maurin V, Neubauer H, Köhler S. Quantitative analysis of the Brucella suis proteome reveals metabolic adaptation to long-term nutrient starvation. BMC Microbiol. 2013;13(1):199.

Allen MM, Smith AJ. Nitrogen chlorosis in blue-green algae. Arch Mikrobiol. 1969;69(2):114–20.

Arias CR, LaFrentz S, Cai W, Olivares-Fuster O. Adaptive response to starvation in the fish pathogen Flavobacterium columnare: cell viability and ultrastructural changes. BMC Microbiol. 2012;12(1):266.

Asayama M, Imamura S, Yoshihara S, Miyazaki A, Yoshida N, Sazuka T, et al. SigC, the group 2 sigma factor of RNA polymerase, contributes to the late-stage gene expression and nitrogen promoter recognition in the cyanobacterium Synechocystis sp. strain PCC 6803. Biosci Biotechnol Biochem. 2004;68(3):477–87.

Azuma M, Osanai T, Hirai MY, Tanaka K. A response regulator Rre37 and an RNA polymerase sigma factor SigE represent two parallel pathways to activate sugar catabolism in a cyanobacterium Synechocystis sp. PCC 6803. Plant Cell Physiol. 2011;52(2):404–12.

Baers LL, Breckels LM, Mills LA, Gatto L, Deery MJ, Stevens TJ, et al. Proteome mapping of a cyanobacterium reveals distinct compartment organization and cell-dispersed metabolism. Plant Physiol. 2019;181(4):1721–38.

Bolay P, Muro-Pastor MI, Florencio FJ, Klähn S. The distinctive regulation of cyanobacterial glutamine synthetase. Life (Basel). 2018;8(4).

Boresch K. Zur Physiologie der Blaualgenfarbstoffe. Lotos (Prag). 1910;58:344–345.

Collier JL, Grossman AR. A small polypeptide triggers complete degradation of light-harvesting phycobiliproteins in nutrient-deprived cyanobacteria. EMBO J. 1994;13(5):1039–47.

Damrow R, Maldener I, Zilliges Y. The multiple functions of common microbial carbon polymers, glycogen and PHB, during stress responses in the non-diazotrophic cyanobacterium Synechocystis sp. PCC 6803. Front Microbiol. 2016;7:966.

Doello S, Burkhardt M, Forchhammer K. The essential role of sodium bioenergetics and ATP homeostasis in the developmental transitions of a cyanobacterium. Curr Biol. 2021.

Doello S, Klotz A, Makowka A, Gutekunst K, Forchhammer K. A specific glycogen mobilization strategy enables rapid awakening of dormant cyanobacteria from chlorosis. Plant Physiol. 2018;177(2):594–603.

Georg J, Dienst D, Schürgers N, Wallner T, Kopp D, Stazic D, et al. The small regulatory RNA SyR1/PsrR1 controls photosynthetic functions in cyanobacteria. Plant Cell. 2014;26(9):3661–79.

Görl M, Sauer J, Baier T, Forchhammer K. Nitrogen-starvation-induced chlorosis in Synechococcus PCC 7942: adaptation to long-term survival. Microbiology. 1998; 144(9): 2449–58.

Grossman AR, Schaefer MR, Chiang GG, Collier JL. The phycobilisome, a light-harvesting complex responsive to environmental conditions. Microbiol Rev. 1993;57(3):725–49.

Gründel M, Scheunemann R, Lockau W, Zilliges Y. Impaired glycogen synthesis causes metabolic overflow reactions and affects stress responses in the cyanobacterium Synechocystis sp. PCC 6803. Microbiology. 2012;158(Pt 12): 3032–43.

Hauf W, Schlebusch M, Hüge J, Kopka J, Hagemann M, Forchhammer K. Metabolic changes in Synechocystis PCC6803 upon nitrogen-starvation: excess NADPH sustains polyhydroxybutyrate accumulation. Metabolites. 2013;3(1):101.

Heidrich J, Thurotte A, Schneider D. Specific interaction of IM30/Vipp1 with cyanobacterial and chloroplast membranes results in membrane remodeling and eventually in membrane fusion. Biochim Biophys Acta. 2017; 1859(4):537–49.

Heilmann B, Hakkila K, Georg J, Tyystjärvi T, Hess WR, Axmann IM, et al. 6S RNA plays a role in recovery from nitrogen depletion in Synechocystis sp. PCC 6803. BMC Microbiol. 2017a;17(1):229.

Hickman JW, Kotovic KM, Miller C, Warrener P, Kaiser B, Jurista T, et al. Glycogen synthesis is a required component of the nitrogen stress response in Synechococcus elongatus PCC 7942. Algal Res. 2013;2(2):98–106.

Imamura S, Asayama M. Sigma factors for cyanobacterial transcription. Gene Regul Syst Bio. 2009;3:65–87.

Keren I, Minami S, Rubin E, Lewis K. Characterization and transcriptome analysis of Mycobacterium tuberculosis persisters. mBio. 2011;2(3):e00100–11.

Klotz A, Georg J, Bučinská L, Watanabe S, Reimann V, Januszewski W, et al. Awakening of a dormant cyanobacterium from nitrogen chlorosis reveals a genetically determined program. Curr Biol. 2016;26(21):2862–72.

Klotz A, Reinhold E, Doello S, Forchhammer K. Nitrogen starvation acclimation in Synechococcus elongatus: redox-control and the role of nitrate reduction as an electron sink. Life (Basel). 2015;5(1):888.

Koch M, Berendzen KW, Forchhammer AK. On the role and production of polyhydroxybutyrate (PHB) in the cyanobacterium Synechocystis sp. PCC 6803. Life (Basel). 2020;10(4).

Koch M, Doello S, Gutekunst K, Forchhammer K. PHB is produced from glycogen turn-over during nitrogen starvation in Synechocystis sp. PCC 6803. Int J Mol Sci. 2019;20(8):1942.

Moreno-Gámez S, Kiviet DJ, Vulin C, Schlegel S, Schlegel K, van Doorn GS, et al. Wide lag time distributions break a trade-off between reproduction and survival in bacteria. Proc Natl Acad Sci USA. 2020;117(31):18729–36.

Osanai T, Oikawa A, Numata K, Kuwahara A, Iijima H, Doi Y, et al. Pathway-level acceleration of glycogen catabolism by a response regulator in the cyanobacterium Synechocystis species PCC 6803. Plant Physiol. 2014;164(4):1831–41.

Perez R, Wörmer L, Sass P, Maldener I. A highly asynchronous developmental program triggered during germination of dormant akinetes of filamentous diazotrophic cyanobacteria. FEMS Microbiol Ecol. 2018;94(1). https://doi.org/10.1093/femsec/fix131.

Pils D, Schmetterer G. Characterization of three bioenergetically active respiratory terminal oxidases in the cyanobacterium Synechocystis sp. strain PCC 6803. FEMS Microbiol Lett. 2001;203(2):217–22.

Reyes JC, Florencio FJ. A mutant lacking the glutamine synthetase gene (glnA) is impaired in the regulation of the nitrate assimilation system in the cyanobacterium Synechocystis sp. strain PCC 6803. J Bacteriol. 1994;176(24):7516–23.

Robertson BR, Tezuka N, Watanabe MM. Phylogenetic analyses of Synechococcus strains (cyanobacteria) using sequences of 16S rDNA and part of the phycocyanin operon reveal multiple evolutionary lines and reflect phycobilin content. Int J Syst Evol Microbiol. 2001; 51(Pt 3):861–71.

Sauer J, Gorl M, Forchhammer K. Nitrogen starvation in Synechococcus PCC 7942: involvement of glutamine synthetase and NtcA in phycobiliprotein degradation and survival. Arch Microbiol. 1999;172(4):247–55.

Sauer J, Schreiber U, Schmid R, Völker K, Forchhammer K. Nitrogen starvation-induced chlorosis in Synechococcus PCC 7942. Low-level photosynthesis as a mechanism of long-term survival. Plant Physiol. 2001; 126(1): 233–43.

Schlebusch M, Forchhammer K. Requirement of the nitrogen starvation-induced protein Sll0783 for polyhydroxybutyrate accumulation in Synechocystis sp. strain PCC 6803. Appl Environ Microbiol. 2010;76(18):6101–7.

Schwarz R, Forchhammer K. Acclimation of unicellular cyanobacteria to macronutrient deficiency: emergence of a complex network of cellular responses. Microbiology (Reading, Engl). 2005;151(Pt 8):2503–14.

Sinai L, Rosenberg A, Smith Y, Segev E, Ben-Yehuda S. The molecular timeline of a reviving bacterial spore. Mol Cell. 2015;57(4):695–707.

Spat P, Klotz A, Rexroth S, Macek B, Forchhammer K. Chlorosis as a developmental program in cyanobacteria: the proteomic fundament for survival and awakening. Mol Cell Proteomics. 2018.

Srivastava A, Summers ML, Sobotka R. Cyanobacterial sigma factors: current and future applications for biotechnological advances. Biotechnol Adv. 2020 May-Jun;40:107517.

Stephan DP, Ruppel HG, Pistorius EK. Interrelation between cyanophycin synthesis, L-arginine catabolism and photosynthesis in the cyanobacterium Synechocystis sp. strain PCC 6803. Z Naturforsch C J Biosci. 2000; 55(11-12):927–42.

Theis J, Gupta TK, Klingler J, Wan W, Albert S, Keller S, et al. VIPP1 rods engulf membranes containing phosphatidylinositol phosphates. Sci Rep. 2019;9(1):8725.

Udikovic-Kolic N, Wichmann F, Broderick NA, Handelsman J. Bloom of resident antibiotic-resistant bacteria in soil following manure fertilization. Proc Natl Acad Sci USA. 2014; 111(42):15202–7.

Watzer B, Forchhammer K. Cyanophycin synthesis optimizes nitrogen utilization in the unicellular cyanobacterium Synechocystis sp. strain PCC 6803. Appl Environ Microbiol. 2018;84(20).

Westphal S, Heins L, Soll J, Vothknecht UC. Vipp1 deletion mutant of Synechocystis: a connection between bacterial phage shock and thylakoid biogenesis?. Proc Natl Acad Sci USA. 2001;98(7):4243–8.

5. Publication 5 (Accepted)

Book chapter

Khaled A. Selim, Erik Zimmer, Heba Yehia, and Sofía Doello

Molecular and Cellular Mechanisms Underlying the Microbial Survival Strategies: Insights into Temperature and Nitrogen Adaptations.

In: Climate Change and the Microbiome

2021. *Springer Cham.* https://doi.org/10.1007/978-3-030-76863-8_36

Chapter 36
Molecular and Cellular Mechanisms Underlying the Microbial Survival Strategies: Insights into Temperature and Nitrogen Adaptations

Khaled A. Selim, Erik Zimmer, Heba Yehia, and Sofía Doello

Abstract Bacteria inhabit almost all ecological niches, including harsh environments of desert, oceans, hypersaline, volcanic and thermal biospheres, representing therefore one of the quantitatively most abundant organisms on earth. To survive under such a variety of ecological habitats, bacteria developed a number of strategies to rapidly adapt and respond to environmental changes by tuning down their metabolic activities, thus overcoming periods of unfavorable growth conditions. Generally, the processes of entering into and exiting from the metabolic stand-by mode are tightly regulated and characterized by a series of signaling events involving various secondary messenger molecules, signaling proteins, and regulatory RNAs. For example, the availability of nitrogen is highly variable in nature and, hence, considered as the limiting factor of microbial growth and development. Therefore, the nitrogen assimilation reactions require a tight regulation and a constant sensing of the quantity and quality of the available nitrogen. Temperature sensing is also essential for microbial survival. Consistently, microbes have developed diverse molecular strategies to sense temperature fluctuations and readjust their metabolism to survive and resume growth at a different temperature. In this chapter,

K. A. Selim (✉)
Organismic Interactions Department, Interfaculty Institute for Microbiology and Infection Medicine, Cluster of Excellence 'Controlling Microbes to Fight Infections', Tübingen University, Tübingen, Germany

Chemistry of Natural and Microbial Products Department, Pharmaceutical and Drug Industries Research Division, National Research Centre, Cairo, Egypt
e-mail: Khaled.selim@uni-tuebingen.de

E. Zimmer · S. Doello
Organismic Interactions Department, Interfaculty Institute for Microbiology and Infection Medicine, Cluster of Excellence 'Controlling Microbes to Fight Infections', Tübingen University, Tübingen, Germany

H. Yehia
Chemistry of Natural and Microbial Products Department, Pharmaceutical and Drug Industries Research Division, National Research Centre, Cairo, Egypt

D. K. Choudhary et al. (eds.), *Climate Change and the Microbiome*, Soil Biology 63,
https://doi.org/10.1007/978-3-030-76863-8_36

we summarize the recent advances in our understanding of the microbial adaptation strategies toward environmental changes, specifically those related to temperature fluctuations and changes in nitrogen availability.

Keywords Chlorosis and resuscitation · Glutamine synthase · Nitrogenase · PII signaling protein · Stress response · RNA thermometers · Cyanobacteria

36.1 Introduction

Climate change, global warming, and greenhouse effects are terms that have been pressingly discussed since the middle of the twentieth century in both scientific and political contexts. They describe the phenomenon of increasing average temperature on Earth, which is posited to reach 4 °C increment by 2100, and the corresponding dramatic and versatile consequences (Yang et al. 2017). Changes in average temperatures are reflected in changes in atmospheric gas composition, water surface and polar regions, the frequency of the freeze–thaw cycles in the alpine region, vegetation, and many other phenomena that affect and/or endanger many forms of life as well as the global food security situation.

Microorganisms are ubiquitous: the microbial pool in any definite ecosystem, whether terrestrial or aquatic, consists of a community of different members each playing a different role and interacting uniquely with their habitat and with their "neighbors" via various metabolic processes (Docherty and Gutknecht 2012; Abatenh et al. 2018; Cronan 2018). Unquestionably, biogeochemistry or the dynamics of any ecosystem, regardless of its size, cannot be studied without considering the microbial community diversity, structure, and contribution to the niche. Classically, microbes are regarded as enzymes' bags that carry out different metabolic activities and control the nutrient load for plants and animals or influence the suitability of the environment for these higher organisms, i.e., controlling the elemental cycles of different key elements in the biosphere (e.g., C and N cycling, redox cycling of different elements, organic compounds decomposition, molecule fixation, and oxygenic photosynthesis). Thus, the diversity of the microbial communities not only is important from the environmental microbiology or taxonomy perspective, but also directly affects the connected environment and living organisms (i.e., mineral resources, agriculture, crop yield, livestock) and hence the global biodiversity, food security, strategic industries, and energy resources (Rodriguez and Durán 2020; Voolstra and Ziegler 2020).

It is only natural then to infer that the microbial pools' structure and function are impacted by environmental changes such as temperature, pH, humidity, and emitted gases as the organisms' bioprocesses respond to the new conditions (Bradford 2013). However, until recently, the microbial factor was underrepresented in most of the modeling studies that describe the influence of varying environmental conditions on the ecosystem cycles and the elemental source-sink flux. Furthermore, studies that attempted to include microbial-related parameters into ecosystem change models

lacked experimental validation due to: (1) the complexity of the microbial communities, (2) the limitation of the necessary techniques, (3) the difficulty to culture some strains under laboratory conditions, or (4) the absence of long-term in situ datasets to monitor the changes in microbiota structure and function (Singh et al. 2010; Dutta and Dutta 2016; Cavicchioli et al. 2019).

Due to the progress in metaomics, it is becoming more feasible to study the mechanisms and dynamics of microorganisms' growth and function (Rodriguez and Durán 2020; Voolstra and Ziegler 2020). Some of the different concepts, strategies, and methods have been summarized by Zak et al. (2006). However, some of these models did not thoroughly consider the ability of microorganisms to tolerate and adapt to changes both on the short and long terms (Docherty and Gutknecht 2012; Bradford 2013; Rousk and Bengtson 2014; Hallin and Bodelier 2020). Usually, short-term adaptation entails a temporary stress response through metabolic regulation and feedback mechanisms, while a long-lasting adaptation is the result of a permanent genetic acclimatization taking place over several generations. Currently, with the average earth temperature getting warmer and the concentration of greenhouse gases, namely carbon dioxide, ammonia, methane, nitrous oxide, and chlorofluorocarbons increasing, many research groups are trying to elucidate how the different microorganism communities react to these disturbances. Yet, it is very challenging to carry out such investigations due to the complexity and heterogeneity of the different microbiomes and the lack of thorough descriptions of their structure, dynamics, function, and relevant food webs at their specific locations (Singh et al. 2010; Dutta and Dutta 2016).

Nevertheless, all prokaryotes, especially the photoautotrophic cyanobacteria (Forchhammer and Selim 2020; Selim et al. 2020c), developed sophisticated strategies on both the molecular and cellular levels to overcome environmental stresses (Selim and Maldener 2021). In contrast, in comparison to prokaryotes, fungi existence in a certain location is minimally affected by ecological perturbations. This is attributed to their ability to form dormant spores, and to their thicker cell wall, especially in response to stress, mycelial growth, etc. (Gionchetta et al. 2019; Perez-Mon et al. 2020). In this chapter, we will discuss in detail the bacterial survival strategies in response to sudden changes in temperature and in nitrogen availability, the latter as an example of nutrient adaptation.

36.2 Various Microbial Responses to Changes in Environmental Conditions

Microorganisms are found all around us, even in the most extreme environments, which are inhabited by so-called extremophiles endowed with special adaptation mechanisms to suit harsh habitats (temperature, salinity, pH, carbon and nitrogen availability) (Rampelotto 2013; Merino et al. 2019). Each microbial genus exhibits optimal features of growth rate, enzyme activities, generation time, etc., in its native habitat conditions (Yang et al. 2017; Kosaka et al. 2019). Thus, mesophiles, which

can only survive at a subglobal warming temperature, are the ones that face the greatest damage threats, in addition to the consequent perturbations in the metabolic cycles in which they are involved (Cavicchioli et al. 2019; Kosaka et al. 2019).

Changes or disturbances can occur at different magnitudes and frequencies resulting in quorum quenching, i.e., unsettling both the normal gene expression and physiologic homeostatic functions of individual microorganisms and the ongoing crosstalk between the microbial communities and their hosts and metaorganisms (Grandclement et al. 2016). These disturbances may either be short-term pulses or long-term pressures that change the nature of local environments (Shade et al. 2012). The organisms' reaction depends on several factors that include, but are not limited to: (1) microorganisms' generation time or doubling time and the disturbance duration relative to this time (discrete or continuous), (2) the microbial robustness against the disturbance (e.g., temperature range, greenhouse gas concentrations, and light intensity in deep waters), (3) the redundancy of the physiologic function(s) of the microorganism in the community (also referred to as the metaorganism), i.e., the ability of the neighboring species to serve the same roles, and (4) whether the microorganism is associated with a host (higher organism) that adds more pressure to the adaptation capacity and speed (Shade et al. 2012; Cavicchioli et al. 2019; Voolstra and Ziegler 2020).

Due to their higher turnover rates, microbial populations show the fastest responses and/or adaptations in comparison to plants and animals. With only the environmental factors in mind, it is generally accepted that the different microbial species respond either (1) directly, by adapting to the warming as allowed by their own features, e.g., critical high temperature (CHT), specific thermal optimum, functional enzymes, and thermal performance curve or spectrum; consequently, the ones that maintain vital functions at warmer temperatures are the ones that survive; or (2) indirectly, as a result of the response of the whole ecosystem to the changes, e.g., altered vegetation, plants and animals migration, and/or dying out (Drigo et al. 2007; Bradford 2013; Dutta and Dutta 2016; Yang et al. 2017; Kosaka et al. 2019; Voolstra and Ziegler 2020).

Different organisms show different survival responses when subjected to changes of the surroundings. They could either take advantage of the changes and undergo a developmental transition (e.g., develop special types of cells like akinetes, heterocyst, and hormogonia of cyanobacteria) or simply alter their food rhythms by consuming different sources of food (Selim and Maldener 2021). However, they could also be vulnerable to the changes and lose their fitness and ability to function on account of the different setup or selection pressure. Hence, what we can describe as adaptation is in fact either resilience or functional plasticity, exploitation or tolerance to the new conditions or disturbances. Several studies interpret the ability to accommodate changing conditions or disturbances as the result of microbial genetic variation (e.g., increasing the frequency of a favorable operon and effective DNA mutations) and, therefore, consider it as evolutionary adaptation (Franks and Hoffmann 2012; Shade et al. 2012; Gionchetta et al. 2019; Kosaka et al. 2019; Voolstra and Ziegler 2020; Wooliver et al. 2020). Nevertheless, it is still a matter of debate whether the adaptation mechanisms of an organism could truly serve to

salvage it against the selection parameter of climate change, or it is inevitable to declare that the world is undergoing a widespread loss of biodiversity and mass extinction.

36.3 Microbial Responses to Warming with Underlying Genetic Disposition

Amid the very few studies that meant to study the microbial genetic adaptation to warming is the one conducted by Xue et al. (2016). These authors screened the active functional genes pool responsible for carbon (C), nitrogen (N), phosphorous (P), and sulfur (S) metabolism in terrestrial microbial communities subjected to temperature increase of 2 ^{o}C over 9 years. However, they did not investigate the behavior of individual organisms as certain species are activated/deactivated more than others. They found that the expression of the genes encoding enzymes responsible for decomposing recalcitrant C sources (e.g., vanillate *O*-demethylase oxygenase, glyoxal oxidase, and manganese peroxidase) increased significantly in comparison to the decrease of those that metabolize labile C (e.g., mannanase, xylanase, and acetylglucosaminidase) (Xue et al. 2016). This is comparable to the results from organic soil reported by Yang and his group. Both the microbial diversity and the availability of functional genes involved in labile C metabolism decreased in the soil incubated at 8 ^{o}C more than that incubated at near-freezing temperature −2 ^{o}C. Yet, genes responsible for recalcitrant carbon digestion did not increase in this report due to the incubation in the absence of oxygen (Yang et al. 2017). With respect to N degradation, Xue and his group documented that four out of 13 relevant genes increased, while three decreased. In a way, this could be attributed to the altered vegetation nature, total organic soil carbon, and C:N ratio after the temperature increase. All the genes playing roles in P and S cycles showed higher abundance after warming, reflecting the increased need for plant growth and carbon fixation as a feedback mechanism to the increased carbon dioxide concentration (Drigo et al. 2007; Xue et al. 2016).

A sound postulation by Kosaka and his group states that in a native habitat, organisms are usually subjected to scarcity of certain elements and, thus, more prone to mutations if compared to those grown in vitro in rich media. Using a thermotolerant mutant of the mesophile *Zymomonas mobilis*, they were able to show that thermal adaptation included reduced activity of NADH dehydrogenase (respiration activity) and, consequently, reduced harmful effects of oxidative stress (accumulation of reactive oxygen species) (Kosaka et al. 2019). Interestingly, different thermo-adapted *Z. mobilis* and *Escherichia coli* strains conserved the wild type-like cell size and shape at their CHT (i.e., not related to σ^{s} responses), and they all showed ratios of mutations in the same order (10^{-2}) to achieve thermal fitness, mostly in genes responsible for membrane stabilization, transporters

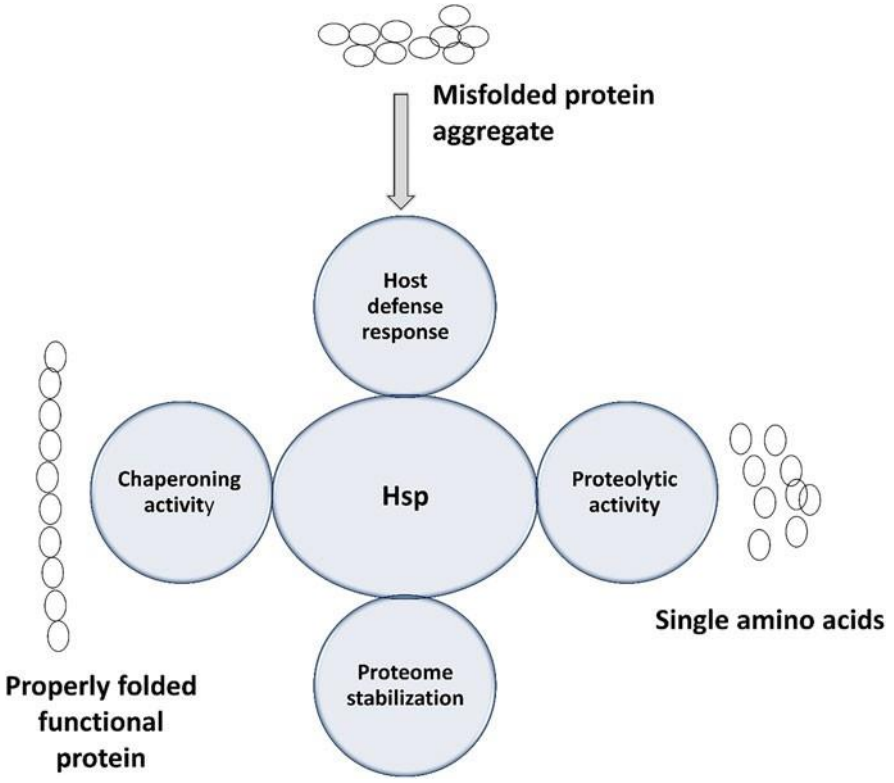

Fig. 36.1 Schematic illustration of heat shock proteins (Hsp) role in controlling proteostasis, modified from Maleki et al. (2016)

synthesis, transcription regulation, and protein proofing (Rudolph et al. 2010; Sandberg et al. 2014; Kosaka et al. 2019).

Furthermore, other mechanisms exist that regulate how bacteria respond to thermal changes, albeit not previously discussed in the context of global warming. However, they definitely fit the narrative when the whole evolutionary picture is evoked. Among these mechanisms are the universally conserved (a) RNA thermometers (RNA-Ts), which modulate the expression of the encoding downstream cistron, and (b) the enhanced or differential expression of heat shock proteins (Hsps), whose function is either to solubilize misfolded proteins that aggregated at high temperature (chaperone activity) or to facilitate their breakdown (protease activity) (discussed below in details; Fig. 36.1).

RNA thermometers are regulatory elements located in the intergenic regions of open reading frames (ORF). Being in the noncoding 5^{0}-untranslated region of some mRNA molecules, they are able to coordinate the ribosomal binding, i.e., controlling the gene expression at the translational level (Narberhaus et al. 2006). At lower temperatures, the mRNA exists in a hairpin-like conformation that masks the

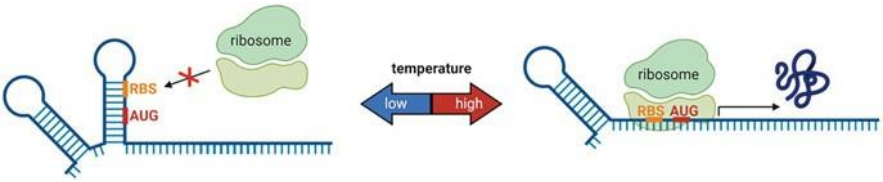

Fig. 36.2 Model for the zipper-like RNA thermometer (RNA-T). RNA-T occluding the ribosomal binding site (RBS) and/or the translation start codon (AUG) of the mRNA by base pairing until temperature is increased, which causes a reversible disruption of the zipper-like RNA structure, to initiate the protein translation, modified from Kortmann and Narberhaus (2012), Righetti and Narberhaus (2014), and Loh et al. (2018)

ribosome binding site (RBS) from ribosomal unit attachment. As the nucleic acid melts and unwinds at higher than ambient temperature, the RNA-T functions as a zipper that switches on/off the expression of the downstream genes that are under its control (Fig. 36.2). These are mainly cold and heat shock proteins and virulence-controlling factors in some pathogenic bacteria. RNA-Ts are extremely sensitive to temperature changes and start reacting to an increase of 1 ^{o}C, with the intensity of the response augmenting as the temperature further increases (Narberhaus et al. 2006; Kortmann and Narberhaus 2012). RNA-Ts contain very short conserved motifs and sometimes none, making their identification in the genome not possible via bioinformatics tools. They can be divided into three families with varying nucleotide length, the common feature among them being the mismatched noncanonical base pairing. The most common family is the repressor of heat shock gene expression family (ROSE), the members of which consist of up to 100 nucleotides that form up to four stem-loops with different heat stabilities and, thus, variable levels of control of RBS occlusion. The double-strand binding strength decreases in the 3^{0} direction where the first to unfold is the one exposing the Shine–Dalgarno sequence (SD) and the AUG start codon (Chowdhury et al. 2006; Kortmann and Narberhaus 2012). The second family is known as the fourU thermometer and was first reported in *Salmonella enterica* to control the production of the Hsp aggregation suppression A (agsA). As the name implies, members of this family consist of four uridine nucleotides that form hydrogen bonds with AGGA in the SD sequence (Kortmann and Narberhaus 2012; Abduljalil 2018). The third and simplest group is the cyanobacterial thermometer detected at the 5^{0}-end of the heat shock protein 17 (Hsp17) gene. This thermometer comprises one hairpin-like secondary structure that normally blocks the expression of Hsp17, which is responsible for both the solubility and structural integrity of cellular proteins (Kortmann and Narberhaus 2012; Cimdins et al. 2014).

The first discovered RNA-T was reported in connection to the alternative sigma factor rpoH gene product (σ^{32}, sigma H) in *E. coli*. Under stress conditions, σ^{32} is liberated from a complex with the chaperones DnaK and DnaJ and binds to the RNA polymerase core enzyme (E) shifting it from the promoters of housekeeping genes to those of stress-related genes. Thereby, the transcription of more than 30 different Hsps transcription is initiated (e.g., ClpB, DnaK, GroEL, GroES, HtpG, YedU)

(Narberhaus and Balsiger 2003; Wang and DeHaseth 2003; Calloni et al. 2012; Righetti and Narberhaus 2014), enabling the cell to salvage aggregated proteins and, hence, secure protein quality control and proteostasis.

Heat shock proteins are ubiquitous molecules, produced in response to biotic and abiotic insults (e.g., temperature, osmotic or oxidative stress, starvation, and infectious agents). They are subdivided into groups depending on their size and function and are located in different parts of the prokaryotic or eukaryotic living cell (cytosol, mitochondria, nucleus, etc). Their sizes range from 8 to 28 kDa in the case of small ATP-independent Hsps to 40–105 kDa for the larger ATP-dependent ones. They either function in solubilizing the misfolded proteins that aggregated at high temperature (chaperone activity) or in facilitating their breakdown (protease activity). They were also reported to have other purposes unrelated to stress protection such as immune system modulation in higher eukaryotes (Tiwari et al. 2015; Maleki et al. 2016; Miller and Fort 2018). In addition to their protein trafficking and chaperoning activity and cell homeostasis/stabilization functions, Hsps were also implicated in rescuing cells from death via an antiapoptotic mechanism. This involves the interaction with several caspase proteins to disrupt the formation of an effective apoptosome, thus inhibiting caspase proteolytic cascade-dependent cell death (e.g., Hsp70 to Apaf-1 and Hsp27 to pro-caspase-3) (Beere 2004).

When it comes to the underlying conceptualization of the microbial response to global warming, many theories are discussed. However, none is yet thoroughly understood and deemed as a correct fact, and many are contradictory and require further investigation. On the one hand, some reports support the idea of "hotter-is-better; HiB." This means that, up to a maximum temperature, all microbial performance and metabolic vital signs (e.g., respiration rate, and growth rate) will increase with increasing temperature, and hence, the microbial population should thrive (Deutsch et al. 2008; Angilletta et al. 2010; Dell et al. 2011; Huey et al. 2012; Smith et al. 2019). The positive thermal response was, for instance, proven by Smith and his group for many mesophilic prokaryotic strains after both short- and long-term exposure to a higher culturing temperature (Smith et al. 2019). Moreover, the increased greenhouse gas concentrations, another feature of global warming, trigger a feedback cycle to control the flux of these gases as modeled in many climate studies. Of special concern is the CO_2 levels as it overlaps with the global carbon cycle and affects the aquatic and terrestrial environments. Elevated temperatures are assumed to result in higher rates of microbial respiration which, in addition to accelerated organic matter decomposition, leads to a positive feedback with a resulting increase in temperature (Bardgett et al. 2008; Singh et al. 2010; Dutta and Dutta 2016; Cavicchioli et al. 2019). On the other hand, other scientists posit reduced metabolic activities and proliferation of microbes in response to environmental warming. This stress response may be mediated by the hyperphosphorylated alarmone tetra- or pentaphosporylated guanosine (p)ppGpp. Albeit usually studied in relation to starvation, (p)ppGpp can also be released in response to changes in temperature, pH, and osmotic pressure. It acts as a sink for activated guanine (GTP) and directly affects some enzymes like GTPases, primases, and RNA polymerases modulating all their relevant activities. Among the negatively influenced

bioprocesses are DNA synthesis (initiation and elongation) as well as RNA and protein synthesis (especially the ribosomal RNA) and ribosomal unit assembly (Steinchen and Bange 2016; Kosaka et al. 2019; Ronneau and Hallez 2019).

36.4 Microbial Adaptation Strategies to Changes in Nutrient Availability (Nitrogen Starvation)

Nitrogen is the most abundant gaseous element in the Earth's atmosphere, representing about 78% of the air. Nitrogen is the simplest building block of life and is essential for all living organisms, since it is a major component of amino acids and nucleic acids. In nature, the availability of nitrogen is highly variable, as most microorganisms are unable to fix atmospheric N_2 (discussed below). Hence, nitrogen is considered one of the limiting factors for microbial growth and development due to its presence in a limited amount of useful forms (i.e., combined nitrogen sources such as ammonia, urea, nitrite, and nitrate) in microbial habitats, especially in the ocean. In this section, we will discuss in detail the microbial adaptation strategies for efficient utilization of nitrogen, with special emphasis on nitrogen assimilation reactions and the mechanisms for overcoming limitation of combined nitrogen.

36.4.1 Adaptation to Variable Nitrogen Availability Via Regulation of the Glutamine Synthetase

Bacterial metabolism requires a tight regulation and a constant sensing of the quantity and quality of the nitrogen and carbon availability. The nitrogen assimilation reactions lead to a consumption of 2-oxoglutarate (2-OG), which represents an indicator of the intracellular carbon/nitrogen balance due to its intermediate positioning between the TCA cycle and nitrogen assimilation cycle (Muro-Pastor et al. 2001; Commichau et al. 2006; Luque and Forchhammer 2008; Forchhammer 2010; Huergo and Dixon 2015; Forchhammer and Selim 2020; Selim et al. 2020c). Generally, the nitrogen and carbon metabolisms are coordinated by a complex crosstalk between different input signals (Fig. 36.3) (Commichau et al. 2006; Luque and Forchhammer 2008). The sensing and regulation of the nitrogen/carbon metabolisms in several bacteria mainly depend on the signal transduction PII protein, which senses the energy/carbon/nitrogen status of the cell through binding ATP/ADP and 2-OG in presence of ATP (see below) (Fig. 36.3; Fokina et al. 2010; Lapina et al. 2018; recently reviewed in Forchhammer and Selim 2020 and Selim et al. 2020c).

For efficient nitrogen assimilation, bacteria possess two pathways to integrate inorganic nitrogen in the form of ammonium (NH_4^+) into organic molecules: the glutamate dehydrogenase (GDH) reaction (Fig. 36.3) and the glutamine synthase/

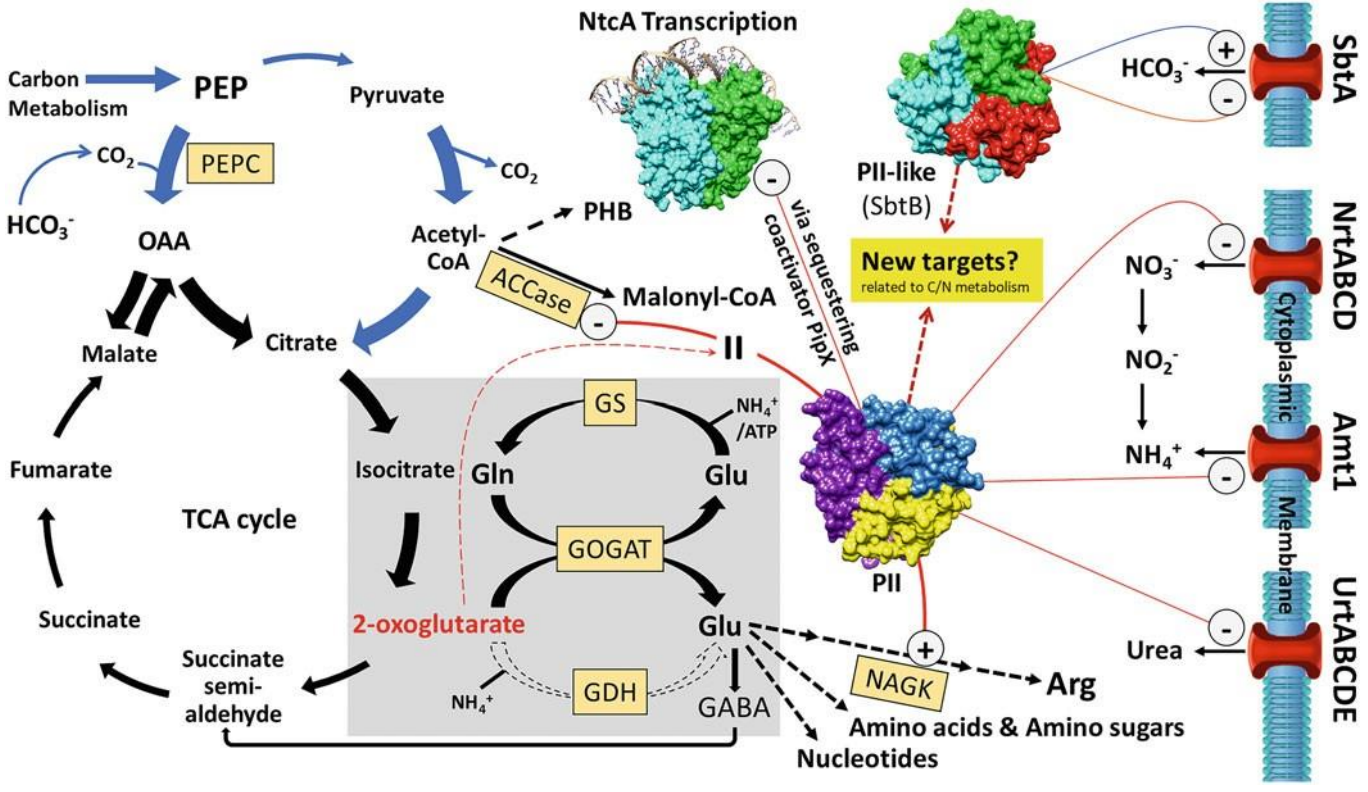

Fig. 36.3 Crosstalk between nitrogen and carbon metabolism is modulated by cell signaling protein of PII superfamily, modified from Forchhammer and Selim (2020). Metabolic basis of C:N balance sensing at the intersection of carbon and nitrogen metabolisms and the role of PII signaling protein in regulating key physiological processes (indicated by red lines). Changes in the 2-oxoglutarate level, which report changes in the C/N balance, are sensed by PII protein. The

2-OG levels are refilled through TCA cycle via carbon anabolic reactions and consumed by the GS-GOGAT cycle (nitrogen assimilation reactions). Glutamate is the primary amino acid and acts as nitrogen donors for several anabolic reactions (indicated by dotted lines), with arginine biosynthesis being of particular interest. PII signaling protein regulates: (1) enzymes through controlling the key reactions of arginine biosynthesis via N-acetyl glutamate kinase (NAGK) (Selim et al. 2020c, 2020b) and of fatty acid synthesis via Acetyl-CoA carboxylase, (ACCase) (Selim et al. 2020c); (2) transcription factors like NtcA (discussed below) (Forchhammer and Selim 2020); (3) as well as the uptake of the nitrogen sources nitrate, ammonium, and urea through their respective uptake systems as indicated (Forchhammer and Selim 2020). Recently, new class of PII-like protein called SbtB was found to control carbon metabolism (Selim et al. 2018; recently reviewed in Forchhammer and Selim 2020). Notably, another class of PII-like protein called CutA was found to be highly abundant in the cells, implying a key role in the intracellular signaling processes. However, at present, the importance of CutA proteins in cell signaling processes waits for further biochemical and physiological investigations (Selim et al. 2020a)

glutamine oxoglutarate aminotransferase (GS-GOGAT) cycle (Figs. 36.3 and 36.4). GDH can aminate 2-oxoglutarate (2-OG) to glutamate (Glu), using NH_4^+ and NAD(P)H/H^+. Since GDH has a relatively low affinity for NH_4^+ and requires no ATP, this reaction mostly takes place under NH_4^+-excess and energy-limiting conditions. The most widely used pathway for nitrogen incorporation in bacteria is the GS-GOGAT cycle, in which NH_4^+ and Glu are condensed to glutamine (Gln) in a reaction catalyzed by the glutamine synthetase (GS; encoded by *glnA*) with the use of one ATP molecule (Forchhammer and Selim 2020). Following this reaction, Gln and 2-OG are transaminated into two molecules of Glu, thereby recovering the Glu molecule initially used by the GS and providing an additional Glu molecule, which can be used as a building block to synthesize other amino sugars and amino acids, such as arginine. This second reaction is catalyzed by the Gln:2-OG amino-transferase (GOGAT) and requires oxidation of one NAD(P)H/H^+ or of one ferredoxin (Figs. 36.3 and 36.4). In summary, the GS-GOGAT cycle uses one 2-OG, one NH_4^+, one ATP, and one reduction equivalent to yield one Glu. Given that the GS-GOGAT cycle is the main metabolic pathway of NH_4^+ assimilation in bacteria, this makes GS one of the central enzymes in nitrogen metabolism and its regulation is of key importance for the optimization of nitrogen utilization (Bolay et al. 2018).

GS is found in all three domains of organisms and can be categorized into three types: GSI, GSII, and GSIII, which differ in their protein structure and regulatory mechanisms. Due to the omnipresence of GS in all clades of life, it is believed that these different types emerged before the evolutionary divergence into eukaryotes and prokaryotes. GSI and GSIII occur in bacteria and archaea, and both are dodecamers consisting of two parallel hexameric rings (Fig. 36.4a). Furthermore, GSIII occurs in a few eukaryotic species. Some bacterial species possess one or multiple GSI genes, while others possess genes for both GSI and GSIII or only for GSIII. It is suggested that GSI and GSIII genes occur in both bacteria and archaea due to multiple lateral gene transfer events. GSI is further divided into GSI-α and GSI-β, whereby GSI-β contains an additional 25-amino-acid insertion and is usually posttranslationally regulated by adenylylation at conserved tyrosine (Tyr) residues that are missing in GSI-α. However, there are some exceptions to this classification. Finally, the decameric GSII is mainly present in eukaryotes, with the exception of few bacterial species (Brown et al. 1994).

Moreover, new types of bacterial GS-like enzymes have been recently discovered as unique adaptation strategies to fulfill new metabolic needs in these bacteria and to utilize a variety of nitrogen sources, other than NH_4^+. The evolution pressure on the *glnA* gene encoding GS led to the emergence of various *glnA*-like genes, which have thus far been less studied (Krysenko et al. 2017, 2019). For example, *Streptomyces coelicolor* possesses two classical *glnA* genes, encoding for GSI and GSII, whose functions are well characterized, as well as three other genes, *glnA2-glnA4*, annotated as GS-like enzymes (Rexer et al. 2006). The GS-like enzyme GlnA3 was found to encode for a gamma-glutamylpolyamine synthetase, which is required for polyamine metabolism and detoxification, allowing *S. coelicolor* to utilize and grow on the toxic polyamines like spermine, spermidine, putrescine, or cadaverine, as a sole nitrogen source (Krysenko et al. 2017). Furthermore, the GS-like enzyme GlnA4

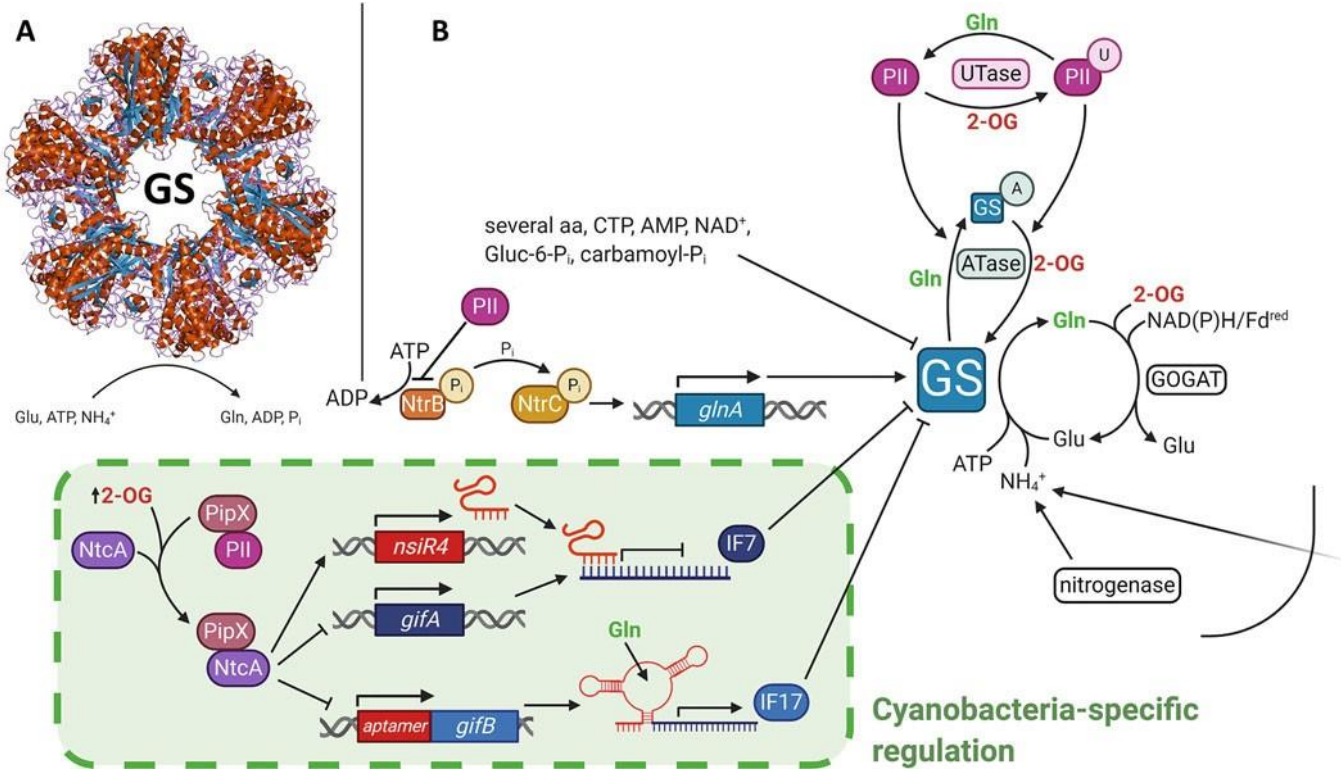

Fig. 36.4 Model for the general modes of GS regulations, with indirect role for PII on GS

was found to encode for a gamma-glutamyl ethanolamine synthetase, which is required for ethanolamine utilization. Through the activity of GS-like GlnA-4, *S. coelicolor* is able to utilize ethanolamine as a sole carbon or nitrogen source, although it grows poorly on ethanolamine as a nitrogen source as it lacks a specific transporter for ethanolamine (Krysenko et al. 2019). The emergence of the evolutionary GS-like enzymes like GlnA3 and GlnA4 clearly reflects survival adaptation strategies of bacteria to compete with other microbes for resources and to occupy a wide variety of ecological niches.

The regulation of GS is complex and takes place at multiple levels (e.g., transcriptional, posttranscriptional, and posttranslational levels) within different bacterial phyla, as each phylum or even bacterium possesses unique regulatory mechanisms for its own GS enzyme(s) (Fig. 36.4b). For instance, in many proteobacteria, GSI is transcriptionally regulated by the NtrB/NtrC two-component histidine kinase system, which has been well studied in *E. coli* (Huergo et al. 2013). Additionally, GS is posttranslationally regulated by feedback inhibition of different metabolites, such as amino acids and adenine nucleotides, and by modification such as (de-)adenylylation of the enzyme. One of the central status reporter metabolites involved in this regulation is 2-OG. Since 2-OG is consumed by the GS-GOGAT cycle to assimilate NH_4^+, its intracellular concentration decreases under N-excess and, vice versa, increases under N-limitation. In addition, 2-OG reports on the C:N balance in bacteria because it is a metabolite in the tricarboxylic acid (TCA) cycle and the origin of many anaplerotic reactions within this metabolic pathway. The signal transduction from 2-OG to GS is indirect, and it is mediated by the PII protein, as well as further signal transduction proteins specific for different bacterial phyla (Bolay et al. 2018; Forchhammer and Selim 2020). Remarkably, the NtrB component of the two-component histidine kinase (NtrB/NtrC) system, which regulates GS transcriptionally, is regulated as well by the PII protein via direct protein–protein interaction to form a PII-NtrB complex under nitrogen-replete conditions (Fig. 36.4b) (Jiang and Ninfa 2009; Huergo et al. 2013).

This complex regulation is required because the availability of nitrogen and the occurrence of different inorganic nitrogen species, like nitrate (NO_3^-), nitrite (NO_2^-), and NH_4^+, are usually highly variable in bacterial environments (Forchhammer and Selim 2020; Selim and Haffner 2020). Therefore, bacteria need to be able to flexibly tune their nitrogen metabolism in accordance with sudden as well as to season-related changes in the environmental conditions. This is especially true for cyanobacteria as primary producers: They possess a particular flexibility in their ability to tune their nitrogen metabolism, since they inhabit all types of aqueous habitats and must often cope with nitrogen limitation (Forchhammer and Schwarz 2019; Selim and Maldener 2021). In the following paragraphs, we will take a closer look into the regulation of GSI in different cyanobacterial species.

Cyanobacteria have evolved unique mechanisms to regulate their GSI (Fig. 36.4b). They do not possess the NtrBC two-component system. The transcription of *glnA* gene is instead regulated by the global nitrogen regulator NtcA, a dimeric transcription factor unique to cyanobacteria (Fig. 36.5). The transcriptional regulation of GSI (*glnA*) by NtcA responds to the levels of 2-OG. Under nitrogen

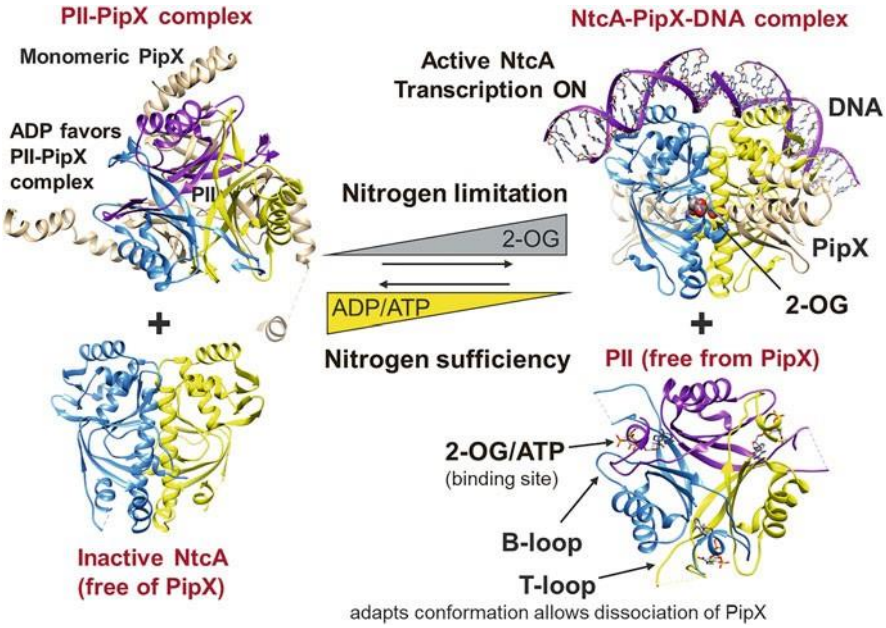

Fig. 36.5 Regulation of NtcA via PipX and PII protein. PipX is an activator of nitrogen transcription factor regulator, NtcA. Under nitrogen excess condition indicated by low 2-OG, high levels of ADP favor the PII-PipX complex formation (PDB: 2XG8), leaving NtcA in an inactive form. When 2-OG levels raise under nitrogen limiting conditions, 2-OG binds to PII and causes dissociation of PII-PipX complex. NtcA binds 2-OG as well and successfully competes for PipX binding. The NtcA-PipX complex (PDB: 2XKO; Llácer et al. 2010) has high affinity to the NtcA-DNA binding sites and switches on the transcription of NtcA-dependent genes, adapted from Forchhammer and Selim (2020)

limiting conditions, the intracellular concentration of 2-OG increases, and the increased 2-OG concentration mediates the interaction of one NtcA dimer with two PipX monomers (summarized in Forchhammer and Selim 2020). PipX is an activator of NtcA and increases the affinity of NtcA for its target promoters characterized by the conserved consensus sequence GTA-N_8-TAC (Espinosa et al. 2007). Thereby, NtcA can either act as an activator or as a repressor of transcription depending on the relative position of the NtcA consensus motif GTA-N_8-TAC to the transcriptional start site (TSS). Expression of *glnA* and other nitrogen assimilation genes is activated by NtcA. Again, the NtcA-PipX interaction is under the control of the master nitrogen regulator PII protein, which also senses the intracellular 2-OG concentrations (Lapina et al. 2018; Selim et al. 2019; Forchhammer and Selim 2020). Upon increasing N availability, lower 2-OG levels lead to the interaction of one PII trimer with three PipX monomers, which prevents PipX (the NtcA activator) from binding to NtcA (Fig. 36.5). Under these conditions, NtcA has low affinity for its target promoters, resulting in a decreased *glnA* expression and, in turn, a reduction in the intracellular 2-OG concentrations due to GOGAT activity

(Forcada-Nadal et al. 2017). The increase in 2-OG levels under N-limitation conditions disrupts the PII-PipX interaction and leaves PipX free again to interact with and activate NtcA (Fig. 36.5).

On the posttranslational regulatory level, GSI of cyanobacteria like GS of other bacteria is regulated via feedback inhibition by several amino acids as well as ATP and AMP. GSI is not regulated by adenylylation. Instead, cyanobacteria possess two regulatory proteins, namely the inactivating factor (IF)7 and IF17 functioning as protein inhibitors of GSI (García-Domínguez et al. 1999; Pantoja-Uceda et al. 2016). In this function, IF7-like proteins exist in most cyanobacterial species. The IF7 and IF17 are small intrinsically disordered proteins, i.e., proteins missing a proper folded structure, which seem to fold upon binding to GSI, although a recent NMR study revealed that IF7 remains disordered even upon binding to GS (Saelices et al. 2011; Neira et al. 2020). Biochemical and physiological analyses revealed that both IF7 and IF17 are required for full inhibition of GS (García-Domínguez et al. 1999). The C-terminus of the 17 kDa IF17 protein displays sequence similarity to the smaller 7 kDa IF7 protein (Saelices et al. 2011). By an unknown mechanism, the additional N-terminus of IF17 seems to enhance the stability of IF17 protein, which is proteolytically degraded in the absence of NH_4^+. In contrast, the degradation of IF7 is performed by the Prp1/Prp2 metalloprotease and is not affected by the availability of nitrogen sources. Both inactivating factors are proposed to bind GSI via electrostatic interactions. Three arginine (Arg) residues in IF7 and IF17 were identified to be important for the interaction with the negatively charged face of GSI. Compared to IF7, IF17 contains an additional lysine (Lys) residue participating in the binding of GSI, which leads to a higher binding affinity of IF17 to GSI than that of IF7. This enhanced binding affinity together with the N-terminus of IF17 is hypothesized to be the reasons for the stronger inhibitory effect of IF17 on GSI compared to IF7. However, the C-terminal part of IF7 appears to be involved as well in the binding of GSI, thus contributing to form the GSI-IF7 complex (Neira et al. 2020). The exact mechanism by which how binding of IF7 inhibits GS activity is so far unknown. However, it is known that the two inactivating factors inhibit GSI independently from each other in a concentration-dependent manner and are able to completely inactivate GS enzymatic activity together. Like *glnA*, also *gifA* and *gifB*, the genes encoding for IF7 and IF17, respectively, are subjected to transcriptional regulation by the master nitrogen transcription factor NtcA (Fig. 36.4b). In contrast to *glnA*, expression of the inactivating factors is repressed by NtcA leading to decreased IF7 and IF17 accumulation under nitrogen-limited conditions. Apart from this transcriptional control by regulatory proteins, both *gifA* and *gifB* genes were recently shown to be regulated by noncoding RNA (ncRNA) molecules as well (Bolay et al. 2018).

In the cyanobacterial genus *Synechocystis*, translation of the *gifA* mRNA into IF7 is regulated by the small regulatory RNA (sRNA) NsiR4 (nitrogen stress-induced RNA 4). *Synechocystis* NsiR4 has a length of 63 nucleotides (nt) and displays a secondary structure with two stem-loops. Furthermore, a shorter form of NsiR4 occurs in some cyanobacterial species inhabiting a *nsiR4* gene. This form is missing the 20 nt at the 5′-end forming one of the stem-loops described for *Synechocystis* NsiR4. The 16-nt-long unpaired region between the two stem-loops is hypothesized

to bind to the 5⁰-untranslated region (UTR) of its target *gifA* mRNA by complementary base pairing. Consequently, translation of this mRNA is inhibited, for example, by blocking the ribosomal binding site (RBS) of the mRNA. Furthermore, binding of a sRNA to its target mRNA usually decreases the stability of the mRNA. The transcription of NsiR4 and, therefore, the repression of *gifA* expression are induced under N-limiting conditions by NtcA, which functions as an activating transcription factor for NsiR4. This leads to increased GSI activity, thereby decreasing the concentration of 2-OG via the GS-GOGAT cycle. The decreased 2-OG concentration then decreases the activity of NtcA and, consequently, enhances the translation of IF7 to inhibit GSI activity. The parallel regulation of IF7 expression by NtcA directly as a transcriptional repressor of *gifA* and indirectly as a transcriptional activator of NsiR4 is known as a feed-forward loop. It is hypothesized that the translational control via NsiR4 is important for the cells to compensate the delayed response of the transcriptional repression alone (Klahn et al. 2015). This is necessary to respond to sudden and strong fluctuations in the concentration of the available nitrogen sources, as it is the case in the aquatic habitats of cyanobacteria (Selim and Maldener 2021). The gene *nsiR4* is conserved in all species of the β-cyanobacterial subsections but is absent in α-cyanobacteria (Klahn et al. 2015). These α-cyanobacteria inhabit oceans, while β-cyanobacteria are found in freshwater and coastal areas. Therefore, it is reasonable to speculate that NsiR4 only evolved in β-cyanobacteria or that it was evolutionary lost in α-cyanobacteria as an adaptation to the often nutrient-deficient saltwater environment. This would be consistent with the hypothesis of marine bacteria's environmental adaptation to N-cost minimizing measures, which will be discussed later on.

In *Synechocystis*, the translation of the *gifB* mRNA into IF17 is controlled by a riboswitch, which is another type of ncRNA. The riboswitch consists of a type 1 Gln aptamer, formerly known as glnA aptamer, located upstream of the *gifB* gene in the 5'-UTR and, therefore, cotranscribed with *gifB* in one mRNA. When transcribed, the aptamer mRNA forms an RNA ring with two stem-loops as a secondary structure. This secondary structure binds Gln specifically promoting a conformational change in the mRNA secondary structure which then leads to translation of the downstream *gifB* mRNA (Fig. 36.4b). The existence of a Gln-binding aptamer is the first proof that Gln functions as a status reporter metabolite in cyanobacteria in parallel to 2-OG. Mechanistically, the binding of Gln to the aptamer is thought to promote a long-range Watson–Crick interaction that subsequently melts a short mRNA double-strand. As this double-strand blocks the RBS, binding of Gln and the ensuing conformational changes free the RBS and allow translation initiation. The activated expression of IF17 then leads to a strong inhibition of GSI activity, thereby decreasing the Gln concentration, which in turn frees the type 1 Gln aptamer in a feedback loop. The regulation of IF17 via the riboswitch is independent from NtcA. However, like for IF7, the expression of IF17 is regulated on the level of transcription (by NtcA) as well as on the level of translation. Like described above, the translational regulation is particularly important for the cells to react to sudden changes of N availability in the cyanobacterial habitats. The binding affinity of the type 1 Gln aptamer to Gln is in the range of the dissociation constant (K_D) values 0.5–5 mM.

This corresponds to the highly dynamic intracellular concentrations of Gln. With respect to the binding kinetics, this perfectly makes sense since binding affinity differs the most with ligand concentrations in the range of the K_D of the target. The binding affinity of the type 1 Gln aptamer to Gln is therefore perfectly tuned to the physiological relevant concentrations of ligand. Type 1 Gln aptamers occur in virtually all cyanobacterial species possessing an IF17 homolog. The wide distribution again undermines the importance of the translational regulation of *gifB* in the control of the cellular nitrogen metabolism in cyanobacteria. Another type of Gln-regulated riboswitch, namely the type 2 Gln aptamer, is solely found in marine picocyanobacteria like *Prochlorococcus*. This type 2 Gln aptamer is located in the 5'-UTR of *gifB*-like genes suggesting a comparable regulatory function on IF17-like proteins as the type 1 Gln aptamer on IF17 in other cyanobacteria. Even though the identified IF17-like proteins lack the C-terminal part of IF17, which is crucial for binding to GSI, another binding mechanism to the target enzyme could have coevolved in *Prochlorococcus*. Marine picocyanobacteria inhabit extremely nitrogen-deficient environments, and they are able to survive along a wide range of the vertical water column. Furthermore, *Prochlorococcus* is believed to be the most widespread and most abundant living organism on earth, and it is responsible for the major stake of oceanic primary production. Therefore, *Prochlorococcus* is a very successful bacterium, and this is in accordance with a perfect adaptation to its nutrient-poor habitat. Like mentioned before, multiple N-cost minimizing mechanisms are believed to be responsible for this adaptation, for instance, genome streamlining. One of these mechanisms is the substitution of regulatory proteins with ncRNAs because less nitrogen is consumed in the transcription of ncRNAs than in the expression of proteins. This is a possible explanation for the occurrence of a unique type 2 Gln aptamer in picocyanobacteria (Klahn et al. 2018).

36.4.2 Metabolic Adaptation to Nitrogen Deprivation

Limitation of a combined nitrogen source (like NO_3 or NH_4^+) is one of the most common hurdles bacteria face in natural environments. Depending on their ability to utilize atmospheric N_2, bacteria can be grouped into two different categories: diazotrophic and nondiazotrophic. Diazotrophic bacteria are able to fix atmospheric N_2 into a more biologically usable form, such as ammonia, via the activity of the nitrogenase enzyme (e.g., *Azospirillum* sp., *Cyanothece* sp., *Nostoc* sp., and *Anabaena variabilis*). On the contrary, nondiazotrophic bacteria cannot fix atmospheric N_2 and require a source of combined nitrogen for growth and for anabolic and catabolic cellular processes (e.g., *E. coli*, *Synechococcus elongatus* PCC 7942 and *Synechocystis* sp. PCC 6803) (Selim and Haffner 2020). In the following sections, we will review the different metabolic strategies adopted by diazotrophic and nondiazotrophic bacteria in response to nitrogen starvation.

36.4.2.1 Nitrogen Fixation by Diazotrophic Bacteria

Nitrogen fixation is a process in which atmospheric N_2 is converted to ammonia or other biologically usable nitrogen compounds. As the nitrogenase is the only enzyme known to catalyze the fixation of gaseous N_2 (Bothe et al. 2010), we therefore would like to summarize in this section the evolutionary and adaptation aspects of the nitrogenase in different bacteria. Nitrogenase is a protein complex formed by the two different proteins dinitrogenase reductase and dinitrogenase. The dinitrogenase reductase, which is also called iron (Fe) protein, is a homodimer and contains a [4Fe-4S] cluster responsible for supplying the catalytic dinitrogenase with electrons from ferredoxin or other reducing equivalents. One molecule N_2 is reduced to two molecules of ammonia NH_3 within the molybdenum-iron (MoFe) cofactor of the dinitrogenase, which is also called MoFe protein (Fig. 36.6a). This reaction requires eight electrons, 16 molecules ATP, and eight protons and releases one molecule of dihydrogen H_2 as side product. The heterotetrameric dinitrogenase consists of two alpha and two beta subunits and receives electrons from the dinitrogenase reductase. It contains two cofactors, the electron-channeling P-cluster located at the interface of one α- and β-subunit, and the mentioned catalytic MoFe cluster located in the α-subunits. Besides the MoFe cofactor containing nitrogenase (Nif), there is also a vanadium–iron (VFe) cofactor containing isoform (Vnf), as well as an isoform with a Fe-only cofactor (Anf). The expression of Vnf- and Anf-type nitrogenases was shown to be dependent on the availability of the trace element Mo, on temperature and on salinity. Both isoforms are believed to have evolved from the ancestral Nif-type nitrogenase since they only occur in prokaryotes possessing Nif nitrogenase (Mus et al. 2019).

The nitrogenase is irreversibly inactivated by oxygen (O_2). A progenitor of the current Mo-dependent Nif nitrogenase is believed to have emerged around 3.5 billion years ago (Bya) in hydrogenotrophic methanogens, which are archaea. This predates the rise of atmospheric oxygen levels due to the emergence of oxygenic photosynthesis around 2.3 Bya (Allen et al. 2019). Consequently, this explains the susceptibility of nitrogenase to O_2, which did not represent an issue at the time of the evolution of the first nitrogenase. By multiple lateral gene transfer events, Nif nitrogenase was passed on to the domain of bacteria in which the enzyme is broadly distributed. Bacteria with many different lifestyles like phototrophs, chemotrophs, and aerobic as well as obligate and facultative anaerobic bacteria, all possess Nif. Generally, aerobic bacteria have a larger number of *nif* genes encoding the enzyme itself, as well as accessory proteins important for synthesis, regulation, and protection of the nitrogenase. This is likely to be an adaptation to the more efficient metabolism of aerobes. Furthermore, the larger gene number is in accordance with the higher turnover and protection of the nitrogenase from the damage caused by O_2 (Mus et al. 2019).

The sensitivity of the nitrogenase to O_2 poses a major challenge for aerobic N_2-fixing bacteria and even more for photoautotrophs that produce oxygen by oxygenic photosynthesis, like cyanobacteria. Bacteria have evolved different

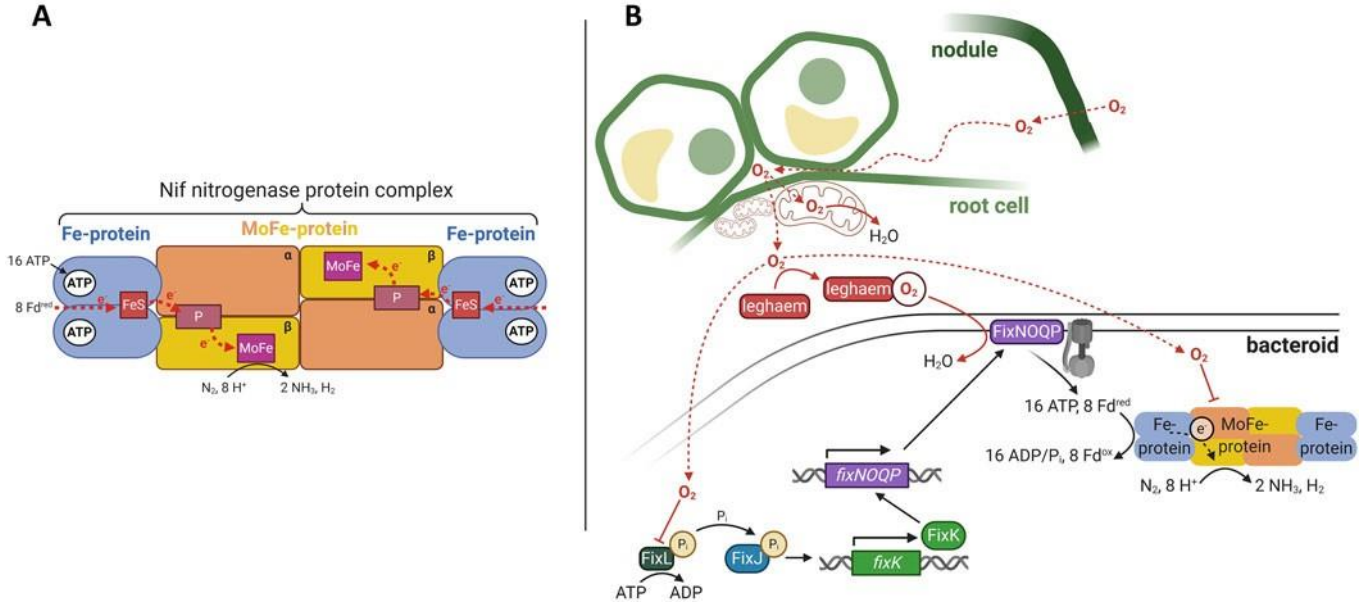

Fig. 36.6 Model for Nif nitrogenase (a) and bacteroid differentiation (b) to protect the O_2-senstive nitrogenase from O_2 damage

solutions to cope with this challenge. For example, facultative anaerobic bacteria perform N_2-fixation under anaerobic conditions only. This can be achieved by temporally controlling nitrogenase expression and activity to occur only under anaerobic growth conditions. The facultative anaerobe *Azotobacter* was shown to protect its nitrogenase from O_2 by encapsulating its cell with the formation of the polysaccharide alginate under aerobic conditions (Sabra et al. 2000). Furthermore, this bacterium shows an elevated respiratory activity, thereby rapidly consuming intracellular O_2 to form an anaerobic environment around its nitrogenase (Oelze 2000).

Concerning the bacterial genus *Rhizobium*, protection of the nitrogenase from O_2 damage is challenging, because these bacteria are obligate aerobes requiring respiration to cope with the high energy demand of their nitrogenase. *Rhizobium* is proteobacteria that has a symbiotic relationship with legume plants fueling the plant with assimilated nitrogen and receiving carbon assimilates in return. In the process of nodulation, *rhizobia* first migrate into nodules, specialized organs in the plant's root. Subsequently, the bacteria are taken up by plant root cells as endosymbionts into so-called symbiosomes. The bacterial cell within one of the symbiosomes undergoes a differentiation process driven by altered *fix* and *nif* gene expression to become a so-called bacteroid (Fig. 36.6b). This morphologically differs from free-living *Rhizobia* and is specialized in nitrogen fixation within the nodule. The bacteroid is protected from O_2 by three main mechanisms, which together result in nearly anoxic conditions at the nitrogenase expressed within the bacteroid. Firstly, the nodule possesses a cortical O_2 diffusion barrier that allows the plant to regulate O_2 entry into the nodules. Secondly, the mitochondria of the root host cells are relocated to the cell periphery, where they function as an additional barrier by consuming O_2 via respiration. Thirdly, the O_2-binding protein leghemoglobin is expressed in the plant cell cytoplasm. Leghemoglobin is structurally similar to myoglobin; however, it has a much higher affinity and much faster binding kinetics to O_2. Thereby, leghemoglobin concentrates O_2 and guarantees its rapid and even distribution in the nodule. Moreover, leghemoglobin-bound oxygen does not harm the nitrogenase, but it is still available to the bacteroid's respiratory chain. The reason for this is the expression of a high-affinity terminal oxidase, complex IV of the respiratory chain, from the *fixNOQP* operon in bacteroids (Bergersen and Appleby 1981; Rutten and Poole 2019).

Regarding oxygen-producing bacteria, almost all cyanobacteria possess a MoFe cofactor containing nitrogenase. In filamentous diazotrophic cyanobacteria, the nitrogenase is protected from oxygen inside cells specialized in N_2 fixation, so-called heterocyst cells, which possess a thick cell wall and lack O_2-producing photosystem II (PSII). Thereby, nitrogen fixation is spatially separated from O_2-evolving photosynthesis, which occurs in undifferentiated vegetative cells. Hence, the ATP needed for nitrogen fixation is produced by photosystem I (PSI) with cyclic photophosphorylation in vegetative cells and then transferred to the neighboring heterocysts in the form of electron-rich substrates like sucrose. Cell differentiation into heterocyst is tightly regulated and characterized by a series of signaling events via many secondary messenger molecules (Agostoni and

Montgomery 2014). Calcium (Ca^{2+}) is one of the most important second messengers, which is known to operate more broadly in metabolic signaling and/or differentiation processes in cyanobacteria. A significant role for Ca^{2+} has been speculated in the tight regulation of heterocyst differentiation and photosynthesis (Zhao et al. 2005; Shi et al. 2006; Walter et al. 2016, 2019, 2020).

A rare mechanism to protect the nitrogenase from oxygen is the differentiation of vegetative cells to diazocytes observed in the filamentous cyanobacterium *Trichodesmium*. In contrast to heterocysts, diazocytes possess no protective cell envelope and contain both photosystems. However, they have a high respiratory metabolic activity; hence, they consume free oxygen as described above for *Azotobacter* (Sandh et al. 2012). In contrast, some unicellular cyanobacteria temporally separate the two cellular processes of N_2-fixation and oxygen-evolving photosynthesis by only fixating N_2 under anaerobic conditions at night and in microbial mat communities with high respiratory activity (Mus et al. 2019). This protective mechanism is the most common among cyanobacteria, while heterocyst-forming filamentous cyanobacteria are thought to only have evolved about 408 million years ago (Mya) (Allen et al. 2019).

Recently, it was proposed that the late emergence of heterocyst-forming filamentous cyanobacteria in evolution is connected to the rise of the atmospheric oxygen level at the Proterozoic eon, which was about 500 Mya. In the great oxidation event (GOE), which lasted from about 2.4 Bya until 2.3 Bya, the atmospheric O_2 content rose to about 2% due to oxygenic photosynthesis conducted by cyanobacteria. Subsequently, oxygen content remained that low for about 2 billion years until it grew up to 21% by oxygenic photosynthesis performed by terrestrial plants. The low atmospheric oxygen content during the 2 billion years period in the Proterozoic, which is therefore also called “the boring billion,” is proposed to be a consequence of the feedback inhibition of nitrogenase by oxygen in cyanobacteria. Only with the increase in atmospheric oxygen content evoked by terrestrial plants did the diverse mechanisms of bacteria to protect nitrogenase from oxygen become necessary (Allen et al. 2019).

The activity of the nitrogenase is tightly regulated. For example, in the diazotrophic bacterium *Azospirillum brasilense*, PII proteins play a key role in the posttranslational regulation of nitrogenase activity. Other main interacting partners of the PII signaling system are the nitrogenase regulatory enzymes DraT (dinitrogenase reductase ADP-ribosyl-transferase) and DraG (di-nitrogenase reductase glycol-hydrolase) (Huergo et al. 2006a,b, 2007, 2009; Rajendran et al. 2011). The mechanism of PII-(GlnB and GlnZ)-dependent activation/inactivation of NifH is summarized in (Fig. 36.7).

36.4.2.2 Adaptation to Nitrogen Starvation in Nondiazotrophic Bacteria

The acclimation response to nitrogen deprivation has been extensively studied in the unicellular cyanobacterial strains *Synechococcus elongatus* PCC 7942 and *Synechocystis* sp. PCC 6803 (Klotz et al. 2016; Selim and Haffner 2020). Unlike

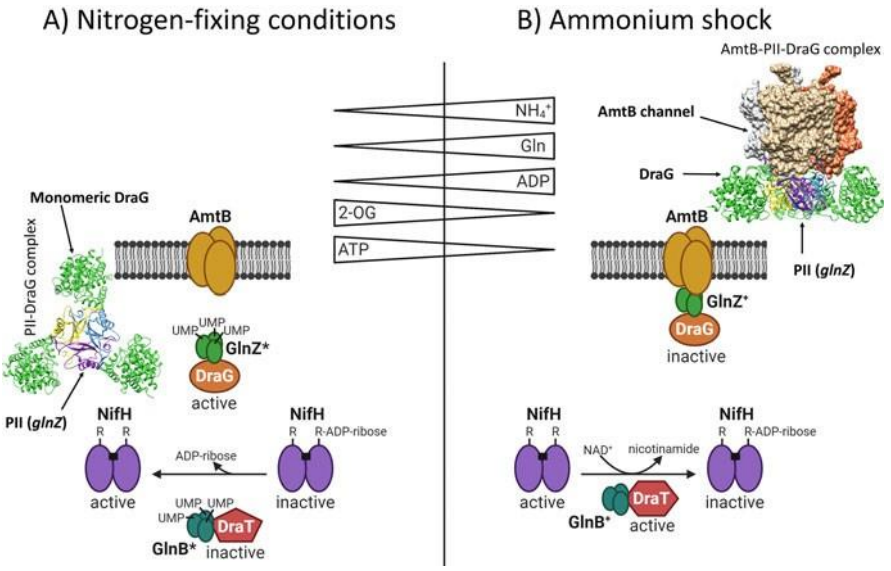

Fig. 36.7 Model for the mechanistic role of PII (GlnB and GlnZ) proteins in the activation/inactivation of NifH nitrogenase activity, through the interaction with DraT and DraG, modified from Huergo et al. (2009). Under nitrogen-fixing conditions, the cytoplasmic-localized PII (GlnB and GlnZ) proteins are fully uridylylated and DraG is active to remove ADP ribosylation (ADP-R) from NifH, while DraT is inactive, allowing NifH nitrogenase activity. Upon nitrogen excess conditions of NH_4^+ shock, the intracellular increase of Gln due to GS activity leads to deuridylylation of the PII protein. Under this condition, the deuridylylated PII (GlnZ) moves to the membrane to close the NH_4^+ transport channel AmtB, and the DraG is sequestered to the membrane through the formation of the ternary AmtB-PII-DraG complex, while DraT starts again to be active leading to ADP ribosylation of NifH (the nitrogenase inactive form). The membrane localization of DraG within the ternary complex separates the DraG from the cytoplasmic NifH and thereby inhibits the DraG ADP-R removing activity. * indicates fully uridylylated and ATP/2-OG bound PII (GlnB and GlnZ) proteins bound, while + indicates deuridylylated/ADP bound PII (GlnB and GlnZ) proteins. The structures of the PII-DraG complex (PDB: 3O5T) and AmtB-PII-DraG complex, which is modeled based on AmtB-PII structure (PDB: 2NUU), are shown

filamentous cyanobacteria, unicellular strains cannot differentiate specialized cells for nitrogen fixation. Instead, in the absence of a combined nitrogen source, these organisms follow a developmental program that leads to metabolic dormancy and allows them to survive under these starvation conditions for a prolonged period of time (Forchhammer and Schwarz 2019). The most immediate metabolic change caused by nitrogen depletion is a rise of the 2-OG levels, since ammonia assimilation via the GS-GOGAT cycle stops operating. As described in the above Sect. 36.4.1. (*Adaptation to variable nitrogen availability* via *regulation of the glutamine synthetase*), 2-OG is a reporter of the intracellular C/N balance (Fokina et al. 2010; Muro-Pastor et al. 2001), and binds both the signal transduction protein PII and the global nitrogen control factor NtcA, increasing its DNA binding affinity and mediating its interaction with the transcriptional cofactor PipX (Forchhammer 2010). One of the

targets of NtcA is *nblA*, a gene encoding for a small protein involved in the degradation of the phycobilisomes (Espinosa et al. 2007; Llácer et al. 2010). When nitrogen assimilation stops, the anabolic pathways involved in amino acid and nucleic acid synthesis are halted, with the consequent intracellular accumulation of ATP and reducing equivalents. Cells respond by adjusting the photosynthetic apparatus to prevent damage due to the extreme reduction of the photosynthetic electron carriers. This adjustment is achieved via degradation of the light-harvesting complexes, the phycobilisomes, which occurs in response to the limitation of various nutrients, but it is particularly rapid under nitrogen deprivation (Forchhammer and Schwarz 2019).

NblA is the main protein involved in phycobilisome degradation. Transcription of the *nblA* gene is induced under nitrogen starvation and is controlled by a very complex regulatory network. As mentioned above, an increase in 2-OG levels and binding of NtcA are required for induction of *nblA* expression under nitrogen-depleted conditions. Moreover, the response regulators NblR, NblC, RpaB, and SrrA are also involved in the regulation of *nblA* expression (Forchhammer and Schwarz 2019). Additionally, *nblA* expression is subjected to redox regulation: Reduction of electron carriers induces *nblA* expression and the initiation of reactions that act as an electron sink represses *nblA* expression (Klotz et al. 2015). This complex system allows a tight regulation of the phycobilisome degradation process, which is essential for survival to environmental changes. In addition to preventing photodamage, phycobilisome disassembly provides amino acids for glycogen synthesis during acclimation to nitrogen starvation. As a result of degrading the light-harvesting complexes, cells experience a color change from blue-green to yellow-orange, gaining a bleached appearance. Therefore, the process of phycobilisome degradation is termed chlorosis (Allen and Smith 1969).

Another immediate metabolic response to nitrogen starvation is the accumulation of glycogen, which has been well investigated in *Synechocystis* (Gründel et al. 2012). When imbalance in the C/N ratio is sensed through elevated levels of 2-OG, the newly photosynthetically fixed carbon is directed toward glycogen synthesis. 3-Phosphoglycerate (3-PGA) is the first stable product of the CO_2 fixation reaction catalyzed by the ribulose-1,5-bisphosphate carboxylase-oxygenase (RuBisCo). 3-PGA can enter the glycolytic route in the catabolic direction, where it is converted to 2-phosphoglycerate (2-PGA) by the phosphoglycerate mutase (Pgam), or in the gluconeogenesis direction, where it is converted to 2,3-bisphosphoglycerate (2,3-PGA) and directed toward glycogen synthesis. The Pgam reaction is a key point in the control of the fate of the photosynthetically fixed carbon. Under nitrogen sufficiency, when 2-OG levels are low, PII binds PirC, a competitive inhibitor of Pgam, and carbon is directed into the catabolic route. When 2-OG levels increase during nitrogen limitation, the PII-PirC complex dissociates and PirC inhibits Pgam, directing carbon into glycogen synthesis (Orthwein et al. 2020). Glycogen accumulation is essential for proper acclimation to nitrogen starvation. Mutants impaired in glycogen synthesis fail to carry out the chlorosis process and do not survive nitrogen depletion (Gründel et al. 2012). Glycogen accumulation starts almost immediately after the onset of nitrogen starvation and reaches a

maximum of 60% of the cell's dry weight after 14 hours (Klotz et al. 2016). As glycogen is being synthesized, cells begin the expression of the glycogen catabolic enzymes, which remain inactive until a nitrogen source is again available (Doello et al. 2018). This anticipatory behavior allows cells to rapidly react to the presence of a nitrogen source. Some cyanobacterial strains of the genera *Anabaena*, *Cyanothece*, *Microcystis*, *Nostoc*, *Oscillatoria*, *Synechococcus*, and *Synechocystis* accumulate an additional carbon polymer called polyhydroxybutyrate (PHB) (Zilliges 2014), which is produced from glycogen after a few days of nitrogen starvation (Koch et al. 2019). The physiological role of PHB in the survival of periods of nitrogen starvation has, however, not been elucidated (Hauf et al. 2013; Klotz et al. 2016; Koch et al. 2020).

After the first events in the adaptation to nitrogen starvation (i.e., chlorosis and glycogen accumulation) have taken place, cells direct their metabolism into a dormant state that allows prolonged survival under these conditions. The chlorotic state is characterized by growth arrest and reduced metabolic activity. Growth arrest occurs after DNA replication, rendering cells ready for division when they can resume metabolic activity and providing a higher polyploidy to protect them in case of DNA damage. During quiescence, a precise regulation of the residual metabolic processes is essential to ensure cell survival. In *Synechocystis*, upon nitrogen starvation, the intracellular ATP content is reduced to approximately 25% of the levels in vegetative cells and is maintained at this level throughout the entirety of the dormant period (Doello et al. 2018). As cells enter dormancy, they degrade most of their thylakoid membranes. Thus, dormant cells rely on residual photosynthetic and respiratory activity to maintain their ATP content to a minimum level. Chlorotic cells conserve a small proportion of their photosynthetic machinery (Sauer et al. 2001; Spät et al. 2018), but the residual activity they are capable of is required to sustain viability, since treatment with inhibitors of photosynthetic electron transport or prolonged exposure to darkness leads to death (Forchhammer and Schwarz 2019). Due to the vast degradation of the thylakoid membranes and the consequent reduced space for proton storage, the bioenergetics of chlorotic *Synechocystis* cells largely depend on sodium. The plasma membrane is energized by its alternative respiratory chain, which consists of a NAD(P)H dehydrogenase type II (NDHII) and an alternative terminal cytochrome c oxidase (ARTO), creating a sodium motive force that can be employed by the ATP synthases in the plasma membrane to provide dormant cells with ATP. This adaptation strategy seems to extend to other high-salt-adapted cyanobacteria, but not to freshwater species such as *S. elongatus* (Doello et al. 2021).

When dormant nitrogen-starved cells encounter a source of combined nitrogen, they are capable of reverting the metabolic and structural changes described above and restore the vegetative cell cycle. The process of exiting dormancy is termed resuscitation, and it involves a genetically determined program (Klotz et al. 2016; Spät et al. 2018). Immediately after nitrogen availability, the genes encoding for the ATP synthesis, nitrogen assimilation and translation machinery are upregulated (Klotz et al. 2016). The first detected metabolic response of chlorotic cells to the presence of nitrogen is an increase in the ATP levels (Doello et al. 2018), which is necessary to fuel nitrogen assimilating reactions. To synthesize ATP, cells cease the

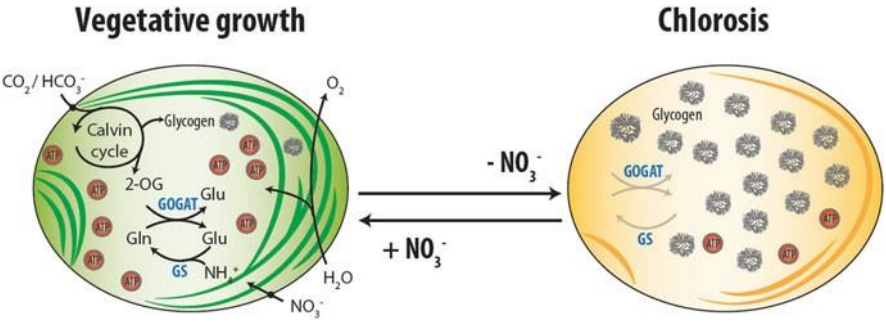

Fig. 36.8 Schematic representation of the adaptation to nitrogen starvation in *Synechocystis* sp. PCC 6803. Under nitrogen deprivation, cells tune down their ATP levels, degrade their photosynthetic machinery and thylakoid membranes, and accumulate glycogen granules, reaching a state of dormancy that allows prolonged survival under these conditions. Upon addition of a combined nitrogen source, cells initiate the resuscitation program: Glycogen degradation is activated, ATP levels rise, and the photosynthetic machinery and thylakoid membranes are rebuilt, restoring vegetative growth within 48 h

residual photosynthetic activity and induce respiration of glycogen, thus switching to a heterotrophic metabolism. Glycogen degradation provides the necessary energy and intermediates to rebuild the photosynthetic machinery, and it is essential for the recovery of dormant cells (Doello et al. 2018). Twenty-four hours after nitrogen availability, cells start to regreen and regain photosynthetic activity, entering a mixotrophic phase. Photoautotrophic growth and cell division resume after 48 h, thereby completing the program (Klotz et al. 2016) (Fig. 36.8).

36.5 Concluding Remarks

Despite all the research efforts, it is necessary to point out that no experimental design truly mimics the complexity of the actual environmental changes experienced by microbes in nature. The seasonal cycles and nutrient scarcity/availability depend on wild or man-made factors, ecosystems, and metaorganisms dynamics. In addition, experiments are time limited, precluding an absolute certainty about the fate of the organisms in question.

Nevertheless, the compilation of information continues to be our strongest tool to prepare for a new norm, as predicted by the intergovernmental panel on climate change, and elaborate accordingly which organisms and locations face the highest degree of risk. This information will serve to inform policy makers on how to control the causes and mitigate the consequences. These can enforce laws and rules for urban sprawl, industrialization, and fuel consumption, but also promote public awareness through campaigns aimed at educating people about waste recycling and the carbon footprint of their own diet.

Acknowledgments The authors gratefully acknowledge Karl Forchhammer for continued support. Furthermore, we would like to acknowledge Libera Lo-Presti for critical scientific and linguistic editing of the manuscript and the infrastructural support by the Cluster of Excellence "Controlling Microbes to Fight Infections" (EXC 2124) of the German research foundation (DFG). We are indebted to the DFG for continuous funding of the work in the authors laboratory. KAS would like to dedicate this chapter to the memory of Dr. Ali Selim, a distinguished father and medical doctor, for his continued support.

Author Contributions KAS conceived and designed this project. All authors analyzed the data and wrote the manuscript, while KSA merged the final version of the manuscript. KAS and EZ prepared the figures (except Fig. 36.8 by SD). All authors but particularly SD commented and edited on the manuscript and approved the final version of the manuscript.

References

Abatenh E, Gizaw B, Tsegaye Z, Tefera G (2018) Microbial function on climate change - a review. Environ Pollut Climate Change 2:1000147

Abduljalil JM (2018) Bacterial riboswitches and RNA thermometers: nature and contributions to pathogenesis. Non-coding RNA Res 3:54–63

Agostoni M, Montgomery BL (2014) Survival strategies in the aquatic and terrestrial world: the impact of second messengers on cyanobacterial processes. Life (Basel, Switzerland) 4 (4):745–769. https://doi.org/10.3390/life4040745

Allen MM, Smith AJ (1969) Nitrogen chlorosis in blue-green algae. Archiv fur Mikrobiologie 69 (2):114–120. https://doi.org/10.1007/bf00409755

Allen JF, Thake B, Martin WF (2019) Nitrogenase inhibition limited oxygenation of Earth's proterozoic atmosphere. Trends Plant Sci 24:1022–1031

Angilletta MJ, Huey RB, Frazier MR (2010) Thermodynamic effects on organismal performance: is hotter better? Physiol Biochem Zool 83:197–206

Bardgett RD, Freeman C, Ostle NJ (2008) Microbial contributions to climate change through carbon cycle feedbacks. ISME J 2:805–814

Beere HM (2004) 'The stress of dying': the role of heat shock proteins in the regulation of apoptosis. J Cell Sci 117:2641–2651

Bergersen FJ, Appleby CA (1981) Leghaemoglobin within bacteroid-enclosing membrane envelopes from soybean root nodules. Planta 152:534–543

Bolay P, Muro-Pastor MI, Florencio FJ, Klahn S (2018) The distinctive regulation of cyanobacterial glutamine synthetase. Life (Basel) 8:52

Bothe H, Schmitz O, Yates MG, Newton WE (2010) Nitrogen fixation and hydrogen metabolism in cyanobacteria. Microbiol Mol Biol Rev 74:529–551

Bradford MA (2013) Thermal adaptation of decomposer communities in warming soils. Front Microbiol 4:333

Brown JR, Masuchi Y, Robb FT, Doolittle WF (1994) Evolutionary relationships of bacterial and archaeal glutamine synthetase genes. J Mol Evol 38:566–576

Calloni G, Chen T, Schermann SM, Chang HC, Genevaux P, Agostini F, Tartaglia GG, Hayer-Hartl M, Hartl FU (2012) DnaK functions as a central hub in the *E. coli* chaperone network. Cell Rep 1:251–264

Cavicchioli R et al (2019) Scientists' warning to humanity: microorganisms and climate change. Nat Rev Microbiol 17:569–586

Chowdhury S, Maris C, Allain FHT, Narberhaus F (2006) Molecular basis for temperature sensing by an RNA thermometer. EMBO J 25:2487–2497

Cimdins A, Klinkert B, Aschke-Sonnenborn U, Kaiser FM, Kortmann J, Narberhaus F (2014) Translational control of small heat shock genes in mesophilic and thermophilic cyanobacteria by RNA thermometers. RNA Biol 11:594–608

Commichau FM, Forchhammer K, Stülke J (2006) Regulatory links between carbon and nitrogen metabolism. Curr Opin Microbiol 9:167–172

Cronan CS (2018) Microbial biogeochemistry. In: Ecosystem biogeochemistry: element cycling in the forest landscape. Springer, Cham, pp 31–40

Dell AI, Pawar S, Savage VM (2011) Systematic variation in the temperature dependence of physiological and ecological traits. Proc Natl Acad Sci U S A 108:10591–10596

Deutsch CA, Tewksbury JJ, Huey RB, Sheldon KS, Ghalambor CK, Haak DC, Martin PR (2008) Impacts of climate warming on terrestrial ectotherms across latitude. Proc Natl Acad Sci U S A 105:6668–6672

Docherty KM, Gutknecht JLM (2012) The role of environmental microorganisms in ecosystem responses to global change: current state of research and future outlooks. Biogeochemistry 109:1–6

Doello S et al (2018) A specific glycogen mobilization strategy enables rapid awakening of dormant cyanobacteria from chlorosis. Plant Physiol 177:594–603. https://doi.org/10.1104/pp.18.00297

Doello S, Burkhardt M, Forchhammer K (2021) The essential role of sodium bioenergetics and ATP homeostasis in the developmental transitions of a cyanobacterium. Curr Biol. https://doi.org/10.1016/j.cub.2021.01.065

Drigo B, Kowalchuk GA, Yergeau E, Bezemer TM, Boschker HTS, Van Veen JA (2007) Impact of elevated carbon dioxide on the rhizosphere communities of Carex arenaria and *Festuca rubra*. Glob Chang Biol 13:2396–2410

Dutta H, Dutta A (2016) The microbial aspect of climate change. In: Energy, ecology and environment, vol 1. Joint Center on Global Change and Earth System Science of the University of Maryland and Beijing Normal University, Beijing, pp 209–232

Espinosa J, Forchhammer K, Contreras A (2007) Role of the Synechococcus PCC 7942 nitrogen regulator protein PipX in NtcA-controlled processes. Microbiology 153:711–718

Fokina O et al (2010) Mechanism of 2-oxoglutarate signaling by the *Synechococcus elongatus* P II signal transduction protein. Proc Natl Acad Sci U S A 107:19760–19765

Forcada-Nadal A, Palomino-Schatzlein M, Neira JL, Pineda-Lucena A, Rubio V (2017) The PipX protein, when not bound to its targets, has its signaling C-terminal Helix in a flexed conformation. Biochemistry 56:3211–3224

Forchhammer K (2010) Network of PII Signalling protein interactions in unicellular cyanobacteria. Recent Adv Phototrophic Prokaryotes 675:71–90

Forchhammer K, Schwarz R (2019) Nitrogen chlorosis in unicellular cyanobacteria – a developmental program for surviving nitrogen deprivation. Environ Microbiol 21:1173–1184

Forchhammer K, Selim KA (2020) Carbon/nitrogen homeostasis control in cyanobacteria. FEMS Microbiol Rev 44:33–53

Franks SJ, Hoffmann AA (2012) Genetics of climate change adaptation. Annu Rev Genet 46:185–208

García-Domínguez M, Reyes JC, Florencio FJ (1999) Glutamine synthetase inactivation by protein-protein interaction. Proc Natl Acad Sci U S A 96:7161–7166

Gionchetta G, Romaní AM, Oliva F, Artigas J (2019) Distinct responses from bacterial, archaeal and fungal streambed communities to severe hydrological disturbances. Sci Rep 9:13506

Grandclement C, Tannieres M, Morera S, Dessaux Y, Faure D (2016) Quorum quenching: role in nature and applied. FEMS Microbiol Rev 40:86–116

Gründel M et al (2012) Impaired glycogen synthesis causes metabolic overflow reactions and affects stress responses in the cyanobacterium Synechocystis sp. PCC 6803. Microbiology (United Kingdom) 158(12):3032–3043. https://doi.org/10.1099/mic.0.062950-0

Hallin S, Bodelier PLE (2020) Grand challenges in terrestrial microbiology: moving on from a decade of progress in microbial biogeochemistry. Front Microbiol 11:981

Hauf W et al (2013) Metabolic changes in Synechocystis PCC6803 upon nitrogen-starvation: excess NADPH sustains polyhydroxybutyrate accumulation. Metabolites 3(1):101–118. https://doi.org/10.3390/metabo3010101

Huergo LF, Dixon R (2015) The emergence of 2-Oxoglutarate as a master regulator metabolite. Microbiol Mol Biol Rev 79:419–435

Huergo LF, Chubatsu LS, Souza EM, Pedrosa FO, Steffens MB, Merrick M (2006a) Interactions between PII proteins and the nitrogenase regulatory enzymes DraT and DraG in Azospirillum brasilense. FEBS Lett 580:5232–5236

Huergo LF, Souza EM, Araujo MS, Pedrosa FO, Chubatsu LS, Steffens MB, Merrick M (2006b) ADP-ribosylation of dinitrogenase reductase in Azospirillum brasilense is regulated by AmtB-dependent membrane sequestration of DraG. Mol Microbiol 59:326–337

Huergo LF, Merrick M, Pedrosa FO, Chubatsu LS, Araujo LM, Souza EM (2007) Ternary complex formation between AmtB, GlnZ and the nitrogenase regulatory enzyme DraG reveals a novel facet of nitrogen regulation in bacteria. Mol Microbiol 66:1523–1535

Huergo LF, Merrick M, Monteiro RA, Chubatsu LS, Steffens MB, Pedrosa FO, Souza EM (2009) In vitro interactions between the PII proteins and the nitrogenase regulatory enzymes dinitrogenase reductase ADP-ribosyltransferase (DraT) and dinitrogenase reductase-activating glycohydrolase (DraG) in Azospirillum brasilense. J Biol Chem 284:6674–6682

Huergo LF, Chandra G, Merrick M (2013) P(II) signal transduction proteins: nitrogen regulation and beyond. FEMS Microbiol Rev 37:251–283

Huey RB, Kearney MR, Krockenberger A, Holtum JAM, Jess M, Williams SE (2012) Predicting organismal vulnerability to climate warming: roles of behaviour, physiology and adaptation. Philos Trans R Soc B Biol Sci 367:1665–1679

Jiang P, Ninfa AJ (2009) α-Ketoglutarate controls the ability of the *Escherichia coli* PII signal transduction protein to regulate the activities of NRII (NtrB) but does not control the binding of PII to NRII. Biochemistry 48:11514–11521

Klahn S, Schaal C, Georg J, Baumgartner D, Knippen G, Hagemann M, Muro-Pastor AM, Hess WR (2015) The sRNA NsiR4 is involved in nitrogen assimilation control in cyanobacteria by targeting glutamine synthetase inactivating factor IF7. Proc Natl Acad Sci U S A 112:E6243–E6252

Klahn S, Bolay P, Wright PR, Atilho RM, Brewer KI, Hagemann M, Breaker RR, Hess WR (2018) A glutamine riboswitch is a key element for the regulation of glutamine synthetase in cyanobacteria. Nucleic Acids Res 46:10082–10094

Klotz A et al (2015) Nitrogen starvation acclimation in *Synechococcus elongatus*: redox-control and the role of nitrate reduction as an electron sink. Life 5(1):888–904. https://doi.org/10.3390/life5010888

Klotz A et al (2016) Awakening of a dormant cyanobacterium from nitrogen chlorosis reveals a genetically determined program. Curr Biol 26(21):2862–2872. https://doi.org/10.1016/j.cub.2016.08.054

Koch M et al (2019) PHB is produced from glycogen turn-over during nitrogen starvation in Synechocystis sp. PCC 6803. Int J Mol Sci 20:1942. https://doi.org/10.3390/ijms20081942

Koch M, Berendzen KW, Forchhammer K (2020) On the role and production of polyhydroxybutyrate (Phb) in the cyanobacterium synechocystis sp. pcc 6803. Life 10. https://doi.org/10.3390/life10040047

Loh E, Righetti F, Eichner H, Twittenhoff C, Narberhaus F (2018) RNA thermometers in bacterial pathogens. Microbiol Spectr 6(2). https://doi.org/10.1128/microbiolspec.RWR-0012-2017

Kortmann J, Narberhaus F (2012) Bacterial RNA thermometers: molecular zippers and switches. Nat Rev Microbiol 10:255–265

Kosaka T, Nakajima Y, Ishii A, Yamashita M, Yoshida S, Murata M, Kato K, Shiromaru Y, Kato S, Kanasaki Y, Yoshikawa H, Matsutani M, Thanonkeo P, Yamada M (2019) Capacity for survival in global warming: adaptation of mesophiles to the temperature upper limit. PLoS One 14:e0218985

Krysenko S, Matthews A, Okoniewski N, Kulik A, Girbas MG, Tsypik O, Meyners CS, Hausch F, Wohlleben W, Bera A (2019) Initial metabolic step of a novel ethanolamine utilization pathway and its regulation in *Streptomyces coelicolor* M145. mBio 10:e00326-19

Lapina T, Selim KA, Forchhammer K, Ermilova E (2018) The PII signaling protein from red algae represents an evolutionary link between cyanobacterial and Chloroplastida PII proteins. Sci Rep 8:790

Llácer JL et al (2010) Structural basis for the regulation of NtcA-dependent transcription by proteins PipX and PII. Proc Natl Acad Sci U S A 107(35):15397–15402. https://doi.org/10.1073/pnas.1007015107

Luque I, Forchhammer K (2008) Nitrogen assimilation and C/N balance sensing, Chapter 13. In: Herrero A, Flores E (eds) The cyanobacteria: molecular biology, genomics and evolution. Caister Academic Press, London

Maleki F, Khosravi A, Nasser A, Taghinejad H, Azizian M (2016) Bacterial heat shock protein activity. J Clin Diagn Res 10:BE01–BE03

Merino N, Aronson HS, Bojanova DP, Feyhl-Buska J, Wong ML, Zhang S, Giovannelli D (2019) Living at the extremes: extremophiles and the limits of life in a planetary context. Front Microbiol 10:780

Miller DJ, Fort PE (2018) Heat shock proteins regulatory role in neurodevelopment. Front Neurosci 12:821

Krysenko S, Okoniewski N, Kulik A, Matthews A, Grimpo J, Wohlleben W, Bera A (2017) Gamma-glutamylpolyamine synthetase GlnA3 is involved in the first step of polyamine degradation pathway in *Streptomyces coelicolor* M145. Front Microbiol 8:726

Muro-Pastor MI, Reyes JC, Florencio FJ (2001) Cyanobacteria perceive nitrogen status by sensing intracellular 2-oxoglutarate levels. J Biol Chem 276:38320–38328

Mus F, Colman DR, Peters JW, Boyd ES (2019) Geobiological feedbacks, oxygen, and the evolution of nitrogenase. Free Radic Biol Med 140:250–259

Narberhaus F, Balsiger S (2003) Structure-function studies of *Escherichia coli* RpoH (σ32) by in vitro linker insertion mutagenesis. J Bacteriol 185:2731–2738

Narberhaus F, Waldminghaus T, Chowdhury S (2006) RNA thermometers. FEMS Microbiol Rev 30:3–16

Neira JL, Ortore MG, Florencio FJ, Muro-Pastor MI, Rizzuti B (2020) Dynamics of the intrinsically disordered inhibitor IF7 of glutamine synthetase in isolation and in complex with its partner. Arch Biochem Biophys 683:108303

Oelze J (2000) Respiratory protection of nitrogenase in azotobacter species: is a widely held hypothesis unequivocally supported by experimental evidence? FEMS Microbiol Rev 24:321–333

Orthwein T et al (2020) The novel PII-interacting regulator PirC (Sll0944) identifies 3-phosphoglycerate mutase (PGAM) as central control point of carbon storage metabolism in cyanobacteria. bioRxiv. https://doi.org/10.1101/2020.09.11.292599

Pantoja-Uceda D, Neira JL, Saelices L, Robles-Rengel R, Florencio FJ, Muro-Pastor MI, Santoro J (2016) Dissecting the binding between glutamine synthetase and its two natively unfolded protein inhibitors. Biochemistry 55:3370–3382

Perez-Mon C, Frey B, Frossard A (2020) Functional and structural responses of arctic and alpine soil prokaryotic and fungal communities under freeze-thaw cycles of different frequencies. Front Microbiol 11:982. https://doi.org/10.3389/fmicb.2020.00982

Rajendran C, Gerhardt EC, Bjelic S, Gasperina A, Scarduelli M, Pedrosa FO, Chubatsu LS, Merrick M, Souza EM, Winkler FK, Huergo LF, Li XD (2011) Crystal structure of the GlnZ-DraG complex reveals a different form of PII-target interaction. Proc Natl Acad Sci U S A 108:18972–18976

Rampelotto PH (2013) Extremophiles and extreme environments. Life 3:482–485

Rexer HU, Schäberle T, Wohlleben W, Engels A (2006) Investigation of the functional properties and regulation of three glutamine synthetase-like genes in Streptomyces coelicolor A3(2). Arch Microbiol 186:447–458

Righetti F, Narberhaus F (2014) How to find RNA thermometers. *Frontiers in Cellular and Infection*. Microbiology 4:132

Rodriguez R, Durán P (2020) Natural Holobiome engineering by using native extreme microbiome to counteract the climate change effects. Front Bioeng Biotechnol 8:568

Ronneau S, Hallez R (2019) Make and break the alarmone: regulation of (p)ppGpp synthetase/hydrolase enzymes in bacteria. FEMS Microbiol Rev 43:389–400

Rousk J, Bengtson P (2014) Microbial regulation of global biogeochemical cycles. Front Microbiol 5:103. https://doi.org/10.3389/fmicb.2014.00103

Rudolph B, Gebendorfer KM, Buchner J, Winter J (2010) Evolution of *Escherichia coli* for growth at high. J Biol Chem 285:19029–19034

Rutten PJ, Poole PS (2019) Oxygen regulatory mechanisms of nitrogen fixation in rhizobia. Adv Microb Physiol 75:325–389

Sabra W, Zeng AP, Lunsdorf H, Deckwer WD (2000) Effect of oxygen on formation and structure of *Azotobacter vinelandii* alginate and its role in protecting nitrogenase. Appl Environ Microbiol 66:4037–4044

Saelices L, Galmozzi CV, Florencio FJ, Muro-Pastor MI, Neira JL (2011) The inactivating factor of glutamine synthetase IF17 is an intrinsically disordered protein, which folds upon binding to its target. Biochemistry 50:9767–9778

Sandberg TE, Pedersen M, Lacroix RA, Ebrahim A, Bonde M, Herrgard MJ, Palsson BO, Sommer M, Feist AM (2014) Evolution of *Escherichia coli* to 42 °C and subsequent genetic engineering reveals adaptive mechanisms and novel mutations. Mol Biol Evol 31:2647–2662

Sandh G, Xu L, Bergman B (2012) Diazocyte development in the marine diazotrophic cyanobacterium Trichodesmium. Microbiol (Reading) 158:345–352

Sauer J et al (2001) Nitrogen starvation-induced chlorosis in Synechococcus PCC 7942. Low-level photosynthesis as a mechanism of long-term survival. Plant Physiol 126:233–243

Selim KA, Haffner M (2020) Heavy metal stress alters the response of the unicellular cyanobacterium *Synechococcus elongatus* PCC 7942 to nitrogen starvation. Life (Basel, Switzerland) 10 (11):275. https://doi.org/10.3390/life10110275

Selim KA, Maldener I (2021) Cellular and molecular strategies in cyanobacterial survival-"In Memory of Prof. Dr. Wolfgang Lockau". Life (Basel, Switzerland) 11(2):132. https://doi.org/10.3390/life11020132

Selim KA, Haase F, Hartmann MD, Hagemann M, Forchhammer K (2018) PII-like signaling protein SbtB links cAMP sensing with cyanobacterial inorganic carbon response. Proc Natl Acad Sci U S A 115(21):E4861–E4869

Selim KA, Haffner M, Watzer B, Forchhammer K (2019) Tuning the in vitro sensing and signaling properties of cyanobacterial PII protein by mutation of key residues. Sci Rep 9(1):18985. https://doi.org/10.1038/s41598-019-55495-y

Selim KA, Ermilova E, Forchhammer K (2020c) From cyanobacteria to Archaeplastida: new evolutionary insights into PII signalling in the plant kingdom. New Phytol 227:722–731

Selim KA, Lapina T, Forchhammer K, Ermilova E (2020b) Interaction of N-acetyl-l-glutamate kinase with the PII signal transducer in the non-photosynthetic alga *Polytomella parva*: co-evolution towards a hetero-oligomeric enzyme. FEBS J 287:465–482

Selim KA, Tremiño L, Alva V, Espinosa J, Contreras A, Marco-Marín C, Hartmann MD, Forchhammer K, Rubio V (2020a) Functional and structural characterization of PII-like protein CutA does not support involvement in heavy metal tolerance in cyanobacteria and hints at a small-molecule carrying/signaling role. FEBS J. https://doi.org/10.1111/febs.15464

Shade A, Peter H, Allison SD, Baho DL, Berga M, Bürgmann H, Huber DH, Langenheder S, Lennon JT, Martiny JBH, Matulich KL, Schmidt TM, Handelsman J (2012) Fundamentals of microbial community resistance and resilience. Front Microbiol 3:417

Shi Y, Zhao W, Zhang W, Ye Z, Zhao J (2006) Regulation of intracellular free calcium concentration during heterocyst differentiation by HetR and NtcA in Anabaena sp. PCC 7120. Proc Natl Acad Sci U S A 103:11334–11339

Singh BK, Bardgett RD, Smith P, Reay DS (2010) Microorganisms and climate change: terrestrial feedbacks and mitigation options. Nat Rev Microbiol 8:779–790

Smith TP, Thomas T, García-Carreras B, Sal S, Yvon-Durocher G, Bell T, Pawar S (2019) Community-level respiration of prokaryotic microbes may rise with global warming. Nat Commun 10(1):5124. https://doi.org/10.1038/s41467-019-13109-1

Spät P et al (2018) Chlorosis as a developmental program in cyanobacteria: the proteomic fundament for survival and awakening. Mol Cell Proteomics 17:1650–1669

Steinchen W, Bange G (2016) The magic dance of the alarmones (p)ppGpp. Mol Microbiol 101:531–544

Tiwari S, Thakur R, Shankar J (2015) Role of heat-shock proteins in cellular function and in the biology of fungi. Biotechnol Res Int 132635

Voolstra CR, Ziegler M (2020) Adapting with microbial help: microbiome flexibility facilitates rapid responses to environmental change. BioEssays 42(7):e2000004

Walter J, Lynch F, Battchikova N, Aro EM, Gollan PJ (2016) Calcium impacts carbon and nitrogen balance in the filamentous cyanobacterium Anabaena sp. PCC 7120. J Exp Bot 67:3997–4008

Walter J, Selim KA, Leganés F, Fernández-Piñas F, Vothknecht UC, Forchhammer K, Aro EM, Gollan PJ (2019) A novel Ca^{2+}-binding protein influences photosynthetic electron transport in *Anabaena* sp. PCC 7120. Biochim Biophys Acta Bioenerg 1860:519–532

Walter J, Leganés F, Aro EM, Gollan PJ (2020) The small Ca^{2+}-binding protein CSE links Ca^{2+} signalling with nitrogen metabolism and filament integrity in Anabaena sp. PCC 7120. BMC Microbiol 20(1):57. https://doi.org/10.1186/s12866-020-01735-5

Wang Y, DeHaseth PL (2003) Sigma 32-dependent promoter activity in vivo: sequence determinants of the groE promoter. J Bacteriol 185:5800–5806

Wooliver R, Tittes SB, Sheth SN (2020) A resurrection study reveals limited evolution of thermal performance in response to recent climate change across the geographic range of the scarlet monkeyflower. Evolution. https://doi.org/10.1111/evo.1404

Xue K, Xie J, Zhou A, Liu F, Li D, Wu L, Deng Y, He Z, Van Nostrand JD, Luo Y, Zhou J (2016) Warming alters expressions of microbial functional genes important to ecosystem functioning. Front Microbiol 7:668. https://doi.org/10.3389/fmicb.2016.00668

Yang Z, Yang S, Van Nostrand JD, Zhou J, Fang W, Qi Q, Liu Y, Wullschleger SD, Liang L, Graham DE, Yang Y, Gu B (2017) Microbial community and functional gene changes in Arctic Tundra soils in a microcosm warming experiment. Front Microbiol 8:1741. https://doi.org/10.3389/fmicb.2017.01741

Zak DR, Blackwood CB, Waldrop MP (2006) A molecular dawn for biogeochemistry. Trends Ecol Evol 21:288–295

Zhao Y, Shi Y, Zhao W, Huang X, Wang D, Brown N, Brand J, Zhao J (2005) CcbP, a calcium-binding protein from Anabaena sp. PCC 7120, provides evidence that calcium ions regulate heterocyst differentiation. Proc Natl Acad Sci U S A 102:5744–5448

Zilliges Y (2014) Glycogen, a dynamic cellular sink and reservoir for carbon. In: Flores E (ed) Cell biology. Caister Academic Press, London

6. Publication 6 (Submitted)

Research article

Sofía Doello, Niels Neumann, Philipp Spät, Boris Maček, and Karl Forchhammer

Regulatory phosphorylation site tunes Phosphoglucomutase 1 as a metabolic valve to control mobilization of glycogen stores.

2021. BioRxiv. doi: 10.1101/2021.04.15.439997

Regulatory phosphorylation site tunes Phosphoglucomutase 1 as a metabolic valve to control mobilization of glycogen stores.

Sofía Doello [1], Niels Neumann [1], Philipp Spät [2], Boris Maček [2] and Karl Forchhammer [1*]

[1]Interfaculty Institute of Microbiology and Infection Medicine, University of Tübingen, Auf der Morgenstelle 28, 72076 Tübingen, Germany

[2] Department of Quantitative Proteomics, University of Tübingen, Auf der Morgenstelle 15, 72076 Tübingen, Germany

*Corresponding author: karl.forchhammer@uni-tuebingen.de

Classification: Biological Sciences; Microbiology

Key words: glycogen metabolism, phosphoglucomutase, glucose-6-phosphate dehydrogenase, phosphorylation, metabolic channeling, carbon flux, oxidative pentose phosphate cycle protein, cyanobacteria

Abstract

Regulation of glycogen metabolism is of vital importance in organisms of all three kingdoms of life. Although the pathways involved in glycogen synthesis and degradation are well known, many regulatory aspects around the metabolism of this polysaccharide remain undeciphered. Here, we used the unicellular cyanobacterium *Synechocystis* as a model to investigate how glycogen metabolism is regulated in dormant nitrogen-starved cells, which entirely rely on glycogen catabolism to restore growth. We found that the activity of the enzymes involved in glycogen synthesis and degradation is tightly controlled at different levels via post-translational modifications. Phosphorylation of phosphoglucomutase 1 (Pgm1) on a peripheral residue (Ser63) regulates Pgm1 activity and controls the mobilization of the glycogen stores. Inhibition of Pgm1 activity via phosphorylation on Ser63 appears essential for survival of *Synechocystis* in the dormant state. Remarkably, this regulatory mechanism seems to be conserved from bacteria to humans. Moreover, phosphorylation of Pgm1 influences the formation of a metabolon, which includes Pgm1, oxidative pentose phosphate cycle protein (OpcA) and glucose-6-phosphate dehydrogenase (G6PDH). Analysis of the steady-state levels of the metabolic products of glycogen degradation together with protein-protein interaction studies revealed that the activity of G6PDH and the formation of this metabolon are under additional redox control, likely to ensure metabolic channeling of glucose-6-phosphate to the required pathways for each developmental stage.

Significance statement

In this study, we showed that post-translational modification of phosphoglucomutase 1 (Pgm1) via phosphorylation at a peripheral residue is a key, evolutionary-conserved regulatory mechanism that controls the utilization of the glycogen reserves. We identified Pgm1 as a central metabolic valve, associating with oxidative pentose phosphate cycle protein (OpcA) and glucose-6-phosphate dehydrogenase (G6PDH) into a metabolon. This interaction is regulated by the phosphorylation state of Pgm1 and the redox state of OpcA, and probably allows direction of the carbon flux into the required metabolic pathways.

Introduction

Glycogen is the major carbohydrate storage compound in a broad range of organisms, from bacteria to humans. This polysaccharide is composed of glucose molecules connected by α,1-4 linkages and branched via α,1-6 linkages, and it is generally considered a carbon sink with energy-storage function. In humans, glycogen is mainly accumulated in the liver and skeletal muscle, and it constitutes a rapid and accessible form of energy that can be supplied to tissues on demand.[1] In many bacteria, glycogen plays a crucial role in survival to an ever-changing environment. It is usually synthesized and accumulated inside the cells under growth-limiting conditions at excess of a carbon source, and degraded when the supply of energy or carbon is not enough to maintain growth or viability, thus allowing cell survival in transient starvation conditions.[2] In cyanobacteria, which generally sustain cell growth by performing oxygenic photosynthesis, glycogen is synthesized towards the end of the day, when photosynthetically fixed carbon is in excess and cells need to prepare to survive the night.[3] Glycogen accumulation also occurs as a response to nutrient limitation. In fact, the greatest amount of glycogen accumulation in non-diazotrophic cyanobacteria, which are unable to fix atmospheric N_2, occurs under nitrogen starvation conditions.[4]

Nitrogen deprivation activates a genetically determined survival program in non-diazotrophic cyanobacteria, which has been extensively studied in the unicellular cyanobacterial strains *Synechococcus elongatus* and *Synechocystis* sp. PCC 6803 (from now *Synechocystis*).[5] When *Synechocystis* encounters nitrogen depletion, the intracellular carbon/nitrogen balance is disturbed, and growth can no longer be supported. This metabolic situation leads to rapid accumulation of glycogen, which serves as a sink for the excess of carbon.[5] In order to survive these starvation conditions, cells undergo an adaptation process termed chlorosis that involves the degradation of the light-harvesting complexes to avoid an excess of energy and reduction equivalents that are no longer consumed by anabolic reactions. As a result of the metabolic and morphological changes induced by nitrogen starvation, cells enter a dormant state, which allows them to survive adverse conditions for a prolonged period of time.[6] Upon nitrogen availability, the glycogen stores accumulated in dormant cells play a key role in the restoration of vegetative growth.[7] When dormant cells have access to a nitrogen source, their metabolism switches towards a heterotrophic mode. They turn off residual photosynthesis, while the production of energy and metabolic intermediates now entirely relies on glycogen catabolism.[8] This extraordinary situation, in which carbohydrate degradation can be completely separated from photosynthetic processes even in the presence

of light, makes awakening *Synechocystis* cells an excellent model to study the regulation of glycogen catabolism.

Although the metabolic pathways involved in glycogen synthesis and degradation are well known, many regulatory aspects around the metabolism of this polysaccharide remain to be deciphered. In nitrogen-starved *Synechocystis* cells, glycogen degradation is known to start soon after addition of a nitrogen source, and the enzymes responsible for this process have been identified (**Figure 1**).[7] However, how glycogen catabolism is induced in dormant cells has not yet been elucidated. The enzymes involved in glycogen metabolism are conserved from bacteria to humans. The glycogen phosphorylase and debranching enzyme are responsible for the excision of glucose molecules from the glycogen granule, releasing glucose-1-phosphate (glucose-1P) and glucose, respectively. Glucose-1P is then converted to glucose-6-phosphate (glucose-6P) by the phosphoglucomutase (Pgm), an evolutionary conserved enzyme that also catalyzes the reverse reaction, while glucose is converted to glucose-6P by the glucokinase (Glk). Glucose-6P is then metabolized by the glucose-6-phosphate dehydrogenase (G6PDH) and enters either the Entner-Doudoroff (ED) or the oxidative pentose phosphate (OPP) pathway. Even though *Synechocystis* also possess the enzymes to catabolize glucose-6P via the Embden-Meyerhof-Parnas (EMP) pathway, this route has been shown not to be relevant for resuscitation from nitrogen starvation. Intriguingly, most of the main glycogen catabolic enzymes are up-regulated during nitrogen starvation, although glycogen degradation does not start until a nitrogen source is available. This suggests that the activity of these enzymes must be tightly regulated: They must remain inactive when cells are dormant and be activated upon nitrogen availability. An exception to the abundance pattern of most glycogen catabolic enzymes is Pgm1, whose expression is suppressed under nitrogen starvation and activated during resuscitation.[8,9] Although *Synechocystis* possesses two Pgm isoenzymes, Pgm1 (*sll0726*) has been shown to be responsible for almost 97 % of the Pgm activity.[10] Pgm1 was recently identified as a phosphoprotein with two localized serine phosphorylation sites: Ser 63 and Ser 68. Ser 168, which is predicted to be in the catalytic center, shows diminished phosphorylation during chlorosis. On the contrary, the phosphorylation of Ser 63 strongly increases during nitrogen starvation, representing one of the most strongly induced phosphorylation events.[9] These findings prompted us to investigate the possible involvement of Pgm1 in the regulation of glycogen metabolism in resuscitating cells, enabling us to unravel some of the key regulatory mechanisms in glycogen catabolism, which seem to be conserved from bacteria to humans.

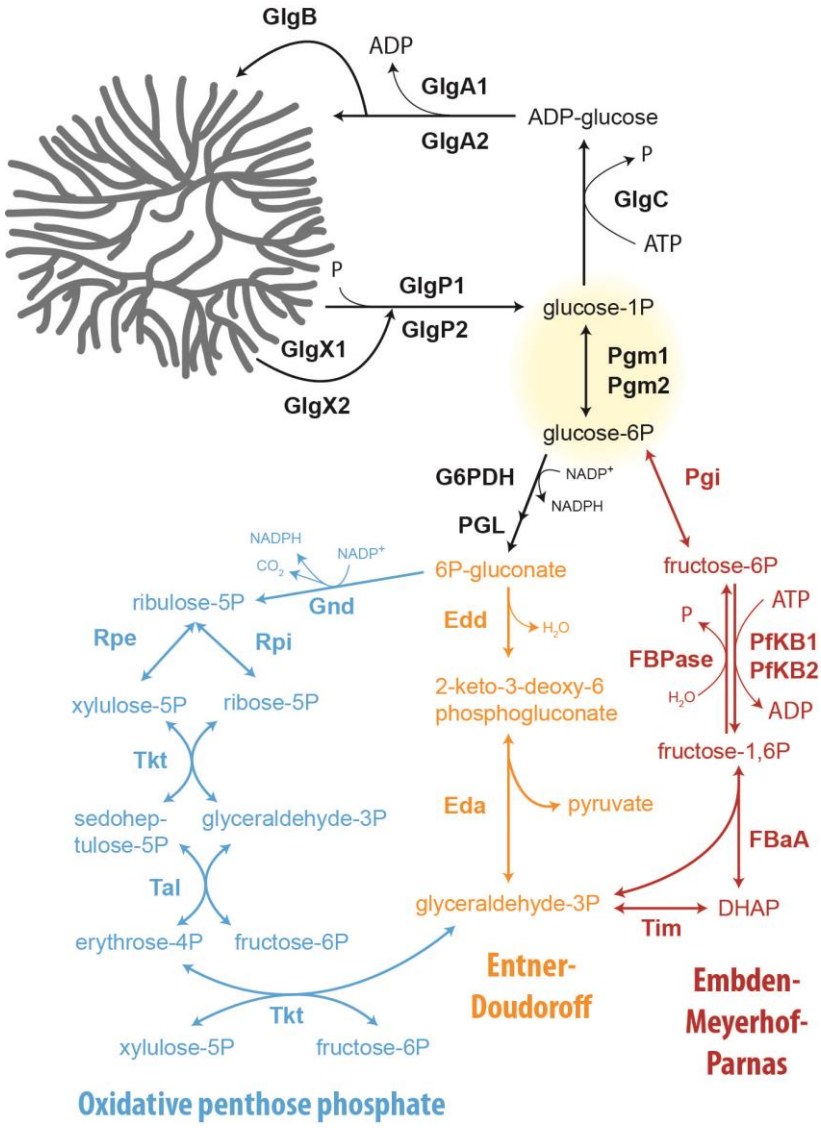

Figure 1. Schematic representation of the pathways involved in glycogen metabolism in *Synechocystis*.

Results

Pgm1 is activated during resuscitation from nitrogen starvation.

The transcription of the glycogen catabolic genes in *Synechocystis* is highly up-regulated during nitrogen deprivation,[11] when glycogen is synthesized, and turned down during resuscitation.[7] In a proteomic study covering the same developmental stages, Spät et al.[9] revealed that the glycogen catabolic enzymes are up-regulated in dormant and resuscitating cells (**Figure 2A**). One exception to this expression pattern is the Pgm1, the abundance of which is low during nitrogen starvation and increases during resuscitation (**Figure 2A**). In the same study, a quantitative analysis of the phosphorylation events during nitrogen starvation and resuscitation revealed that Pgm1 can be phosphorylated at two different residues: Ser 63 and Ser 168.[9] Interestingly, Ser 63 is one of the most phosphorylated residues in chlorotic

cells, being 15 times more phosphorylated under nitrogen starvation than during vegetative growth (**Figure 2B**). These findings suggested that Pgm1 might be a regulatory point in glycogen catabolism. To test if there was any change in the activity of Pgm1 upon addition of a nitrogen source to dormant cells, we assayed Pgm1 activity in cell extracts from chlorotic and resuscitating cells (**Figure 2C**). While Pgm1 activity was detectable in cells under nitrogen starvation, the measured activity was 3 times higher in cells that had been supplemented with nitrate 24 hours before. These results suggested an activation of Pgm1 upon addition of nitrogen to chlorotic cells.

Given the high phosphorylation of the residue Ser 63 in nitrogen-starved cells, we speculated that Ser 63 might be a regulatory phosphorylation site. To determine whether phosphorylation of Pgm1 affects its activity, we treated cell extracts from chlorotic and resuscitating cells with alkaline phosphatase (AP) and measured Pgm1 activity before and after treatment. As shown in **Figure 2D**, a higher Pgm1 activity was measured after 10 min of treatment with AP in cells extracts from chlorotic, as well as from resuscitating cells. According to homology modeling of Pgm1, Ser 168 is the catalytic seryl-residue involved in the phosphor-exchange reaction and it is located in the active site of Pgm1 (**Figure 2E**). This catalytic serine is poorly phosphorylated during nitrogen starvation and it progressively becomes more phosphorylated during resuscitation (**Figure 2B**). Since phosphorylation of the catalytic serine is required for catalysis, the phosphorylation dynamics of this residue corresponds to its state of catalytic activity, with Pgm1 being inactive in chlorotic cells and becoming activated during resuscitation. Ser 63 follows the opposite pattern: The high level of phosphorylation of this residue under nitrogen starvation progressively decreases during resuscitation (**Figure 2B**). As deduced from homology modeling, Ser 63 is located on the surface of the enzyme, close to the access to the catalytic site (**Figure 2E**). Since Ser 168 is buried in the catalytic center, AP is more likely to dephosphorylate the surface-located Ser 63. Thus, the obtained results suggested that dephosphorylation of Ser 63 induces Pgm1 activity.

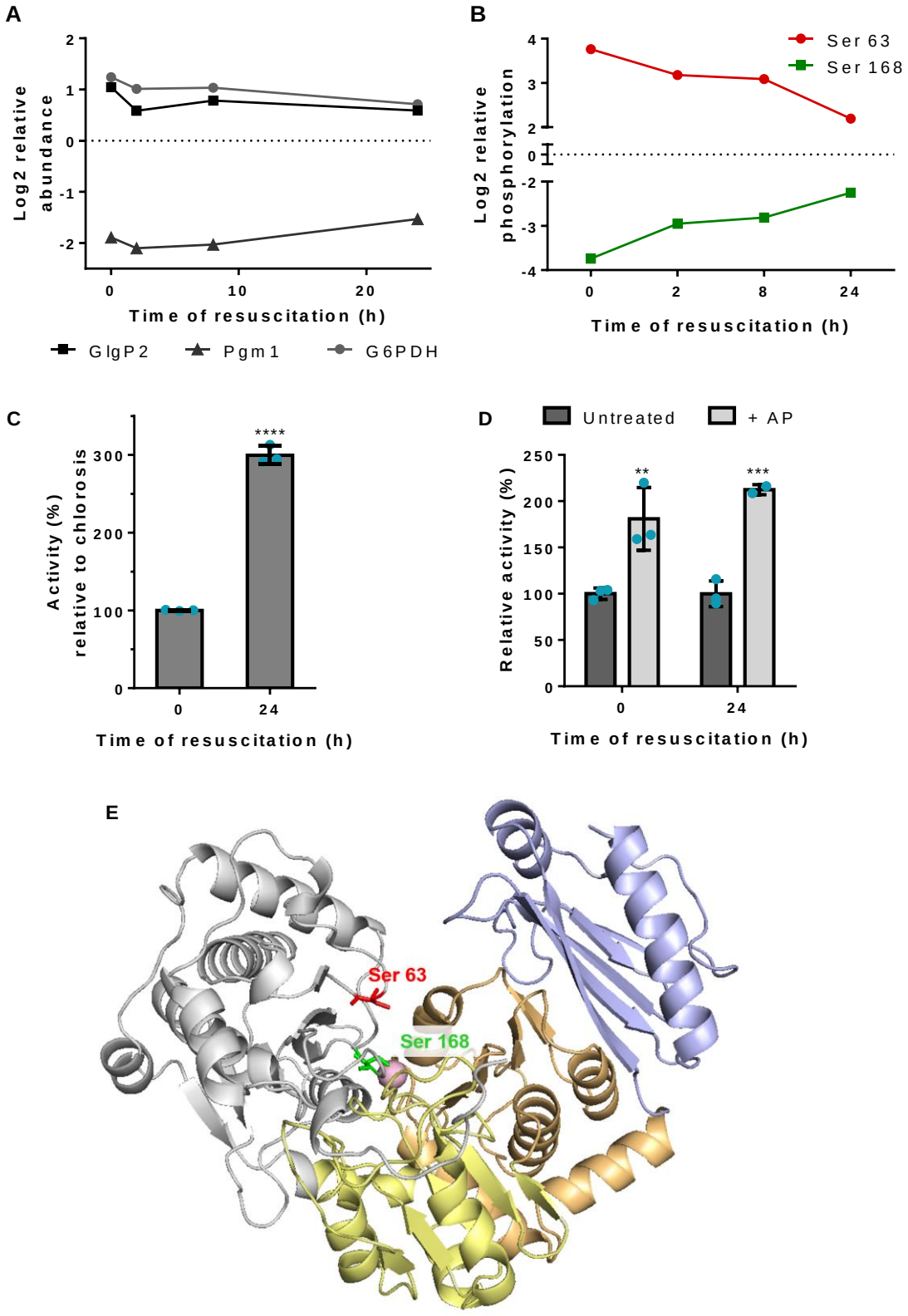

147

148 **Figure 2. Abundance, phosphorylation and activity of Pgm1 during nitrogen starvation and resuscitation.**
149 (A) Protein abundance ratios of GlgP2, G6PDH and Pgm1 during resuscitation from nitrogen starvation. Ratios
150 were calculated comparing the protein abundance during nitrogen starvation and resuscitation with their
151 abundance during vegetative growth. Relative abundance is shown as the Log2 of the calculated ratios. Positive
152 values indicate up-regulation and negative values down-regulation compared to protein levels during vegetative
153 growth (normalized to zero, dotted line).[9] (B) Phosphorylation events of the two phosphorylation sites in Pgm1
154 at the indicated time points during resuscitation from nitrogen starvation. Ratios were calculated comparing the

abundance of phosphorylated and unphosphorylated peptides at different time points during resuscitation to their abundance during vegetative growth. Relative phosphorylation is shown as the Log2 of the calculated ratios. [9] (C) Relative enzyme activity of Pgm1 in cell extracts from chlorotic and resuscitating cells. The activity in chlorotic cells was considered to be 100%. At least 3 biological replicates were measured. (D) Relative enzyme activity of Pgm1 in cell extracts from chlorotic and resuscitating cells before and after treatment with an alkaline phosphatase (AP) for 10 min. The activity before treatment was considered to be 100%. At least 3 biological replicates were measured. Error bars represent the SD, asterisks represent the statistical significance. (E) Structure of *Synechocystis'* Pgm1 obtained from Swiss Model using *Salmonella typhimurium's* Pgm as a template. The two colored resides shown in a stick model represent the two phosphorylation sites: Ser 63 in red and Ser 168 in green. The catalytic site is marked as a blue-shaded area and the Mg^{+} ion required for catalysis is shown as a pink sphere.

Pgm1 activity is regulated via phosphorylation at Ser 63.

To gain more insights on the effect of phosphorylation of Ser 63 in enzyme activity, we created different Pgm1 variants with site-specific amino acid substitutions and measured their activity *in vitro* (**Figure 3A**). First, Ser 63 was replaced by Asp (Pgm1 S63D) to create a phosphomimetic variant: in comparison to Ser, Asp is a larger, negatively charged amino acid that resembles a permanently phosphorylated Ser. The purified Pgm1 S63D seemed to be correctly folded, as deduced from its size exclusion chromatography elution profile (**Figure S1**). However, it presented very low activity *in vitro* (0.32 % of the WT activity), confirming that phosphorylation of Ser 63 inactivates Pgm1. In an attempt to create a Pgm1 variant that would mimic a permanently dephosphorylated enzyme, Ser 63 was substituted for Ala, Gly and Thr (Pgm1 S63A, S63G, and S63T, respectively). All of these variants showed a strongly reduced activity as compared to the wild-type (WT) Pgm1, with Pgm1 S63A presenting the highest activity of all variants (15 % of the WT Pgm1 activity). Comparison of the kinetic parameters of WT Pgm1 and Pgm1 S63A showed that the substitution of Ser for Ala at position 63 strongly affected the maximal velocity (V_{max}) of the reaction, which decreased almost 10-fold, but it did not decrease substrate affinity, as shown by the apparent Michaelis-Menten constant (K_m) (**Figure 3B**). In fact, the calculated K_m was even lower for Pgm1 S63A than for WT Pgm1. These results indicate that replacement of the residue S63 has a direct impact on the mechanism of catalysis rather than hindering substrate binding to the catalytic site.

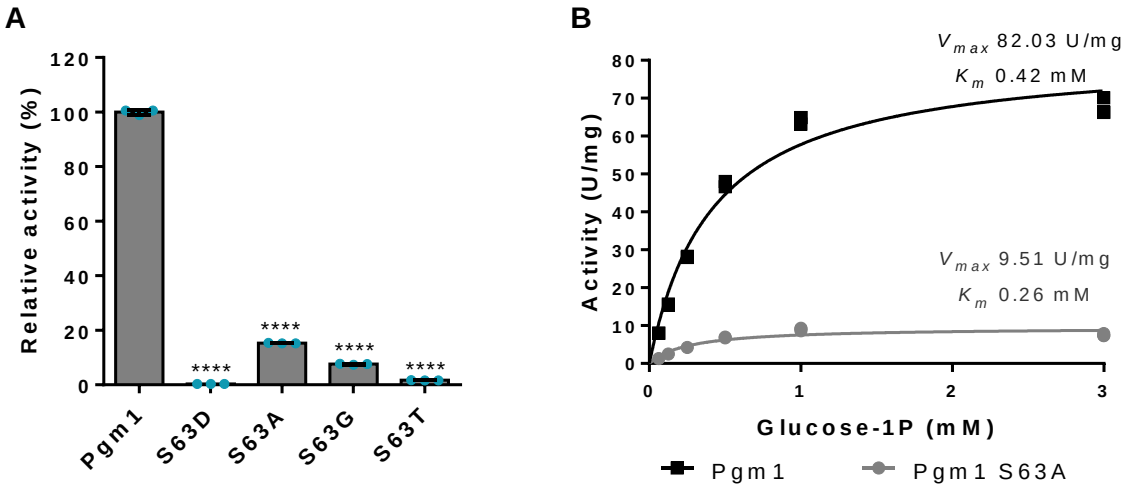

Figure 3. Phosphorylation of Ser 63 regulates Pgm1 activity. (A) Relative *in vitro* activity of wild type (WT) Pgm1 and different mutant variants. The activity of WT Pgm1 was considered to be 100%. At least 3 replicates were measured. Error bars represent the SD, asterisks represent the statistical significance. (B) Michaelis-Menten kinetics of WT Pgm1 (black squares) and Pgm1 S63A (grey circles). Three replicates were measured for each data-point.

Phosphorylation of Pgm1 at Ser 63 is essential for survival under nitrogen starvation.

So far, we could show that phosphorylation of Ser 63 regulates Pgm1 activity *in vitro*. In order to determine what role this regulatory phosphorylation plays during nitrogen starvation in *Synechocystis*, we created and characterized various Pgm1 mutant strains. A Pgm1 knockout strain (Δ*pgm1*) could not properly acclimate to nitrogen-depletion and presented a so-called non-bleaching phenotype: Cells did not degrade their photosynthetic pigments and turned yellow, but stayed greenish instead, progressively looking paler (**Figure 4A**). After two weeks of nitrogen starvation, a very reduced proportion of cells could recover when they were dropped on an agar plate containing nitrate, as compared to the WT (**Figure 4B**). Such a phenotype was previously observed in mutants that were impaired in glycogen synthesis,[12] since accumulation of this polymer has been shown to be indispensable for adaptation to nitrogen-starvation. This phenotype was expected, given that Pgm1 catalyzes the interconversion between glucose-1P and glucose-6P and is therefore involved in glycogen synthesis. Indeed, no glycogen was detected in seven-days-starved Δ*pgm1* cells (**Figure 4C**), indicating that Pgm1 activity is essential for glycogen synthesis under nitrogen deprivation, and that the activity of Pgm2 does not compensate the lack of Pgm1. Consequently, a strain with an inactive Pgm1 variant, such as the Pgm1 S63D, would not be able to enter the chlorotic state due to its inability to synthesize glycogen. To study the physiological consequences of the lack of Pgm1 inactivation via phosphorylation, we complemented the

Δ*pgm1* strain with the WT Pgm1 (Δ*pgm1*+Pgm1) and with the partially active Pgm1 S63A variant (Δ*pgm1*+Pgm1S63A), which lacks the phosphorylation site. Complementation with the WT protein rescued the phenotype: The Δ*pgm1*+Pgm1 strain showed a similar behavior than the WT under nitrogen starvation (**Figure S2A and B**). However, the Δ*pgm1*+Pgm1S63A strain was unable to acclimate to nitrogen deprivation (**Figure S2A and C**), indicating that the low activity of the Pgm1 S63A variant was not enough meet the cellular demand for Pgm activity. Therefore, we transformed wild-type cells with Pgm1 S63A (WT+Pgm1S63A) to study the impact of the lack of phosphorylation of residue 63 on long-term nitrogen starvation. As expected, this strain could initially acclimate to nitrogen depletion like the WT, since it contains the WT version of Pgm1. However, after prolonged exposure to these conditions, in which the WT version of Pgm1 would be highly phosphorylated, the cultures of the WT+Pgm1S63A strain progressively lost their characteristic yellowish color (**Figure 4A**). After one month of starvation, only a reduced number of cells could recover on a nitrate-containing agar plate (**Figure 4D**). WT+Pgm1S63A cells could synthesize glycogen upon nitrogen depletion, but after one week of starvation the glycogen content began to gradually decrease (**Figure 4E**). These findings imply that inactivation of Pgm1 via phosphorylation is crucial for preventing glycogen degradation during prolonged nitrogen starvation, which appears to be essential for survival of these conditions.

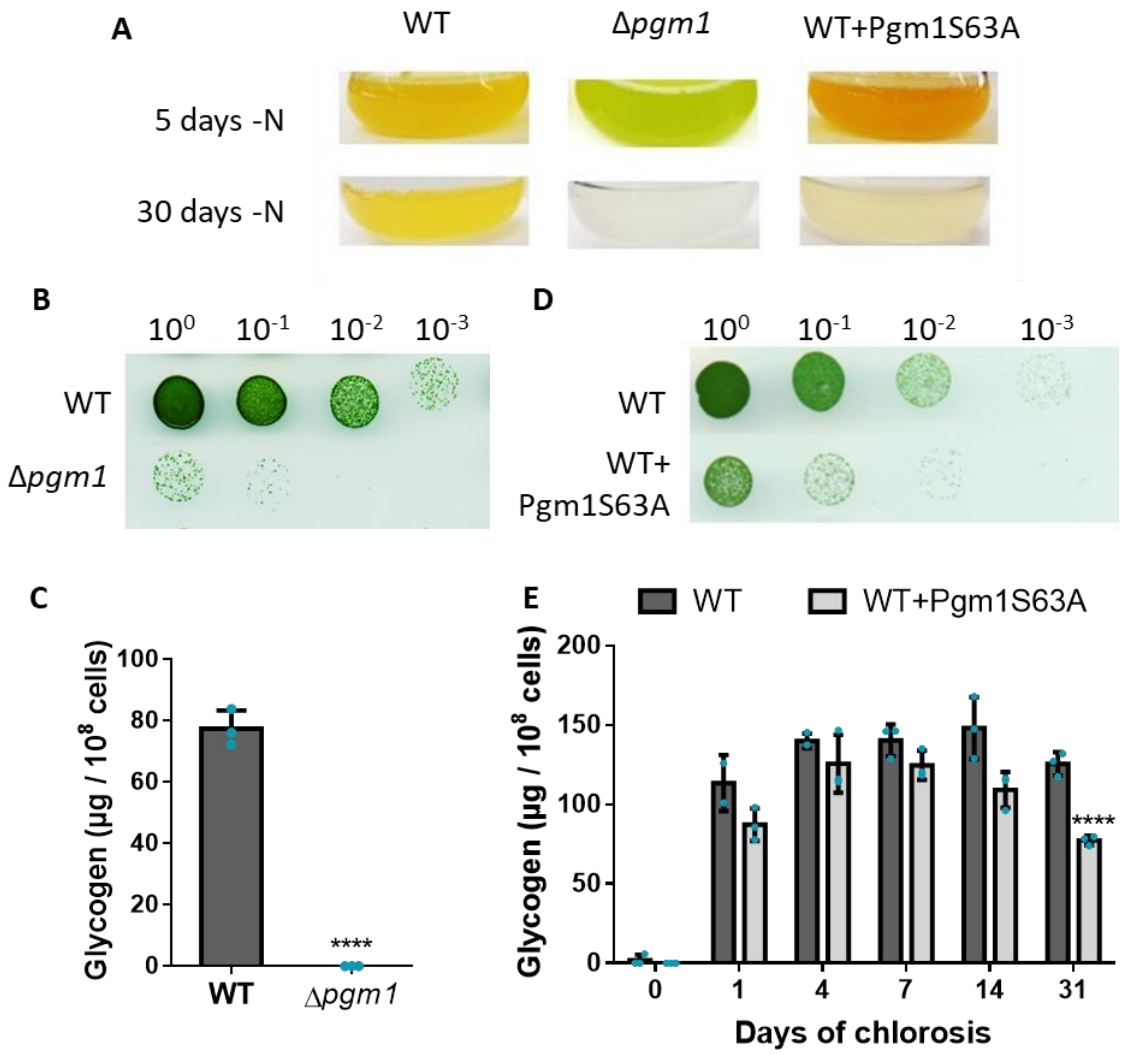

Figure 4. Pgm1 is required for glycogen synthesis and glycogen degradation during nitrogen starvation is prevented by phosphorylation of Ser 63. (A) Pictures of WT, Δ*pgm1*, and WT+Pgm1S63A cultures after 5 and 30 days of nitrogen starvation. (B) Recovery assay on a BG_{11}-agar plate of WT and Δ*pgm1*. Numbers on top represent the dilution factor, starting with an OD_{750} of 1. Pictures were taken 5 days after dropping chlorotic cells on the plate. (C) Glycogen content of WT and Δ*pgm1* after 7 days of nitrogen starvation. (D) Recovery assay of WT and WT+Pgm1S63A. (E) Glycogen content of WT and WT+Pgm1S63A at the indicated time points during nitrogen starvation. In all experiments, three biological replicates were measured. Error bars represent the SD; asterisks represent the statistical significance.

G6PDH activity is regulated by the redox state of its activator protein, OpcA.

To further prove the inactivation of Pgm1 under long-term nitrogen starvation in *Synechocystis*, the levels of glucose-phosphates in chlorotic and resuscitating cells were determined. Given the tight regulation of Pgm1, high levels of glucose-1P were expected in chlorotic cells, which should decrease upon nitrogen repletion. Indeed, an accumulation of glucose-1P during nitrogen starvation was detected: The levels of glucose-1P in chlorotic cells were approximately three times higher than in cells that were 21 h into resuscitation (**Figure 5**), confirming the inactivity of Pgm1 under nitrogen depletion. Intriguingly, glucose-

6P was also found to be accumulated in chlorotic cells (**Figure 5**). In fact, the levels of glucose-6P in both, chlorotic and resuscitating cells, were 100-fold higher than the levels of glucose-1P. This entails that the enzyme that metabolizes glucose-6P must also remain inactive under nitrogen-starvation. During recovery from chlorosis, glucose-6P has been shown to be metabolized mainly via the ED and OPP pathways,[8] implying that the enzyme responsible for glucose-6P catabolism is G6PDH.

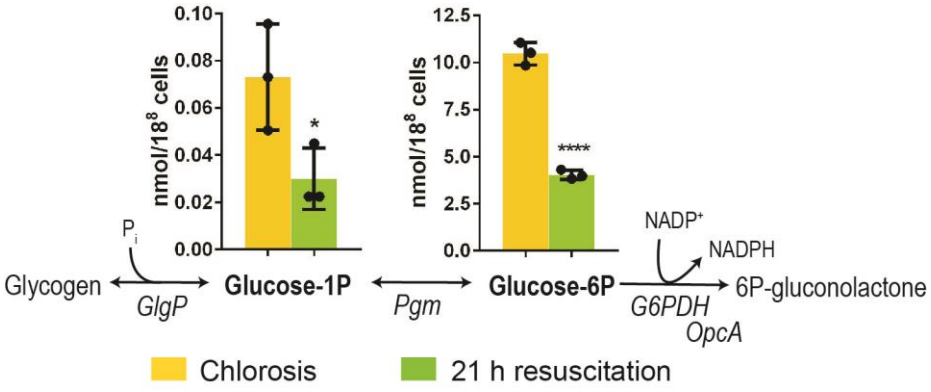

Figure 5. Glucose-phosphates accumulate in the cytoplasm during nitrogen starvation. Glucose-1P and glucose-6P content normalized to 10^8 cells during nitrogen starvation (yellow) and resuscitation (green). Three biological replicates were measured. Error bars represent the SD, asterisks represent the statistical significance.

We were then set to elucidate how G6PDH is regulated during nitrogen starvation in *Synechocystis*. In *Anabaena* sp. PCC 7120 and *Nostoc punctiforme*, the activity of G6PDH is known to be modulated by the redox state of the OPP cycle protein (OpcA), a protein that serves as an activator of G6PDH. OpcA is conserved in all cyanobacteria and it is required for G6PDH activity in *Anabaena* 7120, *N. punctiforme* and *Synechococcus* sp. 7942. In *Anabaena* 7120 and *N. punctiforme*, activation of G6PDH is modulated by the action of thioredoxin (Trx) on OpcA, which can only serve as an G6PDH activator in its oxidized state.[13,14] In the above-mentioned organisms, the *opcA* gene is located directly downstream from *zwf* (the gene encoding for G6PDH), while in *Synechocystis* these two genes are found in different operons. Moreover, the regulation of G6PDH might be different in *Synechocystis* than in nitrogen-fixing cyanobacteria, were this enzyme plays an important role in providing reduction power to the nitrogenase. Therefore, we purified G6PDH and OpcA from *Synechocystis* and studied the effect of the latter on G6PDH activity, as well as the effect of reducing and oxidizing agents on both proteins. As shown in **Figure 6A**, although G6PDH activity could be measured in the absence of OpcA, its substrate affinity increased by 6-fold when OpcA was added to the assay, confirming that OpcA acts as an allosteric activator of G6PDH in *Synechocystis*. When G6PDH was pre-incubated with reduced dithiothreitol

(DTT$_{red}$), trans-4,5-Dihydroxy-1,2-dithiane (DTT$_{ox}$) or $CuCl_2$ (which is known to induce formation of disulfide bonds), we could not detect any significant changes in G6PDH activity when the treated enzyme was assayed either in the absence or in the presence of untreated OpcA (**Figure 6B**), indicating that G6PDH itself is not sensitive to redox regulation. Pre-incubation of OpcA with DTT$_{red}$, on the other hand, reduced G6PDH activity to ~ 30 % as compared to the control, and this inhibitory effect could be partially reverted when the reduced OpcA was re-oxidized by treatment with DTT$_{ox}$. Moreover, pre-incubation of OpcA with *Synechocystis* thioredoxin TxrA had an even stronger inhibitory effect than DTT$_{red}$, reducing G6PDH activity to 10 %, which was the level of activity measured in the absence of OpcA. Pre-incubation of OpcA with DTT$_{ox}$ and $CuCl_2$ did not affect G6PDH activity, suggesting that the untreated OpcA was already in its oxidized state. These results show that in *Synechocystis*, like in the filamentous heterocyst-forming cyanobacteria, the activity of G6PDH is regulated by the redox state of OpcA.

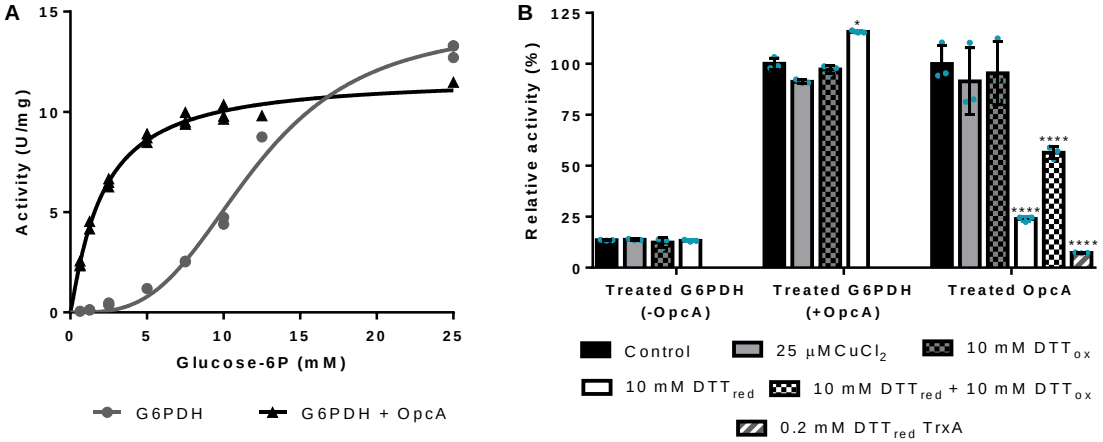

Figure 6. OpcA acts as an allosteric activator of G6PDH when it is in its oxidized state. (A) Effect of OpcA on the enzyme kinetics of G6PDH. OpcA was added as a 4:1 ratio to the amount of G6PDH. 3 replicates were measured for each data point. (B) Effect of incubating G6PDH or OpcA with reducing (DTT$_{red}$) and oxidizing (DTT$_{ox}$ and $CuCl_2$) agents on G6PDH activity. Assays were performed in the absence of the agents. 3 replicates were measured. Error bars represent the SD; asterisks represent the statistical significance.

Pgm1, OpcA and G6PDH form a complex to facilitate metabolic channeling.

The results presented above show the important role of Pgm1 phosphorylation in the regulation of glycogen metabolism. In an effort to find the protein phosphatase responsible for Pgm1 dephosphorylation during resuscitation, we analyzed the Pgm1 interactome through immunoprecipitation. Anti-Pgm1 antibodies were raised in rabbits and used to pull-down Pgm1 from cell extracts of resuscitating *Synechocystis* cells. Serum extracted from the animals before immunization was used as a negative control. The proteins enriched in the

precipitate were analyzed by quantitative proteome analysis. No protein phosphatase was found to be enriched, probably due to the transient interaction with their substrate. Surprisingly, G6PDH and OpcA were significantly enriched in the precipitate (**Figure S3**). Therefore, the interaction between these three proteins was analyzed in more detail using biolayer interferometry (BLI). His8-tagged Pgm1 was immobilized on a Ni-NTA biosensor and was allowed to associate with either Strep-tagged OpcA or Strep-tagged G6PDH. As a negative control, His8-tagged PII-ΔT-loop (a truncated version of *Synechocystis* PII protein, which is not expected to show interaction with the ligands) was immobilized to the biosensor and Strep-tagged OpcA or Strep-tagged G6PDH were used as ligands (**Figure 7A**). OpcA specifically bound to the sensor-immobilized Pgm1, but no binding of G6PDH to Pgm1 was detected. We then studied the formation of the Pgm1-OpcA-G6PDH complex in a two-step experiment, in which the sensor-immobilized Pgm1 was allowed to associate first to OpcA, and then, in a second step, to G6PDH (**Figure 7B**). This experiment showed that G6PDH could bind the sensor-bound Pgm1-OpcA complex, indicating that OpcA mediates the formation of the Pgm1-OpcA-G6PDH complex.

Since the results above showed that OpcA can only induce G6PDH activity when it is in its oxidized state, we studied the formation of the Pgm1-OpcA-G6PDH complex under reducing and oxidizing conditions. The oxidized OpcA (treated with 5 mM DTT_{ox} for 30 min) interacted with the immobilized Pgm1, while the reduced OpcA (treated with 5 mM DTT_{red} for 30 min) showed very poor binding (**Figure 7C**). To analyze the interaction of reduced and oxidized OpcA with G6PDH, His8-tagged G6PDH was immobilized to the Ni-NTA biosensor and allowed to interact with either oxidized or reduced OpcA (**Figure 7D**). The oxidized OpcA also showed better binding to the sensor-bound-G6PDH than the reduced OpcA. To determine whether the redox state of Pgm1 and G6PDH also influences the formation of the Pgm1-OpcA-G6PDH complex, the binding assays showed in **Figures 7C** and **7D** were repeated after treating the immobilized proteins (Pgm1 and G6PDH, respectively) with DTT_{red} or DTT_{ox}. The formation of the complex was slightly better when Pgm1 was in its oxidized state (**Figure S4A**), whereas no difference was observed between the reduced and oxidized G6PDH (**Figure S4B**). Interestingly, the phosphomimetic variant Pgm1 S63D did not show any binding to OpcA (**Figure S4C**). These results indicate that, when Pgm1 is dephosphorylated at Ser 63, it interacts with the OpcA-G6PDH complex in an oxidized state, thus forming a dynamic supramolecular complex of sequential metabolic enzymes.

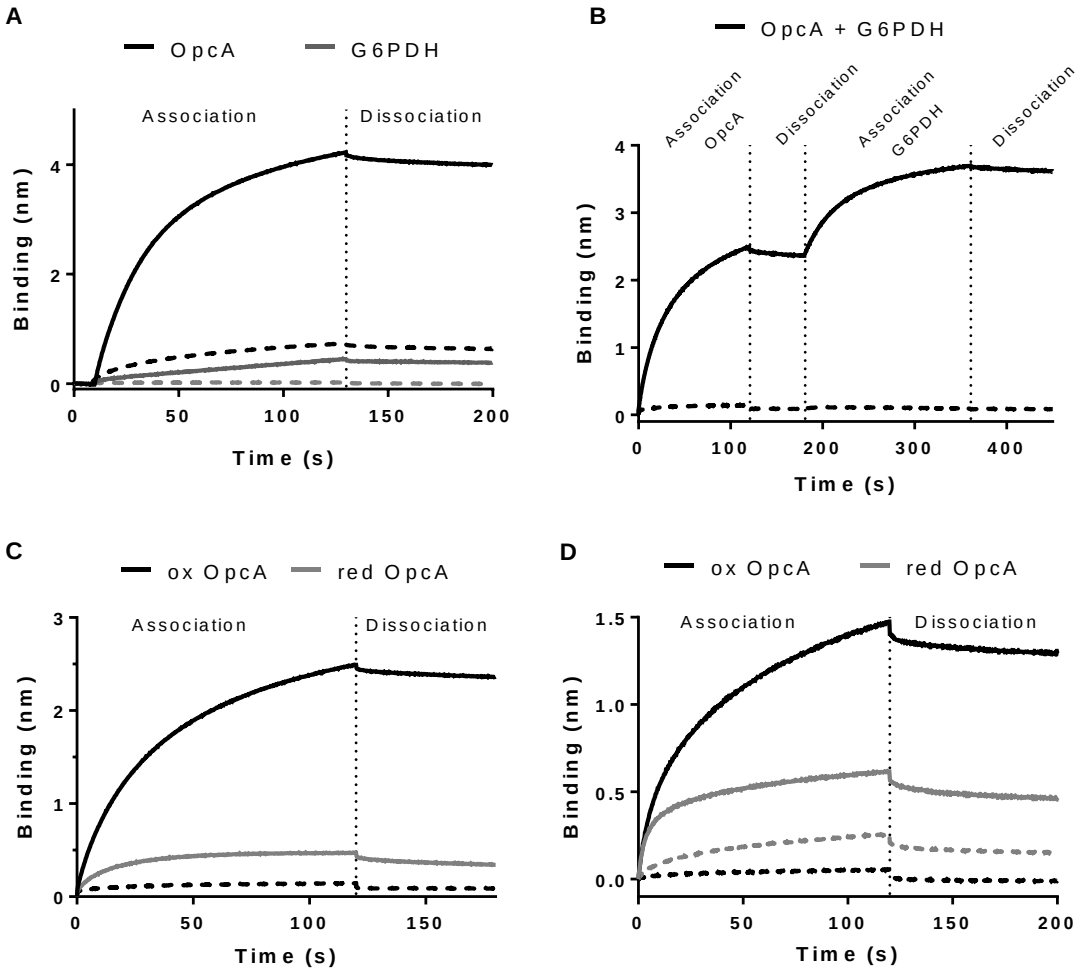

Figure 7. Pgm1, OpcA and G6PDH transiently form a metabolon under oxidized conditions. *In vitro* analysis by Biolayer Interferometry of the interaction between Pgm1, OpcA and G6PDH. Solid lines: (A)(B)(C) His8-tagged Pgm1 was immobilized on Ni-NTA sensor tips, (D) His8-tagged G6PDH was immobilized on Ni-NTA sensor tips. Dashed lines: His8-tagged PII-ΔT-loop was immobilized on Ni-NTA sensor tips. (A) Sensor-immobilized proteins were allowed to associate with either OpcA or G6PDH. (B) Sensor-immobilized proteins were allowed to associate first with OpcA, then with G6PDH. (C) Sensor-immobilized proteins were allowed to associate with oxidized or reduced OpcA. (D) Sensor-immobilized proteins were allowed to associate with oxidized or reduced OpcA.

To determine its size, the Pgm1-OpcA-G6PDH complex was further analyzed via multiangle light scattering coupled to size exclusion chromatography (SEC-MALS) (**Figure S5**). When G6PDH was analyzed alone, most of the protein eluted in a peak with a MALS-determined molar mass of 242.9 ± 0.02 kDa, which corresponds to the tetrameric state of G6PDH (4 x 59 kDa). Additionally, a smaller peak corresponding to the monomeric G6PDH was detected, with a determined molar mass of 59.56 ± 0.071 KDa (**Figure S5A**). OpcA and Pgm1 alone mostly eluted as monomers (55.26 ± 0.009 kDa and 63.61 ± 0.025 kDa, respectively), although higher oligomeric states were also detected (**Figure S5B and C**). When G6PDH was mixed with OpcA in equimolar concentrations, a dominant peak with a

molar mass of 430.3 ± 0.02 kDa was observed, in addition to small amounts of monomeric OpcA (**Figure S5D and F**). The mass difference between the tetrameric G6PDH (4 x 59 kDa) and the G6PDH-OpcA complex (430 kDa) agrees with 4 subunits of OpcA (55 kDa) binding to the tetrameric G6PDH. Analysis of G6PDH, OpcA and Pgm1 together in equimolar concentrations revealed a new peak with a molar mass of 705.57 ± 0.009 kDa, in addition to the previously detected peak of 430 kDa for the OpcA- G6PDH complex (**Figure S5E and D**). The apparent mass difference of 275 kDa agrees with four subunits of Pgm (4 x 63 kDa) binding to the OpcA-G6PDH complex. Overall, the tetrameric G6PDH seems to bind 4 monomers of OpcA, each of which binds a Pgm1 monomer, forming a complex that appears to be stable due to the lack of decay detected in the chromatograms.

Pgm1 regulation is conserved from bacteria to humans.

Regulation of Pgm activity is crucial for the survival of a wide range of organisms to many different conditions. Interestingly, a homologous residue of the phosphorylation site Ser 63 of *Synechocystis* Pgm1 is also found in higher mammals, such as humans, mice and rabbits (**Figure 8A**). In humans, Pgm1 deficiency leads to glycogenosis, a metabolic disorder that causes the abnormal use and storage of glycogen.[15] Despite the importance of the correct activity of this enzyme on human health, little is known regarding its functional regulation. Although Ser 20 of the human Pgm1 (HPgm1), which is the homologous residue of *Synechocystis* Pgm1 Ser 63 in the human protein, has been identified as a phosphorylation site,[16] the role of phosphorylation of this residue has not been investigated. To ascertain whether phosphorylation of HPgm1 at Ser 20 has a similar effect than phosphorylation of Ser 63 in *Synechocystis* Pgm1, we purified HPgm1 along with a mutant variant, in which Ser 20 had been substituted by Asp (HPgm1 S20D), and measured their enzyme activities *in vitro*. As shown in **Figure 8B**, HPgm1 S20D showed no enzyme activity, indicating that, as in *Synechocystis*, HPgm1 activity may be regulated by phosphorylation at Ser 20.

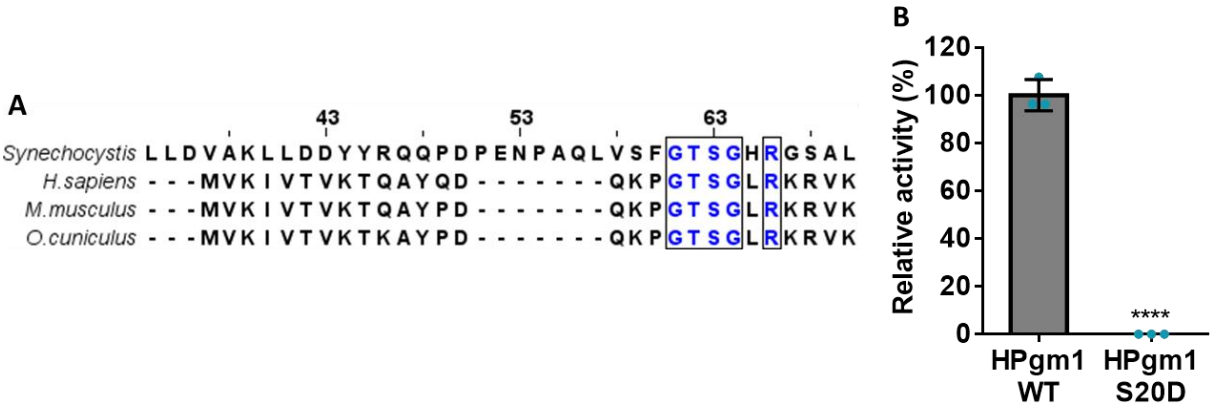

Figure 8. Regulation of Pgm1 by phosphorylation is conserved in mammals. (A) Alignment of the sequence of Pgm1 from *Synechocystis*, *Homo sapiens*, *Mus musculus* and *Oryctolagus cuniculus*. The conserved motif is marked in blue. (B) Relative *in vitro* activity of HPgm1 and HPgm1 S20D. The activity of WT Pgm1 was considered to be 100%. At least 3 replicates were measured. Error bars represent the SD; asterisks represent the statistical significance.

Discussion

Regulation of glycogen metabolism is of vital importance in organisms of all three kingdoms of life. In bacteria, proper control of glycogen synthesis and degradation determines the ability to survive transient periods of nutrient starvation. In mammals, deficiencies in glycogen metabolism lead to a variety of different metabolic disorders, some of them very severe. In this study, we used the unicellular cyanobacterium *Synechocystis* to investigate the regulatory mechanisms of some of the key glycogen metabolic enzymes.

During nitrogen starvation, the activity of the glycogen catabolic enzymes must be regulated to prevent premature glycogen degradation, so that cells can use this reserve polymer once the conditions are favorable for resuscitation. We could show that this control is exerted by the combined regulation of Pgm1 and G6PDH: Pgm1 is inactivated by phosphorylation of Ser 63, whereas G6PDH is under a tight redox control.

Pgm is an evolutionary conserved enzyme that mediates one of the most important reactions in carbohydrate metabolism: It catalyzes the interconversion between glucose-1P and glucose-6P, being thereby involved in both, glycogen synthesis and degradation.[17] Despite its important role in sugar metabolism, Pgm activity has only recently started to be considered as a target for metabolic control.[18–21] At the onset of nitrogen starvation, the activity of the Pgm1 isoform is required for glycogen synthesis, as shown by the inability of a Pgm1 knock-out mutant to synthesize glycogen. Once enough glycogen has been accumulated, Pgm1 activity is inhibited by phosphorylation of Ser 63. When in addition to the WT Pgm1, the non-phosphorylated S63A variant is present, cells degrade glycogen after

prolonged nitrogen starvation and concomitantly lose viability. This highlights the pivotal role of Ser 63 phosphorylation for controlling glycogen catabolism. This residue is highly phosphorylated in long-term-chlorotic cells and it is progressively de-phosphorylated during resuscitation. *In vitro* characterization of a phosphomimic variant of Pgm1 (Pgm1 S63D) strongly suggests that the phosphorylated version of the enzyme is inactive. Analysis of other Pgm1 variants (Pgm1 S63A, S63G, and S63T) indicated that substitution of Ser 63 affects catalysis, as their V_{max} was much lower as compared to WT Pgm1, although the substrate affinity was not impaired (as deduced from the K_m value). Based on structural studies of the reaction mechanism from related proteins,[22] we suggest a role of Ser 63 in a conformational change occurring during catalysis. When Pgm1 is in its open conformation, its catalytic cleft is easily accessible for phosphorylated sugars. When glucose-P enters the catalytic site, the unphosphorylated end of the sugar binds the phosphorylated Ser 168 (see **Figure 2**). The phosphorylated end of the glucose molecule must interact with the phosphate-binding residues present in domain 4. In order for these residues to come in close contact, Pgm1 must undergo a conformational change that involves a rotation of domain 4 and changes the active site from an open cleft to a closed pocket. This conformational change requires the interaction of a group of residues from domain 4 with a group of residues from domain 1, including Ser 63.[23] This explains why any change of Ser 63 has a negative effect on catalysis. When the site of Ser 63 is occupied by a negative residue, as in the phosphomimetic variant, or when the seryl-residue is phosphorylated, the negative charge obstructs this conformational change, preventing the closed conformation of the enzyme and thereby inhibiting catalysis.

Strikingly, this regulatory phosphorylation site located in domain 1 of Pgm1 is conserved in higher organisms, including mouse, rabbit and human. Although Pgm1 deficiency can cause severe disease in humans, its functional regulation remains under-investigated. HPgm1 is known to be phosphorylated and thereby activated by the p21-activated signaling kinase 1 (Pak1) on Thr 466.[17] However, although Ser 20, the homologous of *Synechocystis* Ser 63, had previously been reported as a phosphorylation site in HPgm1,[16] the role of this phosphorylation on enzyme activity had not been characterized. We were able to demonstrate that, as in *Synechocystis*, HPgm1 is also inactivated by phosphorylation at Ser 20. In agreement with our results, a study involving patients suffering from Pgm1 deficiency showed that mutations on the loop in domain 1 where Ser 20 is located in HPgm1 led to a reduced enzyme activity (3.3% of the control) and caused moderate disease in heterozygote patients. [23] These findings suggest that the regulatory mechanism discovered in this study is evolutionary conserved.

Analysis of the steady-state levels of metabolites of glycogen degradation showed high accumulation of glucose-6P, implying that Pgm1 is not the only control point, but also the enzymes that catalyze the glucose-6P consuming reactions are regulated. Although catabolism of the bulk of the glycogen reserves must be prevented during nitrogen starvation, residual glycogen synthesis and degradation constantly takes place in chlorotic cells:[24] A residual carbon flux through the glycogen catabolic pathways results in synthesis of polyhydroxy butyrate (PHB) during prolonged nitrogen starvation. The data presented here also supports the existence of such residual flux, given the considerable glycogen degradation and loss of viability in the WT+Pgm1S63A strain after long-term starvation. This minimal metabolic activity is necessary to maintain the minimum ATP levels to keep viability in dormant cells.[25] As mentioned above, glycogen can be catabolized via three different routes: The EMP, the ED and the OPP pathways. G6PDH directs glucose-6P into the OPP and ED pathways, whereas the glucose-6-phosphate isomerase (Pgi) leads it into the EMP pathway. Koch et al.[24] showed that the main carbon flux from glycogen to PHB synthesis in chlorotic cells happens through the EMP pathway, which is the route with the highest ATP yield, whereas the OPP and ED pathways seem to play a minor role in this process. Our data indicate that G6PDH is inactive in chlorotic cells. The cytoplasm of nitrogen-starved cells is a reducing environment: When cells are nitrogen-depleted, anabolic processes stop consuming the electrons provided by photosynthetic reactions and reducing equivalents accumulate.[26] Under these conditions, OpcA should be reduced by the Trx system, and would be unable to activate G6PDH. However, when a nitrogen source is added to chlorotic cells, the glycogen pool is mainly mobilized through the ED and OPP pathways, and not through the EMP pathway. Although the latter is energetically more productive than the OPP and ED pathways, it does not generate the necessary metabolic intermediates to re-built the previously degraded cellular components in nitrogen-starved cells and it is therefore not the preferred route for carbohydrate degradation during resuscitation[8], or during heterotrophic growth in general.[27] Upon addition of a nitrogen source, the glutamine synthetase – glutamate synthetase (GS-GOGAT) nitrogen assimilation cycle is immediately induced.[7,25] The GOGAT reaction, which produces glutamate from glutamine and 2-oxoglutarate, consumes reduction equivalents, thereby alleviating the over-reduced state of the cytoplasm, which would allow activation of G6PDH by OpcA and utilization of the ED and OPP pathways.

Oxidation of OpcA and dephosphorylation of Pgm1 triggered by nitrate addition also allows the formation of the Pgm1-OpcA-G6PDH complex. Although transient interaction between sequential metabolic enzymes has been observed in a variety of pathways, the

purpose of enzyme assembly remains uncertain. Control of the metabolic flux at a branch point of a pathway has been proposed as a key role of enzyme complex formation: Enzyme assembly may allow channeling of the metabolic product from one enzyme to the next one, avoiding its use by a competing enzyme at a branch point in a metabolic network. In such case, the enzymatic complexes are known as metabolons. However, the functional significance of metabolon formation has not yet been fully clarified.[28] Catabolism of glucose-6P represents a branch point in glycogen degradation. The data derived from the characterization of mutants in key enzymes of the glycogen catabolic pathways strongly suggests that, upon nitrogen addition, the carbon flow is switched from the EMP to the ED and OPP pathways,[8,24] although both G6PDH and Pgi are up-regulated in recovering cells,[9] suggesting the existence of a regulatory mechanism in the control of metabolic flux. We propose that the Pgm1-OpcA-G6PDH complex acts as a metabolon that channels glucose-6P towards the ED and OPP pathways, which provide the metabolites and reduction equivalents required for resuscitation from chlorosis, thereby preventing it from being utilized by Pgi. The fact that the interaction between OpcA, Pgm1 and G6PDH is favored under oxidizing conditions and when Pgm1 is dephosphorylated suggests that formation of the Pgm1-OpcA-G6PDH complex is induced during the transition to heterotrophic growth, when functionality of the OPP and ED pathways is required. Thus, the Pgm1-OpcA-G6PDH metabolon is probably also relevant in the light-dark transitions. Altogether, our study sheds new light on the regulation of the central glycogen metabolic hub, which is at the core of carbohydrate metabolism. Tight regulation of the bi-directional Pgm1 is thereby of special relevance, with its regulation through seryl-phosphorylation being evolutionary conserved from cyanobacteria to humans.

Acknowledgements

We thank Samuel Quinzer for his involvement in G6PDH enzymatic assays, Dr. Nicolas Nalpas for his help with the proteomics data, and Dr. Libera Lo Presti for her assistance writing this manuscript. This work was supported by the German Research Council (DFG) FOR 2816 “The Autotrophy-Heterotrophy Switch in Cyanobacteria: Coherent Decision-Making at Multiple Regulatory Layers”. LC-MS/MS systems at the Department of Quantitative Proteomics were supported by the DFG grants INST 37/935-1 and INST 37/741-1 FUGG. Additionally, we acknowledge the infrastructural support from EXC 2124 “Controlling Microbes to Fight Infections”.

Author contributions

S.D. performed cultivation experiments, cloning, protein purification, enzymatic assays, glycogen and glucose-phosphate determinations, BLI experiments, SEC-MALS experiments, constructed mutants, analyzed data, and wrote manuscript with input from all authors. N.N. contributed cloning and BLI experiments. P.S performed proteomic analysis. K.F. conceived study, interpreted data and edited manuscript.

Competing interests

The authors declare no competing financial interest.

Methods

Cyanobacterial cultivation

The cyanobacterial strains used in this study are listed in **Table S1**. All strains were grown in BG_{11} supplemented with 5 mM $NaHCO_3$ for vegetative growth, as described previously.[29] Nitrogen starvation was induced as previously described by a 2-step wash with BG_{11-0} medium supplemented with 5 mM $NaHCO_3$, which contains all BG_{11} components except for $NaNO_3$.[7,30] Resuscitation was induced by addition of 17 mM $NaNO_3$ to cells residing in BG_{11-0}. Cultivation was performed with continuous illumination (50 to 60 µmol photons m−2 s−1) and shaking (130 to 140 rpm) at 27 °C. Mutant strains were cultivated with the appropriate concentration of antibiotics.[8] All strains used for this study are shown in **Table S1**. Biological replicates were inoculated from the same pre-cultures, but propagated, nitrogen-starved and resuscitated independently in different flasks under identical conditions.

Protein overexpression and purification

Escherichia coli Rosetta-gami (DE3) was used for the overexpression of all proteins. All primers and plasmids used for protein overexpression are shown in **Table S2** and **Table S3**, respectively. Cells were cultivated in 2xYT (1L of culture in 5L flasks) at 37 °C until they reached exponential growth (OD_{600} 0.6-0.8) and protein overexpression was then induced by adding either 0.1 mM IPTG (for His-tagged proteins) or 75 µg/L anhydrotetracycline (for Strep-tagged proteins), followed by incubation at 20°C for 16 h. Cells were harvested by centrifugation at 4000 g for 10 min at 4 °C, and disrupted by sonication in 40 mL of lysis buffer (100 mM Tris-HCl pH 7.5, 150 mm KCl, 5 mM $MgCl_2$, 10 mM imidazole (only for

His-tagged proteins), DNAse, and protease inhibitor cocktail). The cell lysates were centrifuged at 20,000 g for 1 h at 4°C and the supernatants were filtered with a 0.22 µM filter.

For the purification of His-tagged proteins, 1 mL Ni-NTA HisTrap columns (GE Healthcare, Illinois, USA) were used. The cell extracts were loaded into the columns, washed with wash buffer (100 mM Tris-HCl pH 7.5, 150 mm KCl, and 50 mM Imidazole) and eluted with elution buffer (100 mM Tris-HCl pH 7.5, 150 mm KCl, and 500 mM Imidazole).

For the purification of Strep-tagged proteins, 5 mL Ni-NTA Strep-tactin® superflow (Qiagen, Maryland, USA) columns were used. The cell extracts were loaded into the columns, washed with wash buffer (100 mM Tris-HCl pH 7.5 and 150 mm KCl) and eluted with elution buffer (100 mM Tris-HCl pH 7.5, 150 mm KCl, and2.5 mM desthiobiotin).

The buffer of all purified proteins was exchanged via dialysis using dialysis buffer (100 mM Tris-HCl pH 7.5, 150 mm KCl, and 5 mM $MgCl_2$) and a 3 kDa cutoff dialysis tube. 1 mm DTT was also added to the dialysis buffer for Pgm1 and HPgm1. All purifications were checked via SDS-PAGE.

Measurement of Pgm activity in cell extracts

To determine the Pgm activity in *Synechocystis* cell extracts an assay was adapted from Osanai et al.[31] The Pgm reaction was coupled to the G6PDH reaction and the glucose 6-phosphate-dependent conversion of $NADP^+$ to NADPH was monitored by measuring the absorbance at 340 nm. Cells were harvested by centrifugation at 4000 g for 10 min at 4 °C, resuspended in lysis buffer (100 mM Tris-HCl pH 7.5, 10 mM $MgCl_2$) and disrupted by using a "FastPrep®-24"(MP Biomedicals). The lysate was centrifuged for 10 min at 4 °C before the protein content was determined. When indicated, cell lysates were treated with 2 U/mL of alkaline phosphatase for 1 h at 37 °C. Approximately 50 µg of protein were used for each reaction. The reaction buffer was composed of 100 mM Tris-HCl pH 7.5, 10 mM $MgCl_2$, 1 mM $NADP^+$, 1 mM DTT and 1 U/mL G6PDH from *Saccharomyces cerevisiae* (G6378, Sigma Aldrich, Missouri, USA). The reaction was started by the addition of 10 mM glucose-1P. Absorption change at 340 nm was continuously measured for 15 min at 30 °C. As a blank, the change in absorption in the absence of glucose-1P was also measured and subtracted from the experimental values. The enzymatic activity was then calculated. At least three biological replicates were measured.

Measurement of Pgm activity *in vitro*

The reaction buffer was composed of 100 mM Tris-HCl pH 7.5, 150 mM KCl, 10 mM $MgCl_2$, 1 mM $NADP^+$, 1 mM DTT and 1 U/mL G6PDH from *Saccharomyces cerevisiae* (G6378, Sigma Aldrich). 100 ng of His-tagged purified Pgm were added to each reaction. The reaction was started by the addition of glucose-1P and 40 µM glucose-1,6-bisphosphate. Absorption change at 340 nm was continuously measured for 15 min at 30 °C. The enzymatic activity was then calculated. At least three replicates were measured.

Measurement of G6PDH activity *in vitro*

The reaction buffer was composed of 100 mM Tris-HCl pH 7.5, 150 mM KCl, 10 mM $MgCl_2$ and 1 mM $NADP^+$. 500 ng of Strep-tagged purified G6PDH were added to each reaction. When indicated, OpcA was added on 1:4 molar ratio to G6PDH. When stated, the enzymes were pre-treated with DTT_{red}, DTT_{ox} or $CuCl_2$ at the concentration and for the time indicated in the figure legends, but enzyme activity was always measured in the absence of reducing or oxidizing agents. The reaction was started by the addition of 10 mM glucose-6P. Absorption change at 340 nm was continuously measured for 15 min at 30 °C. The enzymatic activity was then calculated. At least three replicates were measured.

Recovery assay

Serial dilutions of chlorotic cultures were prepared (10^0, 10^{-1}, 10^{-2}, 10^{-3}, 10^{-4} and 10^{-5}) starting with an OD_{750} of 1. 5 µl of these dilutions were dropped on solid BG_{11} agar plates and cultivated at 50 µmol photons m^{-2} s^{-1} and 27 °C for five days.

Glycogen determination

Glycogen content was determined as described by Gründel et al.[12] with modifications established by Klotz et al.[7] 2 mL-samples were collected, span down and washed with distilled water. Cells were lysed by incubation in 30% KOH at 95°C for 2h. Glycogen was precipitated by addition of cold ethanol to a final concentration of 70% followed by an overnight incubation at -20 °C. The precipitated glycogen was pelleted by centrifugation at 15000 g for 10 min and washed with 70% ethanol and 98% absolute ethanol, consecutively. The precipitated glycogen was dried and digested with 35 U of amyloglucosidase (10115, Sigma Aldrich) in 1 mL of 100 sodium acetate pH 4.5 for 2 h. 200 µl of the samples were mixed with 1 mL of 6% O-toluidine in acetic acid and incubated at 100 °C for 10 min.

Absorbance was then read at 635 nm. A glucose calibration curve was used to determine the amount of glycogen in the samples. For every condition, at least three biological replicates were measured.

Glucose-phosphate quantification

4 mL of chlorotic and resuscitating (24 h after $NaNO_3$ addition) were harvested (OD_{750} ~ 0.8) by centrifugation at 18,000 g for 1 min at 4°C. Pellets were immediately frozen in liquid nitrogen. Cells were lysed by addition of 0.2 M HCl and incubation at 95 °C for 15 min. Lysates were centrifuged at 18,000 g for 10 min at room temperature, then the supernatants were transferred to clean 2 mL tubes. Samples were neutralized with 1 mL of 1 M Tris-HCl pH 8. A glucose-1P and glucose-6P calibration curve were prepared. $NADP^+$, KCl, and $MgCl_2$ were added to samples and standard solutions to a final concentration of 1 mM, 150 mM and 10 mM, respectively. The absorbance of samples and standards were measured at 340 nm (blank measurement). 3 U of G6PDH from *Saccharomyces cerevisiae* (G6378, Sigma Aldrich) were added to all samples and standards and their absorbance at 340 nm was measured after incubation for 5 min at room temperature (glucose-6P measurement). 3 U of Pgm from rabbit muscle (P3397, Sigma) were added to all samples and glucose-1P standards and their absorbance at 340 nm was measured after incubation for 5 min at room temperature (glucose-1P measurement). The blank measurements were subtracted from the glucose-6P measurements, and the glucose-6P standard curve was used to determine the concentration of glucose-6P in the samples. The glucose-6P measurements were subtracted from the glucose-1P measurements, and the glucose-1P standard curve was used to determine the concentration of glucose-1P in the samples. Data were normalized to the OD_{750} of the sampled cultures. Three biological replicates were measured.

Pull down assay

A pull down assay was performed 4 h after the addition of nitrate to chlorotic cells. Therefore, 250 mL cultures of *Synechocystis* cells were cultivated and nitrogen-starved as described above in three independent biological replicates per condition. Cells were harvested by centrifugation at 4,000 x g for 10 min and cell pellets were resuspended in 2 mL of lysis buffer (50 mM Tris-HCl, pH 7.4) before lysis with a FastPrep®-24 Ribolyser at 4 °C (3 cycles at 7.5 m s-1 for 30 s and 5 min breaks in between). Cell extracts were centrifuged at 16,000 x g for 5 min at 4 °C and supernatants were transferred to a new 1.5 mL tubes. Protein G Magnetic Beads were aliquoted (150 µl) and washed twice with 1 mL of lysis buffer. Then

either pre-immune serum or post-immunization anti-Pgm1 antiserum (PINEDA, Berlin, Germany) was added to the beads and they were incubated for 10 min at RT under agitation on an orbital shaker. Beads were washed again and incubated with the cell extracts for 10 min at RT, then washed again. Proteins were eluted in 2 consecutive steps with 60 µl of elution buffer (200 mM glycine, pH 2.5) each. Both fractions were combined and protein concentration was measured. Pull down eluates were precipitated by the addition of 9 sample volumes of a 8:1 v/v ice-cold acetone:methanol mixture and incubated o.n. at -20°C. Protein precipitates were pelleted (5 min 1000 x g at RT) and washed twice with each 1 mL 80% v/v acetone aq. The resulting protein pellet was air-dried and resuspended in 20 µL denaturation buffer. Protein concentrations were measured by Bradford assay and 10 µg protein per sample were treated with dithiothreitol (1 mM) and subsequently iodoacetmaide (5.5 mM) for each 60 min at RT. Samples were digested with 1 µg Lys-C for 3 h, then diluted 1:5 with 20 mM ABC buffer pH 8.0 followed by addition of 1 µg trypsin and incubation o.n. at RT while shaking. The peptide solution was cleaned by stage-tips.[32] LC-MS analysis was performed as described before on a Q Exactive HF or HF-X as described elsewhere.[9] Raw data was analyzed via MaxQuant 1.6.8.0 using a Target/Decoy Database from Cyanobase (*Synechocystis* sp. PCC 6803; 10.06.2014, user-modified) with 3671 protein IDs. Label -free quantification algorithm was used to calculate LFQ intensities. Data from all pull down experiments was analyzed via the Perseus software (version 1.6.5.0). For the identification of significantly enriched proteins, a t-test was performed with the following requirements: each protein had to be detected in at least two replicates and an FDR of 0.001 at S0 = 0.3 was set.

Biolayer interferometry using the Octet K2 system

Protein-protein interaction was tested *in vitro* by biolayer interferometry using the Octet K2 system (FortéBio). All experiments were performed in HEPES buffer (100 mM HEPES-KOH PH 7.5 and 10 mM $MgCl_2$). For the experiments with one Association/Dissociation step, either His8-Pgm1 or His8-tagged G6PDH was immobilized on Ni-NTA sensor tips (FortéBio) by exposing the sensors to a 500 nM solution of Pgm1 for 120 s (Loading), followed by a 60 s baseline measurement. To avoid unspecific binding, the sensor tips were then dipped in a solution containing 600 nM of His8-PII, followed by a second 60 s baseline measurement. For the binding of OpcA and Zwf, the sensor tips dipped in either a 500 nM solution of Strep-OpcA or a 500 mM solution of Strep-G6PDH for 120 s (Association). When indicated, these proteins were pre-treated with either 5mM DTT_{red} or 5 mM DTT_{ox} for 30 min. The assay was finalized with a 120 s Dissociation step. As a control, Loading was done

using His8-PII instead of His8-Pgm1. For the experiments with two Association/Dissociation steps, the sensors tips were first loaded with Pgm1 as described above. In the first Association step, the sensors were exposed to a 500 nM Strep-OpcA solution, followed by a first Dissociation step. In the second Association step, the same sensors were dipped in a 500 nM Strep-G6PDH solution, followed by a second Dissociation step. As a control, Loading was done using His8-PII-ΔT-loop instead of His8-Pgm1. The biosensors were regenerated after each use with 10 mM glycine (pH 1.7) and 10 mM $NiCl_2$ as proposed in manufacturers recommendations. The recorded curves were aligned to the baseline before the Association step.

Size exclusion chromatography multiangle light scattering (SEC-MALS)

SEC-MALS experiments were performed using an ÄKTA purifier system connected to a Superose 6 Increase 10/300 GL column (GE healthcare) at a flow rate of 0.4 ml/min in running buffer (100 mM Tris-HCl pH 7.5, 150 mM KaCl, and 10 mM MgCl2). The column was calibrated using the gel filtration calibration kit LMW and HMW (GE Healthcare) according to the manufacturer's instructions. To analyze the oligomeric state of the recombinant proteins, the ÄKTA micro was connected to downstream MALS using the miniDAWN TREOS combined with an Optilab T-rEX refractometer (Wyatt Technology, Dernbach, Germany). Data analysis was performed using the software ASTRA 7 (Wyatt Technology) and Unicorn 5.20 (Build 500) (General Electric Company, Boston, USA).

Statistical analysis

Statistical details for each experiment can be found in the figure legends. Samples taken from cultures that were inoculated with the same pre-cultures, but propagated, nitrogen-starved and resuscitated independently in different flasks under identical conditions were considered different biological replicates. GraphPad PRISM was used to perform paired Student’s t-tests to determine the statistical significance. Asterisks in the figures were used to symbolize the p-value: One asterisk represents $p \leq 0.05$, two asterisks $p \leq 0.01$, three asterisks $p \leq 0.001$, and four asterisks $p \leq 0.0001$.

Data availability

Proteome raw data files acquired by mass spectrometry were deposited at the ProteomeXchange Consortium via the Proteomics Identifications Database partner

repository[33] under the identifier PXD024024. FOR REVIEWERS ONLY: Username: reviewer_pxd024024@ebi.ac.uk; Password: YDi7Sztw

References

1. Prats, C., Graham, T. E. & Shearer, J. The dynamic life of the glycogen granule. *J. Biol. Chem.* **293**, 7089–7098 (2018).

2. Klotz, A. & Forchhammer, K. Glycogen, a major player for bacterial survival and awakening from dormancy. *Future Microbiol.* **12**, 101–104 (2017).

3. Welkie, D. G. *et al.* A Hard Day's Night: Cyanobacteria in Diel Cycles. *Trends Microbiol.* **27**, 231–242 (2019).

4. Preiss, J. Bacterial glycogen synthesis and its regulation. *Annu. Rev. Microbiol.* 419–458 (1984).

5. Forchhammer, K. & Schwarz, R. Nitrogen chlorosis in unicellular cyanobacteria – a developmental program for surviving nitrogen deprivation. *Environ. Microbiol.* **21**, 1173–1184 (2019).

6. Schwarz, R. & Forchhammer, K. Acclimation of unicellular cyanobacteria to macronutrient deficiency: Emergence of a complex network of cellular responses. *Microbiology* **151**, 2503–2514 (2005).

7. Klotz, A. *et al.* Awakening of a Dormant Cyanobacterium from Nitrogen Chlorosis Reveals a Genetically Determined Program. *Curr. Biol.* **26**, 2862–2872 (2016).

8. Doello, S., Klotz, A., Makowka, A., Gutekunst, K. & Forchhammer, K. A specific glycogen mobilization strategy enables rapid awakening of dormant cyanobacteria from chlorosis. *Plant Physiol.* **177**, 594–603 (2018).

9. Spät, P., Klotz, A., Rexroth, S., Maček, B. & Forchhammer, K. Chlorosis as a developmental program in cyanobacteria: The proteomic fundament for survival and awakening. *Mol. Cell. Proteomics* **17**, 1650–1669 (2018).

10. Liu, L., Hu, H. H., Gao, H. & Xu, X. D. Role of two phosphohexomutase genes in glycogen synthesis in Synechocystis sp. PCC6803. *Chinese Sci. Bull.* **58**, 4616–4621 (2013).

11. Osanai, T. *et al.* Pathway-level acceleration of glycogen catabolism by a response regulator in the cyanobacterium synechocystis species PCC 6803. *Plant Physiol.* **164**, 1831–1841 (2014).

12. Gründel, M., Scheunemann, R., Lockau, W. & Zilliges, Y. Impaired glycogen synthesis causes metabolic overflow reactions and affects stress responses in the cyanobacterium

719 Synechocystis sp. PCC 6803. *Microbiol. (United Kingdom)* **158**, 3032–3043 (2012).

720 13. Mihara, S. *et al.* Thioredoxin regulates G6PDH activity by changing redox states of
721 OpcA in the nitrogen-fixing cyanobacterium Anabaena sp. PCC 7120. *Biochem. J.* **475**,
722 1091–1105 (2018).

723 14. Hagen, K. D. & Meeks, J. C. The Unique Cyanobacterial Protein OpcA Is an Allosteric
724 Effector of Glucose-6-phosphate Dehydrogenase in Nostoc punctiforme ATCC 29133.
725 *J. Biol. Chem.* **276**, 11477–11486 (2001).

726 15. Lee, Y., Stiers, K. M., Kain, B. N. & Beamer, L. J. Compromised catalysis and
727 potential folding defects in in vitro studies of missense mutants associated with
728 hereditary phosphoglucomutase 1 deficiency. *J. Biol. Chem.* **289**, 32010–32019 (2014).

729 16. Bian, Y. *et al.* An enzyme assisted RP-RPLC approach for in-depth analysis of human
730 liver phosphoproteome. *J. Proteomics* **96**, 253–262 (2014).

731 17. Gururaj, A., Barnes, C. J., Vadlamudi, R. K. & Kumar, R. Regulation of
732 phosphoglucomutase 1 phosphorylation and activity by a signaling kinase. *Oncogene*
733 **23**, 8118–8127 (2004).

734 18. Bro, C., Knudsen, S., Regenberg, B., Olsson, L. & Nielsen, J. Improvement of
735 galactose uptake in Saccharomyces cerevisiae through overexpression of
736 phosphoglucomutase: Example of transcript analysis as a tool in inverse metabolic
737 engineering. *Appl. Environ. Microbiol.* **71**, 6465–6472 (2005).

738 19. Jin, G. Z. *et al.* Phosphoglucomutase 1 inhibits hepatocellular carcinoma progression
739 by regulating glucose trafficking. *PLoS Biol.* **16**, 1–27 (2018).

740 20. Malinova, I. *et al.* Reduction of the cytosolic phosphoglucomutase in Arabidopsis
741 reveals impact on plant growth, seed and root development, and carbohydrate
742 partitioning. *PLoS One* **9**, 1–11 (2014).

743 21. Seibold, G. M. & Eikmanns, B. J. Inactivation of the phosphoglucomutase gene pgm in
744 Corynebacterium glutamicum affects cell shape and glycogen metabolism. *Biosci. Rep.*
745 **33**, 645–654 (2013).

746 22. Müller, S. *et al.* Crystal structure analysis of the exocytosis-sensitive phosphoprotein,
747 pp63/parafusin (phosphoglucomutase), from paramecium reveals significant
748 conformational variability. *J. Mol. Biol.* **315**, 141–153 (2002).

749 23. Beamer, L. J. Mutations in hereditary phosphoglucomutase 1 deficiency map to key

regions of enzyme structure and function. *J. Inherit. Metab. Dis.* **38**, 243–256 (2015).

24. Koch, M., Doello, S., Gutekunst, K. & Forchhammer, K. PHB is produced from Glycogen turn-over during nitrogen starvation in Synechocystis sp. PCC 6803. *Int. J. Mol. Sci.* **20**, 1942 (2019).

25. Doello, S., Burkhardt, M. & Forchhammer, K. The essential role of sodium bioenergetics and ATP homeostasis in the developmental transitions of a cyanobacterium. *Curr. Biol.* **31**, 1–10 (2021).

26. Hauf, W. *et al.* Metabolic changes in Synechocystis PCC6803 upon nitrogen-starvation: Excess NADPH sustains polyhydroxybutyrate accumulation. *Metabolites* **3**, 101–118 (2013).

27. Makowka, A. *et al.* Glycolytic shunts replenish the Calvin-Benson-Bassham cycle as anaplerotic reactions in Cyanobacteria. *Mol. Plant* **13**, 471–482 (2020).

28. Sweetlove, L. J. & Fernie, A. R. The role of dynamic enzyme assemblies and substrate channelling in metabolic regulation. *Nat. Commun.* **9**, 2136 (2018).

29. Rippka, R., Deruelles, J., Waterbury, J. B., Herdman, M. & Stanier, R. Y. Generic Assignments, Strain Histories and Properties of Pure Cultures of Cyanobacteria. *Microbiology* **111**, 1–61 (1979).

30. Schlebusch, M. & Forchhammer, K. Requirement of the nitrogen starvation-induced protein s110783 for polyhydroxybutyrate accumulation in synechocystis sp. strain PCC 6803. *Appl. Environ. Microbiol.* **76**, 6101–6107 (2010).

31. Osanai, T. *et al.* Genetic engineering of group 2 σ factor SigE widely activates expressions of sugar catabolic genes in Synechocystis species PCC 6803. *J. Biol. Chem.* **286**, 30962–30971 (2011).

32. Rappsilber, J., Mann, M. & Ishihama, Y. Protocol for micro-purification, enrichment, pre-fractionation and storage of peptides for proteomics using StageTips. *Nat. Protoc.* **2**, 1896–1906 (2007).

33. Perez-Riverol, Y. *et al.* The PRIDE database and related tools and resources in 2019: Improving support for quantification data. *Nucleic Acids Res.* **47**, D442–D450 (2019).

IX. ACKNOWLEDGMENTS

I must give my most sincere thanks to my Doctoral Father, Karl Forchhammer. I simply could not have asked for better supervision and support than I have received during the last years. I also want to thank my second supervisor, Christiane Wolz, for agreeing to evaluate this work.

I feel very fortunate for having had the opportunity to pursue a doctoral degree in an institution like the University of Tübingen. The Forchhammer/Maldener Lab has been a great place to work at. The privilege of having intellectual freedom, being surrounded by bright people, being allowed to attend all kinds of workshops and conferences, etc. have been fundamental for my scientific development.

I am very thankful to all the people who have been part of this journey. I have to thank Alex for his supervision and his help when I first arrived in Germany. Niels and Moritz, for being the best coworkers and friends. Markus, for always having a positive attitude and being willing to help. Our secretaries and technicians, Michaela, Neus, Louisa, Eva and Claudia, for taking care of very important tasks. And Iris, for her advise whenever it was needed. I also want to thank a couple of external people: Our collaborator Kistin Gutekunst, for the exchange of strains and discussions, the Maček lab, for the proteomic analyses, and Libera Lo Presti, for her help with my manuscripts and with this thesis.

I am as well very grateful for all those moments outside the lab. Thanks to Phil, Eva, Rebeca, Anka and Robert for the climbing and hiking adventures. To Khaled, for the volleyball games, the ice-cream breaks, and for being my companion at conferences everywhere around the world. And to my lunch buddies, Ritu, Rokhsareh, Tchini, Adrian and Ana, for patiently waiting until I finish my food.

The last stage of a doctoral degree is a very stressful period, especially in combination with the situation the whole world is living right now. I want to thank my family and friends for their great support. I must especially mention Loli and Antonio, Mum and Dad, for feeling close when they are far away. David, my little brother, for showing me that it is possible to stay strong in tough times. My Grandma, to whom this thesis is dedicated, for being an inspiration for me. And, of course, Diego, for always, always being there.

Muchas gracias a todos.